B A B A

VE

A N A M A

ELECTRICAL RESISTIVITY AND MAGNETIC ORDERING IN TRANSITIONAL METAL ALLOYS

Thesis Submitted for the Degree of Doctor of Philosophy of the University of London

by

Ahmet TARI

Physics Department,
Imperial College of Science and Technology,
London, S.W.7.

January, 1973

ABSTRACT

Electrical resistivity and magnetisation measurement on a number of alloys of 3d impurities with exchange enhanced hosts have been made. Resistance measurements were made at temperatures $T \leq 40K$ using a 4 probe d c potentiometric technique and magnetisation measurements were made by a vibrating sample magnatometer at temperature range between $1.6^{\circ}K$ up to room temperature.

The main part of the work was the investigation of the Pd-Ni and Rh-Co alloys through their respective critical concentrations. The results show that the Pd-Ni alloys system makes transition from a strongly enhanced paramagnetic region straight into a ferromagnetic phase in which the magnetic properties of the alloys indicate that they are itinerant ferromagnets. In Rh-Co alloys, on the other hand, first the stabilisation of moments on cobalt atoms occurs at about 20 at % and the transition is, unlike Pd-Ni, into a spin glass region. Above about 37 at % Co the system gradually becomes itinerant electron ferromagnets.

Measurements on some Pd-Mn alloys show that there is a gradual transition from ferromagnetism into some type of antiferromagnetic order.

A review of recent theoretical investigations is made and the results of the investigation are discussed in the light of existing theories.

A C K N O W L E D G E M E N T S

The author wishes to express his sincere thanks to Professor B.R. Coles for his continuous interest, encouragement and advice during the progress of this work which was carried out at his suggestion and under his supervision. He is indebted to Dr. M. Rivier and Dr. D. Rainford of the Solid State Group and Dr. G. Grüner of the Central Research Institute for Physics, Budapest for many helpful discussions. Also to Dr D. Caplin for suggestions concerning the design of the cryostat. Further he would like to thank Dr H. Jamieson for his assistance during the investigation of Rh-Co alloys, Mr. R. Rusby of the National Physical Laboratories, for measuring the resistance of several alloys in the He^3 cryostat and all members of the Solid State Group for their valuable assistance during this work. Helpful discussions regarding the metallurgy with Dr H.E.N. Stone are very much appreciated.

Last but not least I would like to thank my wife for her encouragement and for help during the writing of this thesis.

During the course of this work a loan from the Turkish Ministry of Education was gratefully received.

C O N T E N T S

INTRODUCTION

The theoretical and to some extent the experimental study of the alloys has, understandably, been long confined to dilute concentrations where the theoretical treatment is relatively simple and the interpretation of experimental results is usually feasible. Only in recent years have some theoretical attemps been made to explore more concentrated alloys. In this case one has to choose suitable systems for the investigations.

Pd-Ni and Rh-Co alloy systems are fairly simple. They are iso-electronic and the electronic wave function of solute and solvent have the same symmetry. Further, the preparation of samples is quite easy since metallurgically the alloys present no problem. Therefore it was decided to investigate these alloys through their respective critical concentrations. (The concentration at which the alloy has a Curie temperature $Tc=0^{\circ}K$). We also investigated Pd-Mn alloys at intermediate concentrations, 3-10 at % Mn for which no detailed investigation was available.

The arrangement of the thesis is as follows:

In Chapter I a review is made of the theories discussing the formation of localised moments on isolated transition metal atoms dissolved in nonmagnetic hosts. The effect of local environment is considered and the possible interaction mechanisms between the moments are discussed. The chapter ends with a review of some forms of ordering in transition metal alloys relevant to our work.

In Chapter II the electronic properties of alloys, namely, magnetic susceptibility, electrical resistivity and specific heat, are discussed from a theoretical point of view.

A review of the experimental situation is given in Chapter III, apparatus and experimental procedure are described in Chapter IV, and the results of the measurements are presented and discussed in Chapter V.

CHAPTER I

THE DILUTE ALLOY PROBLEM

I THE FORMATION OF LOCALISED MOMENTS

1. Introduction

When an impurity is dissolved into a metal a moment is said to exist if the additional susceptibility, $\Delta\chi$, is strongly temperature dependent i.e. if it follows a Curie law. A Pauli-like susceptibility contribution is taken to mean there is no moment.

When there is a moment the susceptibility is not usually of Curie, but of Curie-Weiss form:

$$\Delta\chi = \frac{C}{T - \theta} \qquad (I.1)$$

i.e. less strongly temperature dependent. In this formula θ may be large and is independent of impurity concentration. C is proportional to the concentration. The above formula is therefore the result of interaction between an isolated impurity and the surrounding conduction electrons.

In a metallic host the formation of localised moment on a potentially magnetic impurity, i.e. which has an unfilled inner shell, depends strongly on the type of shell and the nature of the host matrix. In some cases, where the impurity electronic structure is the same as that of the free atom one expects to observe the presence of localised moment. Examples of such cases being rare earth impurities in simple metals, potentially magnetic ions in insulators etc. where the magnetic electrons are localised. But in the case of 3d transition metal impurities in a metallic host, the states of the magnetic electrons lie in the host

metal conduction band. This makes the situation more complicated.

However one of the main agencies responsible, in all cases, for the formation of a localised moment, is now recognised. This is the Coulomb repulsive energy between two electrons on the same atomic orbital. The same quantity is responsible for the enhanced spin susceptibility of the elements towards the end of 3d, 4d and 5d transitional series. Namely of Pd, Pt and Rh.

The states of a 3d impurity in a metallic host such as copper, silver, aluminium etc. will always lie in the conduction band and will admix strongly with the conduction electrons of the host metal. Under these conditions the magnetic electrons will not be bound to the impurity atom. However this mixing broadens the state of the magnetic electron in space and in energy where the amplitude of the l^{th} component of the state of the conduction electrons is anomalously large, corresponding to an excess of charge density which when summed over the whole region is approximately equal to the charge introduced with initial l^{th} bound state. This is what is called the virtual bound state. This concept was first applied to the impurity problem in metals by Friedel (1) to explain the residual resistivity of 3d elements in simple hosts.

2. Friedel's Virtual Bound State

Let us assume that, with an impurity, a spherically symmetric potential $V_p = V(r)$ is introduced into a matrix. This is the problem of a particle in a central field in quantum mechanics. If the interaction between electrons is neglectedthen the wave function of electrons satisfy

$$\nabla^2 \psi(r,\theta,\varphi) + \frac{2m}{\hbar^2}[E - V(r)]\,\psi(r,\theta,\varphi) = 0 \qquad (I.2)$$

The wave function may be separated into its radial and angular parts.

The equation for the radial part of the wave function is:

$$\frac{1}{r^2}\frac{d}{dr}\left(r^2\frac{dR(r)}{dr}\right)+\frac{2m}{\hbar^2}\left[E-\left(V(r)+\frac{\hbar^2 l(l+1)}{2m\,r^2}\right)\right]R(r)=0 \qquad (I.3)$$

From this equation one can see at once why even though the energy levels of the d-electrons lie in the conduction band they are "virtually" bound to the impurity. The extra term $\frac{\hbar^2}{2m}\frac{l(l+1)}{r^2}$ is $\sim\frac{6}{r^2}$ Rydberg for the d-electrons ($l=2$). It can therefore be quite large and represents a barrier between the impurity cell and the outside region. A d-electron in the virtual state will eventually go through the barrier, the time dependence of its amplitude will be of the form $e^{-i(E_d-i\Delta)t}$ which Fourier transforms to a resonance:-

$$I(E)=\frac{\Delta}{\Delta^2+(E-E_d)^2} \qquad (I.4)$$

Where Δ is the width of the resonant state and E_d is its position in energy. Friedel (1) described this resonance in terms of a scattering phase shift $\eta_l(E)$ obeying an equation of the form:-

$$\eta_l(E)=\mathrm{tg}^{-1}\frac{\Delta}{(E_d-E)} \qquad (I.5)$$

The behaviour of $\eta_l(E)$ is shown in fig.(I.1).

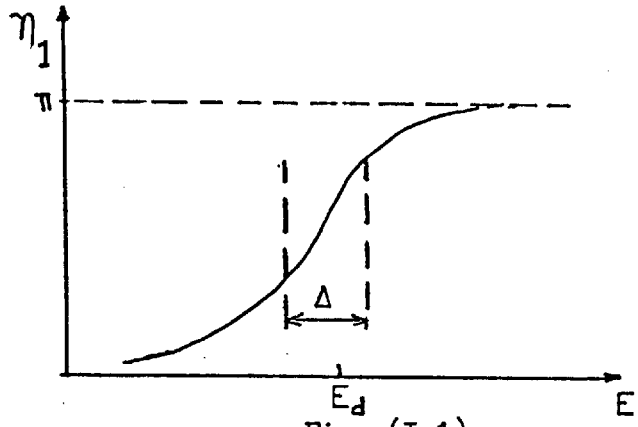

Fig. (I.1)

An important property of the phase shift is that the extra charge introduced into a metallic host with an impurity can be expressed in terms of it. The relationship is given by the Friedel sum rule which states that the total number of states below the Fermi energy of the host conduction electrons is given by the formula:-

$$N(E_F) = N_0(E_F) + 2\sum_l \left(\frac{2l+1}{\pi}\right)\eta_l(E_F) \qquad (I.6)$$

where $N_0(E_F)$ is the number of states in the unpeturbed system. This expression means that there are (2l+1) states for each spin direction between $\eta_l = 0$ and $\eta_l = \pi$.

From formula (I.6) the extra charge around the impurity is obtained as:-

$$\Delta Z = \frac{2e}{\pi}\sum_l (2l+1)\eta_l(E_F) \qquad (I.7)$$

This extra charge is localised in the neighbourhood of the impurity (not too near due to Laue's theorem (2) and has an oscillatory term which has a negligible contribution to ΔZ.

Following the same line as Stoner (3) Friedel qualitatively considered the possibility that the virtual bound state will split into two halves of opposite spin direction due to the exchange energy between electrons in the virtual state and finds the condition for this to be given by:-

$$p \; dE \geq \Delta \qquad (I.8)$$

where p is the number of d electrons (if the level is less than half full) or holes (otherwise) and dE is the energy difference between two electrons with anti-parallel and parallel spins.

3. The Anderson Model

A systematic study, by Matthias et al (4), of the magnetisation of iron in various 4d transitional series metal and alloys, led Anderson (5) to discuss the occurence of localised moments in alloys from a some what different point of view to that of Friedel. Although Anderson recognises the nature of the impurity state for a 3d-element in simple metal hosts, he nevertheless takes it as an extra orbital. This makes the model more explicit and more suitable for mathematical treatment. The hamiltonian is taken to be:-

$$H = \sum_{k\sigma} E_k n_{k\sigma} + \sum_{\sigma} E_d n_{d\sigma} + I n_{d\uparrow} n_{d\downarrow} + \sum_{k\sigma} \left(V_{dk} a^{+}_{k\sigma} a_{d\sigma} + V_{kd} a^{+}_{d\sigma} a_{k\sigma} \right) \qquad (I.9)$$

Where the first and second terms are the unperturbed energy of the conduction electrons of the host and the d-states of the impurity atom respectively. I is the coulomb repulsive energy between the d-electrons in the same orbital. The fourth term is the s-d mixing term which is responsible for the broadening of the d-state into a virtual level.

$n_{k\sigma} = a^{+}_{k\sigma} a_{k\sigma}$ where $a_{k\sigma}$ is the annihilation operator of the conduction electron in the state k with spin σ . $n_{d\sigma}$ is defined in a similar way. In this hamiltonian there is no term representing interaction between host electrons. Therefore the model is applicable to the impurities in metals showing little or no enhancement, such as noble metals. The above hamiltonian is treated in the Hartree-Fock (H-F) approximation. Therefore the hamiltonian for one spin direction is given by:-

$$H^{\sigma} = \sum_{k} E_k n_{k\sigma} + E_{d\sigma}\, n_{d\sigma} + \sum_{k} \left(V_{dk} a^{+}_{k\sigma}\, a_{d\sigma} + V_{kd}\, a^{+}_{d\sigma}\, a_{k\sigma}\right) \qquad (I.10)$$

where $E_{d\sigma}$, the effective one electron energy, is given by:-

$$E_{d\sigma} = E_d + I\langle n_{d,-\sigma}\rangle \qquad (I.11)$$

in which $\langle n_{d\,\sigma}\rangle$ indicates the average number of d-electrons with spin σ . This hamiltonian is treated using the Green's function technique. The Green's operator for such a hamiltonian is:-

$$G^{\sigma}(E) = \eta \to o\,(E - H^{\sigma} + i\eta)^{-1} \qquad (I.12)$$

Computing the matrix elements of the operator $G^{\sigma}(E)$ between the states $|k\rangle$ and $|d\rangle$ one arrives at a set of equations from which the density of states per spin direction of d-electrons is obtained quite simply as:-

$$\rho_d^{\sigma}(E) = -\frac{1}{\pi} \mathrm{Im} \langle d|\ G\ |d\rangle = \frac{1}{\pi}\ \frac{\Delta}{(E - E_{d\sigma})^2 + \Delta^2} \qquad (I.13)$$

where

$$\Delta = \pi \langle V_{dk}^2 \rangle\ \rho_o(E) \qquad (I.14)$$

is the half width of the virtual state and $\rho(E)$ is the density of states of the unperturbed host. The number of d-electrons per spin direction is found from:-

$$\langle n_d^\sigma \rangle = \int_{-\infty}^{E_F} \rho_d^\sigma(E)\, dE \quad = \quad \frac{1}{\pi} \mathrm{Cot}^{-1}\left(\frac{E_d + I\langle n_d^\sigma \rangle - E_F}{\Delta} \right) \qquad (I.15)$$

Hence one has to solve the following two equations simultaneously

$$\langle n_d^+ \rangle = \frac{1}{\pi} \mathrm{Cot}^{-1}\left(\frac{E_d + I\langle n_d^- \rangle - E_F}{\Delta} \right)$$
$$\langle n_d^- \rangle = \frac{1}{\pi} \mathrm{Cot}^{-1}\left(\frac{E_d + I\langle n_d^+ \rangle - E_F}{\Delta} \right) \qquad (I.16)$$

putting $y = \frac{I}{\Delta}$, Anderson finds that when $\frac{y}{\pi} < 1$ the solution of (I.16) gives $\langle n^+ \rangle = \langle n^- \rangle$ i.e. the impurity is nonmagnetic, while $\frac{y}{\pi} > 1$ is found to give magnetic solution i.e. $\langle n^+ \rangle \neq \langle n^- \rangle$. The other condition assumed to exist is $0 < \frac{E_F - E_d}{I} < 1$. Which ensures that E_d is below and $E_d + I$ is above the Fermi level. Thus for a given I and a fixed value of E_d there is a critical value of the width, Δ_c. For widths larger than Δ_c (I.16) has only one solution $\langle n^+ \rangle = \langle n^- \rangle$. The critical value is defined by:-

$$\frac{d\langle n^+ \rangle}{d\langle n^- \rangle} = -1$$

and

$$I\, \rho_d(E_F) = 1 \qquad (I.17)$$

This is of the same form as the Stoner condition for band ferromagnetism (3).

The treatment of Anderson outlined above leads to a sharp boundary between the magnetic and nonmagnetic regions. This results from the use of the H-F approximation. Near the H-F instability the dynamic character of the problem must be taken into account which will smear out the very sharp boundary existing between the two regions.

In the appendix to his paper, Anderson (5) extended his model to the orbitally degenerate states. This was later treated in datail by Yoshida et al (6) and has since been reviewed by Heeger (7). The hamiltonian in this case is given by:-

$$H = H_k + H_d + H_{k-d} \qquad (I.18)$$

where

$$H_k = \sum_{k\sigma} E_k n_{k\sigma}$$

$$H_d = \sum_{\sigma\, m} E_m n_{m\sigma} + (I-J) \sum_{m,n,\sigma} n_{m\sigma}\, n_{n\sigma} + I \sum_{m,n} n_{m\sigma}\, n_{n,\,\sigma}$$

and

$$H_{k-d} = \sum_{km\sigma} (V_{km}\, a^{+}_{k\sigma} a_{m\sigma} + V_{mk}\, a^{+}_{m\sigma}\, a_{k\sigma})$$

In these equations H_k and H_d are the hamiltonians for the conduction and the localised d-electrons and I and J are intra-atomic coulomb and exchange energies respectively. The H_{k-d} is the s-d mixing term and $n_{m\sigma} = a^{+}_{m\sigma} a_{m\sigma}$ is the number operator for electrons in the orbital state labeled by m. The above hamiltonian is treated in the H-F approximation. Hence for the effective one particle energy with spin σ one has:-

$$E_{m\sigma} = E_m + (I-J) \sum_{n \neq m} \langle n_{n\sigma} \rangle + I \sum_{n} \langle n_{m,\,\sigma} \rangle \qquad (I.19)$$

With this, the problem then reduces to the simple one electron problem in which the average numbers of electrons $\langle n_{n\sigma} \rangle$ is to be determined

self consitently. These are given by:-

$$\langle n_{m\sigma} \rangle = \frac{1}{\pi} \cot^{-1}\left(\frac{E_{m\sigma} - E_F}{\Delta_m}\right) \qquad (I.20)$$

In this formula Δ_m is the half width of the virtual level of the m^{th} arbital and is assumed to be independent of energy.

In the absence of the crystal field effects and for the orbitally degenerate d-states the density of states, resulting from the virtual level is obtained as follows:-

$$\rho_d^{\sigma}(E) = \frac{21+1}{\pi} \cdot \frac{\Delta}{(E-E_{d\sigma})^2 + \Delta^2} \qquad (I.21)$$

Where (21+1) arises from the orbital degeneracy in absence of crystal field effects and Δ is the half width of the virtual level. The condition for the quenching of the orbital moment is given by

$$\rho_m^{\sigma}(E_F)(I-J) < 1 \qquad (I.22)$$

and the condition for the appearance of localised moments is found, in the same way as for the case of a single orbital, to be:-

$$(I+4J)\,\rho_m^{\sigma}(E_F) > 1 \qquad (I.23)$$

In (I.21) and (I.22) $\rho_m^{\sigma}(E_F)$ is the added density of states per orbital.

4. Wolff - Clogston Model

Shortly after Anderson, Wolff (8) proposed a model for the occurence of localised moment in alloys. A similar approach was made by Clogston (9). In this model the impurity is represented by a localised potential V_p, which gives rise to a resonance scattering of the conduction electrons of the host. The impurity electrons are assumed to be part of the conduction band. This resonance may be thought

to be created by a partially filled d-shell but no extra orbital is assumed as is done by Anderson. Let the unperturbed hamiltonian of the system be represented by H_o. Then the wave function in the perturbed system is given by:

$$\psi = \varphi_{k,m} + G_o V_P \psi \qquad \text{(I. 24)}$$

where $G_o(E\ ) = \eta \to o(E_m - H_o + i\eta)^{-1}$ is the Green's operator corresponding to H_o, and $\varphi_{k,m}$ is the wave function of the unperturbed system, m is the band index. At this point the following assumption are made.

(a) The perturbing potential does not mix states from different bands. i.e. one band only is considered. This implies that the perturbed wave function can be expanded in terms of the Wannier functions from a single band.

$$\psi = \sum_{R_i} U_\gamma(R_i)\, W_\gamma(r-R_i) \qquad \text{(I.25)}$$

where W is the Wannier function and γ is the index of the band considered.

(b) The only non-zero matrix element of V_p within one band is that taken between two Wannier functions on the impurity site. i.e. V_p is so strongly localised that the only existing term is

$$\langle W(r-R_o) | V_p | W(r-R_o) \rangle = V \qquad \text{(I. 26)}$$

Using the Green's function technique the following expression is obtained for the density of states per atom of the perturbed system

$$\rho(E) = \rho_o(E) + \frac{1}{N}\left[\frac{V^2 F'(E)\rho_o(E) + V\,[1-VF(E)]\rho_o'(E)}{[1-VF(E)]^2 + \pi^2 V^2 \rho_o^2(E)}\right] \qquad \text{(I. 27)}$$

where $F'(E)$ is the derivative of the function

$$F(E) = \frac{P}{N} \sum_{k} \frac{1}{E-E(k)} \qquad (I.28)$$

in which P indicates the principal value and $\rho_o(E)$ is the density of states per atom of the unperturbed host. N is the number of atoms in the crystal. If V is large enough the term in the large bracket may have a resonant character in the nighbourhood of $E = E_o$ for which

$$1-VF(E_o) = 0 \qquad (I.29)$$

Expanding $F(E)$ around E_o and putting the resulting expresion back into (I.27) one arrives at the following

$$\rho(E) \cong \rho_o(E) + \frac{1}{N} \frac{1}{\pi} \frac{\Delta(E)}{(E-E_o)^2 + \Delta^2(E)} \qquad (I.30)$$

where

$$\Delta(E) = \pi \frac{\rho_o(E)}{F'(E)} \qquad (I.31)$$

is the half width of the virtual state.

Depending on the strength of the potential introduced two things may happen:

(a) The perturbing potential is strong enough to capture a bound state. If this state lies outside the band considered then $\rho_o(E_o)=0$ and from equation (I.31) $\Delta \to o$. Hence one has:

$$\rho(E) = \rho_o(E) + \frac{1}{N} \delta(E-E_o) \qquad (I.32)$$

i.e. this state is a real bound state.

(b) The potential is such that the solution of (I.29) is in the band in question then equation (I.30) predicts a sharp peak at $E = E_0$ in the density of states. This is the virtual bound state in this model.

Wolff then goes on, assuming that a virtual level exists for which $F'(E) < 0$, to consider the effect of adding a spin dependent potential δV_σ to V_p. The potentials seen by spin up and spin down electrons are now $V + \delta V_\uparrow$ and $V + \delta V_\downarrow$. These lead to different amplitudes for the corresponding wave functions at the impurity site. These wave functions are then employed to calculate the change in the H-F field of the impurity. By requiring the change in the matrix elements of the H-F field to be equal to δV_σ for each spin direction the problem is made self consistent. The resulting equations are treated in much the same way as Anderson has done in his model and the criterion for the formation of moments for $\frac{\delta V}{V} \ll 1$ is derived. Here too it is found that polarisation arises from the Coulomb repulsion I between anti parallel spins.

This model is siutable for alloys between transition metals because the impurity electrons are assumed to have the same character as those of the host matrix.

5. The Effect of the Local Environment on the Magnetic State of an Impurity

The discussions of Friedel (1), Anderson (5) and Wolff (8) are confined to the simple case of a single impurity embedded in a sea of conduction electrons. Jaccarino and Walker (10) have considered the local environment effect on the state of an impurity due to the presence

of other impurities. As we have seen above, the condition for the existence of a localised moment depends on the width of the virtual state and its position with respect to the Fermi level. These two quantities are directly related to the density of states of the conduction electrons at the Fermi level. Clogstone et al (4) have shown that in Nb–Mo alloys containing 1 at %Fe the magnetic moment per iron atom appears to increase from $0\mu_B$ below 40 at %Mo to $2.2.\mu_B$ above 90 at % Mo. In this concentration range the density of states of iron free Nb–Mo alloys change smoothly as evinced from the susceptibility measurements of this system made by Clogstone et al (4). Therefore it is natural to associate this phenomena with the continuous change in the magnitude of the moment per iron atom. Jaccarino and Walker, however, argue that the magnitisation procedure is essentially a discontinuous one, the moments being either zero or having their full value.

The apparent continous change in the magnitude of the moment is then associated with the probability that individual impurities are magnetised due to the presence of some nighbouring impurities in certain configurations.

In the dilute limit Co is non magnetic in Rh. However in Rh–Pd alloys cobalt acquires a magnetic moment when the Pd concentration exceeds 5 at %. The magnitude of the moment per Co impurity increases with increasing amounts of Pd. In the NMR of Co^{59} however Jaccarino and Walker observe resonance up to at least 12.5 at % Pd, its intensity falling steadily. This behaviour implies that some of the Co atoms are not magnetised even well above 5 at % Pd.

The authors assume that a cobalt impurity will be magnetised if it has a certain number of nearest neighbour Pd atoms and calculate the probability of this event. They find that a Co atom is magnetic if it has at least two nearest neighbouring Pd atoms i.e. eleven or more Rh neighbours demagnetise the Co atoms.

Kim (11) has made a detailed study of the local environment effect on the state of an impurity. He shows that if the interaction among the impurities, between the host metal and the impurities and among the host metal electrons are properly taken into account, the Friedel-Anderson-Wolff condition for the occurence of the localised magnetic moment on an impurity exactly coincides with the condition for the onset of ferromagnetism in transition metal alloys. Anderson's model is extended here to the case of finite concentration. The resulting hamiltonian is treated in the H-F approximation using Greens function techniques.

The hamiltonian considered is:-

$$H = H_k + H_c + H_d + H_{dd} + H_{cd} + H_t \qquad (I.33)$$

where H_k is the one particle energy of the s-electrons and is the first term in the Anderson hamiltonian Eq (I.9). H_c is the hamiltonian representing the repulsive Coulomb energy of the host metal conduction electrons. The Coulomb interaction is assumed to be aδ function of strength v. H_d is the one particle energy, H_{dd} is the Coulomb repulsion of electrons on impurities:-

$$H_d = \sum_{i,\sigma} E_i^o d_{i\sigma}^+ d_{i\sigma}$$

$$H_{dd} = \sum_i U_i d_{i\uparrow}^+ d_{i\uparrow} d_{i\downarrow}^+ d_{i\downarrow} \qquad (I.34)$$

where $d^{+}_{i\sigma}$ is the creation operator for a d-electron at the i^{th} impurity. Here a one-band model is employed and the existence of different types of impurities is assumed. The suffix i on E_i means that E^{o}_{i} depends on the type of impurity. H_{cd} and H_t are the s-d mixing term and the direct transfer integral respectively

$$H_{cd} = \sum_{i,k,\sigma} \left(V_{ik} d^{+}_{i\sigma} a_{k\sigma} + V_{ik} a^{+}_{k\sigma} d_{i\sigma} \right)$$

$$H_t = \sum_{i,j,\sigma} T_{ij} d^{+}_{i\sigma} d_{j\sigma} \qquad \text{(I.35)}$$

where a^{+}_{k} is the creation operator for an s-electron and $V_{jk} = V_k e^{ikR_j}$. R_j being the position of the J^{th} impurity.

Treating the hamiltonian (I.33) within the HF approximation, Kim shows that the effect of the other impurities is to modify the width of an impurity state Δ^{o}_{i} i.e

$$\Delta_i = \Delta^{o}_{i} + \delta\Delta_i \qquad \text{(I.36)}$$

where Δ^{o}_{i} is the width of an impurity in isolation and $\delta\Delta_i$ is the change in Δ^{o}_{i} caused by the surrounding impurities.

The contribution to $\delta\Delta_i$ consists of three parts:-

$$\delta\Delta_i = \delta\Delta^{(1)}_{i} + \delta\Delta^{(2)}_{i} + \delta\Delta^{(3)}_{i} \qquad \text{(I.37)}$$

where $\delta\Delta^{(1)}_{i}$ comes from the indirect interimpurity interaction through the host metal conduction electrons. If one measures the energy from the Fermi level and employs a parabolic band then $\delta\Delta^{(1)}_{i}$ reduces to the following simple form:-

$$\delta\Delta^{(1)}_{i} = \frac{\Delta^{o}_{i}}{k_F^{2}} \sum_{J\neq i} \frac{\cos(2k_F R_{iJ})}{R_{iJ}^{2}} \qquad \text{(I.38)}$$

where $R_{iJ} = R_J - R_i$ and k_F is the Fermi wave-vector of conduction electrons. The oscilatory behaviour has the same origin as RKKY oscilation.

For a simple cubic lattice, taking into account nearest neighbours only, it becomes:-

$$\delta\Delta_i^{(1)} = 4Z_i \Delta_i^{o} \frac{\cos(2k_F d)}{(2k_F d)^2} \qquad (I.39)$$

where d is the interatomic distance and Z_i is the number of nearest neighbours to the i^{th} impurity. This expression can be positive or negative depending on the value of $2k_F d$.

The second contribution $\delta\Delta_i^{(2)}$ comes from the direct transfer interaction between impurities. For the simple case where the virtual level lies at the Fermi level it is given by:-

$$\delta\Delta_i^{(2)} = \sum_{J \neq i} T_{iJ}^2 \frac{1}{\Delta_J^o} \qquad (I.40)$$

If one assumes that $T_{iJ} = T$ for nearest neighbours and is zero otherwise, and further that $\Delta_J^o = \Delta^o$ independent of J, then one obtains

$$\delta\Delta_i^{(2)} = Z_i \frac{T^2}{\Delta^o} \qquad (I.41)$$

The third term is a cross term. Its magnitude is usually between $\delta\Delta_i^{(1)}$ and $\delta\Delta_i^{(2)}$. The author compares $\delta\Delta_i^{(1)}$ with $\delta\Delta_i^{(2)}$ and shows that for the alloys between transitional elements $\left|\frac{\delta\Delta_i^{(1)}}{\delta\Delta_i^{(2)}}\right|$ can

be greater or less than 1. If:-

$$\left|\delta\Delta_i^{(1)}\right| \gg \left|\delta\Delta_i^{(2)}\right| \text{ then } \delta\Delta_i \cong \delta\Delta_i^{(1)}$$

in this case $\delta\Delta_i$ may be negative as well as positive. Thus as in each case the effect of the third term is negligible, the influence of the local environment will be to change the width of an impurity state and the change may be in either direction.

Kim then goes on to consider the magnetic properties of the alloy at $T = 0^{\circ}K$.

His calculation leads to a prediction of an antiferromagnetic coupling between on impurity and the host metal conduction band when the host metal conduction band is almost half full, and to a ferromagnetic coupling otherwise.

It is also found that when the localised state is nearly half full, an antiferromagnetic coupling exists between two impurities and a ferromagnetic one otherwise.

For the susceptibility of the perturbed host electrons, and impurity, and of the set of impurities, a set of coupled equations is obtained. It is shown that all the three susceptibilities, if they diverge at all, diverge simultaneously at the same temperature or concentration. That is, the formation of localised moment on an impurity coincider with the long range ordering throughout the alloy.

The behaviour of pd-Ni, Cu-Ni and some such alloys is discussed within this model. An expresion for the critical concentration for ferromagnetism is derived and is related to the initial increase rate of the alloy susceptibility with the impurity concentration.

6. Localised Spin Fluctuations

The solution of the Anderson hamiltonian within the framework of the H-F approximation leads to a sharp boundary between magnetic and non-magnetic regions. This is because the above approximation excludes the dynamics of the problem.

This aspect of the localised moment problem has been considered by Rivier and Zuchermann (12) and Rivier et al (13). The transverse dynamical susceptibility $X_d(\omega)$ is closely connected to the spin fluctuation lifetime as follows (13), (14):-

$$X_d(\omega) = \frac{X_o(\omega)}{1-IX_o(\omega)} \cong \frac{g^2 \mu_B^2}{\frac{\pi}{T_{sf}} + i\omega\pi} \qquad (I.42)$$

where μ_B is the bohr magneton, g is the lande g factor and $X_o(\omega)$ is the susceptibility of d-states, when $I \to o$, and Tsf is the lifetime of the localised spin fluctuation given by:-

$$T_{sf} = \frac{\pi \rho_d(E_F)}{1-I\,\rho_d(E_F)} \qquad (I.43)$$

In the above expression it should be noticed that $X_d(\omega)$ is

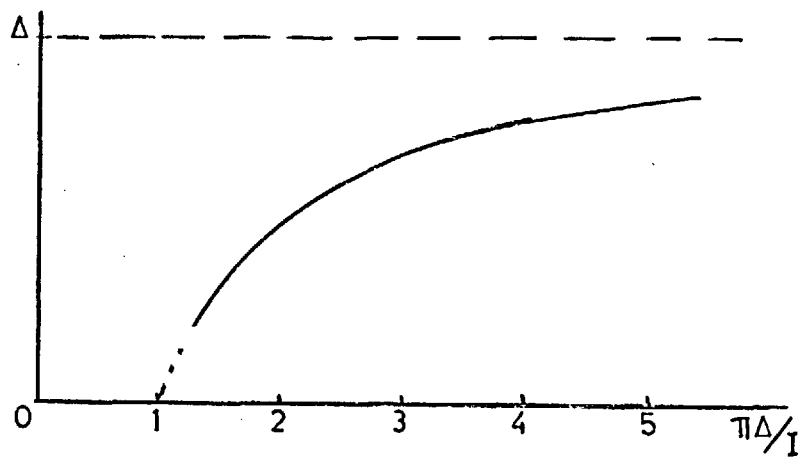

Fig (I.2)

The mean spin fluctuation frequency T_{sf}^{-1} as a function of $\pi\frac{\Delta}{I}$ for the case of virtual state at the Fermi level ($Ed=E_F$)

not dependent on q (hence not on position in real space) as the fluctuations are local. The spin fluctuation lifetime is temperature independent and is essentially a function of I and Δ see fig (I.2).

As I $\rho_d(E_F) \to o$ $T_{sf} \to \infty$ i.e. the spin (or magnetisation) lives a longer and longer life, but never infinite as derived in the H-F approximation. Hence the transition from non-magnetic state to magnetic state is not sudden as derived from Andersons model, but is a gradual process.

7. The s-d Exchange Hamiltonian

When a localised moment is formed it interacts with the conduction electrons via the exchange interaction. This is given by the so-called s-d exchange hamiltonian, in the derivation of which the moments are assumed to be well localised. In the case of a 3d-transition impurity in a metalic host however the moment is not so well localised and hence the validity of the "s-d" exchange model is questionable. Nevertheless when $I \gg \Delta$ this model should be applicable, as in this case a localised moment has a very long lifetime and hence one may assume that the moment is reasonably well defined. In its general form the s-d hamiltonian is given by:-

$$H_{s-d} = -\int J(r-R_n)\, S(R_n)\, \sigma(r-R_n)\, f(r-R_n, \theta, \varphi)\, d^3r \qquad (I.44)$$

where J is the strength of the interaction, S(Rn) is the impurity spin and Rn its position $\sigma(r-Rn)$ is the conduction electron spin density and f represents the spatial extent of the local moment.

The above hamiltonian can be written in the second quantised form as follows:-

$$H_{s-d} = -\frac{1}{N}\sum_{n,k,k'} J(k'-k)\, e^{i(k'-k)Rn}\Big\{(a^{+}_{k\uparrow}a_{k'\uparrow} - a^{+}_{k\downarrow}a_{k'\downarrow})S_n^{Z} + a^{+}_{k\uparrow}a_{k'\downarrow}S_n^{-} + a^{+}_{k\downarrow}a_{k'\uparrow}S_n^{+}\Big\} \qquad (I.45)$$

Where N is the number of atoms in the pure matrix, and $J(k-k')$ is the generalised exchange integral given by

$$J(k-k') = N\, e^{i(k-k')Rn}\int dr_1\, dr_2\, \phi^{+}_{k'}(r_1)\,\phi^{+}_{L}(r_2-Rn)\frac{e^2}{r_1-r_2}\,\phi_k(r_2)\,\phi_L(r_1-Rn) \qquad (I.46)$$

where ϕ_k and ϕ_L are the conduction electrons and impurity states respectively, $S_n^{\pm}$ are the rotational components of the impurity spin given by:-

$$S_n^{\pm} = S_x \pm iS_y \qquad (I.47$$

and S_n^{Z} is the Z component of the spin.

This hamiltonian was first derived by Kasuya (15) and has since been used extensively for the computation of the resistivity, polarisation of the conduction electrons etc. in alloys as will be shown later.

8. Relation of the Anderson Hamiltonian to the Hamiltonian of the s-d Exchange Interaction: The Schrieffer - Wolff Transformation

Both the Anderson and the Wolff theories apply at $T = 0^{\circ}K$. But it is known that experimentally a moment can exist only above a certain temperature T_K. Below this temperature the moment is quenched by the negatively polarised cloud of the conduction electrons as discussed by Nagaoka (16). Alternatively, one can think of the LSF as being fast or slow relative to the thermal fluctuation below and above the temperature $kT_k = T_{sf}^{-1}$ (Rivier; private communucation).

The failure of the theories to account for this, stems again from the use of the H-F approximation. Where it is implicitly assumed that an electron on the impurity stays for such a short time ($T_{decay} = \frac{\hbar}{\Delta}$) that it does not feel the presence of the other spin state which introduces an interaction lifetime ($Tint = \frac{\hbar}{I}$). Thus $\frac{\hbar}{\Delta} < \frac{\hbar}{I}$ i.e. the H-F theory applies when $\frac{I}{\Delta} < 1$. This as we have shown is the non-magnetic limit.

The magnetic limit must be approached in an alternative way, but in this limit it has not been possible to treat the Anderson hamiltonian successfully. For example Scalapino (17) has calculated the magnetic susceptibility (chapter II) using the Anderson hamiltonian. His treatment lead, in the limit of weak s-d mixing, to a susceptibility which diverges below a certain temperature $T_o = \frac{W}{k_B} e^{1/I\rho(E_F)}$, where 2W is the width of the s band. In order to isolate that aspect of the hamiltonian which is responsible for this divergence Schrieffer and Wolff (18) have performed a canonical transformation in the limit of very weak s-d mixing, thereby eliminating V_{kd} to first order. By choosing an appropriate generating function S, they showed that the resulting hamiltonian contains an s-d exchange-like term with an exchange coupling parameter $J_{kk'}$ which at $T = 0^{\circ}K$ is given by:-

$$J_{k_F k_F} = 2 \left|V_{kd}\right|^2 \frac{I}{(I+E_d)} E_d \qquad (I.48)$$

where E_d is the energy of the spin up electron measured with respect to Fermi level. This represents an anti-ferromagnetic coupling between conduction electrons and localised moment because in this limit $E_d < 0$ and $(E_d + I) > 0$. In the above formula we took $k=k \simeq k_F$ since at $T=0^{\circ}K$ only the electrons at Fermi level are effective.

This antiferromagnetic coupling between s-and d-electrons was pointed out earlier by Anderson (5) and Anderson and Clogston (19).

II. BASIC INTERACTION MECHANISMS BETWEEN SOLUTE ATOMS

An impurity in a metallic host may present one, or simultaneously two types of potential to the host conduction electrons, depending on whether it is a simple solute or has a magnetic moment. In the latter case apart from the ordinary potential scattering the electrons are scattered through exchange scattering, giving rise to the polarisation of the conduction electrons. This polarisation will interact with a second impurity when it is not too far from the first, thus providing a coupling mechanism between two impurities.

There are essentially two models describing this coupling. The earliest is based on the s–d exchange model. The more recent is based on the Anderson model.

1. The Interaction Based on the s–d Exchange Model: The RKKY Interaction

A pure metallic host may be represented by a hamiltonian diagonalised to the following form:–

$$H_o = \sum_{k\sigma} E_k a^+_{k\sigma} a_{k\sigma} \qquad (I.49)$$

where $a^+_{k\sigma}$ and $a_{k\sigma}$ are the usual creation and destruction operators and E_k is the energy of a single electron in state k. Addition of an impurity with a localised spin S perturbs the host metal. The magnetic part of this perturbation which concerns us here, is given by the s–d

exchange hamiltonian introduced earlier [eq.(I.45)]. The diagonal part of this hamiltonian is:-

$$-\frac{1}{N}(n^{+}-n^{-})\,J(0)\sum_{n} S_{n}^{Z} \qquad (I.50)$$

where S is the impurity spin, N is the total number of atoms in the lattice, n^{+} and n^{-} are the total number of electrons with spin up and spin down and J(0) is the exchange integral for k=k'

This energy may be considered to represent an effective field acting on conduction electrons polarising $\sigma = \frac{1}{2}(n^{+}-n^{-})$ electrons. As a consequence of this a change in the kinetic energy of the electrons will take place. This is given by $\frac{E_F}{6n}(n^{+}-n^{-})^2$ where 2n is the total number of conduction electrons.

The total change in the energy of the system is the sum of the two terms, which is:-

$$\Delta E_{tot} = \frac{E_F}{6n}(n^{+}-n^{-})^2 - \frac{J(0)}{N}(n^{+}-n^{-})\sum_{n} S_{n}^{Z} \qquad (I.51)$$

The change in energy is minimum when $\frac{d\Delta E_{tot}}{2\,d\sigma} = 0$ leading to:-

$$n^{\pm} = n \pm \frac{3n}{2E_F N} J(0) \sum_{n} S_{n}^{Z} \qquad (I.52)$$

This polarisation is uniform, therefore by hypothesis a second impurity anywhere in the metal will, through this polarisation, be alligned parallel to this. This was suggested by Zener (20) to be responsible for the ferromagnetism of some of the transitional metals.

The exchange parameter J is small compared to the conduction band Fermi energy (e.g. $\frac{J}{E_F}$ 0.03 for Cu-Mn). Therefore one would expect to get reasonable results for various physical properties from lowest order perturbation calculations. But the first order perturbation correction gives, as we have seen, a uniform polarisation. However, the effect of

the uniform spin polarisation of the conduction electrons has not been observed experimentally.

Yosida (21) starting from the first order perturbed wave function has calculated the polarisation of the conduction electrons to second order in J. Assuming a spherical Fermi surface for the conduction electrons, the author calculated the perturbed wave function of electrons for each spin direction and obtained for the density of up and down spins the following expression:-

$$\rho_{\pm}(r) = \frac{n}{V} \pm \frac{3n}{8E_F} \frac{2}{NV} \sum_{q,n} J(q) f(q) S_n^Z \cos q\,(r-R_n) \qquad (I.53)$$

where:-

$$f(q) = 1 + \frac{4k_F^2 - q^2}{4k_F q} \ln \left| \frac{2k_F + q}{2k_F - q} \right| = 2 \frac{X_o(q)}{X_o(0)} \qquad (I.54)$$

here $X_o(q)$ is the q dependent susceptibility of a non interacting gas and $X_o(0)$ is its value at $q \to 0$. At this stage putting $J(q) = J(0)$ (which amounts to a zero range δ function interaction between local moment - conduction electron spins) the author simplifies Eq (I.53). However the resulting expression diverges at $r \to R$ due to this approximation. {which oscillate as $1/r^3$,

Yasida then makes the following approximation:-

$$\begin{aligned} f(q)\, J(q) &= f(0)\, J(0) \quad && \text{for } q < 2k_F \\ f(q)\, J(q) &= 0 && \text{for } q > 2k_F \end{aligned} \qquad (I.55)$$

and obtains for the spin density the following expression which is finite at r->Rn.

$$\rho_{\pm}(r) = \rho_o \left[1 \mp \frac{3\,6\,n}{E_F} \frac{J(0)}{N} \sum_n 2k_F |r-R_n|\, F[\, 2k_F |r-R_n|\,] \right] S_n^Z$$

(I.56)

where $\rho_o = \frac{n}{V}$ is the average spin density in the host and the function F(X) is given (with $X = 2k_F |r-R_n|$) by

$$F(X) = \frac{X \cos X - \sin X}{X^4} \qquad (I.57)$$

The polarisation given by (I.56)is concentrated in the neighbourhood of the impurity and has a long range oscilatory effect outside the impurity cell decreasing with $\frac{1}{r^2}$. The same function was obtained by Rudemann and Kittel (22) in the calculation of the indirect interaction between two nuclei via their hyperfine interaction with conduction electron sea. Therefore it is known as the R K K Y spin polarisation.

In this model there will be an interaction between two impurities via this polarisation if they are not well separated. The interaction energy is given by:-

$$E(R) = 6\pi Z^2 J^2 \rho(E_F) F(2k_F R) \bar{S}_1 \bar{S}_2 \qquad (I.58)$$

where Z is the number of conduction electrons per atom, S_1 and S_2 are the spins of the first and second impurities respectively.

The R K K Y spin polarisation is derived assuming that the conduction electrons of the host have an infinite mean free path. In actual cases it will be modified by all the scattering mechanisms.

2. Interaction Based on Anderson's Model: Caroli

An interaction mechanism between magnetic impurities in normal metals basedon s-d mixing, has been cosidered by Caroli(23).He considers two impurities separated by a distance R which couple through two consecutive resonant scatterings of conduction electrons.

The total wave function of a conduction electron of spin scattered by an impurity is given at a large distance R by:-

$$\psi_k^\sigma(R) \simeq e^{ikr} + \frac{e^{i(kR+\eta_1^\sigma)}}{kR} \operatorname{Sin}\eta_1^\sigma \qquad (I.59)$$

where η_1^σ is the phase shift in the conduction electron wave function caused by the potential of the first impurity. This state then mixes with virtual d-level of the second impurity via its potential V_2 as in the Anderson model but now the matrix element $\langle k | V_2 | d_2 \rangle$ is replaced by $\langle \psi_k^\sigma | V_2 | d_2 \rangle$ which is:-

$$\langle \psi_k^\sigma | V_2 | d_2 \rangle = \langle k | V_2 | d_2 \rangle \left[e^{ikR} + \frac{e^{i(kR+\eta_1^\sigma)}}{kR} \operatorname{Sin}\eta_1^\sigma \right] \qquad (I,60)$$

where $\langle k | V_2 | d_2 \rangle$ is the matrix element of the H-F field of the second impurity taken between s and d-electron states.

Using Anderson's Greens function formalism Caroli calculated the asymptotical form of the interaction energy between two non-degenerate virtual bound states within the H-F approximation. This is given at $T = 0^\circ K$ by:-

$$E_{in}(R) \simeq \frac{E_F}{\pi} \sum_{\sigma = \pm} \operatorname{Sin}\eta_1^\sigma \operatorname{Sin}\eta_2^\sigma \frac{\operatorname{Cos}(2k_F R + \eta_1^\sigma + \eta_2^\sigma)}{(k_F R)^3} \qquad (I.61)$$

The final expression for the interaction energy after level degeneracy is taken into account is:-

$$E(R) - \frac{(2l+1)^2}{\pi} E_F \sum_\sigma \operatorname{Sin}\eta_1^\sigma \operatorname{Sin}\eta_2^\sigma \frac{\operatorname{Cos}(2k_F R + \eta_1^\sigma + \eta_2^\sigma)}{(k_F R)^3} \vec{u}_1 \vec{u}_2 \qquad (I.62)$$

where $\vec{u}_1$ is the unit vector in the direction of the moment on the impurity at R_i. This formula is valid only when $k_F R > 1$ and $k_F R > \frac{E_F}{\Delta}$ Δ being the width of the virtual level. For the range $1 < k_F R \lesssim \frac{E_F}{\Delta}$

the formula takes a very complex form.

Blandin (24) and Blandin and Friedel (25) have proposed a hybrid model of interaction between magnetic impurities in dilute alloys of 3 d elements with simple metals to explain peculiarities shown by such alloys as Cu-Mn.

When a virtual bound state is split, the impurity presents different spin dependant scattering potentials to incoming conduction electrons. If the exchange interaction between conduction electron-spin on the impurity is taken to be of the form $H = -2J(r)S_c\ S_{im}$ then spin-up and spin-down conduction electrons see $V(r) - J\ S_{im}$ and $V(r) + J\ S_{im}$ potentials respectively. This gives rise to a spin density oscillating in sign. At large distances this is given by:-

$$\vec{\rho}(r) = -\frac{5}{8\pi^2}\sum_{\sigma=\pm}\sigma\ \mathrm{Sin}\eta^{\sigma}\ \frac{\mathrm{Cos}\ (2k_F r + \eta^{\sigma})}{r^3}\ \vec{n} \qquad (I.63)$$

where η^{σ} is the phase shift of the scattered conduction electrons with spin σ and $\vec{n}$ is a unit vector in the direction of impurity moment.

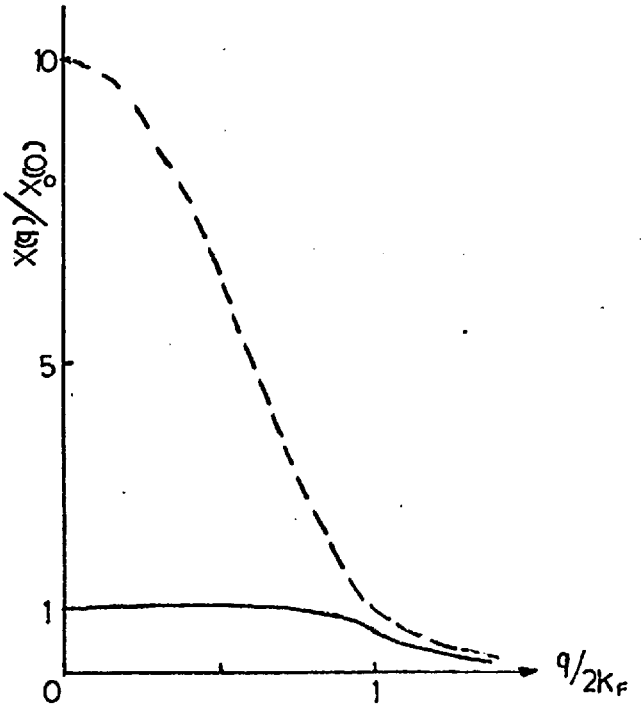

Fig (I.3): The normalised q-dependent susceptibility of an electron gas. The solid curve is drawn for no electron-electron interaction. The dashed curve represents the case $IN(E_F) = 0.9$

An impurity at position R_i induces a spin polarisation $\sigma(r-R_i)$ at r. Assuming a δ function interaction between $\sigma(r-R_i)$ and a second impurity S_J at R_J one has:-

$$E(R_{iJ}) = -2J(0)\sigma(R_J-R_i)\, S_J(R_J) \qquad (I.64)$$

Using (I.63) the interaction between two impurities separated by a distance R via polarised conduction electrons is found to be given by:-

$$E(R) = \frac{15}{S_i}\,\frac{J(0)}{4}\,2\sum_{\sigma}\sigma\,\mathrm{Sin}\eta^{\sigma}\,\frac{\mathrm{Cos}(2k_FR+\eta^{\sigma})}{(Rk_F)^3}\,\vec{S}_i\vec{S}_J \qquad (I.65)$$

where k_F is defined in terms of atomic volume Ω i.e. $k_F^3 = 3\pi^2 Z$ and Z is the number of electrons per atom.

Caroli has compared the strength of the interaction mechanisms discussed above for Cu-Mn alloys for which J = 0.2eV, $E_F \simeq 7$eV, and Z = 1 is assumed. Supposing a Mn atom is in the state Mn^+ and a moment of $4\mu_B$ is associated with each atom, then one has:-

$$n^+ - n^- = 4, \text{ and } n^+ + n^- = 6 \text{ giving } n^+ = 5,\ n^- = 1$$

The phase shift $\eta^{\pm}$ are related to n^+, n^- the numbers of spin-up and spin-down electrons respectively by the Friedel sum rule $n^{\pm} = \frac{1}{\pi}\sum_1 (2l+1)\eta_l^{\pm}$ giving $\eta^+ = \pi$ and $\eta^- = \frac{\pi}{5}$. Taking S = 2 one obtains:-

$$E_{RKKY} \cong 8.10^{-2}\,\frac{\mathrm{Cos}\,(2k_FR)}{(k_FR)^3}\,\bar{U}_1\bar{U}_2(\mathrm{eV}) \qquad (I.66)$$

$$E_{B-Friedel} \cong 9.10^{-1}\,\frac{\mathrm{Cos}\,(2k_FR+\frac{\pi}{5})}{(k_FR)^3}\,\bar{U}_1\bar{U}_2(\mathrm{eV})$$

$$E_{Caroli} \cong 10 \frac{\cos\left(2k_F R + \frac{2\pi}{5}\right)}{(k_F R)^3} \bar{U}_1 \bar{U}_2 (eV) \qquad (I.67)$$

The strength of each interaction mechanism increasing by an order of magnitude.

In the case of rare earth solute atoms the mixing V_{kf} is very small and hence the RKKY mechanism is dominant. The strength of interaction depends naturally on the type (of shell) of magnetic impurities.

MODIFICATION OF THE RKKY INTERACTION

1. The Effect of the Exchange Enhancement

In the derivation of the expression for RKKY spin polarisation the host conduction electrons are assumed to be non-interacting. In the case of a matrix where the susceptibility is enhanced, this expression is no longer valid. The exchange enhancement, which is due to the strong interaction between the itinerant electrons of the metal, reders it easily magnetisable. Therefore a magnetic impurity which may be thought of as an effective field, polarises the host metal electrons easily. This polarisation has a long range and does not oscilate over a large distance. For Pd containing Fe, Law and Holden (26) found no oscilation within a diameter of 10$\mathring{A}$ centred around the Fe impurity. This easy polarisation and its long range, is the origin of the giant moments observed in the exchange enhanced hosts. Where a magnetic moment per impurity, much larger than that expected from the impurity in a metallic host, is found.

This phenomenon has been explained by Wolff (27) and Giovanini et al (28). Wolff calculated the host Pauli spin susceptibility in the random phase approximation including the interaction between electrons which is assumed to be a δ function of strength V and found:-

$$X(q) = g^2 \mu_B^2 \frac{\rho(E_F)\, f\left(\frac{q}{2k_F}\right)}{1-\rho(E_F)\frac{V}{2} f\left(\frac{q}{2k_F}\right)} \qquad (I.68)$$

where $f\left(\frac{q}{2k_F}\right)$ is given by (I.54). As a result of the enhancement X(q) is enhanced for all q's, however the enhancement is much greater for small values of q. For very large enhancement X(q) may be expanded in q giving:-

$$X(q) = \frac{X_o(0)}{1+\left(\frac{q}{K}\right)^2} \qquad (I.69)$$

where K is a constant. Hence, at low q value X(q) has a Lorentzian shape fig (I.3).

The spin polarisation is given by :-

$$\sigma(r) = \frac{1}{g\mu_B} \sum_q H(q)\, X\,(q) e^{iqr} \qquad (I.70)$$

where H(q) is the F·T of the effective field seen by conduction electrons, due to impurity. If the impurity moment-conduction electrons interaction is taken to be δ function s-d interaction then H(q) may be shown to be $H(q) = \frac{J}{g\mu_B} \langle S^Z \rangle$ where J is the exchange interaction constant and $\langle S^Z \rangle$ is the average value of Z component of the impurity spin Substituting H(q) into σ (r) one obtains:-

$$\sigma(r) = \frac{J \langle S_Z \rangle}{(g\mu_B)^2} \sum_q X(q) e^{iqr} \qquad (I.71)$$

As the ferromagnetic transition is approached X(q) peaks strongly at lower value of q and hence the range of $\sigma(r)$ gets longer. At the same time the amplitude of RKKY increases and its first zero is pushed further, covering in some cases a large number of surrounding host atoms. This is the origin of giant moments in the exchange enhanced metals such as Pd.

Due to interaction between these giant moments the alloys of exchange enhanced metals are usually ordered in very dilute limit.

Although the transitional metals Fe; Co and to a lesser extent Mn in Pd induced giant moments, no such effect is produced by the rare earth impurities where the magnetic moment per atom is found to be the value expected from free ion of rare earth solute. This phenomenon seems to be closely connected to the mixing of the host conduction electrons and the localised electron state.

2. The Effect of Approximations Made for J(k,k′) on the RKKY Spin Polarisation

The RKKY spin polarisation is very sensitive to the form of exchange coupling constant J(q). Below, the discussions concerning this quantity are reviewed.

Overhauser (29) has considered the exchange interaction between a localised spin S_i at R_i and the spin polarisation density of the electron gas $\vec{p}(r)$ in which the impurity is embedded. This coupling is represented by:-

$$H_i = - F(q)\ \vec{S}_i \cdot \vec{P}(R_i) \qquad (I.72)$$

Here F(q) is the coupling parameter approximated by the atomic form

factor of the solute:-

$$F(q) = \int e^{i(\underline{k}-\underline{k}')\vec{\rho}} \left| \phi_d(\vec{\rho}) \right|^2 d^3\vec{\rho} \qquad (I.73)$$

where $\rho = (r-R_i)$ and ϕ_d is the state function of the localised spin. This is the spatial F-Transform of the local moment distribution. $F(q)$ is obtained from the exchange interaction parameter $J(k,k')$ given by (I.46), when considering a strong screening of the Coulomb potential i.e. approximating it by a δ function.

The form factor approximation of the exchange coupling parameter leads to a spin polarisation which differs from that obtained from the RKKY theory as shown by Watson and Freeman (30).

Watson and Freeman have investigated quantitatively the exchange coupling constant $J(k,k')$ between conduction electrons and localised magnetic electrons for a range of k, k'. The O.P.W (orthogonalised plane waves) are employed to represent the counduction electron states and the localised moments are taken to be the $4f^7$ and $3d^5$ shells of Gd^{3+} and Fe^{3+} respectively.

The RKKY theory is then employed with and without an exchange enhanced susceptibility. In the case of Gd^{3+} it is found that the approximation $J(\underline{k},\underline{k}') = J(\underline{k}-\underline{k}')$ is well justified as is expected for a short range interaction. However for Fe^{3+} this approximation is found not to be too good. The bulk of the spin polarisation is found to be not on the impurity, but approximately two atomic units away from it in contrast to the RKKY prediction. However the same asymptotical oscilatory behaviour is observed.

3. The Effect of the Magnetic State of the Host on RKKY Spin Polarisation

Kim and Schwartz (31) have considered the effect of the magnetisation of the host on the range of spin polarisation about an impurity. In their calculation a simple non-degenerate band and a δ-function electron-electron interaction is assumed. They found that range is longest for very small value of the host metal relative magnetisation $\zeta = \frac{n^+ - n^-}{n^+ + n^-}$. In the limit of $\zeta = 1$ (an example of this is Ni where at $T = 0^{\circ}K$ one spin direction of holes is completely full while the other is empty) the spin polarisation is found to be the same as the simple RKKY term.

III. SOME FORMS OF ORDERING

1. Introduction

The interaction mechanisms discussed earlier, i.e. RKKY, Caroli (23), Blandin and Friedel (25), describe the exchange coupling between localised spins via conduction electrons. These therefore constitute what is known as indirect exchange. This type of exchange mechanism is operative in metals and alloys with localised moments.

In the transition metals and the alloys between them, the coupling occurs mostly via the exchange between itinerant electrons.

These interaction mechanisms lead to various forms of ordering. These include, what are called spin glasses (of which Cu-Mn is a typical example), long and short range ordering, and various forms of complex spin structure usually seen in rare earth metals.

Below we discuss the types of ordering which are directly related to the alloy systems studied here.

2. Spin Glasses

The common feature of the RKKY interaction and those proposed by Caroli (23) and by Blandin and Friedel (25) is that they oscillated like $\cos(2k_F R + \eta)/(k_F R)^3$ with a wave vector $2k_F$. The wave length of this oscillation is small ($2k_F d \cong 6.92$ for Au, Ag or Cu, where d is the distance between first neighbours.) For dilute alloys the distance between impurities is very large therefore the coupling energy has the same probability of being negative as positive. The moments on the impurities therefore take random orientations at low temperatures. For perfectly disordered dilute alloys of simple metals with transition metal impurities this leads to a sort of ordered state at $T=0^{\circ}K$ in which all the spins are frozen out with no visible regularity.

At high temperatures this state is broken-up by thermal agitations leading to a set of localised moments giving a Curie-Weiss like susceptibility. These types of alloys have been called spin glasses by Prof. Coles.

Marshall (32) has proposed a model, based on the RKKY interaction between manganese ions in noble metals, to account for the behaviour of the excess specific heat of dilute Cu-Mn (33) and Ag-Mn (34) alloys which at low temperatures show a linear temperature dependence independent of solute concentration. He assumes for simplicity that as the alloys are cooled down all spins in the system are oriented parallel or antiparallel to a certain direction $\vec{oz}$. Within this Ising model the effective field seen by a manganese impurity, due to all other impurities, has a probability distribution $p(H,T)$, where $p(H,T)dH$ is the probability that a manganese atom is in a field lying between H and H+dH at temperature T. Marshall's calculation shows that $p(H.T)$ is a Lorentzian having a suitable cut-off limit and a width proportional to concentration. At low temperatures it has a double peak symetrically placed around $p(0,T)$. The minimum at this point was shown later by Klein and Brout (35) to arise from the strong correlations between spins that are close together.

Klein and Brout have developed a statistical theory of the interactions between inpurity spins of very dilute Cu-Mn-like systems. Their detailed analysis, again employing an Ising model for impurity spin system, confirms Marshall's findings. They write down the partition function for a single spin in terms of the probability distribution of the effective field $p(H)$ seen by an impurity moment at some origin due to all other randomly distributed spins in the crystal. To find $p(H)$ they first neglect correlations between impurity spins and assume that the impurities could take up a continuous range of distances from the one located at the origin. In this approximation the authors show that

the distribution function p(H) is a Lorentzian with a width proportional to concentration.

When imposing the condition that no two impurities may come closer than a certain minimum distance r a Gaussian form for p(H) is obtained, again having a width proportional to concentration. To get correction to the distribution function, the authors then consider the two-spin correlation function $\langle S_i S_j \rangle$. They expand the partition function in powers of concentration, perform averages over spins and spatial configurations and thereby obtain the mean free energy of the total system. This procedure at T=0°K and in very dilute limit leads to the break-up of the spin system around an impurity into two regions.

(1) The region within some correlation radius Rc from a certain spin i. Any other spin J within this region is correlated to spin i. The strength of correlation depends on the distance r_{ij} between them.

(2) The rest of the crystal volume for $r_{ij} > R_c$ in which any spin J is weakly correlated to i.

Thus at T=0°K the field experienced by a spin i at certain origin is the sum of the contributions from the two regions. i.e.

$$H_T = H_1 + H_2 \qquad (I.74)$$

The probability distribution of the total field $p(H_T)$ is the convolution of the distributions $p(H_1)$ and $p(H_2)$.

For a Cu-1.8 at % Mn alloy the distribution for the total field $p(H_T)$ is computed and $p(H_T=o)$ is found to be inversely proportional to the concentration in agreement with Marshall's theory.

Klein and Brout's statistical model is applicable to very dilute alloys at T=0°K.

Liu (36) has proposed a model extending Marshalls idea to cover higher temperatures and more concentrated alloys $c \geq 1$ at %. This model is phenomenological and based on self-consistent postulates in analogy with Weiss molecular field model. Therefore Liu makes the assumption that the most probable value of the effective field is temperature dependent and decreases with increasing temperature. This is the main point of disagreement between this model and the theory of Klein and Brout where calculations show that the most probable field shifts to higher values as the temperature is increased. The author takes the distribution function to be of the following form:-

$$p(H) = a\left[\frac{1}{(H-b)^2+C^2} + \frac{1}{(H+b)^2+C^2}\right] \quad \text{for } H < H_c$$

$$p(H) = o \quad \text{for } H > H_c \qquad \text{(I.75)}$$

where Hc is a cut-off value of the field. This function is given in Fig (I.4),

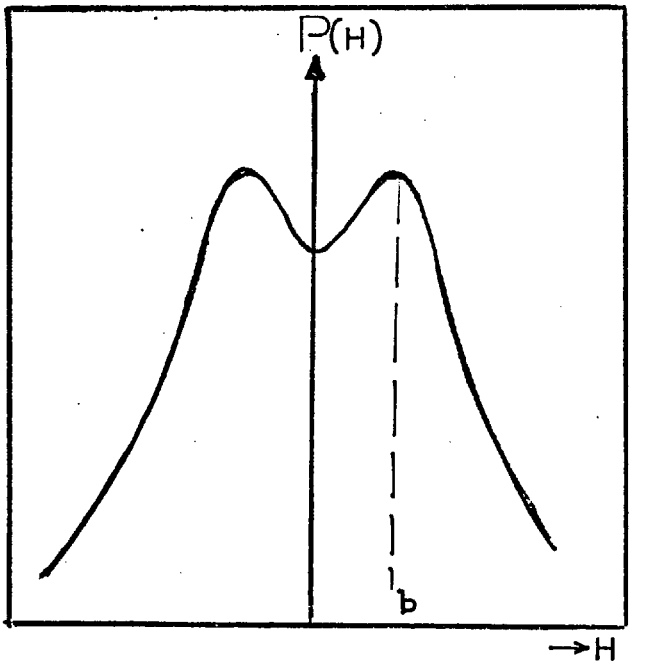

Fig (I.4)

where b represents the most probable value and C the width of the distribution and a is a normalisation constant.

By comparison with the Weiss theory where the magnitude of the molecular field decreases with increasing temperature the parameter b is assumed to be given by:-

$$b = b_o \eta \qquad (I.76)$$

where

$$\eta = \int_0^\infty p(H)dH \; B_s\left(\frac{H}{k_B T}\right) \qquad (I.77)$$

is the reduced average magnetisation per spin.

For dilute alloys Liu assumes b_o and C to be proportional to concentration and that the dependence is complicated for more concentrated alloys.

3. Long Range Ordering

The incomplete 3d shells of the first row transition series elements, play an important role in their magnetic properties. The 3d state functions of these elements are fairly localised and hence cannot overlap strongly with the wave functions of other atoms. This results in a narrow band with a high density of states. This, as we will see soon, is a decisive factor in determining the magnetic state of the transition metals.

There are two models attempting to account for their magnetic properties, the Heisenberg model and the band model. The latter assumes that the magnetic carriers are itinerant, their allowed states lying in a narrow band with a high density of states.

In the Heisenberg model it is assumed that the 3d electrons, which are responsible for the magnetic properties, are localised. The 3d shells of the transition metal atoms not being full, there is, according to Hunds rule, a net magnetic moment associated with each atom. In the case of an interatomic exchange interaction this gives rise to ferro-or antiferromagnetism. Otherwise the metal is paramagnetic. Some of the important results that can be derived from the Heisenberg model are given below:-

(i) The high temperature susceptibility is given, in the molecular field approximation, by the Curie-Weiss law.

(ii) In the ordered ferromagnetic state, at low temperatures, the elementary excitation 'spin waves' of the metal give the Bloch law:-

$$\frac{M(T)}{M(0)} \cong (1-aT^{3/2}) \qquad (I.78)$$

where M(0) is the saturation magnetisation and a is a constant.
The spin wave spectrum for long wave length is given by:-

$$\hbar\omega_q = Dq^2 \qquad (I.79)$$

where:

$$D(T) = D(0)\ (1-bT^{5/2}) \qquad (I.80)$$

and b is a constant.

(iii) At temperatures near Tc the susceptibility behaves as $(T-Tc)^{-\gamma}$. A recent estimate of the exponent γ is $\simeq$ 1.4 (37).

This model explains reasonably well the properties of magnetic transition metals Fe, Co and to some extent Ni as the following examples show.

At high temperatures the susceptibility of Fe and Co follow a Curie-Weiss law in agreement with the prediction of the model. At low temperatures the magnetisation of Fe, Co and Ni follows the Bloch law given by (I.78). The variation of D(T) is also in agreement with the prediction of the model.

At T$\cong$Tc the susceptibility behaves as $(T-Tc)^{-\gamma}$ with $\gamma \simeq 1.4$.

In Fe and Co the magnetic contribution to the electrical resistivity behaves in a similar way to rare-earth metals suggesting that the magnetic components of the resistivity have the same origin.

This model, however, cannot explain other properties of the transition metals some of which are given below

(i) The transition metals have a large electronic specific heat indicating the existence of a high density of states. This can be explained by the participation of the itinerant d-electrons which have a high state density.

(ii) The magnetic transition metals possess a permanent magnetic moment per atom which is not an integer number of Bohr magnetons. For Fe, Co and Ni this number is 2.2, 1.7 and 0.6 respectively. Such a non-integer number follows quite naturally from the band model.

(iii) Transport properties of the transition metals show that the d-electrons take part in the conduction mechanism.

The observed Bloch law in the magnetic transition metals Fe, Co and Ni can also be obtained from band model when including spin wave excitation.

From the above discussion it seems that a proper description of the transition elements should lie in between these two models. At present there seems to be agreement on this point. For this we refer to Herring (38).

Below, the Heisenberg and the itinerant electron model (band model) are described simply and briefly, and the effective field model is introduced via the Heisenberg model.

(a) The Heisenberg and the Effective Field Model

The origin of the effective field in a metal is the exchange interaction between electrons. This concept arises from the use of the determinantal wave functions of the Hartree-Fock (H-F) model. The need for a determinantal wave function arises, ofcourse, from the Pauli principle.

The determinant built up from electrons with parallel spins introduces the exchange term

$$J_{mn}^{iJ} = \langle \phi_{im}(1)\ \phi_{Jn}(2) \mid V_p \mid \phi_{im}(2)\ \phi_{Jn}(1) \rangle \qquad (I.81)$$

where i and J are the sites of atoms, 1 and 2 are the positions of the

electrons and Vp is the repulsive Coulomb potential between the two electrons. The inter-atomic terms ($i \neq J$) are much smaller than the intra-atomic ones ($i = J$) because of the small degree of overlap between atomic states on neighbouring atoms. The intra-atomic terms can be divided into two. The Coulomb term $I = J^{ii}_{mm}$ and the exchange term $J = J^{ii}_{mn}$. Their estimated magnitudes are I = 20eV and J = 1.ev respectively.

The simplest way of introducing the exchange energy is to consider the typical example of the hydrogen molecule (39)

If E_o is the energy of a hydrogen atom in isolation then the energy of the molecule is given by:-

$$E_s = 2E_o + (C+J)/(1+S^2)$$
$$E_{tr} = 2E_o + (C-J)/(1-S^2) \qquad (I.82)$$

Corresponding to the singlet and triplet states respectively where:-

$$C = \langle \psi_i(r_1)\psi_J(r_2) \mid V \mid \psi_i(r_1)\ \psi_J(r_2) \rangle$$
$$J = \langle \psi_i(r_1)\psi_J(r_2) \mid V \mid \psi_i(r_2)\ \psi_J(r_1) \rangle \qquad (I.83)$$
$$S = \langle \psi_i(r_1) \mid \psi_J(r_1) \rangle$$

Here C is the Coulomb integral, J the exchange integral, S is the non-orthogonality integral and V is the perturbing potential introduced when the atoms are brought together. The energy difference between the singlet and triplet states for small S is :-

$$\Delta E = E_s - E_{tr} \simeq 2J \qquad (I.84)$$

Thus if $J > o$, the triplet state is stable. Now if S is zero i.e. if the electrons are completely localised we can write the total energy of the system as

$$H = \text{Constant} \mp J_{12} \qquad (I.85)$$

for the triplet and singlet states respectively. Here J_{12} is the exchange integral for two elctrons having spins S_1 and S_2 on sites 1 and 2 respectively. Apart from some constant terms this can be written as:-

$$H_{12} = -2J_{12}\bar{S}_1\bar{S}_2 \qquad (I.86)$$

Because the eigen value of the operator $-2J_{12}\bar{S}_1\bar{S}_2 - \frac{\hat{I}}{2}J_{12}$ is $\mp J_{12}$ for the parallel and antiparallel spin configurations. Here $\hat{I}$ is the unit operator. Up to this point we have been dealing with the case of the hydrogen molecule where ofcourse $J < o$. The same approach applies to actual cases i.e. to magnetic electrons. Dirac (40) has shown that when taking the Pauli principle into account the spin dependent contribution to the energy due to exchange coupling between localised electrons in orthogonal orbitals may be written as

$$H = -\sum_{i<J} J_{ij}\bar{S}_i\bar{S}_J \qquad (I.87)$$

This hamiltonian is, known as the Heisenberg hamiltonian now.

Below we show how the above Hamiltonian is related to the molecular field model and describe the latter very briefly.

The basic assumption in the molecular field model is that the effective field is proportional to the average magnetisation of the metal i.e.

$$H_m = IM \qquad (I.88)$$

where I is the molecular field constant and M is the magnetisation. With certain approximations a formula of this type may be obtained quite readily from the Heisenberg Hamiltonian (I.87). To show this let us consider the coupling between nearest neighbours only. Then the single atom Hamiltonian, from (I.87), is:-

$$H_1 = -2JS_i \sum_{nn} S_J \qquad (I.89)$$

where it is assumed that J is the same for all nearest neighbours. If this Hamiltonian is replaced by an interaction between a molecular field and the atomic moment, such as:-

$$H_1 = -g\mu_B S_i H_m \qquad (I.90)$$

Then this field is given by:-

$$H_m = \frac{2J}{g\mu_B} \sum_{nn} S_J \qquad (I.91)$$

Where J is the exchange integral between two nearest neighbour atoms, Z is the number of nearest neighbour atoms and g is the Landé g factor. In (I.90) it is assumed that the atomic moment is $\vec{\mu} = g\mu_B \vec{S}$. This is justified for the 3d transition series elements, as in this series the angular momenta of each level is quenched. Now if we assume that each S_J can be replaced by its average value $\langle S_J \rangle$ then it is a simple matter to show that I is given by:-

$$I = \frac{2ZJ}{(g\mu_B)^2 N} \qquad (I.92)$$

When applying an external field H_a to the metal, the total field acting on an atom is:-

$$H_T = H_a + H_m = H_a + IM \qquad (I.93)$$

If one takes H_a in, say, $\vec{oz}$ direction then M and hence H_m lie in the same direction if the system is isotropic. The Hamiltonian of an atom in this field is:-

$$H = - g\mu_B S_z(H_a+IM) \qquad (I.94)$$

and has eigen values

$$E_m = - g\mu_B m(H_a+IM), \; m = -s, -s+1, \qquad s-1, s \qquad (I.95)$$

The reduced magnetisation of the atom is (41)

$$\frac{\mu(T)}{\mu(0)} = B_s\left[\frac{S_z g\mu_B}{k_B T}(H_a+IM)\right] = \frac{M(T)}{M(0)} \qquad (I.96)$$

where $\mu(0)$ is the saturation value of an atomic moment $\mu(0) = g\mu_B S_z$, $B_s(x)$ is the Brillouin function and M(0) is the saturation magnetisation of the crystal. If atoms are of the same sort then $M(0) = N\mu(0)$ where N is the number of atoms per cm^3.

The Curie temperature Tc, at which the spantoneous magnetisation disappears in the absence of an applied field, is easily obtained from this model. For high temperatures and not too large fields H_a, one has (dropping subscript of the spin).

$$B_s(x) \cong \frac{S+1}{3S} x = \frac{S+1}{3S} \cdot \frac{Sg\mu_B}{k_B T} (H_a + IM) \qquad (I.97)$$

hence putting $H_a = 0$

$$\frac{M(T)}{M(0)} = \frac{S+1}{3} \frac{g\mu_B}{k_B Tc} I M(T) \qquad (I.98)$$

giving:-

$$T_c = \frac{S+1}{3} \cdot \frac{g\mu_B}{k_B} \; I\, M(0) \qquad (I.99)$$

which may be shown to be proportional to the molecular field energy.

Above T_c the spontaneous magnetisation is small $\frac{M(T)}{M(0)} \ll 1$ therefore at high temperatures H_a is not negligible compared to H_m hence:-

$$\frac{M(T)}{M(0)} = \frac{S+1}{3S} \; \frac{g^S \mu_B}{k_B T} \cdot (H+IM(T)) \qquad (I.100)$$

giving:-

$$M(T)/_H = \chi = \frac{C}{T-T_c} \qquad (I.101)$$

with:-

$$C = \frac{1}{3k_B} (S+1)\, g\mu_B M(0) \qquad (I.102)$$

(b) The itinerant Electron model of ferromagnetism

This model has been the subject of many recent publications. An excellent review is given by Blandin (42), the most recent by Vogt (43). However we present here the approach originally made by Stoner and Wohlfarth (44).

This model makes use of the concept of energy bands in metals, the Fermi-Dirac statistics and a molecular field, to describe the interaction between carriers, assumed to be holes (3). It must be pointed out however that Fermi Dirac statistics are strictly valid only for the non-interacting particles.

Let $\zeta = \frac{n^+ - n^-}{n^+ + n^-}$ be the relative magnetisation at $T = 0^\circ K$. The molecular field model is brought into the theory by assuming a molecular

field energy per particle $dE_m = -k_B\theta'\zeta$. This energy per atom is then:-

$$E_m = -\frac{n}{2} k_B\theta'\zeta^2 \qquad (I.103)$$

where n is the number of holes per atom and θ' is a characteristic temperature. If $\zeta > 0$ then the spin up and spin down bands split. Fig.(I.5) and are then filled up to $E^{\pm}$ with

$$n^{\pm} = \frac{n}{2}(1 \pm \zeta) = \int_0^{E^{\pm}} \rho(E)\, dE \qquad (I.104)$$

where $\rho(E)$ is the density of states per atom per spin.

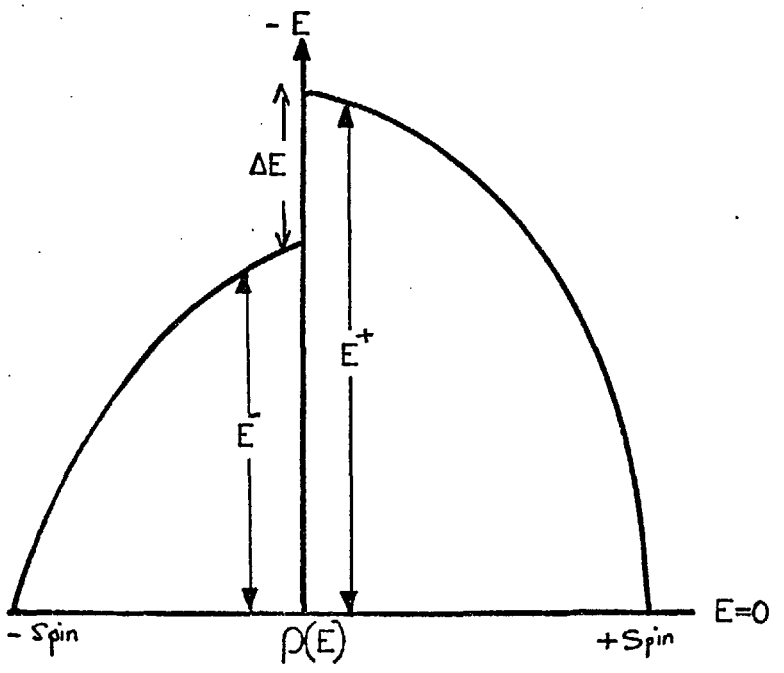

Fig (I.5)

The total energy per atom at T = 0°K is therfore

$$E(\zeta) = E_m + E_K = \int_{E_o}^{E^+} E\rho(E)dE - \int_{E^-}^{E_o} E\rho(E)dE - \frac{nk\theta'}{2}\zeta^2 \qquad (I.105)$$

Minimising $E(\zeta)$ with respect to ζ gives the so called exchange splitting

$$\Delta E = E^{+} - E^{-} = 2k_B\theta'\zeta \qquad (I.106)$$

This splitting exists if the total energy is minimum at a finite value of ζ. From (I.105) one has:-

$$\frac{d^2E(\zeta)}{d\zeta^2} = \frac{n^2}{4}\left[\frac{1}{\rho(E_F^{+})} + \frac{1}{\rho(E_F^{-})}\right] - nk_B\theta' \qquad (I.107)$$

Hence if $E'' < 0$ then $E(\zeta)$ has a maximum at $\zeta = 0$ leading to the so-called Stoner criterion for ferromagnetism at $T = 0^{o}K$.

$$\frac{2\rho(E_F)}{n}\, k_B\theta' > 1 \qquad (I.108)$$

The effect of the high density of states on the magnetic state of the metal is quite clear from this formula. i.e. The high density of states facilitates ferromagnetism.

Equation (I.108) can be written as follows:-

$$I\ \text{eff}.\rho(E_F) > 1 \qquad (I.109)$$

where $I\ \text{eff} = \frac{2k_B\theta'}{n}$

Although in the limit $I\ \text{eff}\,\rho(E_F) < 1$ the system is paramagnetic its susceptibility is now enhanced as:-

$$X = \frac{X_o(0)}{1 - \frac{I_{eff}}{2\mu_B^{2}} X_o(0)} = D\, X_o(0) \qquad (I.110)$$

where $X_o(0) = 2\mu_B^{2}\rho(E_F)$ and D is the enhancement factor. The latest estimate for D is $\simeq 10$ for Pd and 4 for Pt (45).

The generalisation of this formula to finite temperatures is given by:-

$$X(T) = \frac{X_o(T)}{1 - \frac{I_{eff}}{2\mu_B^{2}} X_o(T)} \qquad (I.111)$$

where:

$$X_o(T) = 2\mu_B^2 \int_0^\infty \rho(E) \left|\frac{df}{dE}\right| dE \qquad (I.112)$$

Here: f(E) is the Fermi-Dirac function. The Curie temperature is the temperature at which X(T) becomes infinite. Hence from (I.111) and (I.112) it is given by:-

$$I\ eff \int_0^\infty \rho(E) \left|\frac{df(T_c)}{dE}\right| dE = 1 \qquad (I.113)$$

In alloys, both $\rho(E_F)$ and I_{eff} depend on concentration. Hence the effect of $\rho(E_F)$ and I eff which determine the behaviour of alloys may be separated, at $T = 0^oK$, as follows:-

$$\frac{1}{X(C)} = \frac{1}{X_o(C)} - \frac{I_{eff}(C)}{2\mu_B^2} \qquad (I.114)$$

Thus increasing concentration alters I eff and $\rho(E_F)$, eventually the alloy may become magnetic.

CHAPTER II

THE THEORY OF THE ELECTRONIC PROPERTIES OF TRANSITION METALS AND ALLOYS

I. MAGNETIZATION AND SUSCEPTIBILITY

1. Introduction

At low temperatures low lying spin excitations play an important role in the electronic properties of magnetic and nearly magnetic metals and alloys. The simplest of these are the Stoner excitations. To describe them consider the ground state of a non-interacting electron gas. This may be represented by a solid Fermi sphere. When an electron is removed from within the Fermi sphere it leaves behind a hole. Such an excitation can be represented by the Fermi sphere plus an electron-hole pair. The pair excitations are divided into two: the spin-flip and the non spin-flip excitations. The former, which concerns us here, arises when an electron is transferred to a state outside the Fermi sphere with its spin direction reversed, and its wave vector changed by a certain (wave vector) q. This type of excitation is referred to as Stoner or spin-flip pair excitation.

In magnetic metals and alloys another type of excitation exists. This is the spin wave which is a collective excitation of the spin system.

A spin wave has a wave-vector q, and it represents a bound state of an electron-hole pair. The binding energy is, for small q, given approximately by the exchange splitting Δ of the electron sub-bands, Fig. (II.2). Spin waves are important at low temperatures as they contribute to the resistivity, magnetization and specific heat. They are true excitations and have well defined energies at low temperatures. In the strongly exchange-enhanced systems (e.g. Pd, dilute Pd-Ni alloys) a contribution to the electronic properties comes, apart from Stoner excitations, from the critical spin fluctuations (paramagnons). They have energies which lie in the band of the Stoner continuum, and hence they can decay into pair excitations. Therefore, they are not true elementary excitations. Their existence is indicated by a peak in the imaginary part of the susceptibility as will be shown below. The energies of the above excitations are obtained from the singularities in the imaginary part of the dynamic susceptibility. Therefore, we discuss below the susceptibility function for interacting and non-interacting systems. In each case we consider first the susceptibility in the static limit.

2. The Susceptibility of Non-Interacting Electrons

The bulk susceptibility ($\omega \to o$, $q \to o$) of a non-interacting electron gas is calculated in most textbooks (46). In an applied field H the energy levels of spin-up and spin-down electrons change as follows:-

$$E_{k\uparrow} = E_k - \mu_B H$$
$$E_{k\downarrow} = E_k + \mu_B H \qquad \text{(II.1)}$$

where E_k is the energy of a particle in the absence of the field and μ_B is the Bohr magneton. At $T = 0^oK$ the magnetization is obtained as:-

$$M = \mu_B \int_{\bar{\eta}_o - \mu_B H}^{\bar{\eta}_o + \mu_B H} \rho(E)\, dE = 2H \cdot \mu_B^2 \rho(E_F) \qquad \text{(II.2)}$$

from which the susceptibility is obtained as:-

$$\chi_o(T = 0) = 2\mu_B^2 \rho(E_F) \qquad \text{(II.3)}$$

where $\bar{\eta}_o$ is the highest occupied state in the presence of the field and $\rho(E)$ is the density of states per unit volume. Here it is assumed that $\mu_B H \ll \bar{\eta}_o \cong E_F$ the Fermi energy.

At finite temperatures and for not too large fields, the susceptibility is given by (47)

$$\chi = 2\mu_B^2 \int_o^\infty \rho(E) \left(-\frac{\partial f}{\partial E}\right) dE \qquad \text{(II.4)}$$

Here f is the Fermi function. Notice that as $T \to o$, $\left(-\frac{\partial f}{\partial E}\right) \to \delta(E - E_F)$ giving (II.3). For temperatures not too large the susceptibility is found from (II.4) to be given by (47),

$$\chi_o(T) = \chi_o(0)\left[1 + BT^2\right] \qquad \text{(II.5)}$$

where

$$B = \frac{\pi^2}{6} k^2 \frac{d^2}{dE^2} \log \rho(E_F) \tag{II.6}$$

(II.4) may be written as:-

$$\chi_o(T) = 2\mu_B^2 \sum_k \left[-\frac{\partial f}{\partial E} \right]_{E = E_k} \tag{II.7}$$

This expression may be obtained from:-

$$2\mu_B \sum_{q \to o} \frac{f(k)-f(k+q)}{E(k+q)-E(k)} \tag{II.8}$$

where E(k) is the kinetic energy of an electron. It can further be shown that the general q-dependent susceptibility is given by (48):-

$$\chi_o(q) = 2\mu_B^2 \sum_k \frac{f(k)-f(k+q)}{E(k+q)-E(k)} \tag{II.9}$$

This is the most general formula for the static susceptibility from which, as we tried to show above, the bulk susceptibility (q→o) at any finite temperature is obtained quite readily. $\chi_o(q)$ is, of course, the Fourier transform of the non-local susceptibility, and is the response to a spatially varying field. To find the single particle excitations use is made of the dynamic susceptibility.

For the computation of the dynamic susceptibility, $\chi(q,\omega)$, we refer to White (49). The imaginary part of $\chi(q,\omega)$ is given by:-

$$\mathrm{Im}\chi_{-+}(q,\ ) = \frac{4\pi\mu_B^2}{V} \sum_k f_\downarrow(q)(1-f_\uparrow(k+q)\delta\ (\hbar\omega - E(k+q)_\uparrow + E(k)_\downarrow) \tag{II.10}$$

where V is the volume of the crystal. The single particle excitations are given by the singularities of the δ function, i.e.,

$$\hbar\omega = E(k+q)_\uparrow - E(k)_\downarrow = 2\mu_B H + \left(\frac{k\cdot q}{m} + \frac{q^2}{2m}\right)\hbar^2 \tag{II.11}$$

This is shown in Eq. (II.1).

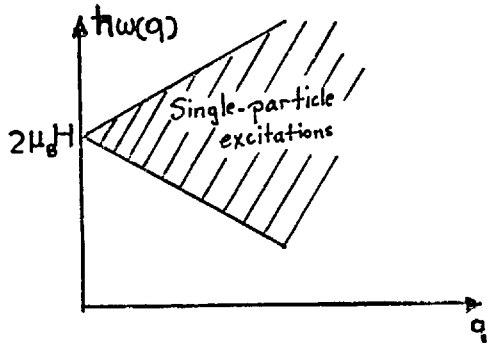

Fig. (II.1)

3. The Susceptibility of an Interacting Electron System

First we calculate the wave vector dependent susceptibility. The procedure is that of Anderson (50).

In an exchange-enhanced system the application of an external field induces an internal exchange field H_{ex} which is taken to be:-

$$H_{ex}(r) = \int I(r-R)M(R)dR \qquad (II.12)$$

where $I(r-R)$ is the exchange interaction between itinerant electrons and $M(R)$ the magnetization.

The total field is then given, in q space, by:-

$$H_T(q) = H(q) + H_{ex}(q) = I(q)M(q)+H(q) \qquad (II.13)$$

and, hence, using $M(q) = \chi_o(q)H_T(q)$

one arrives at:-

$$\chi(q) = \left| \frac{M(q)}{H(q)} \right| = \frac{\chi_o(q)}{1-I(q)\chi_o(q)} \qquad (II.14)$$

where $\chi_o(q)$ is given by (II.9)

This is the so-called exchange enhanced susceptibility and is derived with proper rigour by Wolff(27) in the RPA.

The dynamic susceptibility of an interacting electron gas is calculated, in the one band model, by Izuyama et al (51). It is given by:-

$$\chi_{\alpha\beta}(q,) = (g\mu_B)^2|F(q)|^2\bar{\chi}_{\alpha\beta}(q,\omega) \qquad (II.15)$$

where F(q) is the form factor of the Wannier functions and $\bar{\chi}_{\alpha\beta}(q,\omega)$ is the so-called "reduced susceptibility", α and β label the components of the susceptibility tensor. In the derivation of(II.15)the overlap integrals of Wannier functions and different sites are neglected.

For an isotropic system, in the absence of spin orbit coupling there are three components of the reduced susceptibility, namely $\bar{\chi}_{zz}$, $\bar{\chi}_{-+}$ and $\bar{\chi}_{+-}$.

Among these three components $\bar{\chi}_{-+}$ is the important one as its poles give the energy spectrum of the elementary excitations. It has been calculated in the RPA by Izuyama et al

$$\bar{\chi}_{-+}(q,\omega) = \frac{\Gamma(q,\omega)}{1-I\Gamma(q,\omega)} \tag{II.16}$$

where I is the intra-atomic exchange interaction and

$$\Gamma(q,\omega) = \sum_{k} \frac{f_{\uparrow}(k) - f_{\downarrow}(k+q)}{\bar{E}_{\downarrow}(k+q) - \bar{E}_{\uparrow}(k) - \hbar\omega} \tag{II.17}$$

Here $\bar{E}_{\sigma}(k)$ is the one particle energy modified by the exchange self energy.

There are two types of excitations in (II.76) which occur when $I\Gamma(q,\omega)=1$. This gives both spin wave and Stoner excitations. For the spin wave excitations the dispersion relation is, in the limit of small q, given by (51)

$$\hbar\omega(q) = Dq^2 \tag{II.18}$$

where D is a coefficient involving the Fermi function, number of particles, and the derivative of particle energies with respect to k. (II.18) leads, at low temperatures, to a deviation from the saturation magnetization given by:-

$$M = M(o)(1 - AT^{3/2}) \tag{II.19}$$

where M(o) is the saturation magnetization and A a constant. The energy spectrum of Stoner and spin-wave excitations is shown, for a weak ferromagnet, in Fig. (II.2)

Fig. (II.2)

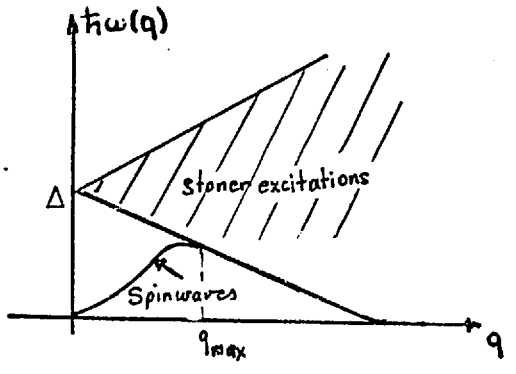

Paramagnons

In the parmagnetic region(II.16)reduces to the following:-

$$\chi_{-+}(q,\omega) = \chi(q,\omega) = \frac{\chi_o(q,\omega)}{1-I\chi_o(q,\omega)} \qquad \text{(II.20)}$$

where $\chi_o(q,\omega)$ is the susceptibility of a non-interacting electron gas. In the limit of $q\to o, \omega\to o$ (II.20) reduces to

$$\chi_s = \frac{\chi_s^o}{1-\bar{I}} \qquad \text{(II.21)}$$

where $\bar{I}=I\rho(E_F)$ and $(1-\bar{I})^{-1}$ is the Stoner enhancement factor. As $\bar{I}\to 1$ the system becomes unstable to a ferromagnetic transition. In the limit of $\bar{I}\to 1$ and for $\frac{\bar{\omega}}{\bar{q}} \ll 1$ and $\bar{q}=\frac{q}{k_F} < 2$ the imaginary part of $\chi(q,\omega)$ has been shown by Doniach (52) to be given by

$$\mathrm{Im}\chi(q,\omega) \cong \rho(E_F) \frac{\frac{\pi}{4}\frac{\bar{\omega}}{\bar{q}}}{\left[(1-\bar{I}) + \frac{1}{I^2}\bar{I}\bar{q}^2\right]^2 + \left(\frac{\pi}{4}\bar{I}\frac{\bar{\omega}}{\bar{q}}\right)^2} \qquad \text{(II.22)}$$

where $\bar{\omega} = \frac{\omega}{E_F}$. This function peaks at certain values of ω given by

$$\omega(q) \cong E_F \left(\frac{1-\bar{I}}{\bar{I}}\right) \frac{q}{k_F} \qquad \text{(II.23)}$$

These peaks define the so-called paramagnons. They are reasonably well-defined for small q's and in the limit of $\bar{I}\to 1$, ie. when approaching the ferromagnetic transition.

The life time of paramagnons is given by

$$\tau_p \cong \frac{1}{\omega(q)} \qquad \text{(II.24)}$$

as the width of the peak in $\mathrm{Im}\chi(q,\omega)$ is approximately proportional to $\omega(q)$. Hence, when $q\to o$ or better still $\bar{I}\to 1$, τ_p increases becoming infinite at $\bar{I}=1$ for which $\omega(q)\to o$.

4. Magnetic Susceptibility Due to Virtual Bound States

(a) Nonmagnetic Limit

Anderson[5] has calculated the susceptibility of an impurity in the non-magnetic limit. An enhanced paramagnetic susceptibility is obtained due to electron-electron interaction I on the impurity. For a 3d impurity with a single orbital, this is found to be:-

$$\Delta\chi = \frac{2\mu_B^2 \rho_d(E_F)}{1-I\rho_d(E_F)} \qquad \text{(II.25)}$$

where μ_B is the Bohr magneton and $\rho_d(E_F)$ is the additional density of states at the Fermi level introduced by the impurity. The condition for the impurity to be magnetic is given by the H-F Stoner condition

$$I\rho_d(E_F) > 1 \qquad \text{(II.26)}$$

The susceptibility contribution by an impurity with full orbital degeneracy has been calculated by Klein and Heeger (53). They find:-

$$\Delta\chi = \frac{2\mu_B^2 \rho_d(E_F)}{1-\frac{(I+4J)}{10}\rho_d(E_F)} \qquad \text{(II.27)}$$

where J is the exchange integral.

(b) Magnetic Limit

Scalapino (17) has derived an expression for the magnetic susceptibility due to the extra orbital of Anderson in the strong magnetic limit.

The mixing term $H_{kd}=\sum_{k\sigma}(V_{kd}a^{+}_{d\sigma}a_{k\sigma}+V_{dk}a^{+}_{k\sigma}a_{d\sigma})$ is treated as a perturbation, and the free energy of the system is obtained from the expansion of the partition function. The susceptibility is then calculated to the fourth order in H_{kd}. This is given by:-

$$\chi = \chi_p + \frac{\mu_B^2}{k_BT}\left[1 + \rho(E_F)J + (\rho(E_F)J)^2 \,\mathrm{Ln}\,\frac{k_BT}{W}\right] \qquad \text{(II.28)}$$

where χ_p is the temperature independent Pauli term, W is the half width of the conduction band, $\rho(E_F)$ is the state density of the conduction electrons, and J is an effective antiferromagnetic coupling between the localized state and the conduction electrons given by:-

$$J = \frac{2|H_{kd}|^2 I}{E_d(E_d+I)} \qquad \text{(II.29)}$$

this is a negative quantity for the case considered here.

The inclusion of higher order terms gives the final expression for χ as follows:-

$$\chi \cong \chi_p + \frac{\mu_B^2}{k_B T}\left[1 + \frac{\rho(E_F)J}{1-J\rho(E_F)\ell n(\frac{k_B T}{W})}\right] \qquad \text{(II.30)}$$

The susceptibility is singular for a certain temperature given by:-

$$T_D = \frac{W}{k_B} - \frac{1}{e|J|\rho(E_F)} \qquad \text{(II.31)}$$

5. The Susceptibility of Random Solid Solutions and of Rare Earth Metals and Alloys

The susceptibility of random solid solutions of some of the transition impurities in simple hosts shows a broad maximum at a certain temperature Tm. Well above this temperature the susceptibility usually fits a Curie-Weiss law. However, the Curie-Weiss temperature θ_c obtained from such an analysis is unrelated to the temperature where the magnetic ordering sets in. The interaction between the magnetic atoms in these alloys in the dilute limit and in rare earth metals and alloys is of the RKKY type. The susceptibility of these substances has been calculated in terms of the RKKY interaction energy.

Blandin and Friedel (25) have obtained a series expansion for the susceptibility per atom in powers of T^{-1} within the RKKY interaction.

The coefficient of T^{-2} gives the paramagnetic Curie temperature.

This is found to be given by:-

$$\theta_c = \frac{S(S+1)}{3k_B} \sum_{n \neq m} E(R_{iJ}) \qquad (II.32)$$

where $E(R_{iJ})$ is the energy of interaction between two impurity spins separated by $(\bar{R}_j - \bar{R}_i)$ in the RKKY model and is given by (I.58).

Performing an ensemble average over possible impurity positions Doniach (54) has found that the sum in this equation is given by:-

$$c\ E\ (q = o)$$

where c is the impurity concentration and $E(q = o)$ is the $q = o$ term of the Fourier transform of $E(R_{iJ})$. Thus the paramagnetic Curie temperature is given by:-

$$\theta_c = \frac{c}{3k_B}\ S(S+1)\ E(q = o). \qquad (II.33)$$

At low temperatures ($T < 100^{o}K$) and for very dilute alloys typified by Cu-Mn, Blandin and Friedel, employing a molecular field model find for Tm, the temperature of the susceptibility maximum, the following expression:-

$$Tm = \frac{4}{3k_B} NI\ c\mu_B^2\ S(S+1) \left[1 + \frac{S}{S+1}\ cZ \right] \qquad (II.34)$$

Here N is the number of sites (magnetic or nonmagnetic) per unit volume, I is the molecular field constant, c is the concentration of impurities and 2Z is the number of neighbouring atoms in the crystal. The agreement of (II.34) with experiments is claimed by the authors.

The case of rare earth metals and alloys has been considered by De Gennes (55). Neglecting the direct f-f overlap when dealing with pure metals, the paramgnetic Curie temperature is found to be given by

$$\theta_c = 3\pi z^2 (g_J - 1)^2 \Gamma^2\ J(\frac{J+1}{4k_B}) \sum_{J \neq i} E(R_{iJ}) \qquad (II.35)$$

where g_J is the Landé factor and J is the total angular momentum of an atom, Γ is the coupling parameter between the s and f electrons, and z is

the number of valence electrons per atom. For an ordered structure the sum over $E(R_{iJ})$ may be performed. For metals having hexagonal structure and 3 conduction electrons per atom, θ_c is found to be positive in accordance with experimental results for the heavy rare earth metals.

II. RESISTIVITY

1. Introduction

At temperatures very much less than certain characteristic temperatures T* (e.g. Debye, Curie, etc.) the ideal or temperature dependent part of the resistivity has a functional form which can help in some cases to identify the nature of the predominant scattering mechanism. For simple metals and alloys the main contribution comes from the scattering of electrons from phonons. But in transition metals and alloys two or more physically quite distinct mechanisms may lead to the same form of temperature dependence, in which case it is quite difficult to decide which one is the most important.

Below, after giving the formal transport theory briefly, we discuss basic scattering mechanisms and the form of temperature dependence they lead to, especially at low temperature.

2. Formal Transport Theory

We give here a brief derivation of a general relaxation time for scattering of conduction electrons from excitations such as phonons, spin waves and so on. In this we follow Jones (56).

Let us define a distribution function f(k,r,t) such that

$$(4\pi^3)^{-1} f(\vec{k},\vec{r},t)\ d^3k\ \ d^3r \qquad \text{(II.36)}$$

is the number of electrons in a volume $d\Gamma = d^3k\ \ d^3r$ of phase space at time t. Here it is assumed that $d\Gamma$ can contain large numbers of electrons while it is so chosen that within it the temperature and external field are approximately constant. After a time dt the electrons in volume $d^3k\ d^3r$

at t will, according to Liouville's theorem, lie in an equal volume of space about $\vec{k}+\dot{\vec{k}}dt, \vec{r}+\vec{v}dt$ at time t + dt. Hence the difference between $f(\vec{k}+d\vec{k}, \vec{r}+d\vec{r}, t+dt)$ and $f(\vec{k},\vec{r},t)$ must be due to the electrons scattered into the new volume during the time dt. One may write this as

$$\frac{\partial f}{\partial t} + \dot{\vec{k}}\,\vec{\nabla}_k f + \vec{v}.\vec{\nabla}_r f = \left(\frac{\partial f}{\partial t}\right)_{coll} \qquad (II.37)$$

where $\left(\frac{\partial f}{\partial t}\right)_{coll}$ denotes the rate of change of $f(\vec{k},\vec{r},t)$ due to scattering.

Now we calculate this quantity.

Consider an electron in a state k at time t. If $p(\vec{k},\vec{k}')$ is the probability per unit time that the electron is scattered into state $\vec{k}'$ (assumed to be vacant) then the number of electrons per unit volume of crystal scattered into d^3k' in time dt is:

$$\tfrac{1}{2}(4\pi^3)^{-2}p(\vec{k},\vec{k}')\ f(\vec{k})(1-f(\vec{k}'))\ d^3k'.\ d^3k\ dt \qquad (II.38)$$

A similar expression holds for the scattering in reverse direction. Here $\frac{1}{2}$ occurs because we are considering the process in which there is no spin flip. The difference between these two expressions when integrated over the final state dk' gives the $\left(\frac{\partial f}{\partial t}\right)_{coll}$ as:

$$\left(\frac{\partial f}{\partial t}\right)_{coll} = \frac{N\Omega}{8\pi^3}\int\left(p(\vec{k}',\vec{k})f(\vec{k}')(1-f(\vec{k}))-p(\vec{k},\vec{k}')f(\vec{k})(1-f(\vec{k}'))\right)d\vec{k}' \qquad (II.39)$$

where N is the number of atoms in crystal and Ω is the atomic volume. If very small displacements from the equilibrium state are considered then one may write for the distribution function

$$f(\vec{k}) = f_o(\vec{k}) + f_1(\vec{k}) \qquad (II.40)$$

where $f_1(\vec{k})$ is the deviation of the distribution function from its equilibrium value, $f_o(\vec{k})$, and is a small quantity.

Now employing the principle of detailed balance in the equilibrium state and neglecting the second power of $f_1(\vec{k})$ one arrives at the following:-

$$\left(\frac{\partial f}{\partial t}\right)_{coll} = \frac{N}{8\pi^3 k_B T}\Omega \int p(\vec{k},\vec{k}')f_o(1-f_o')\left[\chi(\vec{k}')-\chi(\vec{k})\right] d\vec{k}' \quad (II.41)$$

where k_B is the Boltzmann constant, T the absolute temperature and $\chi(k)$ comes from the following transformation:-

$$f_1 = -\chi(\vec{k})\frac{df_o}{dE} \quad (II.42)$$

In the above expressions f_o' is used to indicate $f_o(\vec{k}')$. Now we recall that the group velocity of an electron in state k is given by:-

$$\vec{v} = \frac{1}{\hbar}\vec{\nabla}_k E_k \quad (II.43)$$

and the rate of change of momentum by:-

$$\hbar\dot{\vec{k}} = e\left[\vec{\mathcal{E}} + \frac{1}{c}\vec{v}\wedge\vec{H}\right] \quad (II.44)$$

Where E_k is the energy of the electron in state k, $\vec{\mathcal{E}}$ and $\vec{H}$ are electric and magnetic fields respectively.

Considering steady states for which $\frac{\partial f}{\partial t} = o$ and assuming that no thermal gradient or magnetic field are present, one obtains from (II.37), (II.41), (II.43) and (II.44) the following:-

$$\frac{e}{\hbar}\vec{\mathcal{E}}\cdot\vec{\nabla}_k f = \frac{N\Omega}{8\pi^3 k_B T}\int P(\vec{k},\vec{k}')f_o(1-f_o')\left[\chi(\vec{k}')-\chi(\vec{k})\right] dk' \quad (II.45)$$

We now proceed from this equation to calculate the electrical conductivity in terms of the relaxation time which we introduce immediately.

3. Time of Relaxation

In Eq(II.45) $p(\vec{k},\vec{k}')$ is determined by the nature of the interaction between electrons and the lattice irregularities, hence it can be regarded as a known function. Therefore, the only unknown term in this equation is $\chi(\vec{k})$. Let us assume that Eq.(II.45) has been solved giving the unknown $\chi(\vec{k})$. Using this, the right hand side of the equation becomes a known function of $\vec{k}$. Following Jones (56) we take this to be

$$-\frac{f1}{\tau(\vec{k})} \quad (II.46)$$

The function $\tau(\vec{k})$, it should be noticed, depends on external fields as well as on k.

In the situation where P(k,k') is small except when

$$E_{k'} - E_k \ll k_B T \tag{II.47}$$

One finds from (II.41), (II.42) and (II.46) the following for $\tau(k)$:-

$$\frac{1}{\tau(\vec{k})} = \frac{N\Omega}{8\pi^3} \int p(\vec{k},\vec{k}') \left(1 - \frac{\chi(\vec{k}')}{\chi(\vec{k})}\right) d\vec{k}' \tag{II.48}$$

In this case if $\chi(\vec{k}')/\chi(\vec{k})$ is independent of the external fields then $\tau(\vec{k})$ depends on k only and is called the relaxation time. Because under these conditions any arbitrary distribution, when left to its own devices, will relax exponentially to its equilibrium value.

At low temperatures the scattering of electrons from lattice waves involves an energy exchange by an amount $\Delta E \leq k_B T$, hence the condition (II.47) is not satisfied. At high temperatures, however, the maximum energy an electron can exchange with lattice is equal to $k_B\theta_D$ hence, if $T \gg \theta_D$ the condition $E_{k'} - E_k \ll k_B T$ is satisfied. Therefore in pure metals a time of relaxation exists at sufficiently high temperatures only. For scattering by an impurity this condition is always satisfied. Therefore in this case the relaxation time exists at all temperatures.

We now consider a uniform electric field given by $\vec{\mathcal{E}}(o,o,\mathcal{E})$. When Ohms law is applicable one may replace f by f_o on the left hand side of (II .45). This is equivalent to neglecting powers of $\mathcal{E}$ higher than the first.

Then using $\left(\frac{\partial f}{\partial t}\right)_{coll} = -\frac{f_1}{\tau(k)}$ one has from (II.45)

$$\frac{e\mathcal{E}}{\hbar} \cdot \frac{\partial f_o}{\partial k_z} = -\frac{f - f_o}{\tau(\vec{k})} \tag{II.49}$$

This equation may be written as:-

$$f = f_o(k_x,\ k_y,\ k_z\ - \frac{e\mathcal{E}}{\hbar}\tau(\vec{k})) \tag{II.50}$$

For free electrons if one assumes $\tau(\vec{k})$ is independent of $\vec{k}$ then the change in the momentum of n electrons in a unit volume of the metal is $ne\mathcal{E}\tau$. The current density is therefore:-

$$J_z = \frac{ne^2\tau\mathcal{E}}{m} \tag{II.51}$$

and, hence, the resistivity is given by:-

$$\rho = \frac{m}{ne^2} \cdot \frac{1}{\tau} \tag{II.52}$$

where m is the mass of the electron and e is the electronic charge. Thus the calculation of the resistivity reduces to that of the relaxation time which is given below.

In order to make the calculation of the transition probability p(k,k') feasible, the following assumptions are made:-

(i) The energy of the electrons depends on the magnitude of the wave vector as follows:-

$$E(k) = \frac{\hbar^2}{2m} |\vec{k}|^2$$

where m is the effective mass of the electron.

(ii) The metal is regarded as an isotropic elastic solid.

The most important consequences of these two assumptions are that $P(\vec{k},\vec{k}')$ now depends only on the magnitude of $\vec{k}$ and $\vec{k}'$, and the angle α between them. A second consequence of these assumptions is that $\tau(k)$ can depend on the magnitude of $\vec{k}$ only. These have been shown by Jones (56) to simplify (II.48) to:-

$$\frac{1}{\tau} = \frac{N\Omega}{8\pi^3} \int P(k,k',\alpha)\left(1 - \frac{k_z'}{k_z} \cdot \frac{C(E')}{C(E)}\right) d\vec{k}' \tag{II.53}$$

where C(E) is some unspecified function of the energy. In this equation

we need to know $P(k,k',\alpha)$ the transition probability. This can be calculated as follows, using time dependent perturbation theory. Let $V_o(r)$ be the potential energy of the electron at $\vec{r}$ in the perfect lattice and $V(\vec{r},t)$ be the potential of the electron at the same point after a time t in the crystal which contains irregularities due to thermal motion of the atoms, or impurities. Then

$$U(\vec{r},t) = V(\vec{r},t) - V_o(\vec{r}) \tag{II.54}$$

is the perturbation giving rise to transitions between electronic states. We calculate this assuming that at some instant the displacement of atoms is frozen-out. This amounts to excluding all but elastic scattering. In this case, of course, U is independent of time. A wave function in the perturbed lattice can be expressed as

$$\psi = \sum_{\vec{k}} a(\vec{k},t)\, \varphi_{\vec{k}}(\vec{r},t) \tag{II.55}$$

where $\varphi_{\vec{k}}$ is a Bloch function of the unperturbed lattice assumed here to be normalized to the volume of the crystal. Using the perturbation calculation one obtains:-

$$|a(k',t)|^2 = 4\langle \varphi_k | U(r) | \varphi_k \rangle \frac{\mathrm{Sin}^2\left(\frac{E(k)-E(k)}{2h}\right)t}{(E(k)-E(k'))^2} \tag{II.56}$$

which is interpreted as the probability of finding an electron in state $\vec{k}'$ at time t after starting from state $\vec{k}$ at t = o, hence the rate of change of $|a(\vec{k}',t)|^2$ has the same meaning as $p(\vec{k},\vec{k}')$. Taking the derivative of $|a(\vec{k}',t)|^2$ with respect to time, substituting into (II.53) and integrating over all final states k' one finally arrives at

$$\frac{1}{\tau} = \frac{mkN\Omega}{2\pi\hbar^3} \int_0^{\pi} |\langle \varphi_k | U | \varphi_k \rangle|^2 (1-\mathrm{Cos}\alpha)\, \mathrm{Sin}\alpha\, d\alpha \tag{II.57}$$

This integral may be written as (57)

$$\frac{1}{\tau} = 2V k^2 \pi \int_0 (1-\mathrm{Cos}\,\alpha)\, p(\alpha)\, \mathrm{Sin}\alpha\, d\alpha \tag{II.58}$$

where $V = N\Omega$ is the volume of the crystal. If one uses the wave function ψ

normalized to the crystal volume V then this term does not show in this last equation. $p(\alpha)$ is the probability per unit time that an electron is scattered through an angle α.

We now use this formula to calculate the resistivity arising from the scattering of electrons from well defined excitations such as phonons, magnons, etc.

4. Contribution to Resistivity from Electron-Phonon Scattering

The thermal motion of atoms in a lattice may be resolved into a set of travelling plane waves. For a perfect lattice, and in the case of harmonic interactions, these are the normal modes of vibration, each mode having an energy which,when quantized, is called a phonon. This is usually denoted by $\hbar\omega(q)$ where q is the phonon wave vector. At temperatures above a certain characteristic temperature all these modes are thermally excited. Well below this temperature, however, only modes with long wave lengths (small q's) are excited. Therefore, different forms of temperature dependence are obtained for resistivity in these two regions. We derive below the expression for resistivity in the simplest case, ie: for free electrons and neglect the scattering through more than 79° (the Umklapp processes).

(a) Resistance at Low Temperatures

If k and k' are the wave vectors of an electron before and after scattering, and α is the angle between them, then from(II.58)the resistivity is obtained as:-

$$\rho = C \int_0^{\alpha_{max}} p(\alpha)(1 - \cos\alpha) \sin\alpha \, d\alpha \qquad \text{(II.59)}$$

At low temperatures $p(\alpha)$ is roughly independent of α and is proportional to $\frac{T}{M\Theta^2}$ for all angles less than $\alpha_{max} = \frac{q_{max}}{k_F}$ (58) where q_{max} is the

maximum phonon wave-vector excited at this temperature, M is the mass of an atom in the crystal and θ is a characteristic temperature. Hence:-

$$\rho = C \int_0^{T/\theta} \frac{T}{M\theta^2} (1-\cos\alpha) \sin\alpha \, d\alpha = C' \frac{T^5}{M\theta^6} \qquad (II.60)$$

where C and C' are constants. This formula is derived under the assumption that $E(k')-E(k) \ll k_B T$ which is not true for temperatures $T \lesssim \theta$, hence it cannot be used to obtain a quantitative expression for resistance.

(b) Resistance at High Temperatures

At high temperatures the resistivity for a Debye Solid is given by Jones (56) as :-

$$\rho = \frac{m^2 \pi T \Omega}{3e^2 \hbar k_B M \theta_D} C_D^2 \qquad (II.61)$$

where M is the ionic mass, θ_D is the Debye temperature and C_D is a constant expressing the coupling between electrons and the lattice vibration.

At low temperatures the Umklapp processes may be neglected because the electrons are scattered through small angles. At high temperatures, however, it may account for ~75% of the total resistance (59). To represent the variation of the resistivity in the intermediate temperature range, the so-called Bloch-Grüneisen formula has been used extensively. This is given by (60):-

$$\rho = \frac{C}{M\theta^6} T^5 \int_0^{\frac{\theta}{T}} \frac{z^5 \, dz}{(e^z-1)(1-e^{-z})} \qquad (II.62)$$

In II.60 and II.62 θ is a characteristic temperature for the lattice resistivity and is slightly higher than the Debye temperature (61). When θ and C have been suitably chosen, the above expression is found to represent the experimental temperature variation of the resistivity of a wide range of metals quite well.

5. Magnetic Disorder and Spin Wave Scattering in Pure Metals

In magnetic materials the disorder in spin orientation and in its location gives rise to an extra term in resistivity. At low temperatures relative to a magnetic ordering temperature, the disorder in the spin orientation is best described by the spin waves. At sufficiently low temperatures the dispersion relation for spin waves is of the form (58)

$$E(q) \sim Jq^2 \tag{II.63}$$

where q is the wave vector and J is the exchange integral. The scattering of the conduction electrons by the spin waves occurs through the s-d(f) exchange interaction. When such a scattering takes place it results in the destruction of a spin wave and the change in the spin direction of the conduction electrons. In this case it can be shown that the $(1 - \cos\alpha)$ term does not appear in the expression of the time of relaxation. Hence, the resistivity arising from this mechanism is given by:-

$$\rho \sim \int_0^{\alpha_{max}} p(\alpha) \sin\alpha \, d\alpha \tag{II.64}$$

where $\alpha_{max} \sim (\frac{kT}{J})^{\frac{1}{2}} \cdot \frac{1}{k_F}$. As $p(\alpha)$ is proportional to T one finds the resistivity to be proportional to T^2.

The different form of temperature dependence of the resistivity due to the lattice and spin waves arises from the difference between their energy spectra. Mannari (62) has discussed the resistivity due to phonon and spin waves in ferro and antiferromagnets. He finds a T^5 term for phonon and a T^2 term for spin waves in ferromagnets. In an antiferromagnet, where the energy is linearly dependent on q, the author obtains a T^4 term in the resistivity.

Liu (63) has criticized the use of the s-d interaction as a small perturbation on a gas of free electrons and magnetically coupled spins. Assuming that the coupling between spins arises entirely from the indirect

s-d(f) interaction, he obtains for a ferromagnet a $T^{3/2}$ term in addition to T^2 term and claims that the former may be dominant at temperatures below 10% of the ordering temperature.

In the rare earth and magnetic transition elements the magnetic part of the resistivity drops abruptly below the ordering temperature. Above this temperature the resistivity is constant in rare earth metals and may have a T^2 dependence in transition metals (64). This anomalous behaviour of the resistivity has been discussed by several authors whose models can be classified into two types. The one is the spin disorder resistivity based on the s-d exchange model and the other is the resistivity due to the s-d interband scattering.

The s-d interband scattering proposed by Mott (65) is based on the band structure of the transition metals. The states of d-electrons in these metals, according to the band model, form a narrow band with a high density of states as well as the broad s-band. The effective mass of d-electrons being large, the current is mainly carried by the s-electrons. But as the transition probability is proportional to the density of final states of the Fermi level, the s-electrons are mostly scattered into d-states. Hence, at temperatures where the band for one spin direction is full, the conduction electrons can only be scattered

into the unfilled band. Hence, the resistivity of these metals depends on the magnetization of the d-band. This model is appropriate for Ni and Co where the magnetic electrons are itinerant.

In the s-d exchange model the magnetic electrons are assumed to be localized on the lattice point. The coupling between conduction electrons and localized moments is described by the s-d exchange hamiltonian (I·45) which is treated as a perturbation. The anomalous electrical resistance occurs because the exchange energy between conduction electrons and localized spins depends on the relative orientations of the latter which is not periodic at finite temperatures. This model is most appropriate for iron and rare earth elements. Among these Gadolinium has been chosen for theoretical treatments by Kasuya (66) and by De Gennes and Friedel (67).

In his treatment Kasuya made the following assumptions:-

(i) The energy spectrum of the conduction electrons is given by $\frac{\hbar^2 |k|^2}{2m}$ where m is the effective mass of electrons.

(ii) The Fermi energy is much larger than the exchange constant $J(q = o) = J$ and $k_B T$.

Using the molecular field approximation the author obtains the following expression for the resistivity:-

$$\rho(T) = C\left[S-\sigma(T)\right]\left[S+\sigma(T)+1\right] \qquad \text{(II.65)}$$

where C is a constant depending on the metal in question, S is the magnitude of the impurity spin at absolute zero and $\sigma(T)$ is its average value at temperature T. At $T = 0^{\circ}K, \sigma(o) = S$, therefore resistivity goes to zero. At $T \geq Tc, \sigma(T) = o$, hence at $T \geq Tc$, $\rho(T)$ is constant. Its value being

$$\rho_m = C\,S(S+1) \qquad \text{(II.66)}$$

When temperature is lowered below Tc, $\sigma(T)$ increases, therefore $\rho(T)$ decreases. Hence, the resistivity decreases with decreasing temperature. Formula (II.66)

shows that the magnitude of the resistivity at and above Tc depends on the magnitude of the spin. This is, indeed, observed experimentally.

De Gennes and Friedel (67) have calculated the magnetic part of the resistivity in the Born approximation using the molecular field model. Employing an effective mass approximation for the conduction electrons they obtained the following expression for the resistivity above the ordering temperature:-

$$\rho_o = \frac{\hbar k_F}{4\pi z} \left(\frac{mG}{e\hbar^2}\right)^2 S(S+1) \qquad \text{(II.67)}$$

where z is the number of valence electrons per atom, G is the strength of the coupling energy between conduction electrons and atomic spins, and is assumed to be δ function-like, m is the effective mass of the conduction electrons and S is the magnitude of the atomic spin.

The authors argue that the wave-length of the conduction electrons at the Fermi level is sufficiently short, and therefore neglect the interference between scattered waves. In this case they find the following for the resistivity:-

$$\rho(T) = \rho_o\left(1 - \frac{\langle S\rangle^2}{S(S+1)}\right) \qquad \text{(II.68)}$$

They further discuss the effects of short range ordering above the transition temperature, and find that in the above case these effects are negligible.

Both Kasuya's and De Gennes and Friedel's models are not valid at very low temperatures where the molecular field model is not applicable.

6. Resistivity Due to the Magnetic Disorder and Spin Waves in the Alloys of Transition and Rare Earth Metals

(a) Finite Concentration

The resistance of certain alloys of the transition and rare earth metals with noble and with some other transition metals (e.g. Pd) shows an anomalous behaviour.

In most of these alloys the resistance shows a sudden decrease on cooling through the ordering temperature, but it does not tend to a very low value at the lowest temperatures because of the spatial disorder of the localized spins. Here again the spin disorder scattering mechanism explains this anomolous resistivity. The theories developed to account for the behaviour of the resistivity in some of these alloys typified by dilute Cu-Mn (excluding the resistance minimum) and Pd-Fe are given by Yosida(68) and by Long and Turner (69).

Yosida has discussed the behaviour of Cu-Mn alloys containing more than about 1 at % manganese. He assumes that the main parts of the perturbation in these alloys are the spin dependent potential, resulting from the s-d interaction, and an ordinary screened Coulomb potential $V(\underline{r})$ around the manganese ions. The author makes the following assumptions:-

(1) The energy of the conduction electrons can be approximated by $E = \frac{\hbar^2 k^2}{2m}$, where m is the effective mass of the conduction electrons.

(2) At low temperatures the Mn ions are ordered in an antiferromagnetic fashion.

(3) The exchange integral $J(k,k')$ and the potential $V(k,k')$ depend on $|k-k'|$ only

(4) Mn ions are distributed at random and there is no interference between

the waves scattered from different ions.

With these approximations Yosida calculates the resistivity and finds:-

$$\rho = Ac\left[G+D\left[S(S+1) - \tfrac{1}{2}\sum_{m}^{\pm} m\,\omega_m^{\pm} \tan h \left(\frac{g\mu_B H^{\pm}}{2k_B T}\right)\right] \right] \qquad (II.69)$$

where A, G and D are constants, c is the concentration of Mn atoms, $H^{\pm}$ are the molecular fields acting on up and down spins and ω_m^{+} is the probability with which the component of a localized up-spin takes the value m. At temperatures above the ordering temperature all the spins are oriented randomly. Hence: $\sum_m m\,\omega_m^{\pm}=o$ and $H^{+}=H^{-}=o$, therefore (II.69) reduces to:

$$\rho = Ac\left[G+D\ S(S+1)\right] \qquad (II.70)$$

i.e. independent of temperature but dependent on the magnitude of the impurity spin. The model clearly does not take into account the effect of the short range ordering above the transition temperature. Below the ordering temperature the expression (II.69) decreases and at absolute zero it reaches:-

$$\rho\,(T\rightarrow o) = Ac(G+DS^2) \qquad (II.71)$$

The difference between the value at absolute zero and that above the ordering temperatures is given by:-

$$\Delta\rho = AcDS \qquad (II.72)$$

Using the values of the constants A and D which are related to the physical parameters of the alloys, Yosida calculates $\Delta\rho$ and shows that it would agree with experiments if the exchange integral for the s-d interaction were taken to be larger than that of a free Mn^{+} ion by a factor 1.7.

For a comprehensive review of spin disorder effect in rare earth and transition metals and their alloys we refer to Coles (70).

Long and Turner (69) have calculated the resistivity of dilute ferro-

magnetic alloys of the type Pd-Fe using the hamiltonian originally given by Doniach and Wohlfarth (71). They describe the dynamical state of the localized spins at low temperatures by spin-waves and at temperatures near the Curie temperature by independent spins moving in a molecular field. The authors follow the calculation of Yosida and obtain for the incremental (the impurity part of the) resistivity a complicated expression which, as the temperature approaches the Curie temperature Tc, reduces to:-

$$\Delta\rho\,(T \rightarrow Tc) = Ac\ (1 - \frac{T}{Tc}) \qquad \text{(II.73)}$$

where A is a constant and c is an impurity concentration.

At temperatures well below the ordering temperature the form of the incremental resistivity is:-

$$\Delta\rho\,(T \rightarrow o) = Bc + Dc^{-\frac{1}{2}}\ T^{3/2} \qquad \text{(II.74)}$$

Here B and D are numerical factors. The first term in (II.74) arises from the elastic scattering. Both the elastic part of the exchange scattering and the spin independent potential contribute to this term. The second term has two contributions:-

(i) The term arising from the temperature dependence of the elastic part of the exchange scattering which yields a contribution proportional to the square of the magnetization. For spin waves as $T \rightarrow o$ the square of the magnetization varies as $M(o)^2 - AT^{3/2}$ (See Eq. I.78).

(ii) The term coming from the inelastic scattering. Long and Turner argue that in a system which is not translationally invariant the momentum is not conserved. This leads to a scattering rate proportional to the number of spin waves present, which is again proportional to $T^{3/2}$.

(b) Single Magnetic Impurity Taken to Higher Order

The magnetic part of a single impurity resistivity arises from scattering of conduction electrons from the spin dependent part of the impurity potential. Kondo (72) has calculated this using the s-d exchange hamiltonian given by(I.45) in which he took $J(k-k')$ to be a constant J. The author carried the calculation to 2nd order using the Born approximation and found:-

$$\rho = c\rho_m(1 + 3Z \frac{J}{E_F} \log T) \qquad \text{(II.75)}$$

where ρ_m is given by(II.66), z is the number of conduction electrons per atom and c is the impurity concentration.

7. Resistivity Due to Non-magnetic Impurities and Defects

The contribution to the resistivity from a non-magnetic impurity is due to simple potential, resonance scattering and defects. Here we will be concerned with the contribution due to resonance scattering . The calculation of the residual resistivity arising from the resonance scattering has been done by Friedel (1). The author, using phase shift analysis, found the following expression:

$$\Delta\rho = \frac{4\pi n_i}{ne^2k_F} \sum_{\ell} (\ell + 1)\sin^2 (\eta_\ell - \eta_{\ell+1})_{E=E_F} \qquad \text{(II.76)}$$

where n_i is the number of impurities, n is the concentration of electrons, k_F is the Fermi wave vector and η_ℓ is the phase shift for the 1^{th} partial wave. If only the resonant phase shift is large, then using the Friedel sum rule (Eq.I.7), the resistivity per impurity is found to be given by:-

$$\Delta\rho = \frac{10\ m}{n\pi e^2\hbar\rho(E_F)} \sin^2 \frac{\pi}{10}N \qquad \text{(II.77)}$$

where m is the electronic mass, N is the number of d-electrons of the

impurity and $\rho(E)$ is the density of states of host conduction electrons. From the above formula it is clear that the resistivity of 3d elements should go through a maximum when $N \sim 5$, i.e. near Cr and Mn. This is indeed observed by Boato et al (73), for 3d impurities in Al and in Zn.

8. Scattering of Electrons from Persistent Spin Fluctuations in Metals and Alloys

In a strongly enhanced paramagnetic metal such as Pd there is an additional contribution to the usual resistivity (electron-electron and electron-phonon scattering) due to the scattering of conduction electrons from persistent spin fluctuations in the d-band. These so-called paramagnons are not true excitations. Their existence is indicated, as we have shown (Eq.II.22) by a peak in the imaginary part of the susceptibility, which is essentially the spin fluctuation spectral density function. Therefore, the computation of the resistivity due to the scattering of the conduction electrons from paramagnons involves the spectral density function quite naturally.

The first calculation of the electrical resistivity arising from the scattering of conduction electrons from itinerant d-electrons in which a spin flip of the electrons occurs, was made by Mills and Lederer (64). They considered an exchange interaction of the form:-

$$H_{s-d} = J\, V_c \int \sigma(r)\, S(r)\, d^3r \qquad \text{(II.78)}$$

where Vc is the volume of the unit cell, J is the s-d interaction parameter, $\sigma(r)$ and $S(r)$ are the spin density operators of the s and d electrons respectively. They retain in the hamiltonian only the terms in which a spin flip of an s-electron is described. Employing for the d-electrons the one band, short range, interaction model, they computed the susceptibility

and, hence, the spectral density function. They then calculated the relaxation time for a variety of cases.

Relevant to our discussion here is the case of a ferromagnetic system of itinerant electrons at temperatures above the Curie temperature, where they showed that the resistivity should be proportional to T^2 and pointed out that the result of their calculation should also apply to a paramagnetic transition metal such as Pd at low temperatures.

Schindler and Rice (74) have calculated the resistivity of dilute Pd-Ni alloys using the above hamiltonian and the Mills and Lederer formalism. They assumed that the addition of Ni impurities enhances the alloy's d-band uniformly. They used a variational principle to solve the Boltzmann equation and related the scattering rate to an integral equation containing a spectral density function. For this function a simple triangular approximation is made which assumes a linear variation of the spectral density function $A(q,\omega)$ with the frequency up to a certain phenomenological cut-off value ω_Q. The calculation yielded the following expression for the resistivity:-

$$\rho = \frac{\alpha}{\theta^2}\, T^2 \left[J_2\left(\frac{\theta}{T}\right) - \left(\frac{T}{\theta}\right)^3 J_5\left(\frac{\theta}{T}\right) \right] \qquad \text{(II.79)}$$

Where θ is a characteristic paramagnon temperature defined by $k_B\theta = k\omega_Q \sim \frac{1-\bar{I}}{\bar{I}}$, $J_n\left(\frac{\theta}{T}\right)$ denotes the Bloch-Grüneisen integral, and α is a concentration-dependent parameter.

Close to the ferromagnetic transition $\bar{I} \sim 1$ hence:-

$$\theta \sim (1 - \bar{I}) \qquad \text{(II.80)}$$

In the above expressions $\bar{I} = I\rho_d(E_F)$. Here I is the Coulomb repulsion between d-electrons and $\rho_d(E_F)$ is their density of states at the Fermi level.

For sufficiently small $(\frac{T}{\theta})$, the Bloch-Grüneisen integrals may be replaced by the constants $J_n(\infty)$. Therefore the formula (II.79) reduces to:-

$$\rho = \frac{\alpha}{\theta^2} J_2(\infty) T^2 - \frac{\alpha}{\theta^5} J_5(\infty) T^5 \qquad \text{(II.81)}$$

Thus at very low temperatures and for a system near to the ferromagnetic transition (i.e. θ very small) the first term may suppress the T^5 term hence allowing the T^2 law to be observed. One aspect of the theory which is not satisfied is the variation of the coefficient of the T^2 term with the exchange enhancement factor $(\frac{\chi}{\chi_o})$. The theory suggests that this coefficient should vary as $(\frac{\chi}{\chi_o})^2$ while the experimental evidence is that this variation is linear. This was explained later by Lederer and Mills (75).

These authors argued that in the Pd-Ni type alloys the enhancement due to the impurity is confined to the impurity cell, and hence the uniform enhancement model of Schindler and Rice (74) cannot give an adequate description of such alloys. They considered an enhanced matrix containing a single impurity which tends to drive the host to the ferromagnetic transition in the region of the impurity. They used the Wolff model (8) and employed a dynamic molecular field approximation to obtain the susceptibility of the alloy from which the spectral density function is obtained. This function consists of two parts as expected, the host and the impurity parts.

They then used their earlier method to compute the resistivity at low temperatures and found

$$\rho \sim A(o)\left[\, 1 + \left(\frac{\delta I}{I_o}\alpha\right)^2 \Gamma\, c \,\right] T^2 \qquad \text{(II.82)}$$

where the constant A(o) refers to the host matrix, c is the impurity concentration, I_o is the intra-atomic Coulomb repulsion between d-holes of the host, δI is the change in the strength of the interaction within the impurity cell. Γ is a parameter related to the number of holes in

the d band, the exchange enhancement factor $\left[1 - I_o \rho(E_F)\right]^{-1}$ of the host metal and $\alpha = \left[1 - \delta I \cdot \bar{\chi}_R(o)\right]^{-1}$, where $\bar{\chi}_R(o)$ is the real part of the function

$$\bar{\chi}(\omega) = \frac{1}{N} \sum_k \chi_o(k,\omega) \qquad \text{(II.83)}$$

in the limit of $\omega \to o$. Here N is the total number of atomic cells in the pure metal, χ_o is the susceptibility of the pure host metal. The calculation showed that, in the dilute limit, A(c) varies roughly linearly with concentration, hence linearly with the susceptibility.

Kaiser and Doniach (76) have extended the calculation of Lederer and Mills (75) to higher temperatures and obtained a universal curve for the impurity spin fluctuation contribution to the resistivity of dilute alloys. They applied their model to alloys in which local exchange enhancement is large (e.g. Pd-Ni, Rh-Fe, Rh-Co, etc.). Employing a variational principle to solve the Boltzmann equation they arrived at the following for the reduced impurity resistivity:-

$$\bar{\rho} \sim \frac{1}{\bar{T}} \int_o^\infty \frac{\bar{\omega}^2}{(e^{\bar{\omega}/\bar{T}} - 1)(1 - e^{-\bar{\omega}/\bar{T}})(1 + \bar{\omega}^2)} \, d\bar{\omega} \qquad \text{(II.84)}$$

Here $\bar{\rho} = \frac{\rho}{\rho_o}$, where ρ_o is a constant, $\bar{T} = \frac{T}{\theta}$, $\bar{\omega} = \frac{\omega}{k_B \theta}$, $\hbar\omega$ is the energy of the paramagnon and $k_B\theta = \frac{(1 - \delta I \bar{\chi}_R)}{\Delta I \quad \bar{\chi}_I} \omega$ is the energy of the peak in the localized spin fluctuation excitation spectrum. $\bar{\chi}_R(\omega)$ and $\bar{\chi}_I(\omega)$ are the real and the imaginary parts of the susceptibility given by (II.83). At very low temperatures $\bar{\omega}^{-2}$ can be neglected in the denominator if the system is not too near to the Stoner instability limit leading to:-

$$\rho(T \to o) \sim \left(\frac{T}{\theta}\right)^2 \qquad \text{(II.85)}$$

At high temperatures, all paramagnons are excited, hence one has:-

$$\rho(T \to \infty) \sim \frac{T}{\theta} \qquad \text{(II.86)}$$

They showed that the region of T^2 extends to temperatures up to 25% of θ.

Hence, as the system approaches the Stoner instability region, θ goes to zero and, therefore, the power of T at a given low temperature decreases. Eventually the resistance becomes linear over the whole temperature range. This fact can be used as a criterion to select the alloy with the critical concentration, i.e. the alloy nearest to the ferromagnetic transition. The authors also discuss the resistivity of the host metal and show that it varies as T^2 over a considerable temperature range, since in this case θ is large. They further discuss the effect on the resistivity of the variation with temperature of the local exchange enhancement factor, and find a fall of the resistivity below the linear portion of the curve at higher temperatures. The effect is found to be greater, the greater the enhancement factor at absolute zero. Comparison with experiments on dilute Rh-Fe, Ir-Fe, Rh-Co, Pd-Ni is made and it is shown that theory and experiment agree reasonably well, especially in the case of Ir-Fe.

Rivier and Zlatić (77) have critized the high temperature calculation of Kaiser and Doniach (76). The latter authors' calculation leads to a resistivity which varies linearly with temperature at high temperatures. This implies that in this temperature range the effective perturbing potential is large. Therefore the proper treatment is to carry perturbation calculation to higher orders. This has been done by Rivier and Zlatić. These authors found the following for the reduced resistivity:-

$$\bar{\rho} = \frac{\rho}{A} = \left[1 - \left\{1 + \frac{\pi T}{\theta} + \psi\left(\tfrac{1}{2} + \frac{1}{2\pi}\ \frac{\theta}{T}\right) - \psi\left(1 + \frac{1}{2\pi}\ \frac{\theta}{T}\right)\right\}^{-1}\right] \qquad \text{(II.87)}$$

which is plotted in Fig. (II.3) as a function of $2\pi\frac{T}{\theta}$. In the above expression A is a constant involving the number of impurities, mass and charge of electrons, etc. It is chosen so that as $T\to\infty$ $\bar{\rho}\to 1$. ψ is the digamma function and θ is the localized spin fluctuation temperature. The resistivity $\bar{\rho}$ is a universal function of temperature and varies with temperature as follows:-

(a) At very low temperatures the resistivity increases as:-

$$\bar{\rho} = \frac{3\pi^2}{4}\left(\frac{T}{\theta}\right)^2 \qquad \text{(II.88)}$$

(b) At temperatures of the order of0.2θ it becomes linear:

$$\bar{\rho} = c(T - D\theta) \qquad \text{(II.89)}$$

where $c = \frac{1.12}{\theta}$ and $D = 0.67$

(c) Above the spin fluctuation temperature θ, $\bar{\rho}$ varies as

$$\bar{\rho} = 0.68 + 0.24 \ln \left(\frac{T}{\theta}\right) \qquad \text{(II.90)}$$

(d) At temperatures well above θ the variation of $\bar{\rho}$ is:

$$\bar{\rho} = \left(1 - \frac{\theta}{T}\right) \qquad \text{(II.91)}$$

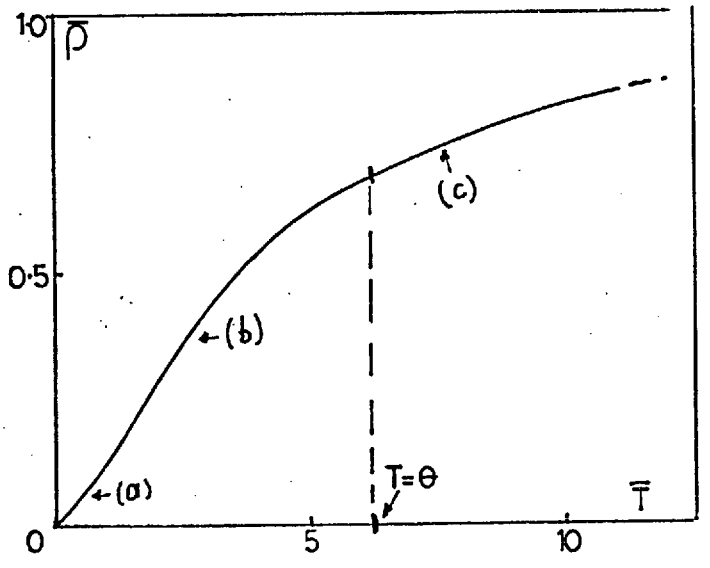

Fig. (II.3). The normalized resistivity versus the reduced temperature $\bar{T}=2\pi(T/\theta)$

Mathon (78) has employed the uniform exchange enhancement model of Schindler and Rice (74) to investigate the behaviour of the resistivity through the critical concentration. Using a variational principle the author calculated the resistivity which is found to increase with decreasing power of T on approaching from either side of the critical concentration. About the critical concentration the resistivity is symmetrical and has a

$T^{5/3}$ limiting behaviour with temperature. Away from the critical region the resistivity varies as T^2 due to the paramagnons or spin waves.

The temperature dependence of the resistivity arising from spin fluctuations or paramagnons seems now to be explained satisfactorily by the Lederer and Mills-Kaiser and Doniach-Rivier and Zlatič model. However, no satisfactory investigation has been carried out through the critical concentration.

III. SPECIFIC HEAT

1. Introduction

By specific heat, sometimes called heat capacity, we shall usually mean the specific heat at constant volume. This quantity is defined by

$$C_V = \left(\frac{dE}{dT}\right)_v \tag{II.92}$$

where E is the energy and T is the temperature. The specific heat at constant pressure, which is the quantity measured experimentally, is defined in a similar manner and is denoted by C_p. The thermodynamic formula which connects these two quantities is:

$$C_p - C_v = \beta^2 KVT \tag{II.93}$$

where β is the volume coefficient of thermal expansion at constant pressure, V is the volume, T is the absolute temperature and K is the isothermal bulk modulus given by : $K = - V \left(\frac{dp}{dv}\right)_T$. In solids the difference between C_p and C_v is usually very small and may often be neglected below room temperature. At room temperature the specific heat of almost all solids is approximately $3Nk_B$. Where N is the number of atoms in the speciment and k_B is the Boltzmann constant.

At low temperatures the specific heat drops markedly and approaches zero as T in metals and as T^3 in insulators. In ferromagnetic and in strongly paramagnetic metals and alloys there is a large contribution to the specific heat near the critical concentrations in paramagnets and the ordering temperatures in ferromagnets.

Below we discuss some of the contributions to the specific heat which are relevant to the alloy systems investigated here.

2. The Electronic Specific Heat

In classical statistical mechanics an energy of $\frac{3}{2}k_BT$ is associated with a free particle. Therefore, a crystal made of N atoms each giving one valency electron to a gas of free electrons should make a contribution of $\frac{3}{2}Nk_B$ to the electronic specific heat. But it is found experimentally that at room temperature the contribution to the specific heat is less than 1% of this value. This discrepancy which concerned the early workers was explained later by the discovery of the Pauli exclusion principle.

At absolute zero all the electronic states of a free electron gas are occupied up to a certain maximum energy E_F, the Fermi energy. When heating the system some electrons will be thermally excited above the Fermi level. The number of excited electrons is of the order of the number of states within an energy range k_BT of the Fermi level. Hence, if the total number of electrons is N then $N\frac{k_BT}{E_F}$ fraction of these electrons are excited. Each of these electrons has an average thermal energy of the order of k_BT. Hence the total electronic energy is of the order of $\frac{Nk_B^2}{E_F}T^2$, and the electronic specific heat is $C_v \sim Nk_B^2\frac{T}{T_F}$.

This quantitative argument shows that the specific heat should be linear in temperature in agreement with experimental results. Now a rigorous calculation of the electronic specific heat, vali d at temperature $T \ll T_F$, will be given.

The change in the energy of an electron gas on heating from zero to a certain temperature T is:

$$E = \int_0^{E_F} (E_F-E)\left(1-f(E)\right)\rho(E)\,dE + \int_{E_F}^{\infty} (E-E_F)f(E)\rho(E)\,dE \qquad \text{(II.94)}$$

where the first term is the energy required to bring electrons from below the Fermi level to the Fermi level, and the second term is the energy needed to take the electrons from the Fermi level to the states lying above the Fermi energy. f(E) is the Fermi distribution function, $\rho(E)$ is the density of states, and the factor $[1 - f(E)]$ takes into account the fact that the state with energy E below the Fermi level is empty.

Taking the derivative of the energy with respect to the temperature, integrating the resulting expression and using $T \ll T_F$ the specific heat is found to be given by

$$C_v^{\,o} = \frac{2}{3} \pi^2 \, k_B^{\,2} \, \rho(E_F) \, T \qquad \text{(II.95)}$$

At temperatures well below the Debye temperature θ_D, and very much below the Fermi temperature T_F, the specific heat of non-magnetic metals and alloys may be written as:

$$C_v = \gamma T + \beta T^3 \qquad \text{(II.96)}$$

where γ and β are constant. At room temperature the electronic term γT is insignificant compared to the lattice (2nd) term, while at sufficiently low temperatures it dominates the lattice term. The standard way of analyzing a set of experimental data on specific heat is to plot $\frac{C_v}{T}$ versus T^2. Then the points should lie on a straight line with slope β, and intercept γ.

3. Paramagnon Contribution to Specific Heat in Strongly Enhanced Metals and Alloys

In strongly enhanced paramagnetic metals the strong interaction between the itinerant electrons increases the effective mass of electrons and, hence, the electronic specific heat. This interaction is taken into account by adding a term to the hamiltonian. ie:—

$$H = H_o + I \sum_i n_{i\uparrow} n_{i\downarrow} \qquad \text{(II.97)}$$

where H_o is the kinetic energy term, and the second term is the term

representing the interaction. $n_{i\uparrow}$ is the number operator for up-spin electrons at site i, and I is the intra-atomic electron-electron repulsion between electrons of opposite spin.

Starting from the above hamiltonian Doniach and Engelsberg (79) have calculated the mass enhancement due to the interaction between the itinerant d-electrons and paramagnons and found at $T = 0^{o}K$:

$$\frac{m^*}{m} = 1 + 3\,\bar{I}\,\ell n\,(1 + \frac{\bar{q}^2\,\bar{I}}{12(1-\bar{I})}) \qquad \text{(II.98)}$$

where $\bar{q}$ ($= \frac{k}{k_F}$) is a cut-off value for the wave vectors and is of the order of unity, $(1 - \bar{I})^{-1}$ defines the Stoner enhancement factor. This mass enhancement leads to an enhancement in the low temperature electronic heat capacity.

$$\frac{C_v}{C_v^o} \cong \frac{m^*}{m} + \frac{6}{5}\pi^2 \frac{\bar{I}^2}{(1-\bar{I})}(\frac{T}{\theta})^2 \ell n\,(\frac{T}{\theta}) \qquad \text{(II.99)}$$

where C_v^o is given by (II.95) and

$$\theta = \frac{4}{\pi}\,T_F\,(\frac{1-\bar{I}}{\bar{I}}) \qquad \text{(II.100)}$$

is a characteristic spin fluctuation temperature and T_F is the Fermi temperature.

When approaching the ferromagnetic transition $\bar{I}$ approaches unity. Therefore, in this case $\frac{m^*}{m}$ should increase and θ should decrease resulting in a considerable increase in $\frac{C_v}{C_v^o}$. The presence of the $\mathrm{Ln}(\frac{T}{\theta})$ term is detected when plotting $\frac{C_v}{T}$ versus T^2. If such a term exists then the initially straight line should show an upturn at very low temperatures.

The above model is based on the uniform exchange enhancement model and, therefore, is suitable for pure metals. A model for the dilute alloys in which the enhancement due to the impurity is localized within the impurity cell has been proposed by Engelsberg et al (80). The hamiltonian used is:

$$H_{Alloy} = H + \Delta I \sum_i n_{i\uparrow} n_{i\downarrow} \qquad (II.101)$$

where H is the hamiltonian of the pure matrix and is given by (II.97), ΔI is the increase in the strength of the interaction within an impurity cell. The sum in the second term is over the impurity sites.

In the dilute limit they determine ΔI in terms of the local exchange enhancement parameter $\frac{1}{\eta}$ as follows:-

$$\frac{1}{\chi_{pd}} \frac{d\chi_{Alloy}}{dc}\Big]_{\substack{(\omega=o)\\(q=o)}} = (1-\bar{I})^{-1} \frac{\rho(E_F)\Delta I}{1-\Delta I\, \chi_{pd}(r=o,q=o)} = \frac{1}{\eta}$$

and calculate the contribution to the specific heat from impurities. This is given by

$$\frac{\Delta C_v}{C_v^o} = \frac{3c}{2\eta}\left[\alpha_+^{-1} \frac{6\pi^2}{5} \frac{\bar{I}}{(1-\bar{I})} \left(\frac{T}{\theta}\right)^2 \ell n\left(\frac{T}{\theta}\right) - \frac{9\pi^4}{2} n_e^2 \left(\frac{T}{\eta T_F}\right)^2 \alpha^{-3}\right] \qquad (II.102)$$

where n_e is the number of electrons per atom. T_F and θ are the Fermi and the spin fluctuation temperatures of the host. α is given in terms of the range parameter σ and $\bar{I}$ as:

$$\alpha = (1 - \bar{I}) + \frac{\bar{I}}{3}\sigma \qquad (II.103)$$

and c is the impurity concentration.

This result shows that the local enhancement does not only yield an increase in the specific heat but also introduces a new T^3 term which could add to the lattice specific heat and give an apparent concentration-dependent Debye temperature.

4. Molecular Field Calculation of the Specific Heat

In the Weiss molecular field approximation the calculation of the specific heat is fairly simple.

In the presence of an applied field H the total field acting on a

magnetic metal is

$$H_T = H + IM \tag{II.104}$$

where I is the molecular field constant and M the magnetization. The magnetization at temperature T is given by

$$\frac{M(T)}{M(o)} = B_s(X) \tag{II.105}$$

where B_s is the Brillouin function, $M(o) = N g \mu_B S$ is the saturation magnetization, and

$$X = g \mu_B S(H + IM)/k_B T \tag{II.106}$$

The magnetic energy in the presence of a constant applied field is:

$$E_m = -\int H_T \, dM = -\int (H + IM) \, dM \, . \tag{II.107}$$

From which

$$C_m = -(H + IM) \frac{dM}{dT} \, . \tag{II.108}$$

In order to obtain C_m, M has to be calculated as a function of temperature. For this we refer to Morrish (81).

The calculation leads to the following expression for the specific heat.

$$C_m = -\left[B_s(X) + \frac{H}{IM(o)} \right] \frac{dB_s(X)}{dT} \quad IM\,(o)^2 \tag{II.109}$$

In the absence of the applied field this formula reduces to

$$C_m = -\frac{1}{2} \, N k_B I \frac{d}{dT} \quad M\,(T)^2 \tag{II.110}$$

CHAPTER III

EXPERIMENTAL SITUATION

1. Introduction

During the last decade, particularly in the last few years, considerable attention has been given to the alloys of Pd and Rh with the elements in the middle of the 3d transition series. Sufficient interest has also been given to the alloys of Pd with some rare earth metals. Despite such a short period of time the number of investigations has grown so rapidly that it is not feasible to discuss all the works reported. Here we give a review of the experimental work which is closely related to the alloys investigated here and discuss in detail only the cases which will be used for the interpretation of data.

In the first part of this chapter, investigations on the electrical resistivity will be reviewed. This will be followed by those on the susceptibility and magnetization. Finally the specific heat will be discussed.

2. ELECTRICAL RESISTIVITY

The first measurements of the electrical resistivity of dilute Pd-Ni alloys with Ni concentration between 0 and 1.7 at % were made by Schindler and Rice (74) in order to test their theoretical predictions. According to their calculation, which assumes that the addition of Ni enhances the alloy susceptibility uniformly, s electron-paramagnon scattering in which spin flip of the s-electrons occurs should contribute a term to the low temperature resistivity which should vary as in Eq.(II.79).For

$T \ll \theta$ it may be written as:

$$\rho = \frac{\alpha}{\theta^2} J_2(\infty)\ T^2 \qquad \text{(III.1)}$$

here α, θ and $J_2(\infty)$ are the same quantities entering Eq.(II.79). Such a T^2 term was indeed observed in their alloys.

The range of this term was seen to increase with Ni concentration. They observed that the variation of $\frac{\alpha}{\theta^2}$ with the exchange enhancement is almost linear in contrast to the prediction of the theory where a quadratic variation is predicted.

Schriempf et al (82) have measured the lectrical resistivity of Pd-Ni alloys with concentrations ranging from 0 to 1.0 at .% Ni between 2 and 20°K.

They fit their low temperature data to the following expression:-

$$\rho = AT^2 + BT^5 \qquad \text{(III.2)}$$

where A and B are two concentration dependent parameters. They observed that A is large and increases with increasing Ni concentration, while B is found to be small and decreasing.

The resistivity of the ferromagnetic Pd-Ni alloys with 2.9, 3.1 and 4.3 at .% Ni, has been measured by Leger and Muir (83) between 2 and 77°K. They fit their data to Eq(III.2) for temperatures up to 20°K for the two dilute alloys and for temperatures up to 30°K for the concentrated one. They plot A/A_{Pd} versus concentration using their data and data from Schriempf et al (82). They argue that the decrease of this quantity after a maximum at the critical concentration (2.3 at .% Ni) is generally slower than the initial increase. They relate this to the removal of some Ni sites from the exchange enhancement process as a result of the clustering of Ni impurities, where Ni-Ni interaction magnetises Ni atoms in a given cluster, thus removing them from the above process. They further observe

a large reduction in the phonon term BT^5 of the two more dilute alloys and attempt without success to relate this to a similar reduction and recovery of the lattice specific heat observed by Chouteau et al (84).

Fluitman et al (85) have measured the electrical resistivity of a series of strongly paramagnetic and weakly ferromagnetic alloys of Ni_3Al near the critical concentration ($Ni_{74.6}\ Al_{25.4}$) below 20°K. The resistivity of all the alloys is found to be very strongly temperature dependent and varies as $T^{1.6}$ between 10 and 20°K and as $T^{1.8}$ around 3°K. They fit their data around 3°K to Eq.(II.79) and calculate θ and α . They find that θ takes its lowest value at the critical concentration in agreement with Schindler and Rice's theory. They further observe that as in the case of Pd-Ni series α goes through a maximum at the critical concentration. In these alloys, as in the Pd-Ni alloys, the coefficient of the T^2 term varies linearly with the exchange enhancement factor $\left(\frac{\chi}{\chi_o}\right)$ which is determined from the susceptibility measurements of de Boer (86).

The low temperature electrical resistivity of Ni_3Al and Ni_3Ga alloys has been reported by Fluitman et al (87). They discuss the behaviour of the alloys with temperature in the light of the existing theories on the scattering of conduction electrons from spin-density fluctuations. They analyze their data at temperatures below 4.2°K using Eq.(II.79) i.e. in terms of Rice's calculation and a simple power law

$$\rho = CT^n \qquad \text{(III.3)}$$

They find that θ goes through a minimum and α through a maximum at the critical concentration. Similar effects are obtained for C and n when they analyze their data in terms of the simple power law. They obtain a value of $n = \frac{3}{2}$ for alloys close to the critical concentration which is somewhat lower than the value predicted ($^5/_3$) by Mathon (78).

For the alloys close to the critical concentration the plot of $\frac{\rho}{c}$ versus temperature gives a universal curve. They further investigate the effect of adding iron impurities to these alloys and find that it results in a decrease of the power n and an increase in C.

Electrical resistivity measurements on Pt-Fe alloys with iron concentration of between 0.03 and ~1 at % over the temperature range from 0.4 to 50°K have been done by Loram et al (88). The alloys containing less than 1 at % Fe have an incremental resistivity which increases approximately logarithmically with concentration. Below 8°K the impurity resistivity of the three most dilute alloys (containing 0.03, 0.05 and 0.1 at % Fe) scales approximately linearly with concentration. For the alloys with less than 1 at % Fe they fit their data for temperatures below 8°K to:

$$\Delta\rho = E + F \ln (T^2 + \theta^2)^{\frac{1}{2}} \qquad \text{(III.4)}$$

where E and F are two parameters depending on concentration approximately linearly and θ is a characteristic spin fluctuation temperature which is found to be 0.4°K for the three most dilute alloys. For the other two (0.3 and 0.6 at % Fe) alloys θ increases approximately linearly with concentration. Correlating the temperature dependent impurity resistivity with the magnetic state of the impurities the authors give a simple phase shift calculation assuming a free electron model for the conduction electrons. They do not take into account the contribution to the impurity resistivity from spin-flip scattering which will affect the magnitude of the resistivity but leave the quantitative behaviour unaffected.

In recent years a number of investigations have been reported on the electrical resistivity of Pd-Mn alloys.

According to the work by Shaltiel et al (89) both dilute Pd-Mn and Pd-Gd alloys undergo transition to a ferromagnetic state at low temperatures. Furthermore, their work and EPR g shifts (90), (91) indicated that the effective host-local moment exchange coupling is positive for dilute Pd-Mn and is negative for Pd-Gd. Therefore according to a naïve application of the Kondo (72) theory, a resistivity minimum should be observed in the dilute Pd-Gd alloys and a logarithmic decrease in Pd-Mn. To test these predictions and to obtain the ordering temperatures of the alloys, Sarachik and Shaltiel (92) have measured the resistivity of Pd-Mn alloys containing $\frac{1}{2}$, 1 and 2 at % Mn and of Pd-Gd alloys with Gd concentration ranging from .1 to 3 at % Gd. In Pd-Mn alloys a sudden change in the resistance-temperature curve at the ordering temperature is observed. But no such behaviour and also no resistance minimum is found in the Pd-Gd alloys.

However, what is really involved in Kondo's calculation is conduction electron-local moment interaction and this is probably positive for Pd-Gd.

Resistivity measurements of Chen et al (93) indicated, contrary to the result of Sarachik and Shaltiel, that Pd-Gd dilute alloys in fact show a magnetic ordering anomaly in the resistivity. For Pd-1 at % Gd this anomaly is at 2.4^{o}K.

Electrical resistivity of a series of Pd-Mn alloys with 1, 2.4 and 2.9 at % Mn has been measured by Williams and Loram (94) between 0.4 and 300^{o}K. In all three alloys the incremental resistivity $\Delta\rho$ ($=\rho_{alloy}-\rho_{Pd}$) shows a sharp transition at the ordering temperatures of the alloys.

Below this temperature $\Delta\rho$ decreases linearly with temperature. At temperatures well below the ordering temperature the incremental resistivity shows a limiting $T^{3/2}$ behaviour. These behaviours are in agreement with the prediction of Long and Turner (69) discussed in Chapter II One aspect of the theory which is not obeyed is the behaviour of the coefficient of the $T^{3/2}$ term with the impurity concentration. The theory predicts that it should vary as $C^{-\frac{1}{2}}$, while experiment shows that its variation is as C^{-1}.

In Pd-Mn alloys the variation of Tc with concentration is unlike those of Pd-Fe and Pd-Co where Tc increases with increasing concentration. In Pd-Mn, Tc first increases and then starts decreasing with further addition of Mn. For this behaviour Williams and Loram suggest two competing mechanisms in these alloys. The first is the relatively long range indirect ferromagnetic coupling between Mn impurities, due to the polarization they induce in the Pd d-band. The second is the direct Mn-Mn exchange coupling which becomes increasingly important with increasing manganese concentration. The direct Mn-Mn coupling should, according to Moriya (95) and Kim (11)) result in an antiferromagnetic coupling. Williams and Loram point out that the competition between the above two mechanisms accounts qualitatively for the behaviour of Tc with Mn concentration.

Niewenhuys and Boerstoel (96) have made careful measurements of the resistivity of Pd-1 at % Mn in the vicinity of the ordering temperature of the alloy which is approximately 3.4°K. The incremental resistivity $\Delta\rho$ is found to be linear in temperature above, as well as below, the ordering temperature Tc. At temperatures very close to Tc they observe a rounding off in the $\Delta\rho$ -T curve. They ascribe the rounding off to local concentration variation which results in a distribution of local ordering temperatures t_c which they assumed to be a Gaussian of the form:

$$\frac{}{e} (tc-Tc)^2/2(F\ Tc)^2 \qquad \text{(III.5)}$$

They determine F by doing a best fit calculation to their data, and show that this procedure is consistent with the experimental results, i.e. the calculation yields a mean transition temperature $\bar{T}_c$ which is equal to Tc, and the measured and the calculated values of the quantities

$$d\left(\frac{\Delta\rho}{dT}\right)\Big]_{T\to Tc} \text{ and } \Delta\rho(Tc) - \Delta\rho(o) \qquad \text{(III.6)}$$

are in very good agreement. They therefore conclude that the definition of Tc, as being the temperature at which $d\left(\frac{\Delta\rho}{dT}\right)$ is maximum, as is done by Kawatra et al (97) for Pd-Fe alloys, is not correct.

The electrical resistivity of dilute Pd-Fe alloys containing less than 1 at % Fe has been measured between 0.5 and 77°K by Williams and Loram (98). The behaviour of the resistivity is very much like that of Pd-Mn alloys, ie. the transition to the ordered state is sharp, below the ordering temperature the incremental resistivity is linear with temperature and at the lowest temperatures it has a limiting $T^{3/2}$ behaviour. The authors therefore analyze their data using the theory of Long and Turner (69) and Yos ida (68). The coefficient of the $T^{3/2}$ term is found to vary again as C^{-1} as in Pd-Mn alloys.

Williams (99) has measured the resistivity of Pd-Co alloys containing between 0.1 and 1 at % Co in the temperature range 0.45-300°K. In almost all respects the behaviour of Pd-Co alloys are similar to those of Pd-Fe alloys. In both these alloys Tc increases with impurity concentration continuously, unlike those of Pd-Mn.

The electrical resistivity of Pd-Co alloys, with concentrations ranging from 2 - 7.5 at % Co, has been measured between 1.4 and 77°K by

Colp and Williams (100). For all the alloys the incremental resistivity is found to vary, at temperatures well below the ordering temperature, as:

$$\Delta\rho = Ac + Bc^{-0.75}\ T^2 \qquad \text{(III.7)}$$

where A and B are two numerical constants. According to the authors this T^2 behaviour is due to a considerable homogeneity in the palladium d-band magnetization at these concentrations. In this case the alloy behaves approximately as a uniform ferromagnet and,hence,its resistance varies as T^2. In the incremental resistivity of Pd-Fe alloys with similar concentration, a T^2 behaviour has also been observed by Skalski et al (101).

The interest in the Rh based alloys started with the observation of an anomalous behaviour of dilute Rh-Fe alloys by Coles (102). In these alloys the incremental resistivity is a strong function of temperature and the residual resistivity per iron impurity is very small, even smaller than that of Fe in Cu. This peculiar behaviour has been explained by the scattering of conduction electrons from magnetic impurities, taking into account their electrostatic potentials. This calculation shows that the exchange interaction between conduction electrons and the electrons of a magnetic impurity J_{s-d} may be written as J_{s-d} Cos 2η, and predicts that η may be larger than $\frac{\pi}{4}$ for iron impurities in rhodium. But this theory does not explain the small residual resistivity of dilute Rh-Fe alloys which is about two orders of magnitude smaller than those of Cu-Fe. The residual resistivity is proportional to $\mathrm{Sin}^2\eta$ as given by Eq(II.76). For Rh-Fe $\eta > \frac{\pi}{4}$ and, hence it is expected to be large contrary, as Nagasawa (103) points out, to the experimental findings.

In order to investigate the relationship between the residual resistivity and phase shift, Nagasawa (103) has measured the electrical resistivity of dilute Rh-Co alloys and found a residual resistivity which

is larger than that of Rh-Fe. However, no satisfactory explanation has been offered by the author.

The electrical resistivity of a Rh-0.5 at % Fe alloy has been measured down to 0.035°K by Labord and Radakrishna (104). They discuss their results in terms of the scattering of conduction electrons from localized spin density fluctuations. This mechanism results in a resistivity which, according to the theory of Kaiser and Doniach (76) behaves as T^2 at temperatures well below the spin fluctuation temperature Θ and as T at temperatures comparable to Θ. Such a behaviour is indeed observed in this alloy for which Θ is found to be 0.5°K in reasonable agreement with the value predicted by Kaiser and Doniach, who deduced this from a comparison between high temperature data on Rh-Co and Rh-Fe.

However, examination of more dilute alloys by both the Grenoble Group and Rusby (105) show that at 0.5 at %, Θ in Rh-Fe is already being depressed by interactions. A T^2 behaviour is found in the resistivity up to approximately 2°K for concentrations of about .1 % Fe.

Electrical resistivity of a series of Ni-Rh alloys in the region of the critical concentration ($\sim Ni_{62}$-Rh_{48}) has been measured by Houghton et al (106) in the temperature range from 2 to 700°K. In all alloys the variation of resistance with temperature is similar. At temperatures where the phonon contribution is negligible the resistivity varies as T^2 up to a certain temperature which is lower the closer the alloys is to the critical composition. Above this temperature the variation is linear. The authors discuss their results in terms of the theory of Kaiser and Doniach (76) which is formulated essentially for dilute nearly magnetic impurities in a metallic host. They argue that, although in Ni-Rh alloys there are localized magnetic moments contained within giant polarization clouds, it is reasonable to expect that there are large numbers of Ni atoms whose local environments are such that they are not yet magnetized, but are close

to the ferromagnetic transition. Hence, spin fluctuations may exist in Ni-Rh alloys but selectively on those Ni atoms which are not yet magnetized.

3. MAGNETIZATION AND SUSCEPTIBILITY

The alloys of the exchange enhanced metals such as Pd with some of the iron group metals have unusual magnetic properties. The magnetic moments per impurity atom are large. In the case of Pd the so-called giant moments are observed. Although the presence of giant moments for Fe and C_o impurities were noted in the early works, recent investigations have shown that Mn too produces giant moments in Pd. The analysis of the susceptibility data of these alloys is difficult due to the temperature dependence and the enhancement of the Pd susceptibility.

In one of the early measurements of the susceptibility of the alloys of Pd with Fe, Co, Ni and Mn, Shaltiel et al (89) were forced to assume that the magnetic moment associated with a magnetic impurity is a linear function of the susceptibility of the pure Pd. They took this relationship to be of the following form:-

$$p(T) = P_o\left[\, 1 + \alpha\chi_o(T)\right] \qquad \text{(III.8)}$$

where p_o is the unenhanced magnetic moment, α is the enhancement factor and $\chi_o(T)$ is the pure matrix susceptibility. They further assumed a certain value for the enhancement factor. Only after these were they able to fit their data to a Curie-Weiss law $\chi = \chi_o + \frac{C}{T-\theta}$ at temperatures above 100^oK. However, they found that this procedure could not give a unique value for the enhancement factor because little change was observed between the slopes corresponding to very different values of the enhancement factor.

The authors measured the susceptibility of Pd-Ni alloys containing up to 3.5 at % Ni. They showed that the alloys containing up to approximately 2 at % Ni are not magnetic. Above this concentration the alloys showed a Curie-Weiss behaviour. For the alloy containing 3.5 at % Ni they obtained a Curie temperature of 40^oK from $\frac{H}{M}$ versus M^2 and of 45^oK from the intersection

of $\frac{1}{(\chi-\chi_o)}$ with the temperature axis. An alloy of Pd-Mn containing 3 at % Mn was also studied and was found to have a Curie temperature of 8°K. For this alloy a value much smaller than those used for Fe, Co impurities for the enhancement factor was found to be sufficient to get a linear $(\chi-\chi_o)^{-1}$ dependence on temperature. From the slope of the curve a value of $6.3\mu_B$ is obtained for this alloy at 80°K for the effective moments.

Shaltiel et al (89) also measured the susceptibility of rare earth impurities in Pd. For these alloys it is found that the total alloy susceptibility can be decomposed as:-

$$\chi = \chi_o + \chi_{ion} \qquad \text{(III.9)}$$

where χ_o (the background susceptibility) is obtained by measuring the susceptibility of Pd alloys in which rare earth is replaced by Lu. This is found to give a linear dependence of $(\chi-\chi_o)^{-1}$ on temperature. The effective Bohr magneton per impurity, obtained from the slope of the curve $(\chi-\chi_o)^{-1}$ versus temperature is very close to the free ionic value. The background susceptibility χ_o at room temperature is found to be as large as 40 to 90% of the total susceptibility. Therefore, the authors give less weight to these temperatures.

Crangle and Scott (107) have measured the magnetization and the susceptibility of some of the dilute alloys of Pd and Pt with Fe, Co, Ni and Gd in fields up to 20kG, and at temperatures between 1.5°K and the respective Curie temperatures of the alloys. They obtained the spontaneous magnetization M(T,O) of each alloy at various temperatures from the linear extrapolation to H=o of the high field part of $\left[M(H,T),H\right]$ isothermals and the saturation magnetization M(o,o) from the extrapolation of the graphs of M(o,T) against T^2 to where T=o. From M(o,o) the number of Bohr magnetons per atoms is calculated. The Curie temperature of each alloy is determined

from the graphs of $(\frac{H}{M})$ against M^2 at different temperatures. In this type of analysis the graph plotted at $T=T_c$ passes through the origin.

For the Pd-Ni alloys the Curie temperatures obtained by this method are plotted in Chapter V , Fig.(V.18) versus concentration, using additional data from other sources.

Crangle and Scott (107) observed the following for their alloys:-

(a) Ferromagnetism exists in some of the alloys even in very dilute impurity concentration (0.15 at % Fe in Pd still produces ferromagnetism);

(b) The rise of the Curie temperature with the impurity concentration is, in all the alloys, very rapid;

(c) The magnetic moment per solute atom is always larger than the value associated with the bare impurity.

In some cases the moment per impurity rises to such a high value that it cannot possibly be associated with the solute atom, since in these elements the magnetism arises from the unfilled 3d shells which can lead to a maximum moment of $5\mu_B$ for a single atom. The authors explain these properties as follows: A solute atom having a localized moment interacts with its nearest neighbour solvent atoms and polarizes primarily their d-band which has a high density of states. This polarization is expected to extend over a large distance from the impurity atom. The magnetic ordering of these alloys in the dilute limit is the result of the ferromagnetic interaction between these long range polarization clouds. In the very dilute alloys a smaller moment per atom is observed. This the authors argue occurs because at these concentrations some of the polarization clouds are decoupled from the magnetization of the whole speciment. In small fields, not all the moments are polarized. This is evinced from the observation that in most dilute alloys the magnetization-field isothermals are markedly curved

in fields of up to 20kG. Therefore, if very high fields are used this decrease would not occur.

On the high concentration side of impurities a reduction in the size of the moment is observed. Crangle and Scott associate this with the fact that each host palladium atom has only 0.36 holes. After these are polarized the addition of impurities does not contribute to the polarization process and, hence, the size of the moment reduced.

The authors have also measured the susceptibility of some of the Pd-Gd alloys. The moment per Gd impurity obtained is found to be less than the free ionic value. They attribute this to a probably negative polarization of palladium d-electrons by the moments on the Gd impurities. In these alloys the Curie temperature changes very slowly with Gd concentration.

Chouteau et al(84) have measured the susceptibility of Pd-Ni alloys containing up to 10 at % Ni at temperatures from 0.05°K to 4°K in fields of up to 35kG. They found that at high fields and at temperatures below 2°K the M-H isothermals become linear, therefore they split the magnetization into two terms

$$M = M_m(H,T,c) + \chi(c)H \qquad \text{(III.10)}$$

where $\chi(c)$ represents the paramagnetic susceptibility of the alloys which is independent of external magnetic field H and temperature for T 2°K. M_m is found to saturate easily for any concentration c if H >20kG. Below 1.5 at % Ni the saturation value of M_m is found to be constant corresponding to the saturation magnetization of about 70ppm iron impurity. Above this concentration the saturation magnetization increases rapidly with Ni concentration, thus indicating the presence of magnetic Ni atoms. The relative

increase of the paramagnetic susceptibility $\frac{(\chi_{Alloy}-\chi_{pd})}{\chi_{pd}}$ with Ni concentration rises to a maximum of about 2.5 at % Ni then decreases. This concentration is, of course, close to the value where the Pd-Ni alloy system makes a transition into long range ferromagnetic ordering.

In the Pt-Ni alloy system the transition to long range ordering takes place at a very high Ni concentration (~41 at % Ni). The magnetization measurements on the Pt-Ni alloys with Ni concentration ranging from 25 to 50 at % Ni have been done by Besmus and Herr (108). The alloys with more than approximately 41 at % Ni are ferromagnetic. Their respective Curie temperatures are obtained by means of M^2 versus $\frac{H}{M}$ plots which are found to be linear. The alloys with $41<c<37$ at % Ni are strongly enhanced paramagnets. For these alloys the linear parts of the M^2 versus $\frac{H}{M}$ plots start at increasingly higher fields. Below 37 at % Ni the M-H isothermals are linear. The initial susceptibility χ_i, obtained from the intercept of the straight line with the $\frac{H}{M}$ axis, peaks in the vicinity of $C_F \sim 41$ at % Ni. In the lowest temperature (1.4^oK) for the ferromagnetic alloys a marked increase of M with field is found. This and the fact that no curvature is observed in the M^2 versus $\frac{H}{M}$ plots at low fields lead the authors to characterize these alloys as weak itinerant ferromagnets. They further observe that there is a linear relationship between the concentration and Tc^2, χ_i^{-1} and the square of the spontaneous magnetization $M^2(T,o)$. Such relationship are derived by Mathon (78) for spatially homogenous ferromagnets. The authors therefore conclude that in their alloys the magnetization is spatially uniform.

Magnetization and susceptibility measurements on Pd-Mn alloys containing between 0.5 and 25 at % Mn have been done by Rault and Burger (109). The variation of the transition temperature and the magnetization of the alloys at 4.2^oK in a field of 6kG show a gradual transition from ferromagnetism to antiferromagnetism. The authors argue that above 8 at % Mn the ordering

is antiferromagnetic. However, we found that here the alloys are spin glass over a considerable concentration range. For ferromagnetic alloys no remanent magnetization is observed. The authors attribute this to a very small anisotropy energy. For the alloys with more than 8 at % Mn, hysteresis behaviour is observed. This behaviour is,of course, a property of what is lately known as "spin glass". The alloys with high Mn content are expected to show antiferromagnetism due to antiferromagnetic coupling of Mn impurities as suggested by Moriya (95) and Kim (11).

Until recently it was thought that manganese does not produce giant moments in palladium. Recent work by Star et al (110) showed that manganese produces a giant moment of approximately $7.5\mu_B$ per Mn atom . A diffuse neutron scattering experiment by Coles (private communication) also shows clearly the existence of giant moments. Star et al.measured the magnetization of a series of Pd-Mn alloys containing between 0.05 and 2.5 at % Mn at liquid helium temperatures in fields of up to 210kG. They were able to saturate the impurity moments of all the alloys at $1.3^{o}K$ with fields of $H \geq 30kG$. However, they could not saturate the moments of the alloys with concentrations of more than about 1 at % Mn at $4.2^{o}K$ even in the maximum field employed

The moment, in the dilute alloys ($c \leq 0.5$ at % Mn) that could be saturated at $4.2^{o}K$ was found to be approximately 7.5 Bohr magneton per manganese atom. Choosing a spin value of $S = \frac{5}{2}$ which is found from the entropy of Mn in Pd by Boerstoel et al (111), the authors were able to account for the behaviour of the magnetization M(H,T) of the alloys with less than 0.23 at % Mn (inclusive) using the Weiss molecular field model which required a g value of about 3. The Curie temperatures obtained from the molecular field model, were found to be consistent with the values found experimentally.

Magnetic measurements on a series of Ni_3Al and Ni_3Ga have been done by

De Boer (86). He obtained the initital susceptibility and the Curie temperatures of the alloys from the plot of M^2 versus $\frac{H}{M}$. The saturation magnetizations were also obtained from these plots. De Boer was not able to saturate the magnetization of the alloys at 4.2°K even at 200kG. In these alloys the plots of M^2 versus $\frac{H}{M}$ are perfectly linear at all temperatures up to 77°K, and the inverse susceptibility has a Stoner type behaviour. This and the T^2 dependence in the decrease of the spontaneous magnetization with increasing temperature, has lead De Boer to describe the magnetic properties of these alloys in terms of the itinerant electron model satisfactorily.

Susceptbility measurements on dilute Rh-Co alloys have been done by Walstedt et al (112), Murani (113) and by Nagasawa (103). They find a weakly temperature dependent excess susceptibility due to cobalt impurities. Walstedt et al (112) associate this with local exchange enhancement on the cobalt sites. Nagasawa has made a Curie-Weiss fit to his data for Rh-1 at % Co, and obtained an effective moment of $5\mu_B$ per cobalt impurity and a Curie-Weiss temperature of $1200^{\circ}\pm100^{\circ}$K. Murani has measured a Rh-Co alloy containing 11 at % Co, and found that the temperature dependence of the excess susceptibility is similar to that of dilute alloys. He has concluded that the threshold value for moment formation is at a much higher concentration.

It has become evident from recent investigations that numerous properties of Cu-Ni and Rh-Ni alloys are affected by clustering. Therefore, in the recent works this aspect of the alloys is brought into the procedure of analysis and satisfactory explanation of the experimental results has been possible.

The magnetic measurements on paramagnetic Cu-Ni alloys have been made

by Kouvel and Comly (114). They measured the initial susceptibility χ_i, of the alloys at different temperatures and observed that away from the critical concentration ($\sim$ 43 at % Ni) χ_i not only gets smaller but becomes more nearly constant. They fit their data to:-

$$\chi_i = \chi_o + \frac{C}{T-\theta} \qquad \text{(III.11)}$$

where χ_o is the background susceptibility and the second term is attributed to the superparamagnetism of large polarization clouds. χ_o is found to vary slightly with concentration in the region of the critical concentration, but does not show any singularity. The lack of singularity leads the authors to conclude that, in these alloys, the critical enhancement occurs while the alloys are still paramagnetic. From C they obtained an average magnetic moment per cluster of the order of 10-12μ_B, and an average cloud concentration, defined as being the number of clouds divided by the total number of atoms, which increases from 0.012% at 32 at % Ni to about 0.34% at 44 at % Ni. The authors concluded that the formation of the clouds occurs in local highly Ni rich regions and that the long range ordering is caused by the ferromagnetic coupling of these clouds.

Magnetization measurements of Ni-Cu alloys containing between 0 and 60 at % Cu on fields of up to 60kG, and in the liquid helium range have been made by Acker and Huguenin (115). They split the measured magnetization into three components:-

$$M(H,T) = M_o + \chi_o H + \sum_i N_i M_i \left(\text{Coth} \frac{M_i H}{k_B T} - \frac{k_B T}{M_i H} \right) \qquad \text{(III.12)}$$

where N_i and M_i are the numbers and the magnetic moments of the clusters, M_o is the ferromagnetic contribution to the magnetization, and the second term is the paramagnetic band contribution. In high fields they approximate (III.12) by

$$M(H,T) = \chi_o H + \left(M_o + \sum_i N_i M_i\right) - \frac{k_B T}{H} \sum_i N_i \qquad \text{(III.13)}$$

and from a least squares fit obtain the values for χ_o, $(M_o+\sum_i N_i M_i)$ and $\sum_i N_i = N$, the density of clusters. The result of analysis shows that χ_o presents a singularity at c≃43 at % Ni which is the critical concentration for ferromagnetism.

Magnetic measurements on Rh-Ni alloys with nickel content varying between 0 and 100 at % Ni have been made by Buchler et al (116). The initial susceptibility is found to vary as $(C-C_F)^{-1}$ and to have a maximum at the critical concentration $C_F \simeq 63$ at % Ni. The enhancement in the susceptibility is found to be approximately 70 at this concentration. The authors explain their experimental findings in terms of the interaction between conduction electrons and low lying spin excitations (paramagnons) in nearly ferromagnetic metals. It has been shown by Doniach and Engelsberg (79) that this interaction gives rise to an effective mass which increases with the enhancement factor: $(1-\bar{I})^{-1}$. Hence, the susceptibility (the enhancement factor) reaches its maximum value when the effective mass (specific heat) is maximum.

Measurements on three Rh-Ni alloys containing 58, 60 and 62 at % Ni have been made by Muellner and Kouvel (117) in fields of up to 56kG and at temperatures down to 4.2°K. They analyzed the total susceptibility into a temperature independent matrix term χ_o and a Curie-Weiss component. The matrix susceptibility is found, as in the case of Cu-Ni alloys, to be insensitive to the impurity concentration. They therefore concluded that the ferromagnetism arises entirely from the Curie-Weiss component which is attributed to the giant polarization clouds. The analyses of Kouvel and Comley (114) and Muellner and Kouvel (117) indicate that both in Rh-Ni and Cu-Ni there is a tendency towards an antiferromagnetic coupling (negative θ) between the polarization clouds when the alloys' compositions become more

rhodium or copper rich.

The class of alloys, of which Cu-Mn is a typical example, have some unusual magnetic behaviours. At very low temperatures the spin orientations are frozen out without any well defined long range orderings. If a specimen is cooled well below certain temperatures Tm in a zero applied field, and measurements are made at increasing temperatures in a constant field, the magnetization shows a maxima at Tm. In constrast, if the measurements are made in a constant field from above Tm, the magnetization first increases toward a maxima around Tm then stays approximately constant there. In some alloys it may increase further. The increase is usually steeper if the alloy is cooled in a higher field.

In recent years a large number of alloys showing these effects have been discovered. They were first found in Cu-Mn and Ag-Mn alloys by Owen et al (118). They were able to fit their high temperature susceptbility data to a Curie-Weiss low $\Delta\chi = \frac{C}{T-\theta}$ and found that the paramagnetic Curie temperatures θ of the alloys were close to their respective susceptibility maxima temperatures, and were always positive. Tm (and hence θ) was found to increase with Mn concentration. The Curie constant C was found to correspond to a spin value which lies between S = 2 and S= $\frac{5}{2}$. They cooled from 77°K two alloys containing 1.4 and 5.6 at % Mn in a field of 5kG to helium temperature and obtained a remnant magnetization which decayed exponentially as the temperatures were increased, vanishing at the respective Tm of the alloys. When cooling the alloys in a zero field down to 4.2°K and, subsequently increasing the field to 5kG the magnetization was found to be proportional to the field. When the field was then reduced to zero, there remained a very small magnetization, i.e. the alloys showed hysteretic

behaviour. In spite of these observations Owen et al (118) concluded that in the Cu-Mn alloys they studied there is a gradual transition to antiferromagnetism.

Magnetization measurements on Cu-Mn alloys containing less than 2 at % Mn have been carried out by Schmitt and Jacobs(119). The analysis of the high temperature data of these authors agrees well with those of Owen et al. All the samples containing 0.4 at % Mn or more were seen to exhibit hysteresis at liquid helium temperatures. They cooled a Cu-Mn alloy containing 1.8 at % Mn ($T_m \sim 15^{\circ}K$) in different fields from above $77^{\circ}K$, and found that a saturation value for the remanence could be achieved in fields larger than 5kG. Subsequent work by Kouvel (120) on Cu-Mn and Ag-Mn alloys of Mn concentration about 25 at % showed further that when the specimens are cooled in a zero field the magnetization is proportional to the field for negative as well as positive fields. However, if they are cooled in a field then hysteresis curves are obtained which are displaced from their symmetrical position. In the latter case it was found that the M-H line was parallel to the line obtained from the M-H plots after cooling the specimens in zero field. These and the previous observations by Schmitt and Jacobs and by Owen et al lead Kouvel to explain the observed effects in terms of a microscopic exchange anisotropy. According to this model the ferro-and antiferromagnetic interactions between Mn atoms of different separation gives rise to a mixed magnetic state in these alloys. Magnetization and susceptibility measurements have been done on Rh-Fe alloys by Murani and Coles (121). Alloys containing 3 at % and more Fe show magnetic properties similar in many respects to those of Cu-Mn and Ag-Mn. Here too a maximum was found in the plot of the susceptibility versus

temperature which broadened with increasing impurity concentration. The temperature of the susceptibility maximum,Tm, was seen to increase with increasing iron concentration. When alloys with high Tm were cooled to helium temperature in a zero field a linear M-H plot was obtained. However, when the same alloys were cooled in a field the M-H plots were found to be displaced from the origin (i.e. a remanence is obtained at H=o) and a hysteresis loop enclosing a very small area was observed.

The remanent magnetization was found to decrease with increasing temperatures, disappearing completely around the temperature of the susceptibility maximum. When cooling an alloy in a field the susceptibility rose to a maximum at Tm of the alloy, but did not remain constant there. A further increase was observed with decreasing temperature, the rise being sharp.er for higher fields.

Magnetization measurements of Bancroft (122) on Au-Co alloys containing 5 and 7 at % Co, show that in these alloys too, susceptibility maxima, hysteretic magnetization curves, time and temperature dependent remanence are present. Dilute alloys of cobalt with gold form a weak moment in the sense that in these alloys there is a weak temperature dependent moment, indicated by a large negative θ obtained from the fit to a Curie-Weiss law $\frac{C}{T-\theta}$ of high temperature data. If Tm is taken to be a measure of the strength of interaction between moments, its variation with Co concentration is found to be slower than those of good moment systems such as Au-Fe. This further confirms that cobalt in gold cannot be included into the class of strong moments such as iron or manganese in gold.

It has been shown by Chakravorty et al (123) that the alloys of Pd-Cr containing Cr ranging from 25 to 35 at % and V-Mn containing 50 to 76 at % Mn demonstrate some of the effects common to the alloys reviewed in this section. In these and other alloys mentioned above the authors consider

the possibility that magnetic clusters with giant moments might be present.

A brief review of investigations on this subject is given by Beck (124).

4. SPECIFIC HEAT

The first specific heat measurement to be done in order to observe the electron-paramagnon mass enhancement effect was by Bucher et al (116). They investigated Rh-Ni alloys which are paramagnetic between pure Rh and Rh-63 at % Ni. The alloys with more than 63 at % Ni are ferromagnetic. The paramagnetic alloys are exchange enhanced, and the enhancement is greater in alloys containing more Ni. The alloys containing between 60 and 63 at % Ni are strongly enhanced paramagnets. The susceptibility and the coefficient of the linear term in the specific heat γ, peaks about Rh-63 at % Ni. Although both γ and χ are enhanced considerably, the authors point out that the enhancement of χ at the critical concentration is $\simeq 70$ while that of γ is 2.

More significant, however, was that the specific heat showed an upturn below $8^{\circ}K$ when plotted in the usu al way, i.e. when $\frac{C}{T}$ is plotted versus T^2. This effect was found to decrease on either side of the critical concentration. Such an upturn is predicted by Engelsberg and Doniach (79) as has been discussed in Chapter II, section III.

However, there is now evidence that in the Rh-Ni alloys, near the critical concentration, giant magnetization clusters are present which can provide an alternative explanation for the effect observed in the low temperature specific heat.

A more suitable system for the observation of the effect of the electron-paramagnon interaction on the specific heat is Pd-Ni alloys. In this system the alloys containing between 0 and 2.3 at % Ni are paramagnetic with susceptibilities that increase rapidly with increasing Ni concentration, and no giant magnetization clusters are present in these alloys. The

specific heat measurements of Schindler and Macliet (125) and Chouteau et al (84) show no upturn in plots of $\frac{c}{T}$ versus T^2, i.e. no $T^3 \ln T$ term was observed in these alloys. This fact has been explained by Schindler (126) as follows: The coefficient of the $T^3 \ln T$ term (Chapter II, Eq.II.102) in dilute alloys is approximately that of pure Pd times a factor of $\frac{3c}{2\eta}$. This is about 2.6 for the alloy: Pd-2 at % Ni. The author therefore concludes that, since a $T^3 \ln T$ term is not observed in pure palladium, it is unlikely that it would be observed in paramagnetic Pd-Ni alloys.

However, the data of Chouteau et al (84) and Schindler and Macliet (125) shows that specific heat peaks on the ferromagnetic side of the critical concentration. Chouteau et al (84) have further observed that the Debye temperature θ_D first increases and then decreases with nickel concentration. In Pd-10 at % Ni, θ_D reduces to that of pure palladium.

Specific heat measurements on Pt-Ni alloys containing between 1 and 12.8 at % Ni have been made by Macliet et al (127) at temperatures between 1.2 and 4.2°K. The data fit well to a relation of the form $c = \gamma T + \beta T^3$ where the coefficient γ increases linearly with nickel concentration. The coefficient β of the T^3 term is found to decrease significantly with increasing nickel concentration.

We conclude that clear evidence for the presence of a $T^3 \ln T$ term, expected from electron-paramagnon interaction in the low temperature specific heat of the exchange enhanced metals and alloys has not yet been obtained.

The low temperature specific heat measurements on five Pd-Mn alloys containing between 0.08 to 2.45 at % Mn has been made by Boerstoel (128). Except for the most dilute alloy a sharp peak is observed when measurements are done in zero applied field. This system is quoted by Boerstoel, to

be the only dilute magnetic system to show such a sharp peak. Such a sharp peak, of course, implies that the interaction between the manganese impurities is uniform. Boerstoel analyzes his data using molecular field model of the specific heat, and showsthat the theory gives a very good description of the alloys when they are placed in large magnetic fields which can suppress the influence of short range ordering.

CHAPTER IV

APPARATUS AND EXPERIMENTAL METHODS

I. ELECTRICAL RESISTIVITY

1. Introduction:

The electrical resistivity measurements were made by the standard four probe dc potentiometric technique in the temperature range from 1.6 to 40°K. In some cases measurements were made at temperatures lying outside this range.

A Tinsley potentiometer of Diesselhorst pattern, together with a Tinsley photocell galvanometer amplifier is employed. The power supply is a bank of lead-acid accumulators. A high dissipation resistance box is used in the current circuit to obtain a steady current.

The magnetisation and susceptibility measurements were made with a vibrating sample magnetometer in magnetic fields up to 7.5 Kilo Gauss and at temperatures between 1.6 and 300°K.

2. The Design of Cryostat and the Dewar System

The previous "two concentric cans arrangement"+ is modified here Fig.(IV.1). The tufnel disc, onto which the specimen holders are positioned in a symetrical fashion, is suspended from the main top plate by a $\frac{3}{8}$" diameter tube made of German silver which has an 0.006" wall thickness. A Copper can with a wall thickness of approximately 0.05" slides onto the tufnel disc from above. The block of araldite,

---

+: R.V. Bellau. Thesis. University of London 1963

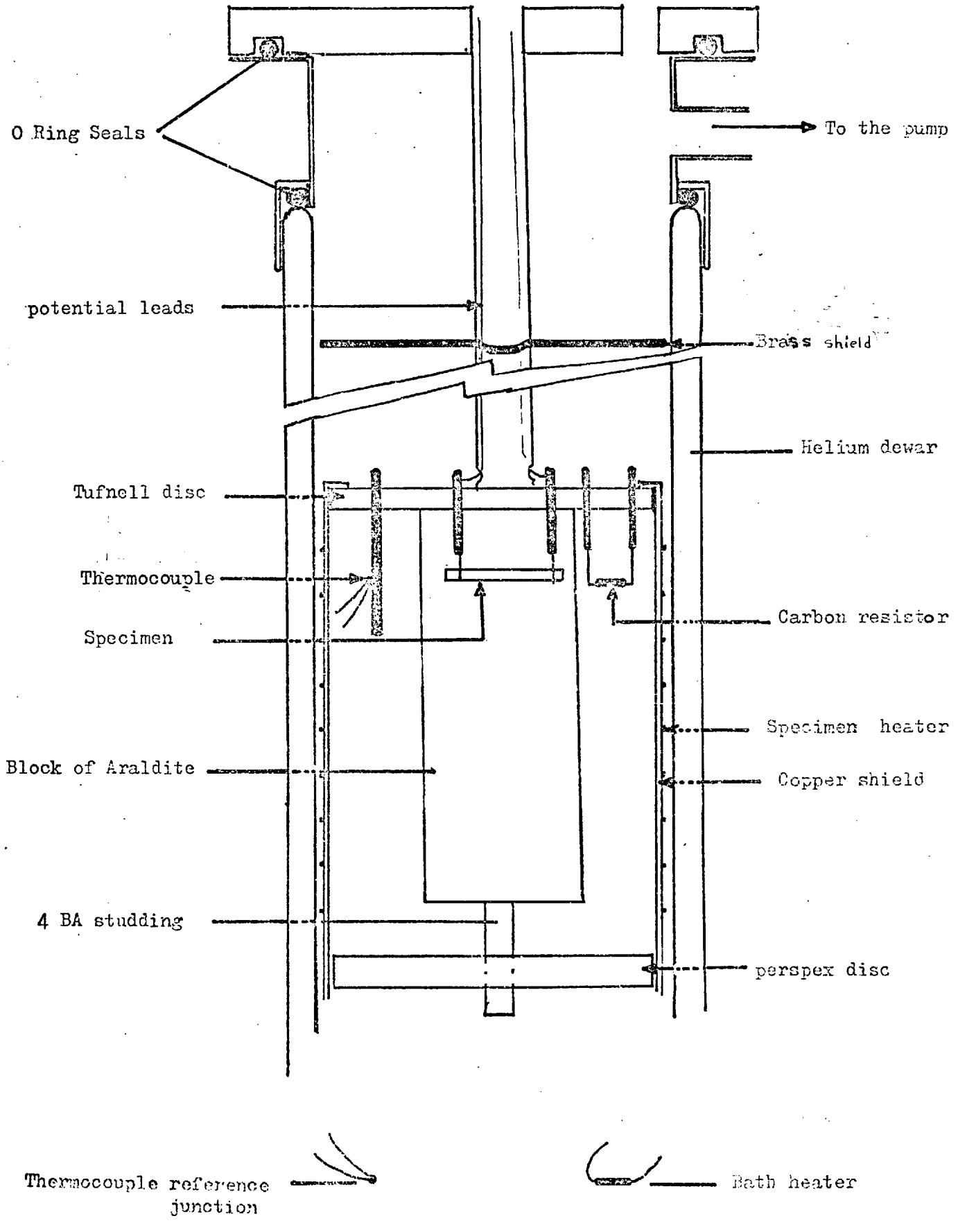

Fig (1.1) The cryostat

cast with 4BA studding in the centre, and machined into a perfect cylidrical form for reasons of symmetry, is screwed onto the centre of the disc from below. The lower end of the can is closed with a perspex disc which is also screwed onto the studding, thus forming the specimen chamber which can accomodate five holders.

Holes are drilled in the perspex disc to let helium gas into the specimen chamber during warm-up.

An opening of approximately 3 mm between the dewar and the copper can ensures the free flow of helium gas. A brass shield of circular form fixed onto the main tube approximately 10 cm above the copper can, acts as a shield against the radiation.

A length of insulated constantan wire of 36 S.W.G. is wound uniformly along the full length of the copper can using G.E. varnish. This is used as a specimen heater. The bath heater, a wire wound resistor of 100 Ω , is at the bottom of the inner dewar. The block of araldite ensures steady warm-up due to its high specific heat at low temperatures. The potential leads are 40 S.W.G. enamel coated copper wires, which are brought down through the main supporting tube, and where they emerge from the top are brought out through a short length of small bore brass tubing and sealed with araldite. At regular intervals holes are drilled in the main tube to prevent thermal oscillations when the system is immersed in helium.

Each current lead consists of seven single eureka wires of 26 S.W.G. They and leads for the heaters are brought into the inner dewar via a lead-through soldered onto the main top plate.

The dewar system consists of a conventional glass double dewar. The top of the cryostat forms an "O" ring seal with the inner dewar. Nitrogen is used in the outer dewar to reduce the flow of heat into the helium dewar.

3. Thermometry

At the start of this project we intended to find among other things, the critical concentration of the Pd-Ni and Rh-Co alloy systems. Hence great importance was attached to the very low temperature region. For this reason a carbon resistor and an Au + 0.03% Fe versus Chromel (Ni_{90} Cu_{10}) thermocouple were employed for the thermometry.

(a) The Thermocouple

We chose from among the three usefull low temperature thermocouples the Au + 0.03% Fe-Chromel thermocouple for it is very stable, and retains a thermoelectric power in excess of 10 μV/°K at all temperatures greater than 1°K. The other two; Au + 2.1% Co-Cu, and the copper constantan are sufficiently sensitive only at temperatures $\gtrsim$ 20°K. The reference junction of the thermocouple was at helium temperature for the temperature range from 4.2 to 77°K. The other junction was fixed at a position which was thermally equivalent to those of the specimens.

Using a D.C. amplifier, with a large input impedence (approximately 10 K Ω), having a noise level less than 1 μV and a DVM, the thermocouple e.m.f's were directly read in micro-volts, the corresponding temperatures were obtained from a calibration curve plotted using data given by Berman et al.(129). Using the nitrogen boiling point as the reference temperature the entire temperature range from 77°K up to room temperature could be covered.

(b) The Carbon Thermometer

An Allen-Bradley resistor of nominal value 47Ω , (1/4) watt is used as the primary thermometer. This is wound by its lead-out wires and then G.E. varnished onto a short, thick, insulated copper wire in

the specimen circuit. These resistors are very sensitive in the temperature range from 2 to 25°K. Their resistance-temperature relationship is assumed to be of the form:-

$$\text{Log } R + A/\text{log } R = B + C/T \qquad \text{(IV.1)}$$

as originally suggested by Clement and Quinell (130). A, B and C are three parameters to be determined by calibration for a given resistor. For this the values of the resistor at temperatures below 4.2°K and above 25°K, usually nitrogen boiling point, must be known accurately.

The nitrogen temperature value of the resistor is obtained simply by dipping it into a can of fresh nitrogen. To obtain its values in the liquid helium range the circuit shown in Fig. (IV.2) is used.

The circuit is constructed in such a way that the range of temperatures from 1.6 to 25°K is divided into three to obtain better sensitivity. For each temperature range, the galvanometer deflection was calibrated in terms of resistance by replacing the carbon resistor with a resistance box.

The calibration of the carbon thermometer is fairly simple. The values of the resistors at known temperatures below 4.2°K were obtained sufficiently accurately from the deflections of the galvanometer. Then the quantities $\text{Log } R + A/\text{log } R$ were plotted against $\frac{1}{T}$ at each temperature assuming a certain initial value for A which is usually close to 2.5. This procedure was repeated for different values of A until the graph was straight and passed through the points corresponding to the nitrogen and room temperatures. The value of A corresponding to this is the best. From the gradient and the intercept of the straight line with the $\frac{1}{T}$ axis the other two parameters, B and C, were obtained. These three parameters completely define the resistance-temperature calibration. For accuracy the calibration was also checked on a computor. This procedure was repeated fairly often, though it was found that the same resistance

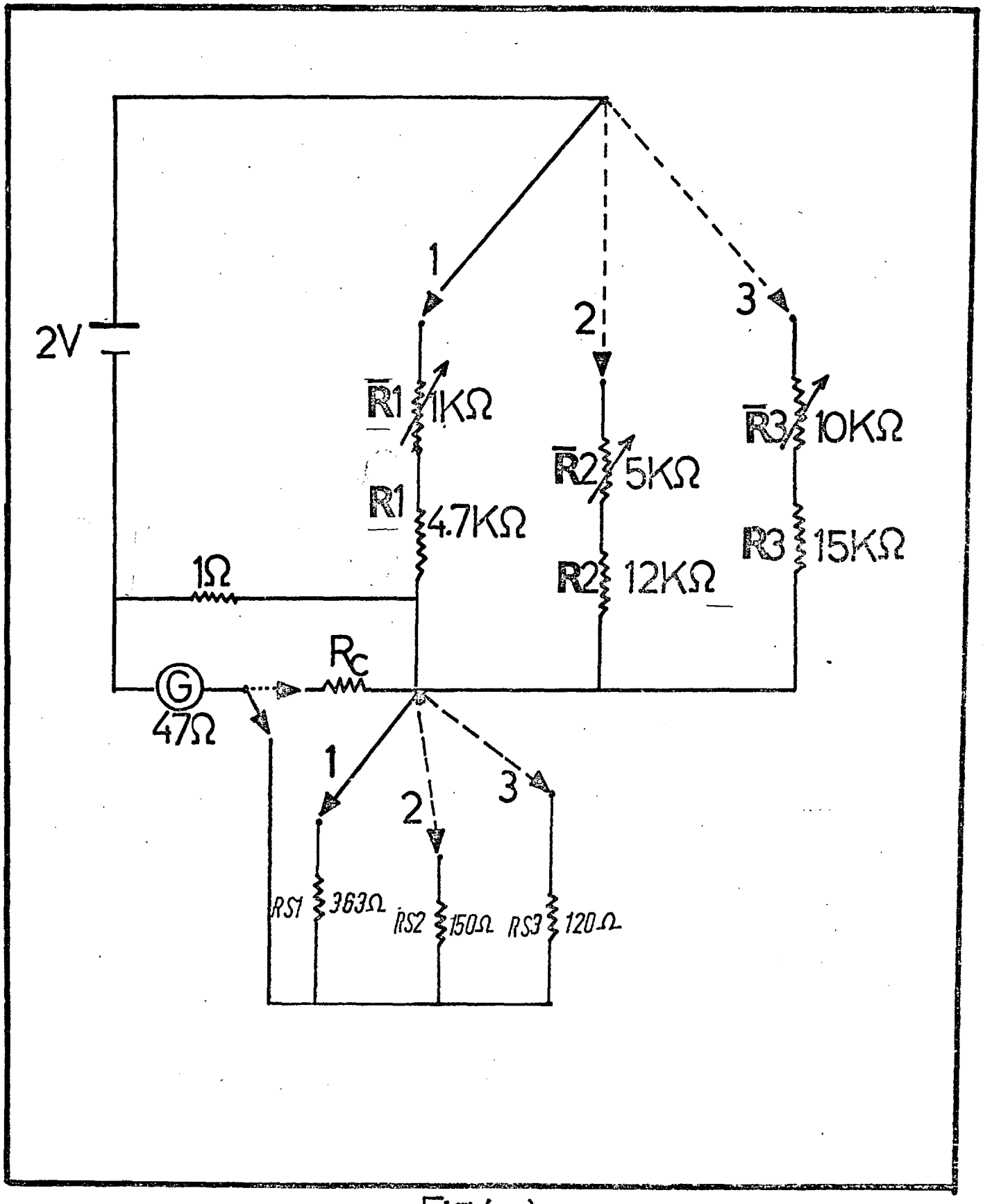
2V
1
2
3
R1 1KΩ
R1 4.7KΩ
R2 5KΩ
R2 12KΩ
R3 10KΩ
R3 15KΩ
1Ω
Rc
G
47Ω
1
2
3
RS1 363Ω
RS2 150Ω
RS3 120Ω

Fig (IV.2)

temperature calibration was reproducible over a long period of time.

4. Temperature Control

In the liquid He range the temperature is controlled by maintaining a constant pressure in the inner dewar using a rubber diaphragm type monostat .

Between 4.2 and 77°K the temperature is controlled in the following manner. First using the bath heater, the helium level is lowered to below the specimen chamber. It then remains there for a very longtime. Following this a suitable rate of warm-up is selected by dissipating an appropriate amount of power in the specimen heater. Return to a lower temperature could be made by boiling some helium from the residual helium pool. In this range the temperature indicated by the carbon thermometer is compared with that of the thermocouple. For a warm-up rate of 10°K/hour the two agreed to within $\pm$ 0.1°K upto 20°K. In a very slow warm-up procedure the agreement was even better.

Above 20°K we relied on the thermocouple though the carbon thermometer was still used as a check on the former. Above 77°K the measurements had to be made while cooling down very slowly. This was achieved by pumping very hard on the helium interspace with a rotary pump. Some nitrogen was then put into the nitrogen dewar and its level raised gradually. Helium was used in the inner dewar as the exchange gas.

However it must be noted that the resistance measured in this way is approximate.

5. The Resistance Measuring Equipment

The resistance measured by the standard four probe technique is that of the part of the specimen lying between the two points where the

potential leads make contact with it. The contact and lead resistances of the potential leads are not part of the resistance to be measured because in the null potentiometric method used here the leads carry (no) negligible current in the (perfect) balance position. Thus in this way the potential developed across a specimen is measured in the open circuit mode. All four leads of pure platinum wires of approximately 0.006" diameter, were spot welded onto the specimen. These were then attached to a specimen holder using a low melting point tin-lead eutectic solder (50 wt% of each metal melted together in a crucible and then quenched in water).

The measurements were made on a five decade Tinsley potentiometer of Diesselhorst pattern, together with a Tinsley type 5214 galvanometer amplifier and a secondary galvanometer. The latter was used as null indicator. The lowest decade of the potentiometer is of 0.1 μ V steps, and by adjusting the sensitivity of the galvo-amplifier a total potential of up to 10 mV could be measured to 10^{-8} volts. All specimens, together with a very high precision four terminal standard resistor and a high dissipation resistance box, were connected in series to a battery. The resistance box was used to set current and also act as a buffer resistance. The battery provided a current stable to better than 2 parts in 10^5 for 10 to 15 minutes which was much longer than the time required to make a set of measurements. The potential leads were brought out to a Tinsley selector switch which was immersed in oil to minimise switching thermals. The specimen resistance is obtained by comparing the potential drop across it with that across the standard resistor. Thermal E.M.F's in the potential leads are eliminated by simultaneous reversal of the potentiometer and the specimen currents with an oil filled type 4092 thermo-electric free Tinsley reversing switch. The E.M.F's in the potentiometer circuit are eliminated by the Diesselhorst design.

6. Experimental Procedure

Having given a description of the cryostat and the measuring equipment, we now go on to describe the experimental procedure which was followed during the course of a typical run.

After mounting the specimens, a check was made to ensure that they were not touching the copper can. The electrical circuit was also examined for continuity. Following this the system was lowered into the dewar which was then sealed off.

For helium work it was necessary to precool the cryostat to the nitrogen temperature. This is done in the following way:-

Using a rotary pump, the interspace of the inner dewar was pumped and flushed out three or more times with pure nitrogen. After the final flushing the interspace was pumped on until the pressure was down to about 1 m.m. This procedure of flushing the interspace was repeated during each run because most glasses are permeable to helium.

Helium gas which diffuses through the glass into the interspace will conduct heat from the nitrogen dewar into the inner dewar resulting in a very quick boil-off of the helium in the inner dewar.

The helium dewar was next pumped out. After this approximately one atmospheric pressure of helium gas was let into the inner dewar which was then isolated from the helium storage vessel. Following this the nitrogen dewar was topped up with nitrogen.

After the cryostat was cooled to 77°K liquid helium was transfered into the inner dewar using a siphon.

Measurements in the helium temperature range were made while pumping on helium at various pressures down to the lowest temperature. After shutting off the pump the bath heater was used to return to 4.2°K. Following this some helium was boiled until its level was below the specimen chamber. This was followed by the warm-up procedure for which

the specimen heater was used.

II. MAGNETIC SUSCEBTIBILITY

Vibrating Sample Magnetometer

1. Description

Magnetic measurements were made with a vibrating sample magnetometer, originally built in this laboratory by Murani (113). The principle of the magnetometer is quite simple. The sample is vibrated in a pick-up coil, placed in a magnetic field, by means of a piezo-electric bimorph tuning fork driven by an a.c voltage from an oscilator. The vibration of the sample induces a signal in the pick-up coil. This signal is amplified and detected in a suitable manner.

The basic arrangement of the apparatus is shown in fig. (IV.3). The nulling coil consist of two layers of 48 SWG enamel coated copper wire, wound on a thin walled pyrextube. The specimen machined into a cylinder of 0·05" diameter and 0·6" length, fits inside the pyrextube and held there firmly by dabbing some G.E. varnish to the open end. A lip made at the other end of the tube prevents the specimen from slipping out of the nulling coil when it is vibrated.

The coil housing and vibrators are enclosed in a glass tube closed at the lower end, with a quick fit ground glass joint at the others thus forming a specimen chamber. The whole system is enclosed within a standard glass double dewar system. The dewar tails are positioned

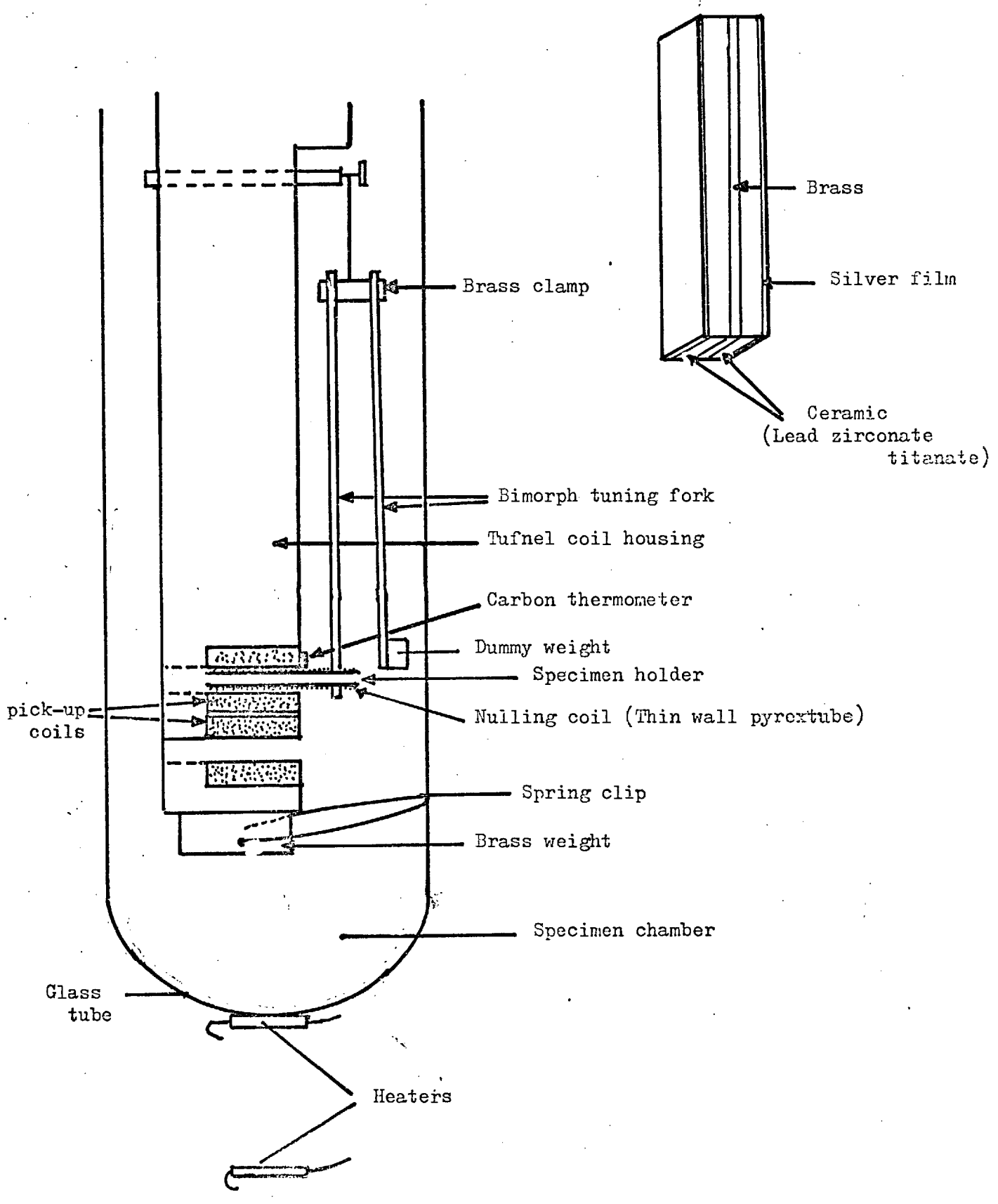
Brass
Silver film
Ceramic
(Lead zirconate
titanate)
Brass clamp
Bimorph tuning fork
Tufnel coil housing
Carbon thermometer
Dummy weight
Specimen holder
pick-up
coils
Nulling coil (Thin wall pyrextube)
Spring clip
Brass weight
Specimen chamber
Glass
tube
Heaters

Fig (IV.3)

between the poles of a Newpost type D water cooled electro-magnet used inconjuction with a 15 Amper Wareham power supply. The field is measured with a Hall effect Bell-Model 620 gauss meter which was calibrated against an NMR probe.

2. Operation

The block diagram of the magnetometer is shown in Fig. (IV.4). The signal from the oscillator is divided into two channels. One output goes via a phase shifter to the double beam cathode ray oscilloscope, while the other is connected directly to one of the bimorphs. When the bimorphs are loaded equally it is sufficient to drive only one of them, the second follows in antiphase. The specimen is vibrated axially in the pick-up coil. A second identical coil situated just above the main pick-up coil and connected in opposition, minimises the synchronous noise which is due to the pick-up coils vibrating at the same frequency as the specimen. The induced voltage in the pick-up coil is amplified by a low noise Brook Deal type 450 amplifier and fed into a Brook Deal type 411 phase sensitive detector. The output from the latter is read on a digital voltmeter (DVM).

For weakly magnetic specimens a null method of measurement is used. The magnetisation of the specimen is compensated by passing a current through the nulling coil so as to produce a moment of the same magnitude in the opposite direction. The nulling coil is calibrated in terms of magnetic moment per unit current by measuring the susceptibility of a pure Pd sample. To avoid heating effects in the nulling coil the maximum current used is 120 mA when the "specimen chamber" is immersed in helium bath and 12 mA when the helium level drops below it.

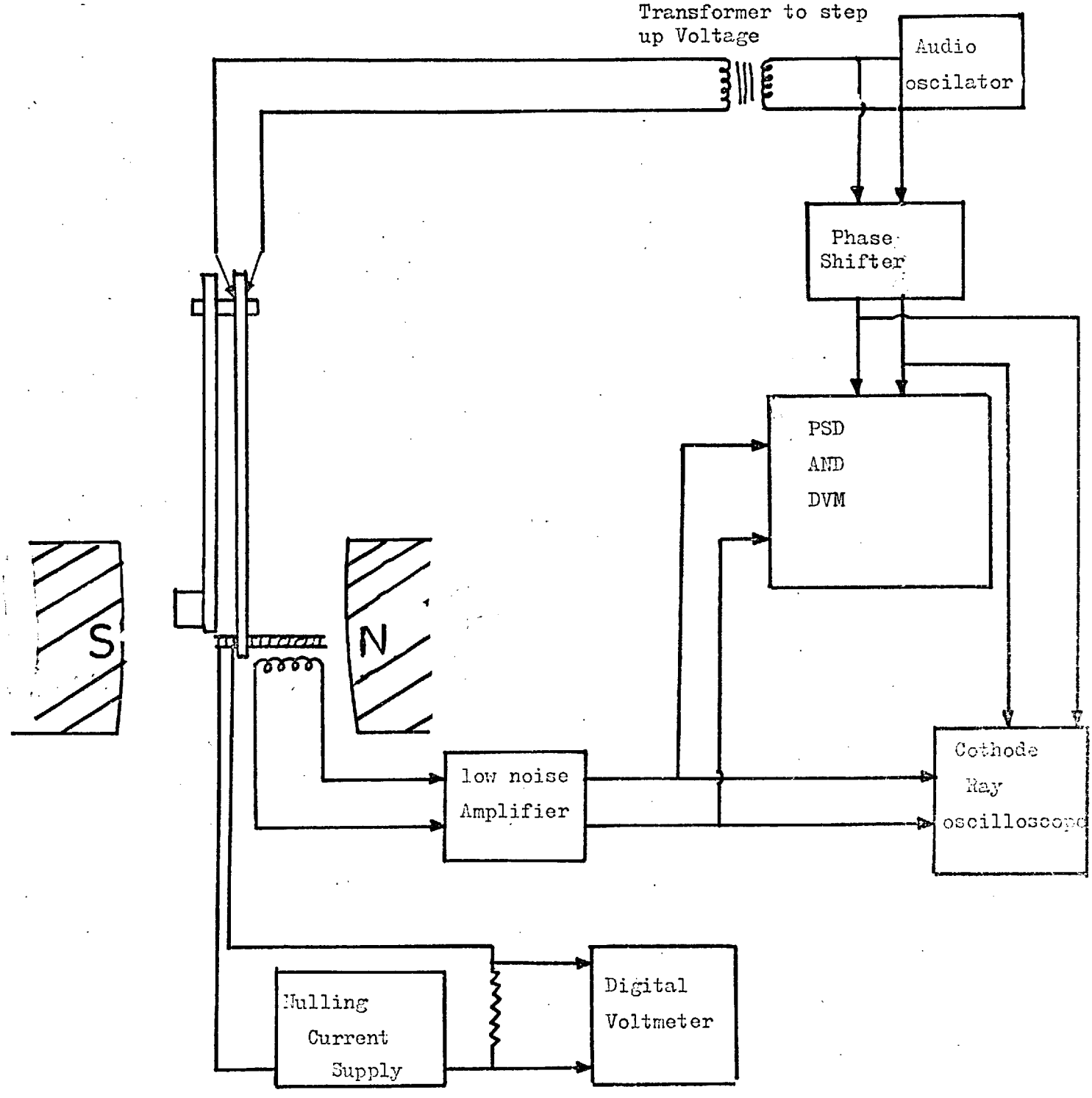
Transformer to step up Voltage
Audio oscilator
Phase Shifter
PSD AND DVM
S
N
low noise Amplifier
Cothode Ray oscilloscope
Nulling Current Supply
Digital Voltmeter

Fig (IV.4)

For strongly magnetic specimen the measurements are done in the following way. First the induced voltage in the pick-up coil, obtained as a dc output from the phase sensitive detector, is read on a DVM. Then 10 and 25 mA stabilised currents are passed through the nulling coil and the change in the output signal is recorded for each current. By a simple extrapolation the current required to compensate the total signal is calculated and thus the voltage induced in the pick-up coil by the sample is expressed interms of an equivalent nulling current. When employing this procedure care is taken to keep within the linearity limit of the amplifier and the phase sensitive detector.

3. Thermometry

Two thermometers, a copper and a carbon resistance thermometer, are employed for two different temperature ranges. The carbon resistor is an Allen-Bradley $(\frac{1}{4})$ watt resistor of 47 Ω nominal value at room temperature. It is mounted on the pick-up coil and used for temperatures below $20^{\circ}K$.

The calibration procedure is the same as that described in the section on the resistivity measurements. Its resistance is measured by two terminal methods (as the leads resistance is negligible compared to that of the carbon resistor) using a standard resistor and a lead-acid cell.

Above $20^{\circ}K$ the nulling coil itself is used as the Copper resistance thermometer. A four terminal method is employed to determine the resistance of the coil. The pontential drop across the coil is read directly from a DVM and the current through it is determined by reading the voltage drop produced across a 1 Ω standard resistor connected in series in the circuit.

The resistance-temperature calibration of the coil was made by measuring its resistance as 4.2°K and at ice point and using the tabulated value of the function:-

$$Z = \frac{R(T) - R(4.2)}{R(273) - R(4.2)} \qquad \text{(IV.2)}$$

given by White (131). For the samples measured a small field value, usually much less than 1kG, was chosen for which the correction to the resistance of the coil due to magneto resistivity was found to be negligible above 20°K. This was checked by switching off the field, measuring the resistance of the coil then comparing it with the value obtained in the field.

4. Temperature Control

Below 4.2°K the temperature is controlled by pumping on helium bath through a manostat. After the helium level has dropped below the glass tube enclosing the system, the apparatus begins warming-up at a rate of approximately 10°K. per hour.

The rate of warm-up can be controlled reasonably well by the two heaters while there is a residual helium pool in the tail of the helium dewar. One of the heaters is in the tail of the helium dewar, the other is positioned below the pyrex tube enclosing the coil housing and the bimorphs.

Between 77° and 300°K the measurements were taken while cooling down slowly. This is achieved by pumping hard with a rotary pump on the helium interspace after flushing it with fresh nitrogen. The specimen chamber and the helium dewar were also flushed with nitrogen. This procedure ensures that any oxygen inside the specimen chamber is pumped out. After this is done, nitrogen is poured into the outer dewar

and its level is raised gradually.

The experimental procedure is described in detail by Murani. After mounting the specimen the magnet is wheeled into position and the signal from the sample is checked on a cathoderay osciloscope. For a freely vibrating sample the signal is a smooth sine wave.

If the vibration of the sample is not free, which is indicated by a distorted sine wave on the oscilloscope, the Aluminium foil by which the bimorphs are suspended from the coil housing can be twisted slightly until the free vibration of the sample is ensured. After this the dewars are replaced around the apparatus. The apparatus is now ready for measurements.

PREPARATION OF SPECIMENS

(a) Pd-Ni alloy system

Ni in Pd form a continuous series of solid solutions (132), therefore the preparation of specimens was fairly simple. The starting materials were palladium ex Johson Mattey "specpure" grade (The upper limit of Fe content is given as 3pp), and nickel from Koch-Light Laboratories (nominally 99.998 wt% Ni). Nine different alloys with concentration of Ni between 2.25 and 6 at % were made by careful arc melting of their components on a water cooled copper hearth(+) under $\frac{2}{3}$ atmospheric pressure of pure argon gas. They were melted and remelted several times to ensure better homogeneity. The buttons, usually about 1,3 gms, were cold forged with non-ferrous implements then homogenised at 1200°C for 2 days. They were then rod rolled between protective plastic sheets (melinex), and subsecuently drawn to wires of about 0.8mm diameter. At the first stage of drawing, the surfaces of the wires were cleaned several times using fine sand paper to prevent iron contamination from the steel dies.

After the total length of each of the specimens was carefully measured, they were bent into hairpin shapes and given a heavy pickle using Aqua-regia (3 parts HC1: 1 part HNo_3). They were then sealed into quartz tubes under a vacuum of 10^{-5} torr and annealed again for two days at 1200°C. Following the annealing procedure they were quenched in brine and were given a light etch. Then spot welding was done and the distances from the potential leads to the nearest ends were measured, thus obtaining the length of the specimens.

(+) H.E.N. Stone: J. Sci Instr. (J. Phys. E) 1971 (DEC).

(b) Pd-Mn Alloy system

The solubility limit of Mn in Pd is 26 at% at room temperature (132) (133) and the alloys made here have Mn concentrations of between 3 and 8.4 at%. Therefore the preparation of alloys was again simple. The alloys, of mass usually around 1.5 gms., were prepared in the same way as the Pd-Ni alloys by arc melting of the component metals. Pd was spec-pure sponge ex Johnson Mattey and Mn was 99.995% pure supplied by Koch-Light Laboratories. Care was taken that Mn was not blown away by the initial strike of the arc. The alloys were melted and remelted five times. After final melting they were cast into a copper mould 2.3 mm in diameter. They were etched with aqua-regia and sealed under a pressure of 10^{-5} torrs. After being homogenised for a day at 750°C they were brine quenched. Following this the Mn depleted layer was taken off using a "Servomet" spark machine manufactured by Metal Research Ltd. which uses the technique of spark erosion. They were then drawn to wires of about 1 mm in diameter using tungsten carbide dies. After this they were bent into hairpin shapes and were given a final annealing at 400°C for about 20 minutes. After the leads were spot welded the dimensions were measured in the same way as those of the Pd-Ni alloys.

(c) Rh-Co Alloys

The alloys, usually weighing about 1.5 grms., were prepared in the same way as alloys of the previous two systems, by arc melting of component metals. Rh was 99.99% pure sponge from Engelhard Industries and Co was 99.995% pure sponge from Koch-Light Laboratories. The melting procedure was repeated several times and after the final melting they were cast into a copper mould of 1.6mm in diameter. They were then etched with aqua-regia, homogenised for two days under a vacuum of 10^{-5} torr. Following

this the alloys were spark machined to the required dimensions. The leads were attached using a spot welder, and the length of samples measured.

Samples of all three alloy systems were analysed to determine their homogenity and concentration by an electron microprobe analyser. The samples were homogenous and their concentrations were very close to their nominal values.

CHAPTER V

RESULTS AND DISCUSSIONS

In this chapter, results of the electrical resistivity measurements on Pd-Ni, Rh-Co and Pd-Mn alloy systems are given. Also magnetization and susceptibility measurements on the Pd-Ni and Rh-Co alloys are reported and a discussion of the results is presented.

1. Pd-Ni Alloy System

The Pd-Ni system has been investigated extensively (107), (134)etc. as an example of a system in which the local exchange enhancement on Ni atoms increases as their concentration is increased, leading to a long range ferromagnetic ordering at a certain nickel concentration C_F. This concentration is suggested by Bozorth et al (135), by Crangle and Scott (107) and Chouteau et al (84) to be $\leq$ 2 at %. However, the present investigation shows clearly that it is at a value which is considerably larger than 2.0, and indicates 2.32% as the critical composition.

This concentration is easily obtained from the electrical resistivity measurements. At low temperatures where the phonon term is negligible the resistivity of alloys of Pd-Ni type is mainly due to the scattering of conduction electrons from localized spin fluctuations or paramagnons. The spin fluctuation temperature θ of the alloys is proportional to the inverse of the enhancement factor. At a certain temperature T the number of paramagnons excited is of the order of $\frac{T}{\theta}$. For the alloys near the critical concentration the enhancement factor is large and, hence, θ is small. Therefore, the number of paramagnons excited at temperature T increases reaching a maximum value at the critical concentration where the

enhancement factor is largest (infinite in theory) and, hence, θ has its lowest value. Thus at the critical concentration the temperature dependent resistivity reaches its maximum value.

Electrical resistivity and magnetic measurements show that the magnetic alloys of this system are like Ni_3Al and Ni_3Ga (136) and $ZrZn_2$ (137), weak itinerant ferromagnets.

Below we discuss the behaviour of the alloys as a function of Ni concentration after consdering each alloy individually.

Pd-2.25 at % Ni

The resistivity of the alloy as a function of temperature is plotted in Fig. (V.1), where the dotted line represents the experimental points. The solid line is the curve of the form AT^n fitted to the experimental points below 4.2°K. Up to 10°K the resistivity varies as $T^{1.4}$ Fig. (V.2). Above 10°K deviation from $T^{1.4}$ law occurs Fig. (V.3). The resistivity in this region appears to be linear Fig. (V.1).

This alloy is paramagnetic and is just below the critical concentration (C_F=2.32%). Hence it is very strongly enhanced and its spin fluctuation temperature θ is very low. We recall that (Chapter II)

$$\theta \sim (1-\bar{I})$$

For this sample $\bar{I} \sim 1$.

According to the theories of Kaiser and Doniach (76) and Rivier and Zlatič (77), at $T \ll \theta$ the resistivity due to LSF varies as T^2 and at $T \sim \theta$ as T. The variation of the resistivity of the alloy with temperature confirms the predictions of the above theories which, although they are formulated for dilute alloys, seem to have a more general validity.

Fig. (V.1)

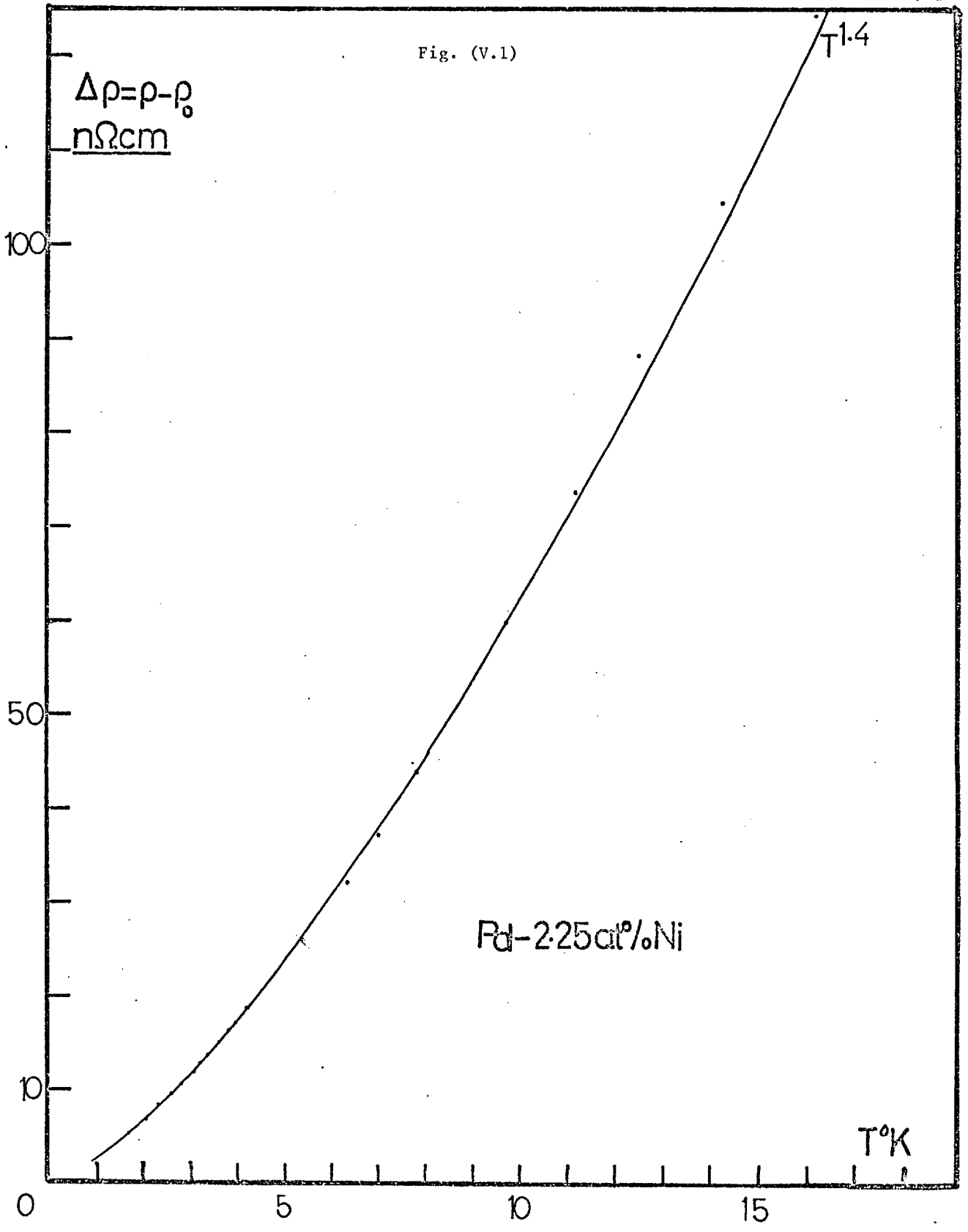

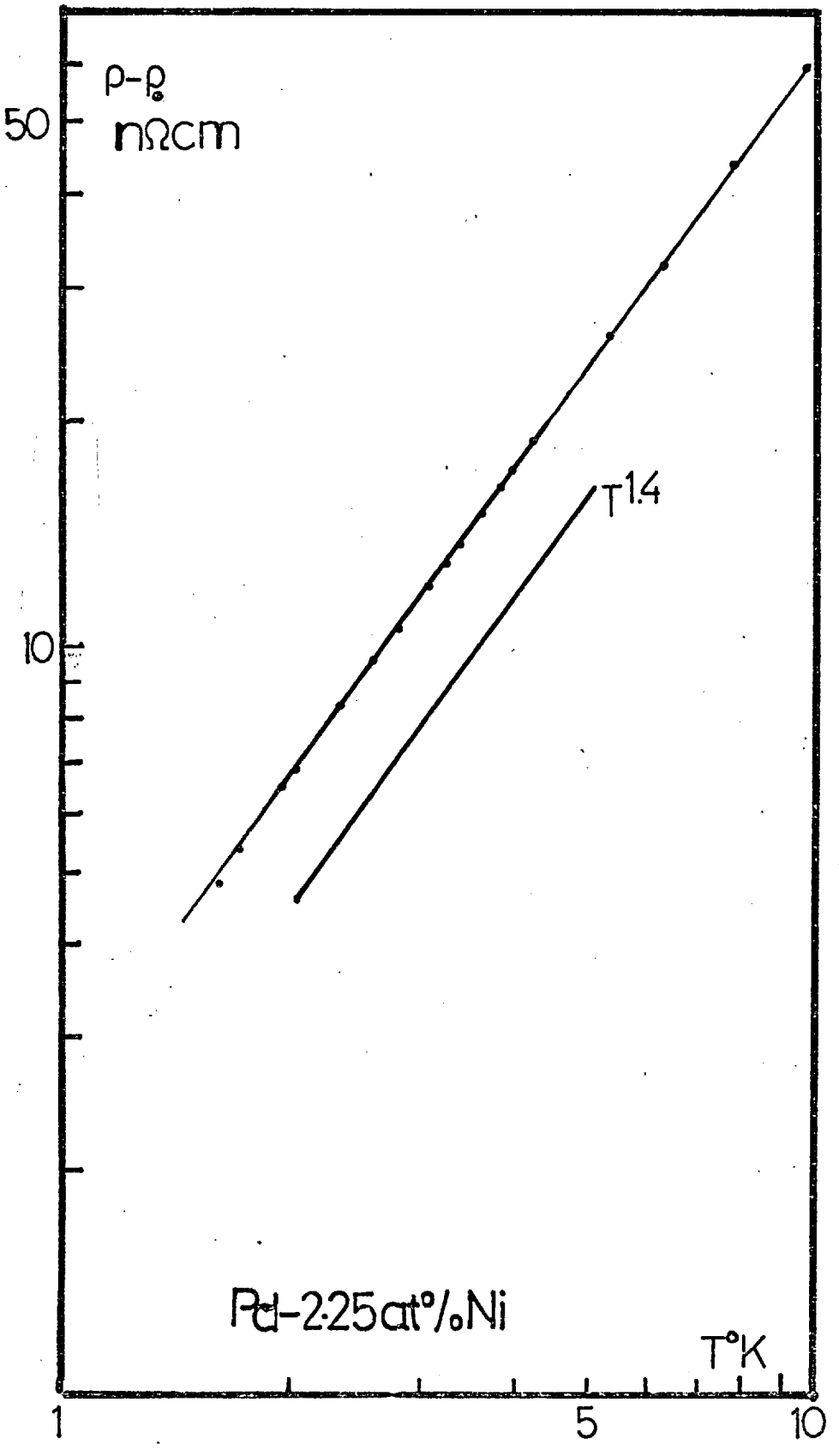

Fig. (V.2)

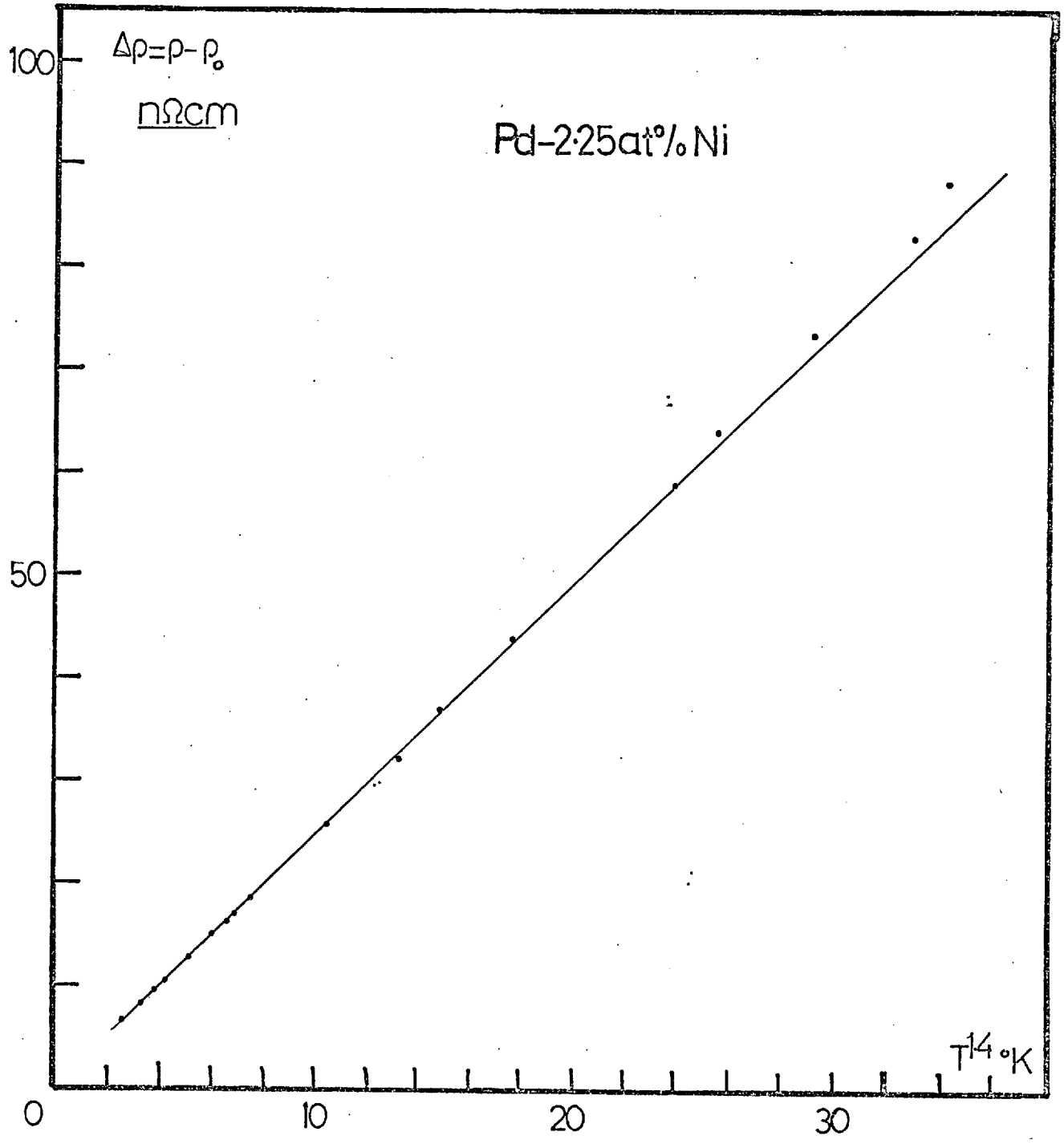

Fig. (V.3)

Mathon (78) has calculated the resistivity about the critical concentration. According to him it should vary as $T^{5/3}$ very close to the critical concentration, and the experimental points should fall below the initial power law at higher temperatures.

As we have shown above, the resistivity varies as $T^{1.4}$ and the experimental points fall above the initial $T^{1.4}$ low.

Pd-2.35 at % Ni

This sample is just ferromagnetic. No anomaly in the resistance-temperature curve is found down to the lowest temperature.

Below 4.2°K the resistivity varies as $T^{1.49}$ Fig. (V.4). Between 7° and 14°K it appears to be linear Fig. (V.5). Above 6°K the experimental points (dots) fall below the initial $T^{1.5}$ power law Figs. (V.5) and (V.6). This behaviour is consistent with the theory of Mathon (78) which will be discussed later after studying all the alloys closely.

Magnetization measurements have been made in the helium temperature range in fields of up to 7.5kG. The data have been analyzed in the conventional way ($\frac{H}{\sigma}$ versus σ^2) Fig. (V.7). To demonstrate the behaviour of the alloy only a few plots are shown.

It is clear that this type of analysis does not apply here. This is not surprising as $|C-C_F| \sim 0$ for this alloy, and hence the Landau theory breaks down as shown by Mathon (78) and Hargitai et al (138).(Here C is the Ni concentration and C_F is its critical value).

The plots of magnetization versus field are shown in Fig. (V.8) for 77°K, 4.2°K and 2.1°K. From the plots the alloy seems to be almost ferromagnetic at 2.1°K. At 4.2°K there is an atypical anomaly in the

Fig. (V.4)

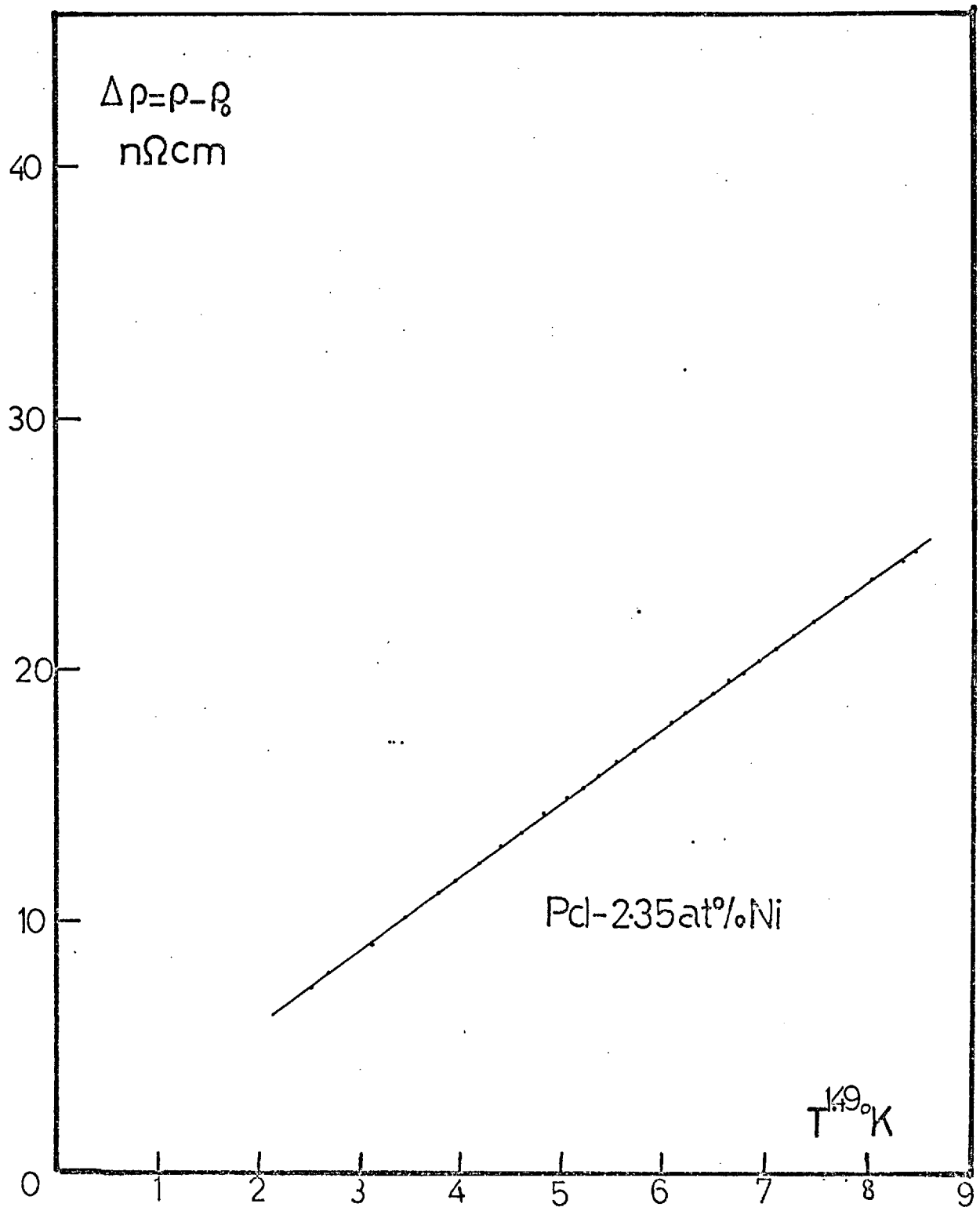

Fig. (V.5)

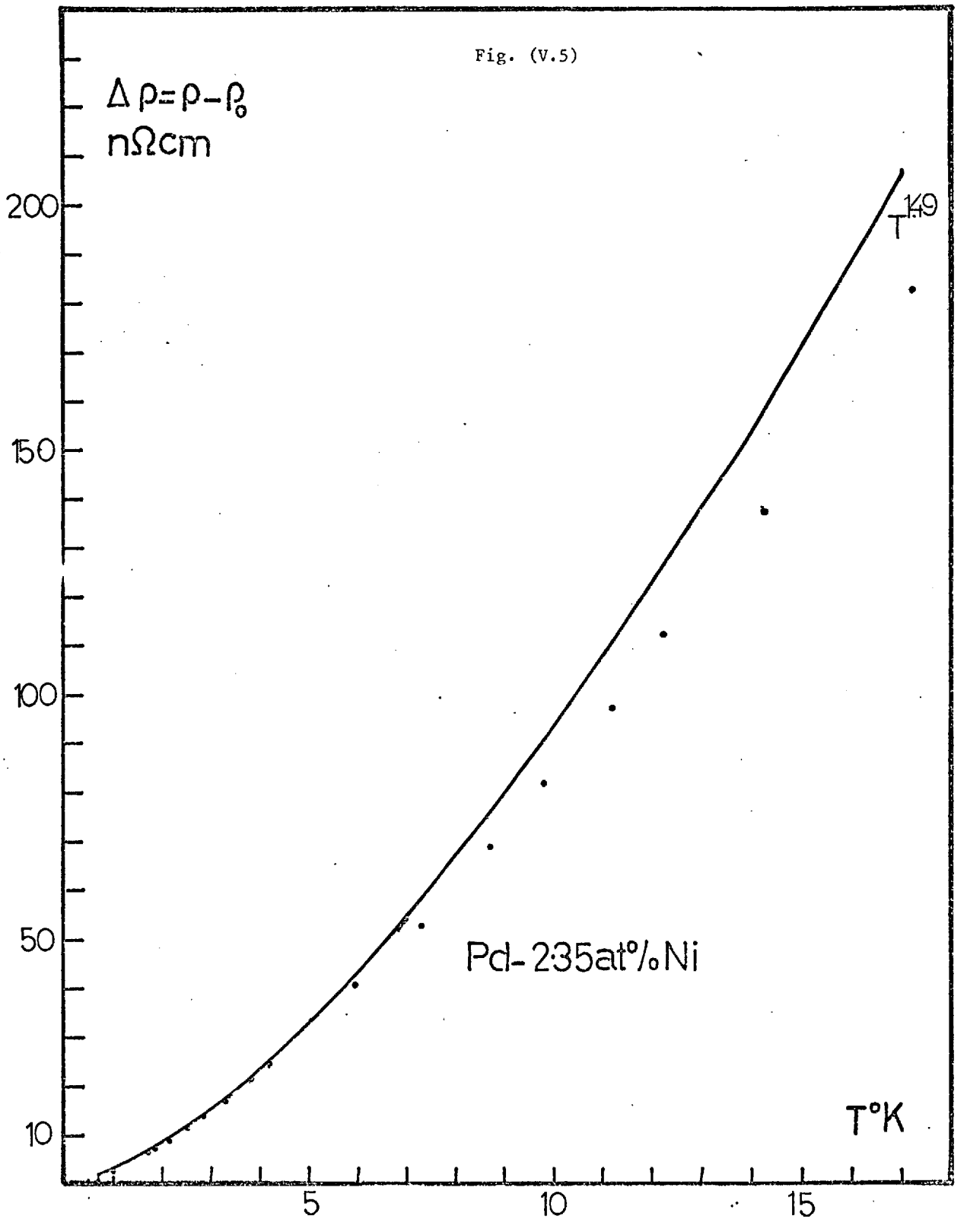

Fig. (V.6)

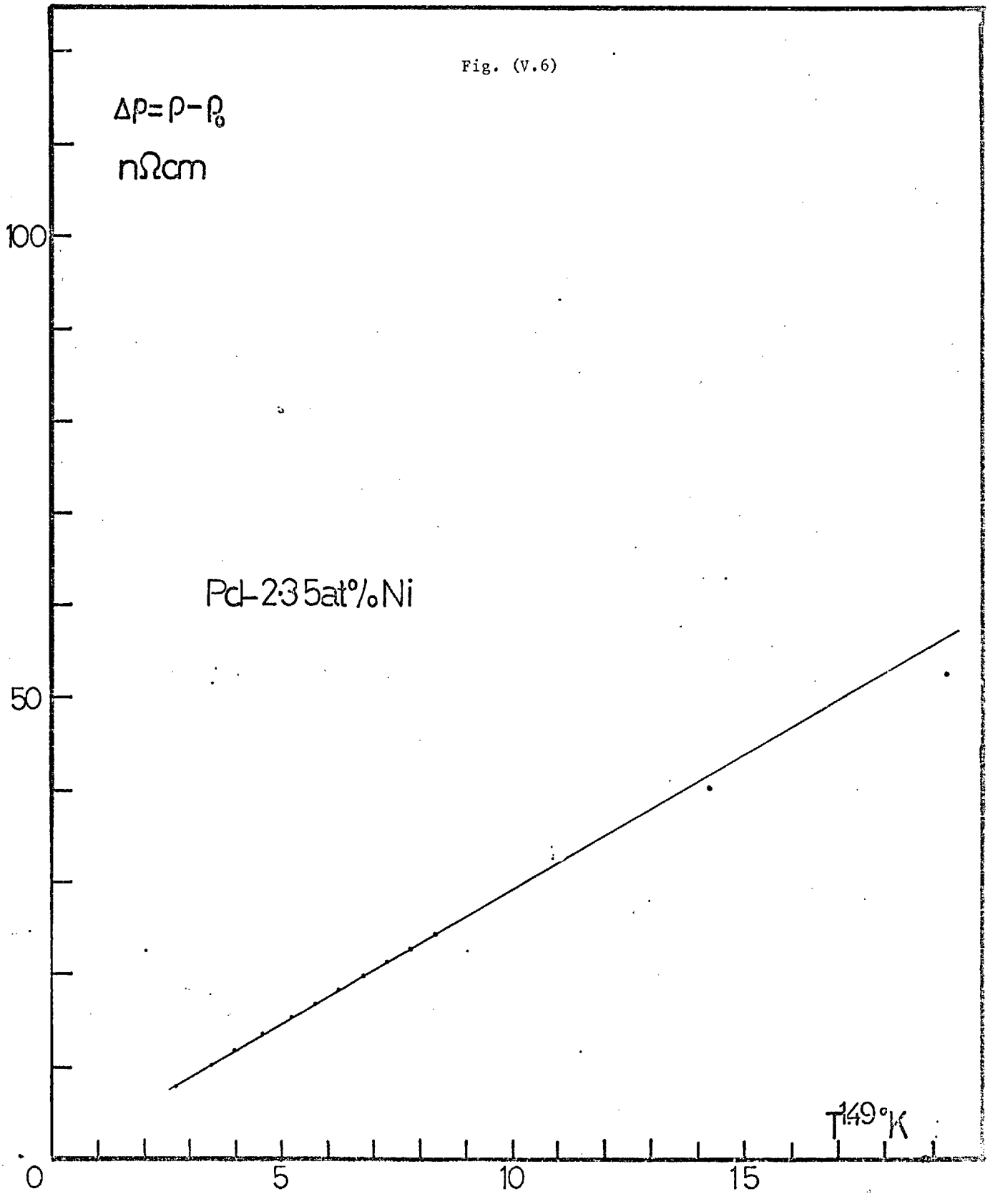

Fig. (V.7)

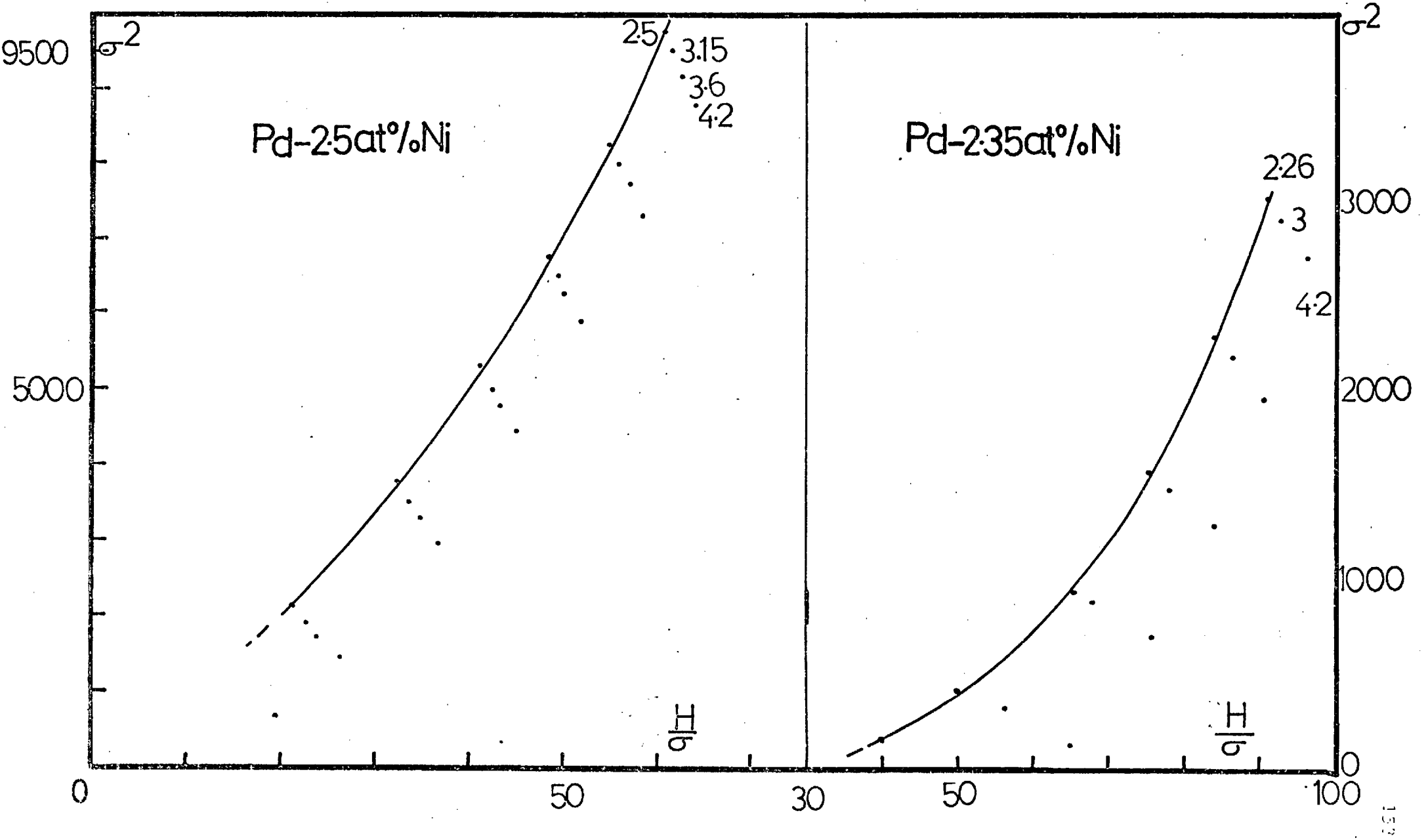
σ2
9500
5000
0
50
H/σ
2·5
3·15
3·6
4·2
Pd-2·5at%Ni
σ2
3000
2000
1000
0
30
50
100
H/σ
2·26
3
4·2
Pd-2·35at%Ni

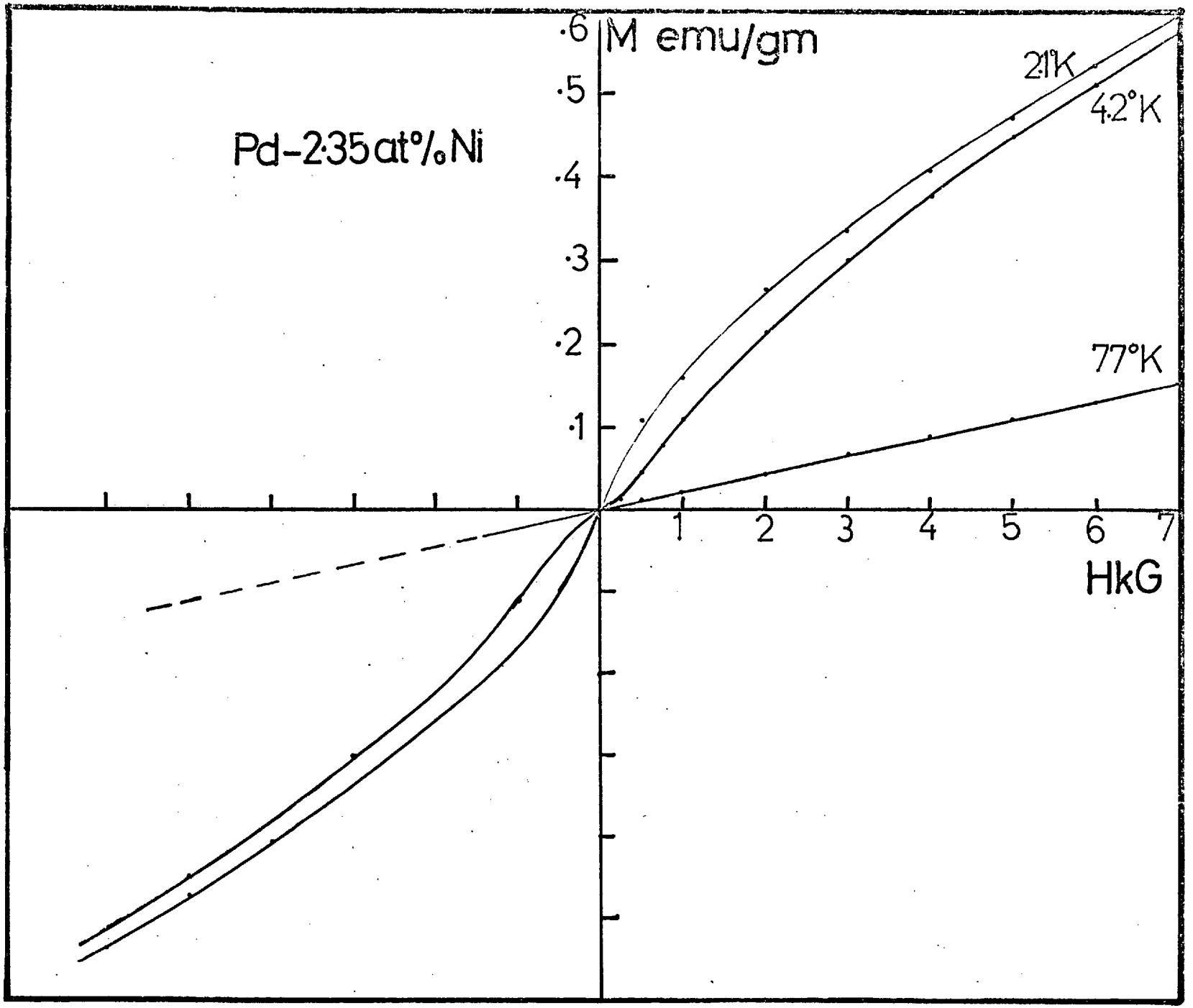

Fig. (V.8)

Fig. (V.9)

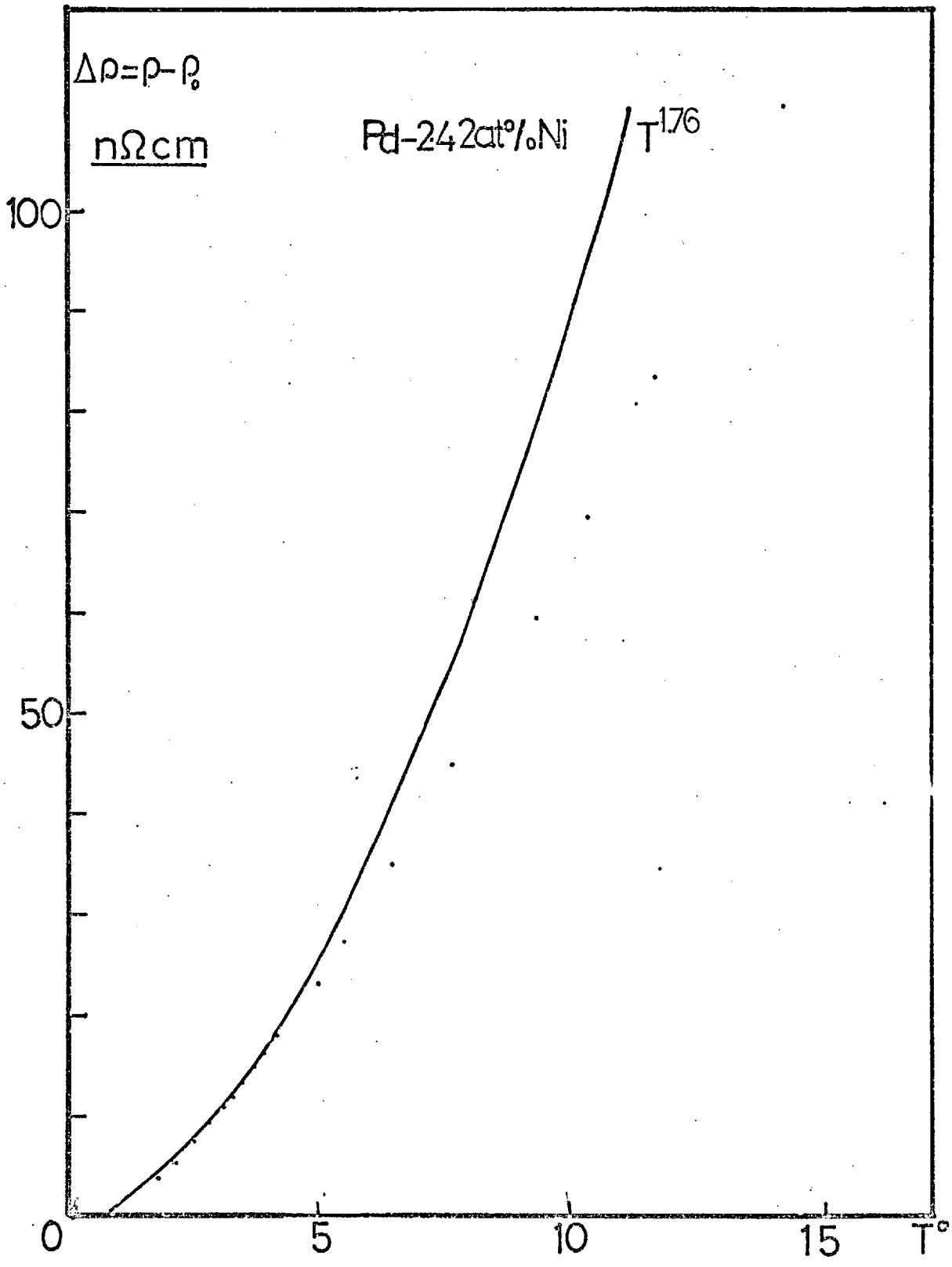

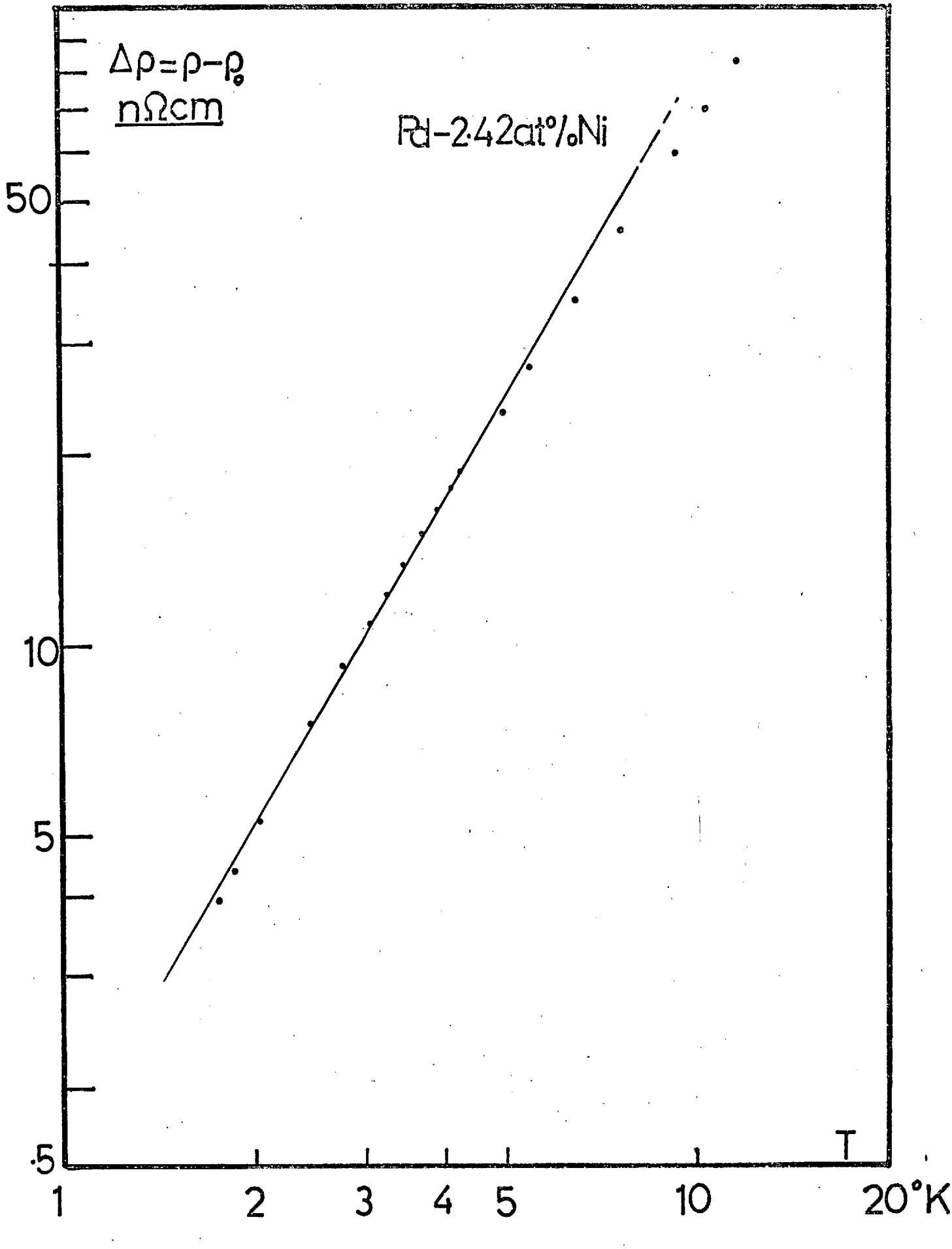

Fig. (V.10)

curve. Only in fields above approximately 0.5kG does the magnetization start increasing rapidly with the applied field.

Pd-2.42 at % Ni

The plot of the resistivity versus temperature is shown in Fig. (V.9). At low temperatures the resistivity varies as $T^{1.76}$. It is clear that the deviation occurs from the initial $T^{1.76}$ law at about 4.5°K. Above this temperature the power of T falls below 1.76. Just above 5°K the resistivity appears to be linear over a limited temperature range. At the lowest temperatures, a tendency towards a higher power of T can be seen from Fig. (V.10). The qualitative behaviour of the alloy is similar to that of the Pd-2.35 at % Ni.

Pd-2.5 at % Ni

The variation of the resistivity with temperature is shown in Fig. (V.11) on a log-log scale. The resistivity varies as $T^{1.75}$ below 4°K. Above this temperature the experimental points gradually fall below the initial power law.

The fall-off of the experimental points below the initial $T^{1.75}$ law is again observed here Fig. (V.12).

The magnetization of the alloy as a function of field up to 7.5kG has been measured at 5.1°, 4.2°K, and at several other points in the helium temperature range. The data obtained are analyzed in terms of σ^2 versus $\frac{H}{\sigma}$ some of which are plotted in Fig. (V.7) where the numbers indicate the temperature at which the magnetizations versus field are measured. There is a clear curvature in the plots; the curvatures increasing at the lower fields. From the figure it is clear that the alloy is ferromagnetic at low temperatures, but the curvature makes firm conclusion

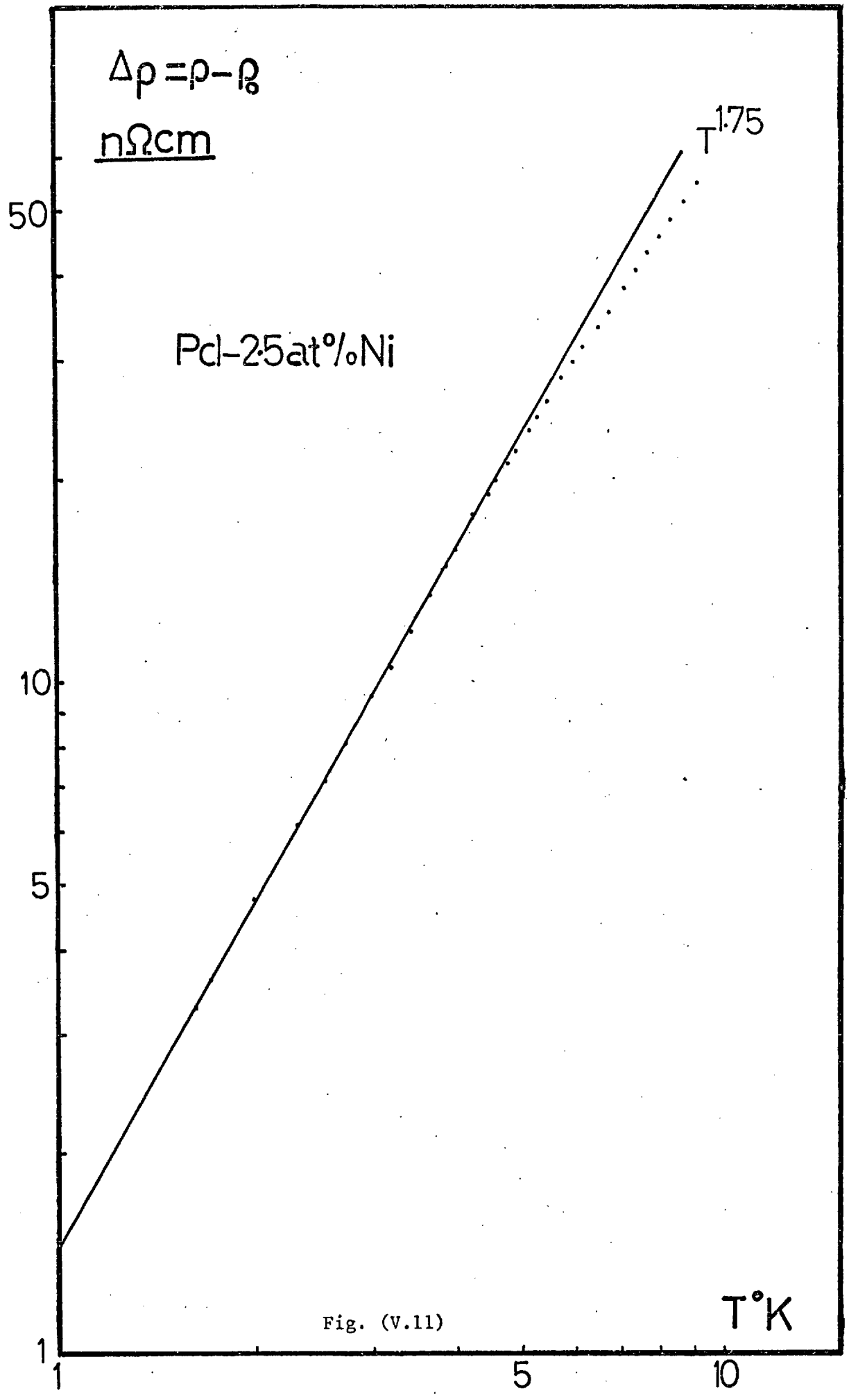

Fig. (V.11)

Fig. (V.12)

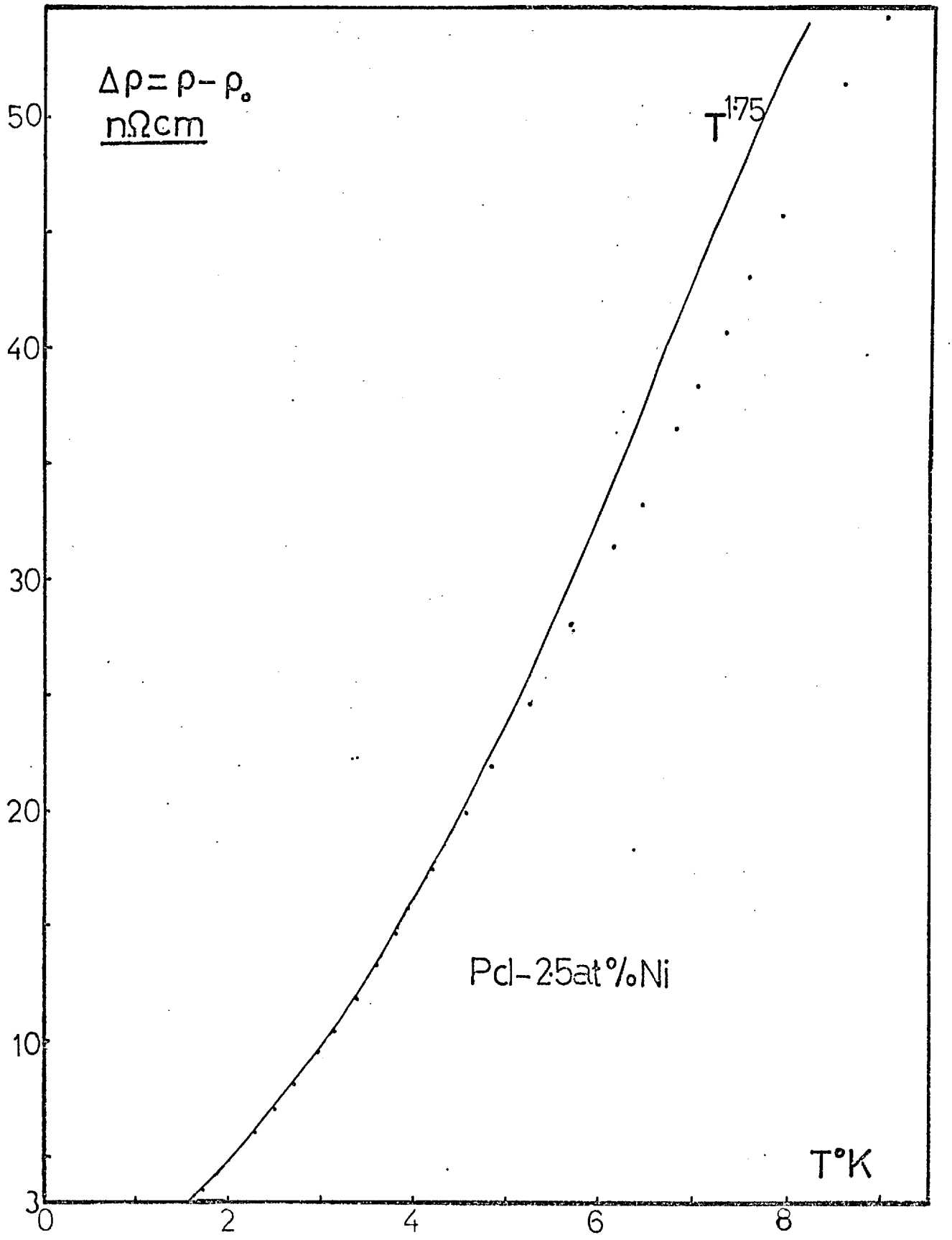

Fig. (V.13)

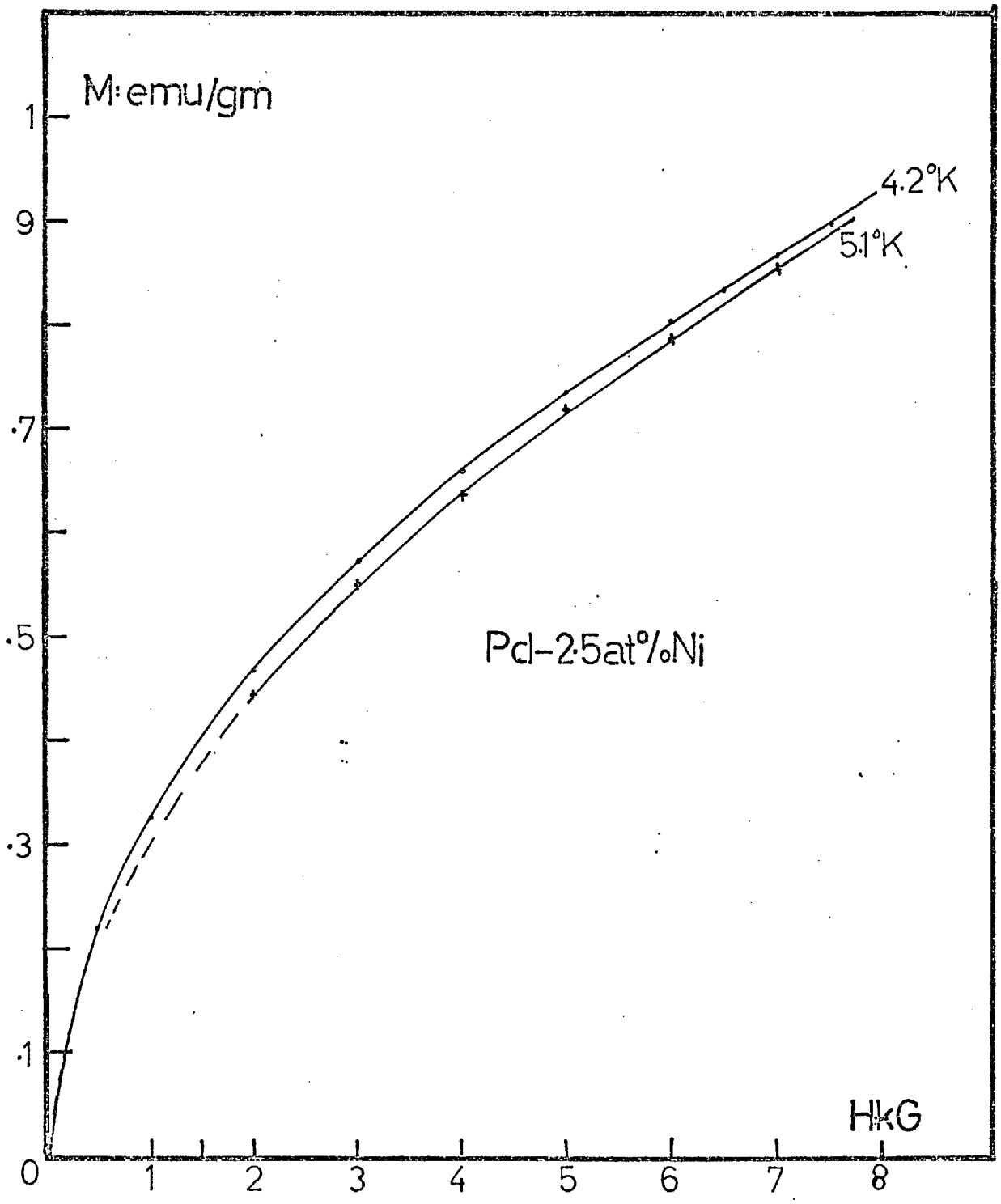

Fig. (V.14)

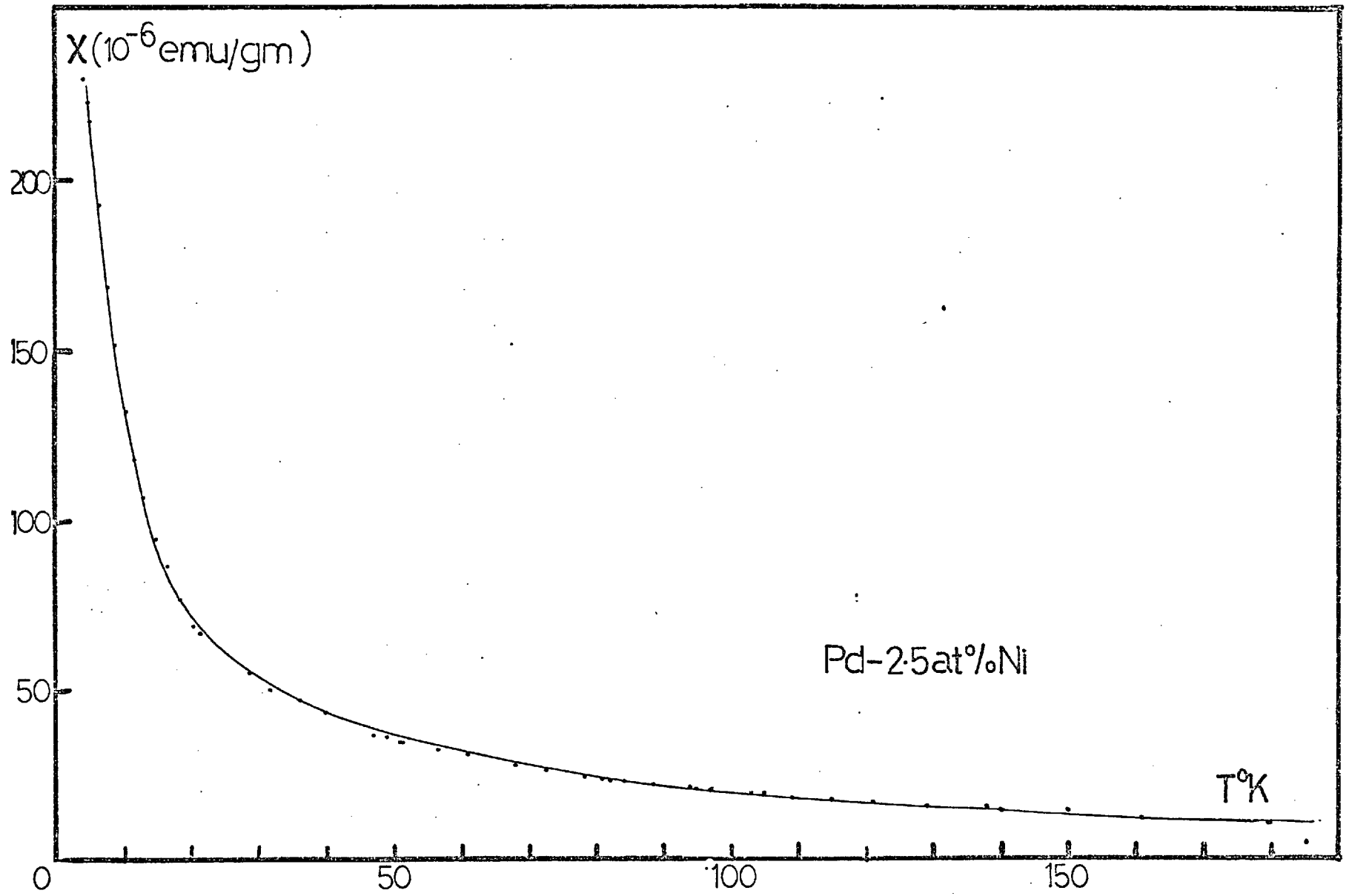

from the data impossible.

The plots of magnetization versus field at tmperatures 5.1° and 4.2°K are shown in Fig. (V.13). These curves are typical of alloys near critical temperature.

The susceptibility (ratio of the magnetization to the field) of the sample has been measured in 2kG over the temperature range from 1.6° to 300°K. The portion lying between 4° and 190°K is plotted in Fig. (V.14). Due to the strong temperature dependence of the pure Pd no Curie-Weiss fit is attempted. However, the reciprocal of the total susceptibility versus temperature is found to be almost linear, which indicates that the matrix susceptibility is small compared to that of the alloys.

Pd-3 at % Ni

Resistivity data for this alloy are plotted against temperature in Fig. (V.15). The resemblance of the plot to those of previous alloys is clear. Above about 5°K the experimental points again fall below the initial $T^{1.9}$ law which is obtained from the best fit to the temperature below 4.2°K. However, the deviation seems to be less and there is a linear region which is at comparatively higher temperatures.

Magnetization measurements have been done at different temperatures in fields of up to 7.5kG. The data, analyzed in terms of σ^2 versus $\frac{H}{\sigma}$ plots which are shown in Fig. (V.16), indicate a Curie temperature of 10.8°K. This temperature is given as 21°K by Crangle and Scott (107). The plots have a slight curvature, in the way which has been predicted by Strickman and Wohlfarth (139). Namely in the low fields the curves turn upward in the paramagnetic region and downward in the ferromagnetic region.

The magnetization has been measured in 100 Gauss between 4.2° and 300°K.

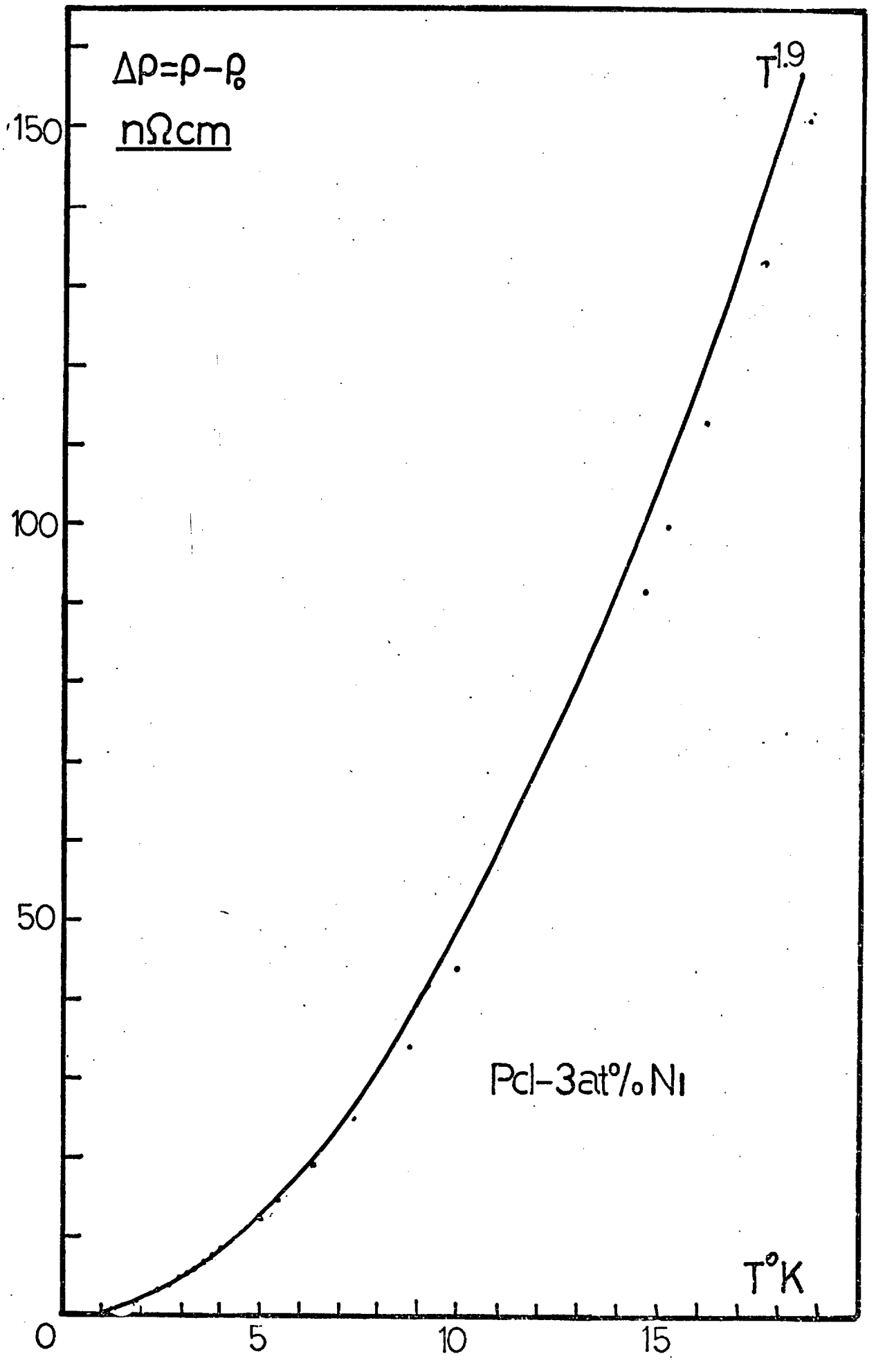

Fig. (V.15)

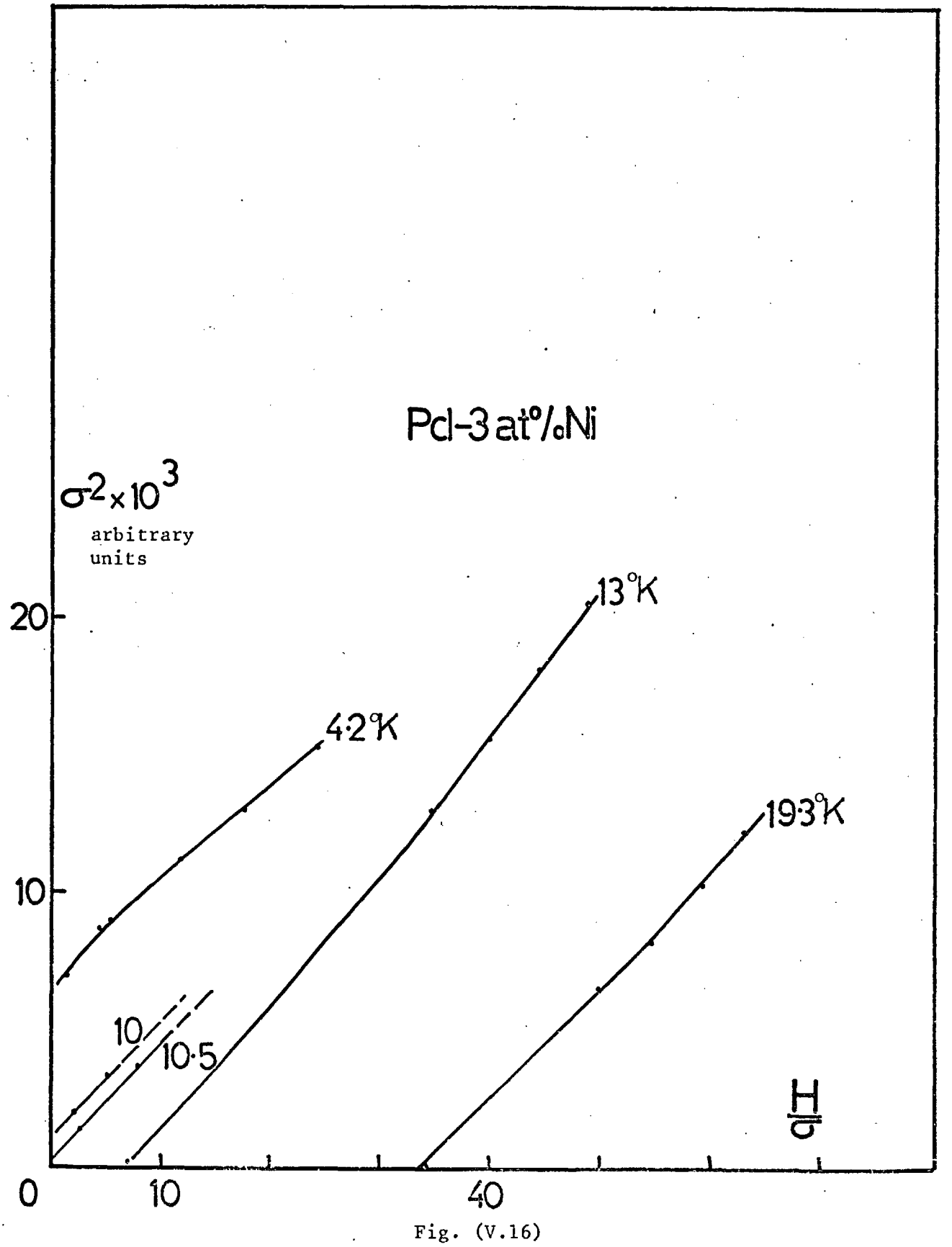
Pd-3 at% Ni
σ² x 10³
arbitrary units
20
10
0
10
40
13°K
4·2°K
19·3°K
10
10·5
H/σ

Fig. (V.16)

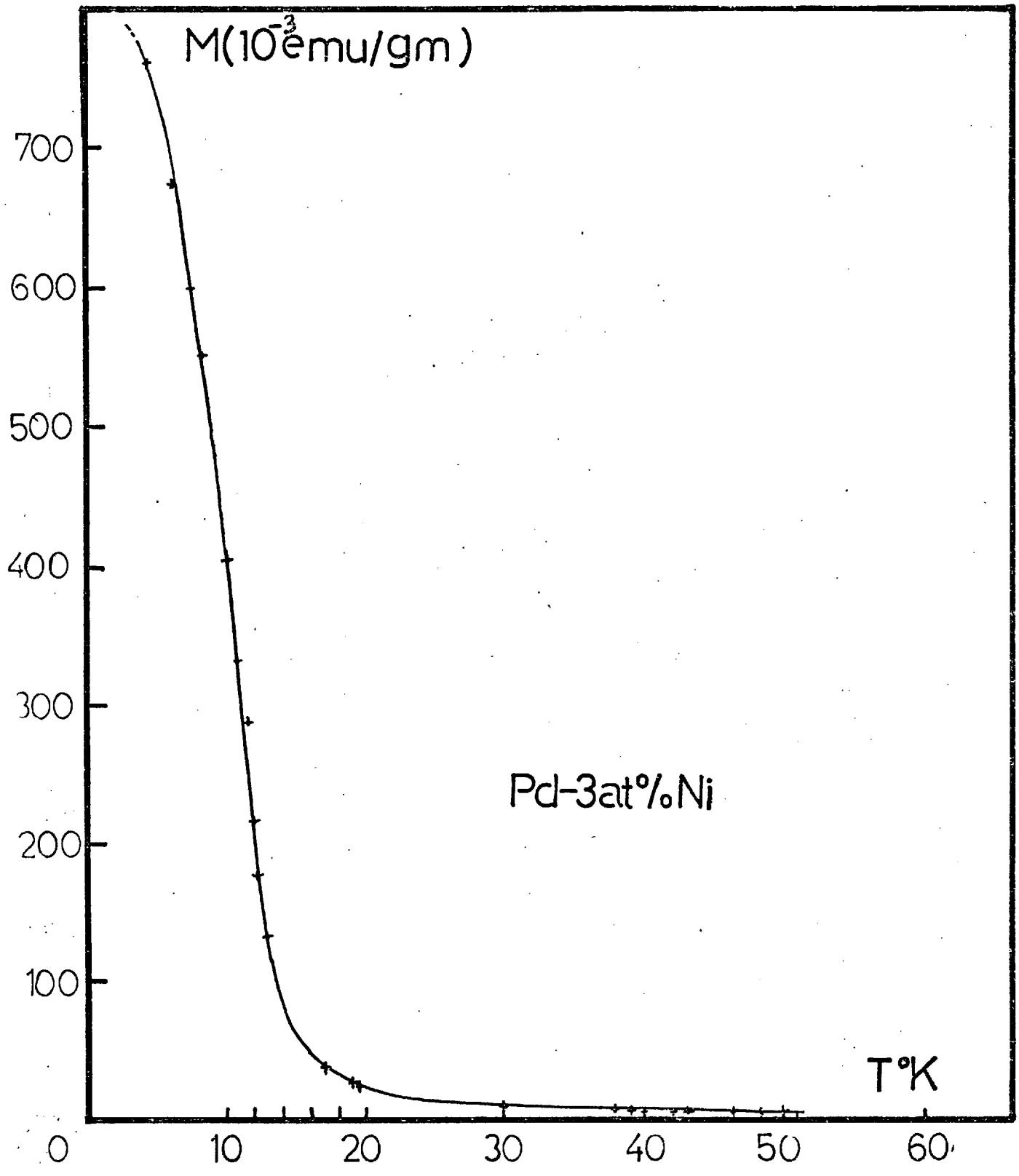
M(10⁻³emu/gm)
700
600
500
400
300
200
100
0
10
20
30
40
50
60
Pd-3at%Ni
T°K

Fig. (V.16a)

Fig. (V.17)

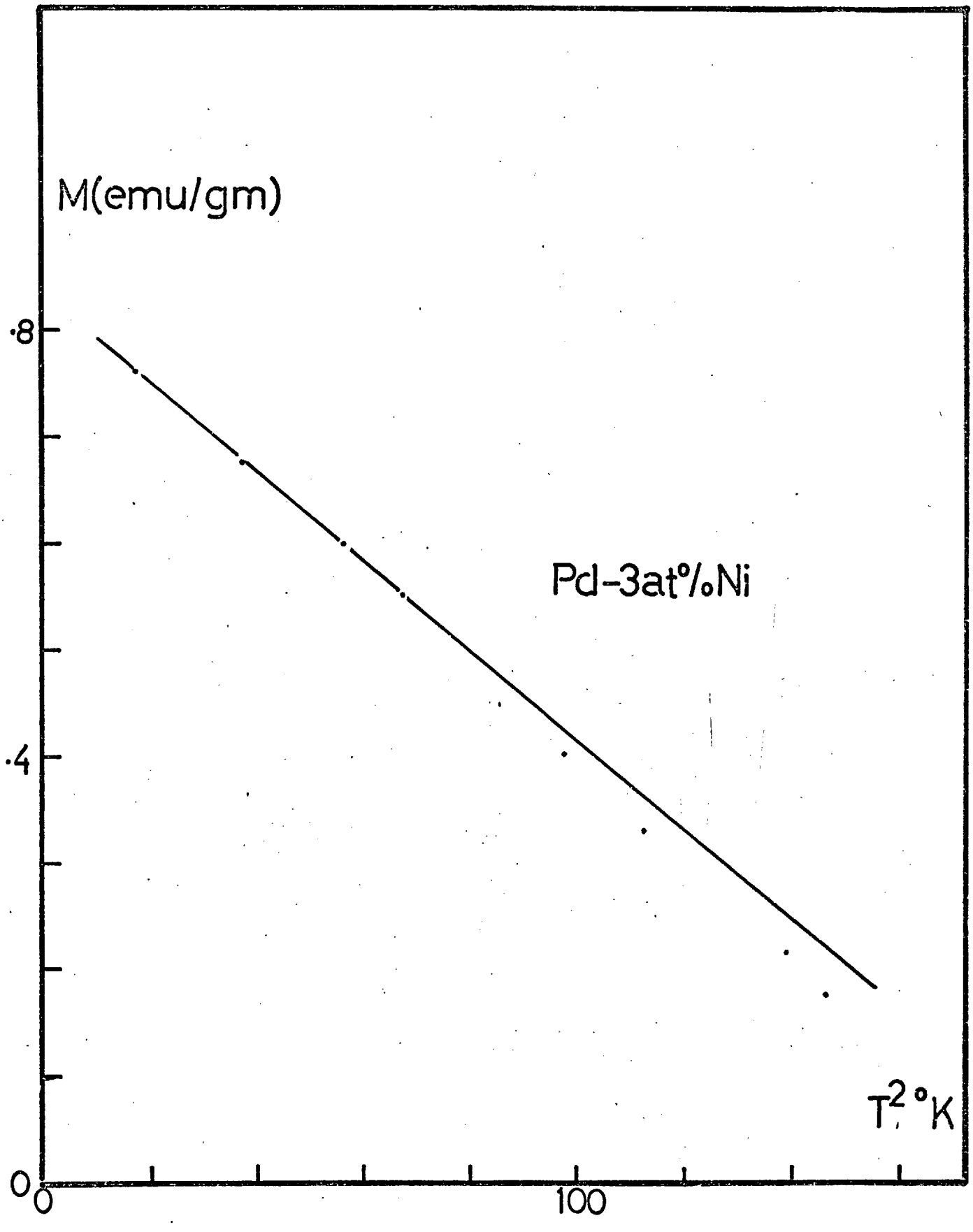

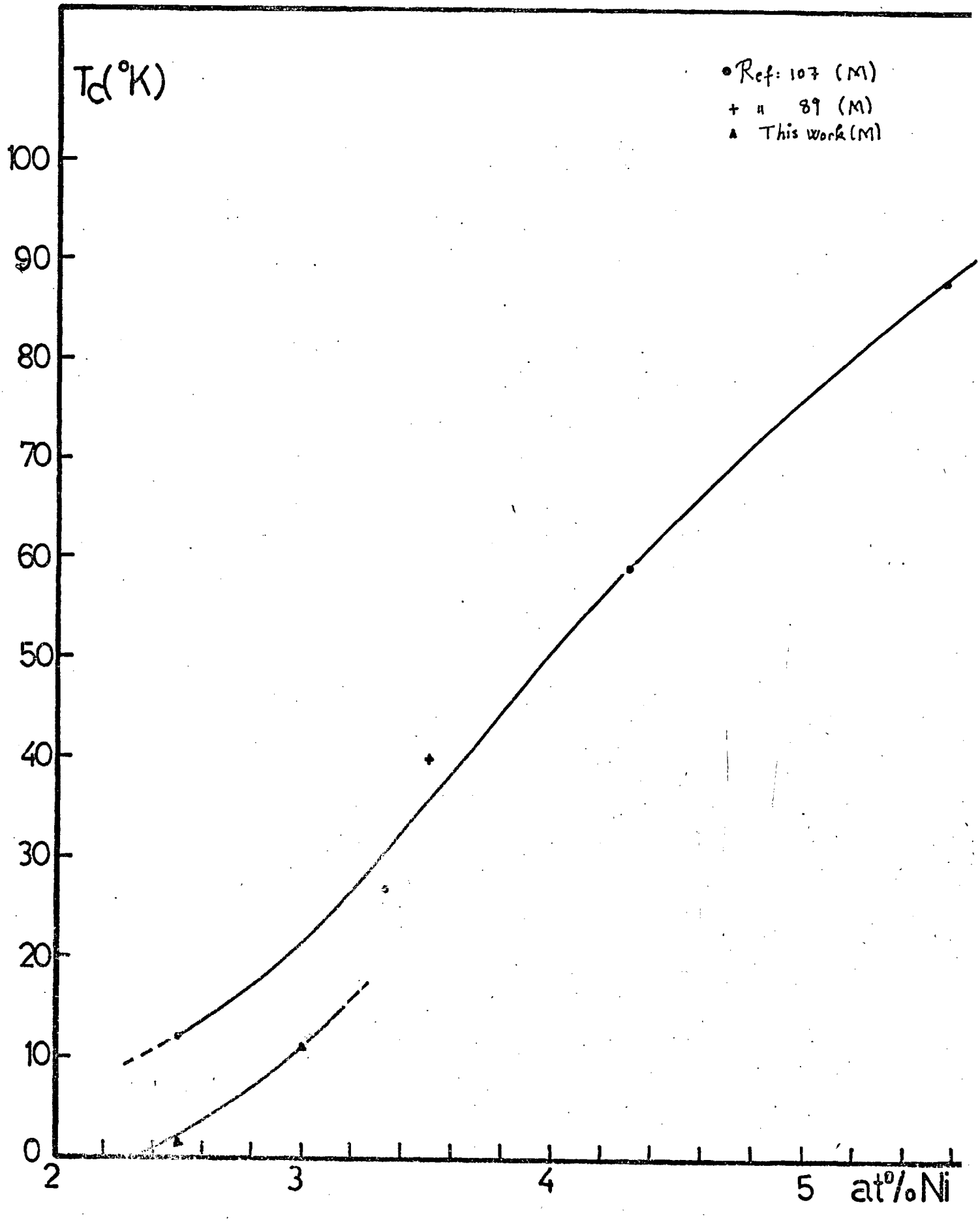
T_c(°K)
● Ref: 107 (M)
+ " 89 (M)
▲ This work (M)
100
90
80
70
60
50
40
30
20
10
0
2
3
4
5
at% Ni

Fig. (V.18)

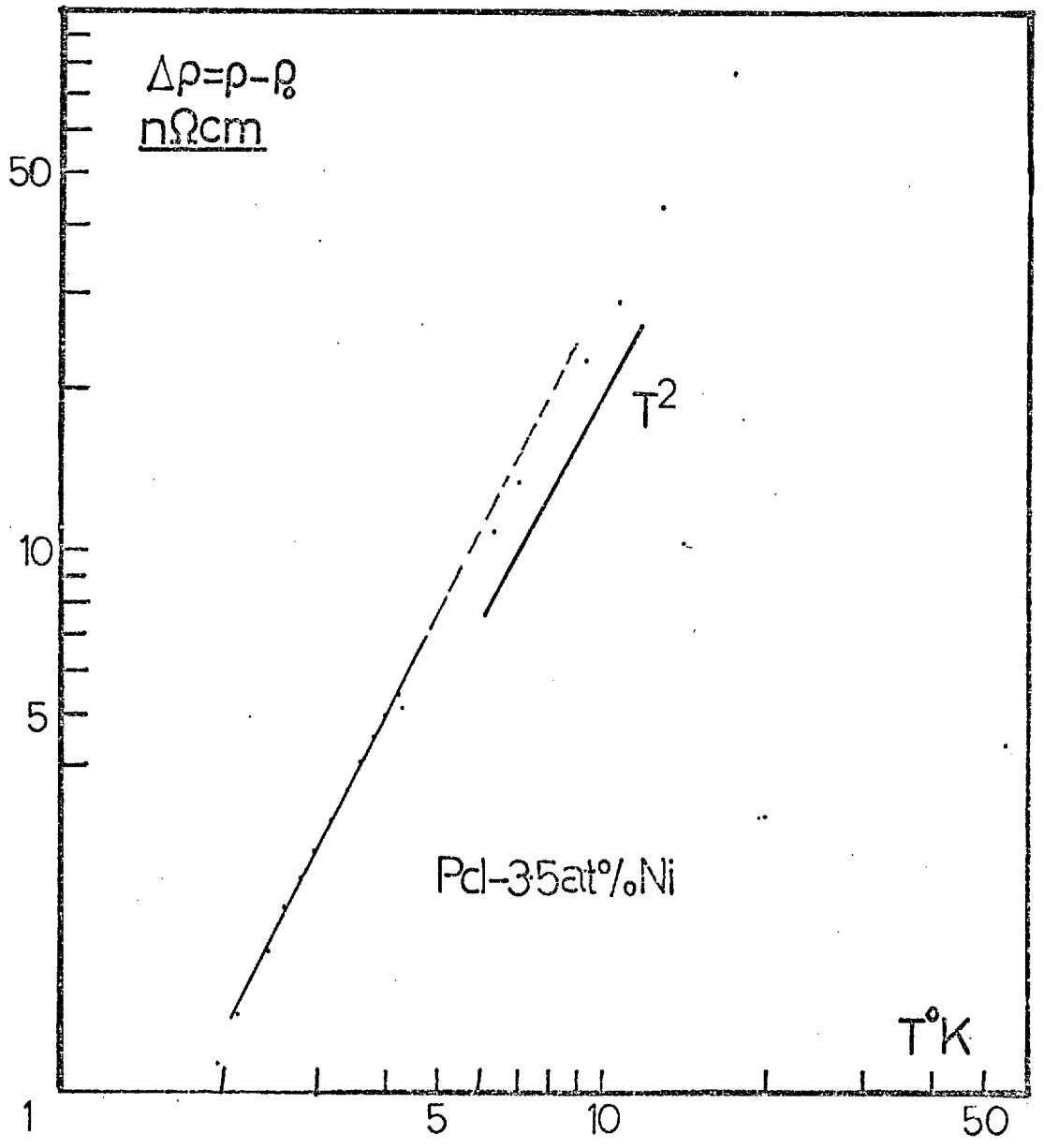

Fig. (V.19)

The data between 4.2° and 80°K are plotted on Fig. (V.16a). Up to 8°K the magnetization varies as T^2 Fig. (V.17). Such a T^2 law is expected from single particle excitations in weakly ferromagnetic alloys on the basis of the Stoner-Wohlfarth theory (140).

Pd-3.5 at % Ni

This alloy has a Curie temperature of 40°K as given by Shaltiel et al (89) Fig. (V.18). At the lowest temperatures the resistivity varies at $T^{2.05}$. Above 4°K the resistivity falls below the initial power law. However, around 10°K, the phonon term dominates and resistivity becomes more strongly temperature dependent. The variation of the resistivity with temperature is shown in Fig. (V.19) on a log-log plot which summarises the behaviour of the alloy.

Alloys containing 4, 4.5, 5.83 at % Ni

The behaviour of these alloys is similar as shown in Fig. (V.20) where the numbers indicate nickel concentrations in at %. At low temperatures the resistivity of the alloys varies as $T^{2.04}$, $T^{2.06}$ and $T^{2.2}$, in order of increasing nickel concentration. Deviations from these initial power laws occur at 10°, 9° and 8°K respectively. These deviations are due to phonons as the following argument shows:-

The Curie temperatures of the samples are approximately 50°, 60° and 90°K respectively Fig. (V.18). Therefore, in the temperature range in which measurements are done, the number of spin waves excited are fewer for 5.83 at % alloy than for the alloy containing 4.5 at % Ni. Hence, the effect of phonons comes in for the former alloy at a lower temperature. The same reasoning applies to the alloys containing 4.5 and 4 at % Ni.

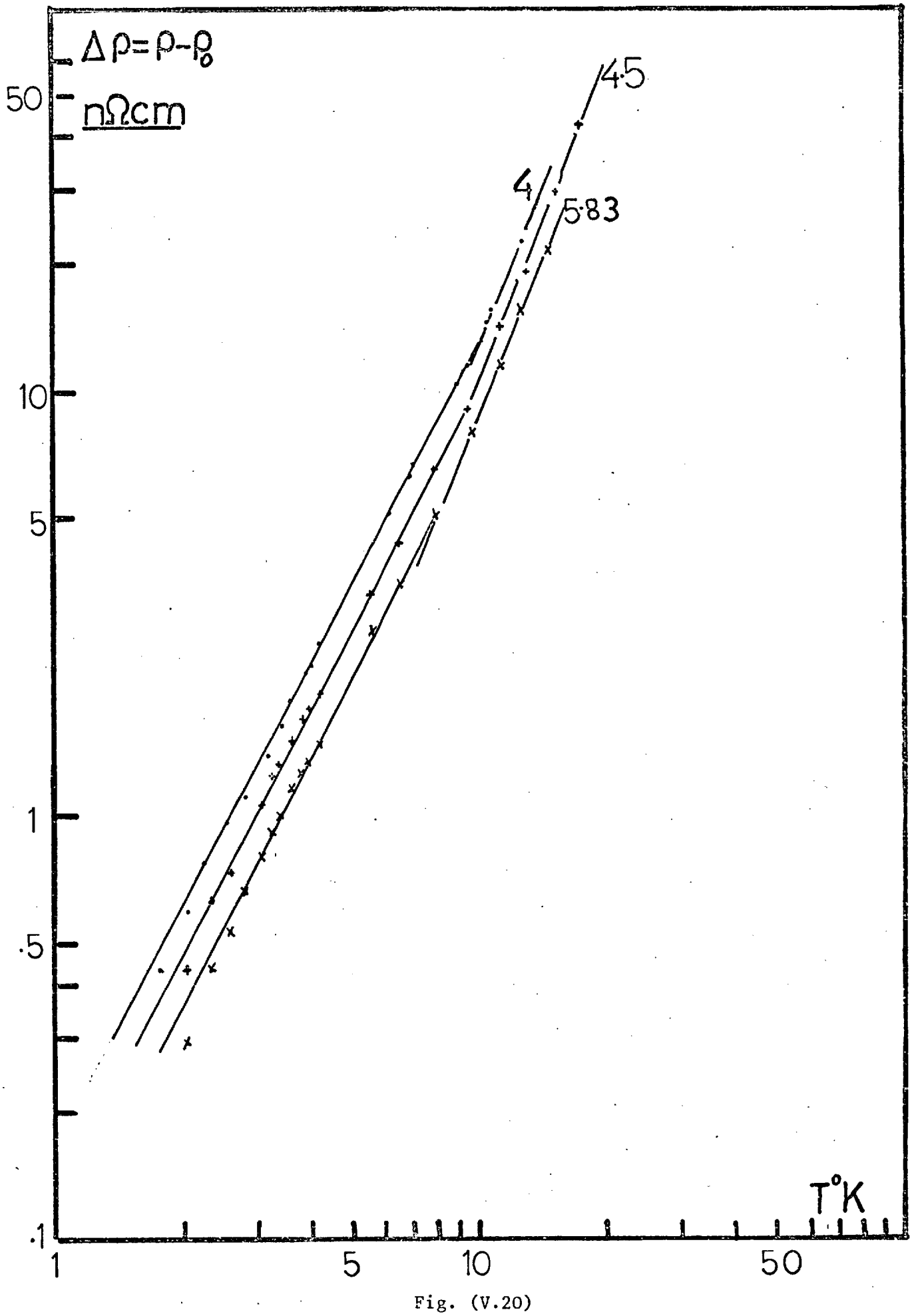

Fig. (V.20)

DISCUSSION

From the previous section it is clear that the temperature dependence of the resistivity is described by a low power of T when approaching the critical concentration (2.32 at % Ni). The power of T clearly falls well below 2, a power expected from electron-electron or from electron-magnon scattering.

The participation of d-electrons in the conductivity phenomena is corroborated by the clear relation of the temperature dependence of the resistivity to the magnetic state of the alloys.

The common feature of the resistivity temperature curves is that in all alloys (except the alloy containing 2.25 at % Ni) the experimental points fall below the initial power law. The effects mentioned above, i.e. lower power of T, negative deviation of the resistivity from the initial temperature dependence, etc., are predicted by the theories of Mathon, Kaiser and Doniach-Rivier and Zlatić. Mathon (78) has carried out the calculation of the resistivity through the critical concentration. Using the hamiltonian employed by Mills and Lederer (64), and uniform enhancement model of Schindler and Rice (74), he has calculated the resistivity using a variational method (141). The resulting expressions are:-

$$\rho = C_1 \frac{J^2}{T} \int_{-\infty}^{+\infty} d\omega \cdot \omega \int_{0}^{2k_F} \frac{q^3 dq \ \mathrm{Im}\, \chi^{-+}(\omega,q)}{(e^{\hbar\omega/k_B T}-1)(1-e^{-\hbar\omega/k_B T})} \qquad (V.1)$$

in the paramagnetic region and

$$\rho = C_2 \frac{J^2}{T} \int_{-\infty}^{+\infty} d\omega \cdot \omega \int_{0}^{2k_F} \frac{q^3 dq \left[\mathrm{Im}\chi^{-+}(\omega,q) + \mathrm{Im}\chi^{zz}(\omega,q)\right]}{(e^{\hbar\omega/k_B T}-1)(1-e^{-\hbar\omega/k_B T})} \qquad (V.2)$$

in the ferromagnetic region where C_1 and C_2 are two constants involving

physical parameters of the alloy, and J is the coupling constant between s- and d-electrons. The above formulae show immediately the depedence of ρ on the imaginary part of the susceptibility, $\mathrm{Im}\,\chi^{-+}(q,\omega)$. This function has been calculated by Doniach (52) and is shown in Fig. (V.21).

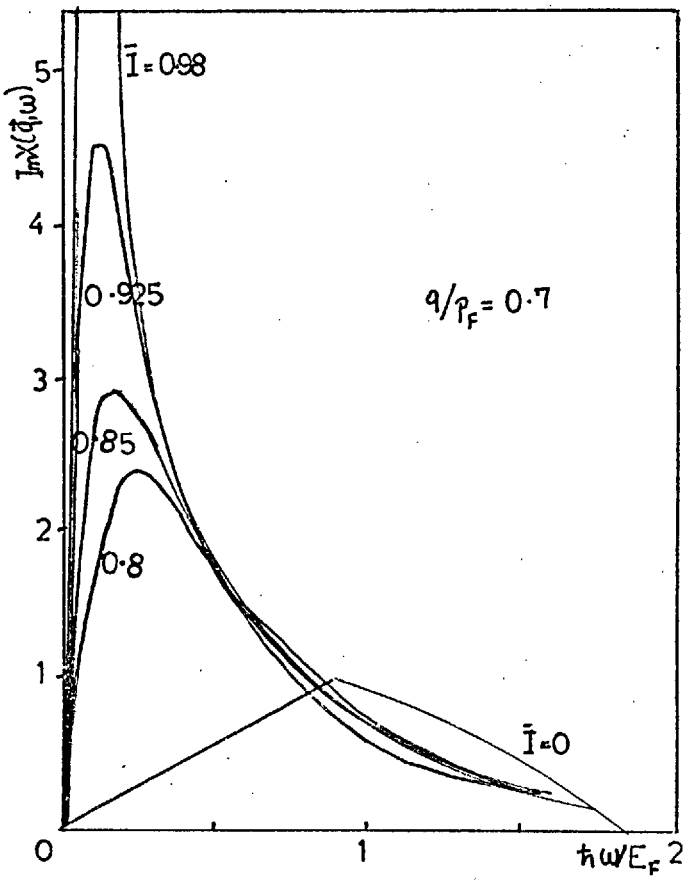

Fig.(V.21) Effect of electron-electron interaction on Im χ $(\vec{q},\omega)$ for a fixed $\vec{q}$.

The peak in the $\mathrm{Im}\,\chi^{-+}(\vec{q},\omega)$ moves to a lower value of ω as the enhancement increases, reaching a maximum at the critical concentration, i.e. when $\bar{I}\sim 1$. Thus at this concentration the resistivity has its maximum value.

Employing a model function for $\mathrm{Im}\,\chi^{-+}(\vec{q},\omega)$ Mathon has calculated these integrals. Away from the critical concentration he obtains for the resistivity the following:-

$$\rho_{para} = A.J^2.N_D(E_F)\ k_F^4\ E_F\ \frac{1}{K_o \bar{I}^{3/2}}\ \left(\frac{T}{T_F}\right)^2 \qquad (V.3)$$

where k_F, E_F and T_F are the d-electrons Fermi wave vector, energy and temperature respectively, and A is a constant $K_o^{-2} = (1-\bar{I})^{-1}$ is the Stoner enhancement factor.

At the critical concentration the expression obtained is:-

$$\rho_{Ferro} = \rho_{para} \cong B.J^2 N_D(E_F) k_F^4 \frac{E_F}{\bar{I}^2} \left(3\pi \frac{T}{T_F}\right)^{5/3} \left[3 - \left(3\pi \frac{T}{T_F}\right)^{1/3}\right] \quad (V.4)$$

where B is a constant.

The expression for the resistivity at the critical concentration shows that at the lowest temperatures the resistivity varies as $T^{5/3}$, however, at higher temperatures the second term in the square bracket will cause a negative deviation as is observed.

Apart from the predicted $T^{5/3}$ law for the alloy with the critical concentration, the experimental results are in overall qualitative agreement with the prediction of Mathon.

The values of A together with those of n and ρ_o, obtained by fitting the data below 4.2°K to the expression $\rho = \rho_o + AT^n$, are listed in Table 1, and those of A are plotted in Fig. (V.22) together with coefficient of the T^2 terms extracted for more dilute alloys by Schindler (126).

Table 1: The values of the parameters in the expressions $\rho = \rho_o + AT^n$ at temperatures below 4.2°K.

Composition (at % Ni)	ρ_o^+ ($10^{-6}\Omega$cm)	A ($10^{-12}\Omega$cm/K^n)	n*
2.25	0.676	2500	1.40
2.35	0.893	2800	1.49
2.42	0.803	1580	1.76
2.50	0.988	1420	1.75
3.00	1.139	607	1.90
3.50	1.284	320	2.00
4.00	2.048	138	2.04

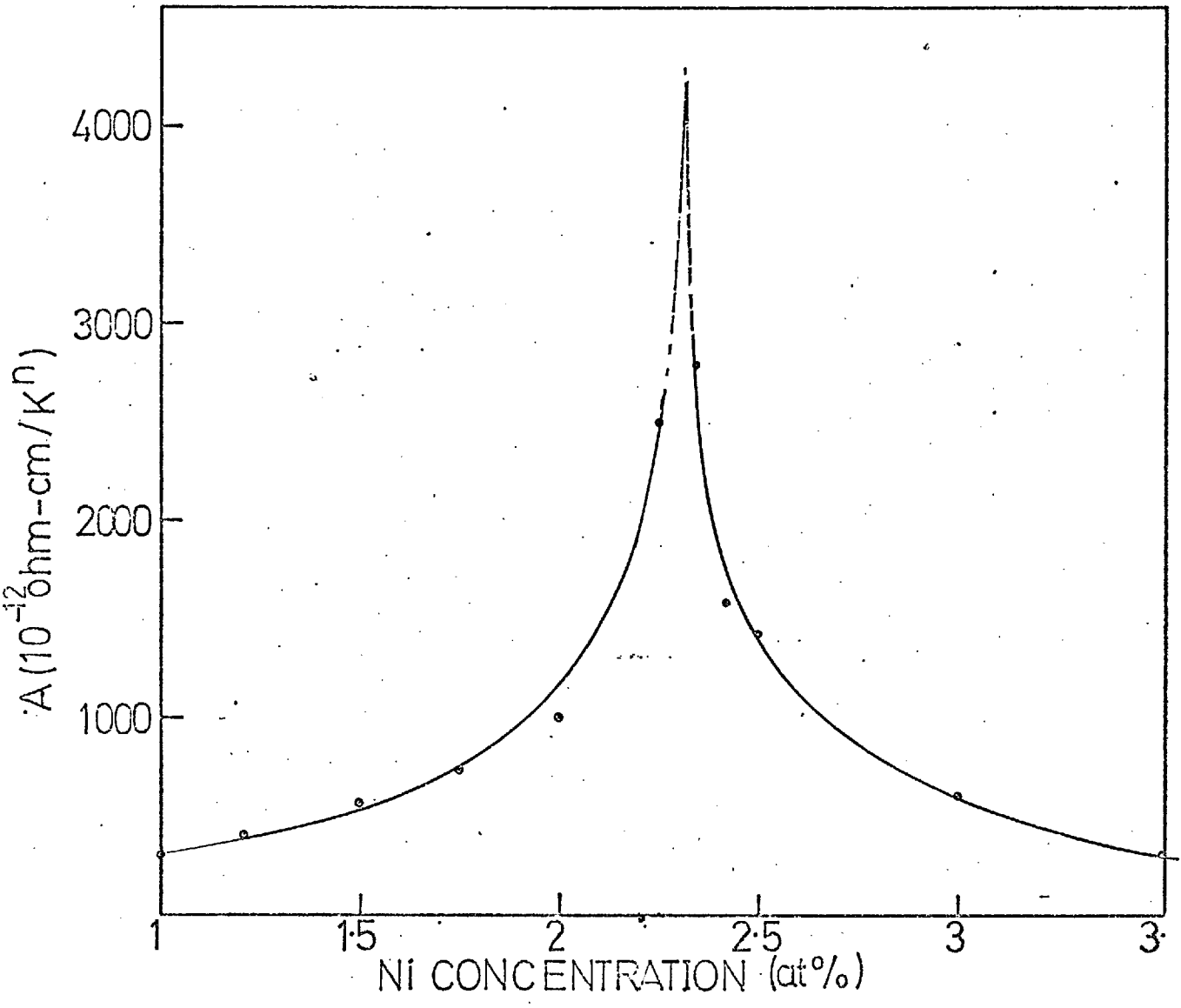

Fig(V·22) Plot of the coefficient A against Ni concentration

4.50	2.477	120	2.06
5.83	3.065	80	2.20

+ The uncertainties in these values arise mainly from inaccuracies in determining the dimensions; it is rather larger for 2.42% alloy.

* The uncertainties are ±0.05 for alloys near the critical concentration rising to ±0.1 at 5.83% Ni.

The peak in A is extremely pronounced giving C_F as 2.32±0.03 at %. The curve for A clearly approaches the symmetry required by Mathon's theory.

Fig. (V.22) summarises the variation of the ideal (temperature dependent part) of the resistivity with concentration. When approaching the critical concentration from the paramagnetic side the local exchange enhancement increases and the spin fluctuation temperature decreases. Hence, more and more paramagnons are excited below 4.2°K until the spin fluctuation temperature is zero (critical concentration) in which case all the paramagnons are excited at any finite temperature. Therefore, the resistivity reaches a maximum at this concentration.

In the ferromagnetic region below 4.2°K fewer and fewer spin waves are excited with increasing nickel concentration as the Curie temperature increases with increasing concentration, consequently the resistivity decreases.

The variation of Tc with nickel concentration is shown in Fig. (V.18). The lower points are obtained by us using low field data in Arrott plots. The higher points are those of Crangle and Scott (107) and Shaltiel et al (89) obtained from the Arrott plots using high field data.

The magnetization measurement of Pd-3 at % Ni in 100 Gauss Fig (V.16a) shows clearly the justification of the use of the low field Arrott plots.

McDougald and Manuel (142) have shown that in dilute Pd-Fe alloys too,

the transition temperatures are consistent with those obtained from resistivity and specific heat measurements when using low field Arrott plots.

2. Pd-Mn Alloys

Introduction

The dilute Pd-Mn alloys show a ferromagnetic ordering, while at sufficiently high concentration some type of random antiferromagnetic ordering sets in. There is thus a concentration range where a gradual transition from ferromagnetism to antiferromagnetism occurs. Although the dilute alloys have been investigated extensively, no satisfactory research has been carried out in the intermediate region.

The present work is part of a general research done in conjunction with Mr R.H.Taylor who performed electron spin resonance (ESR) experiments and Dr H.Jamieson who made the susceptibility and magnetization measurements to investigate the behaviour of Pd-Mn alloy system at intermediate concentrations.

Pd-3.75 at % Mn

The incremental resistivity ($\Delta\rho = \rho_{alloy} - \rho_{Pd}$) of this alloy is shown in Fig. (V.23) as a function of temperature. The alloy has an ordering temperature of $T=6.3^{o}K$ which is well defined as is clear from the figure. Below this the incremental resistivity is linear in temperature. At the lowest temperatures it varies as $T^{1.5}$ Fig. (V.24).

The run on the magnets resistance is shown in Fig. (V.25) where the resistance in zero field and in a field of 7.65kG are plotted as a function of temperature. It is clear that the application of an external field results in a decrease in the resistance and an increase in Tc. Measurements on Pd-2.9 at % Mn made by Williams (143) show the same effect.

Fig. (V.23)

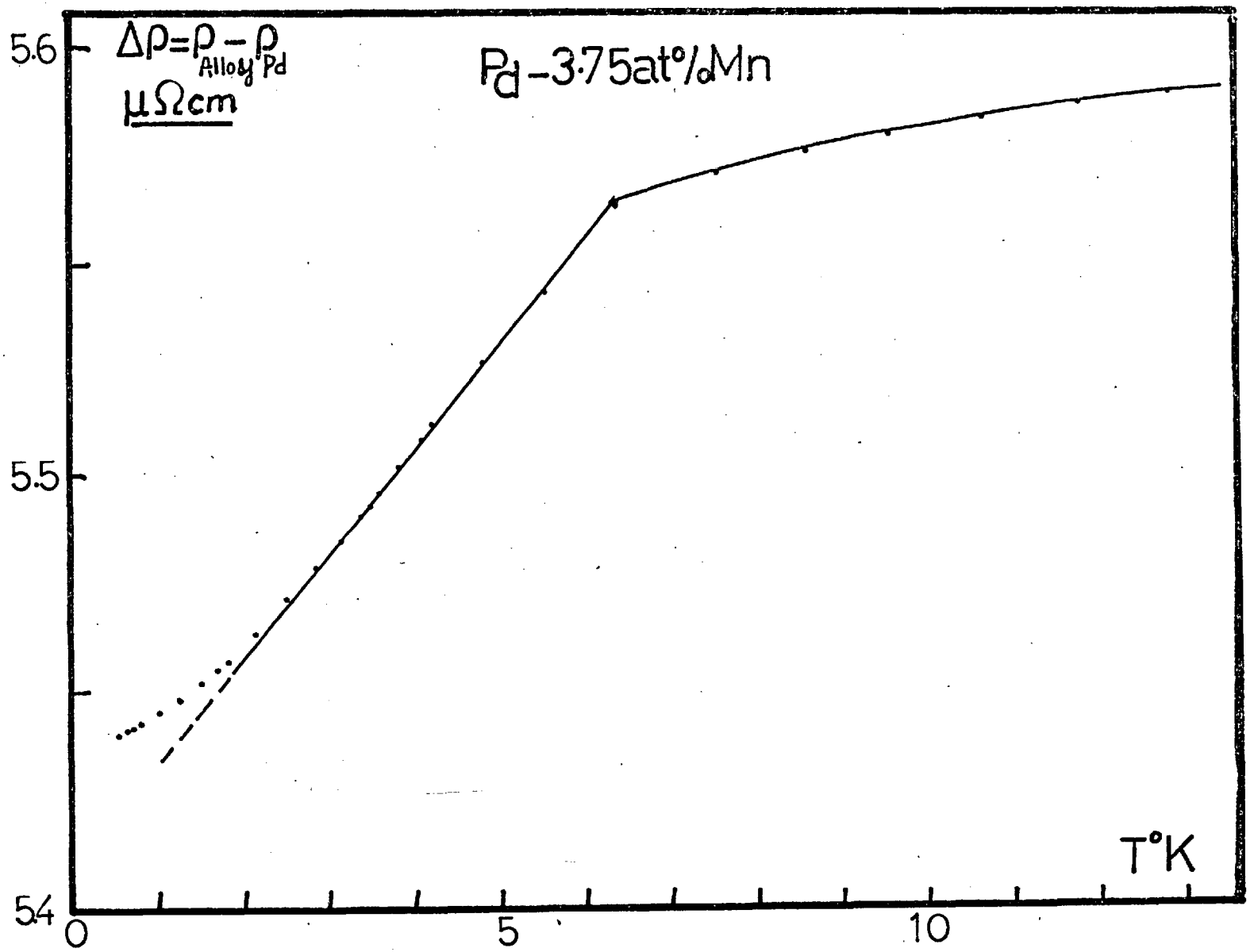

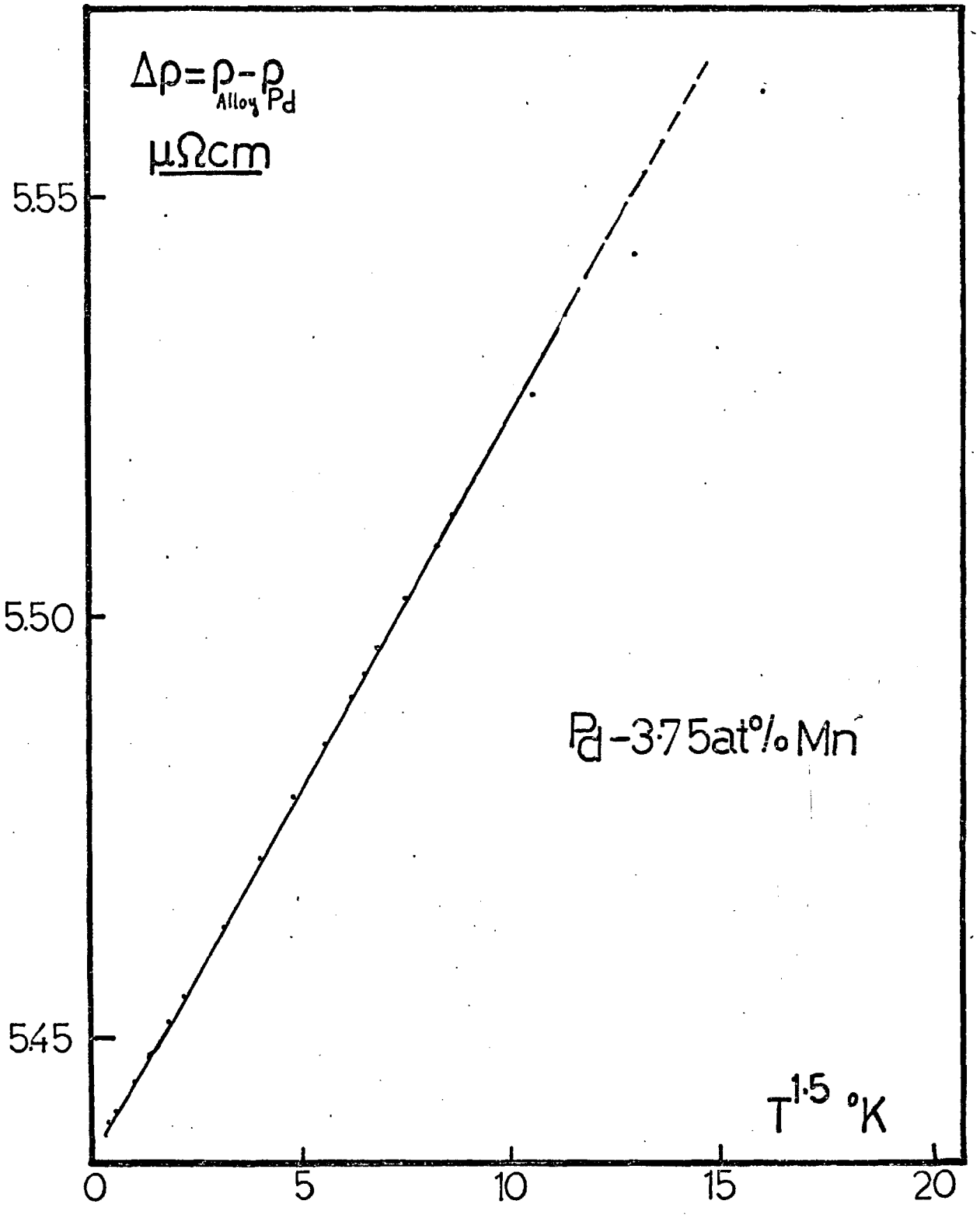

Fig. (V.24)

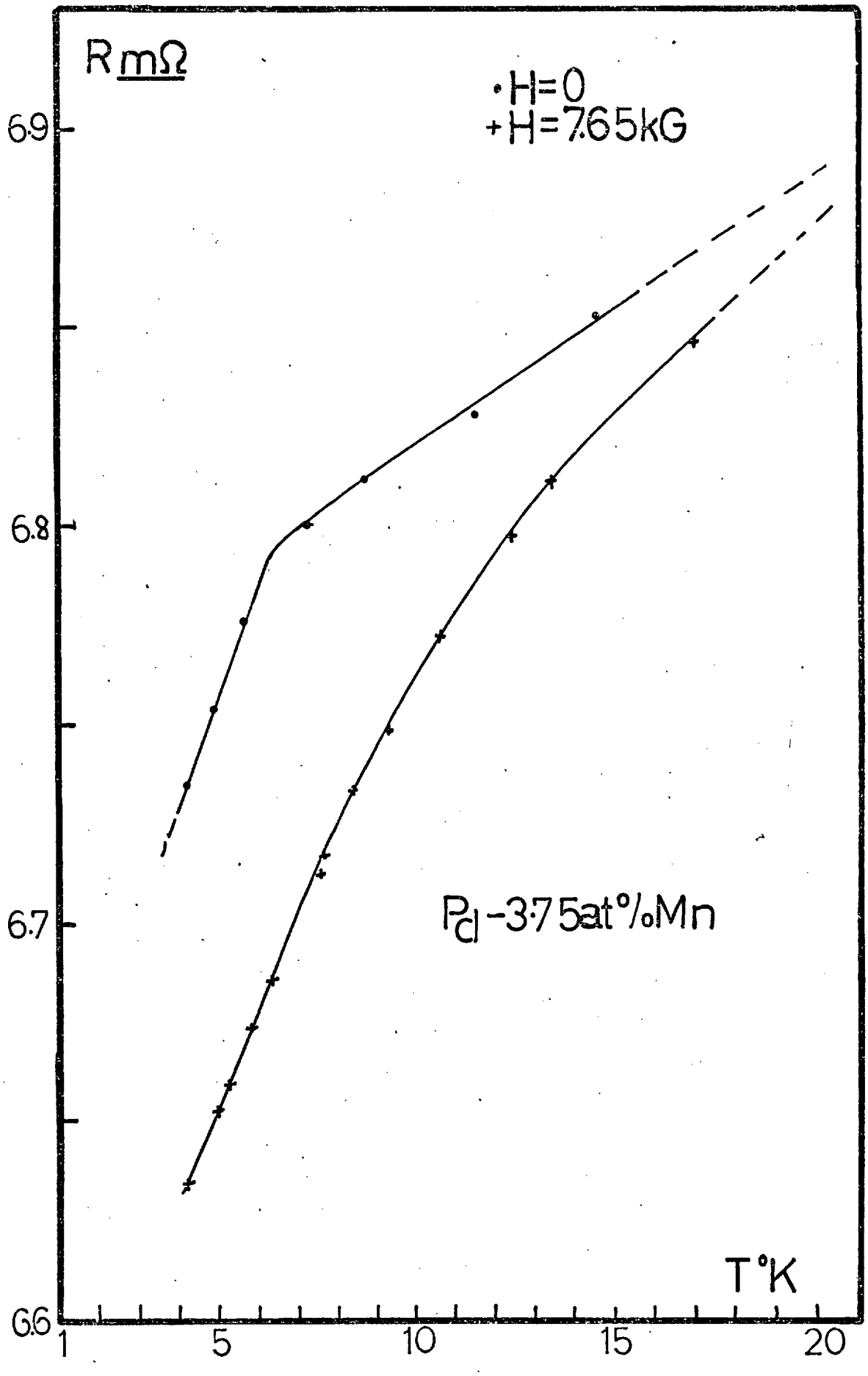

Fig.(V.25)

Such a negative magneto resistance is in agreement with the prediction of Yosida (68). The increase in Tc and the rounding-off of the resistance-temperature curve at Tc is, of course, expected.

Pd-4.1 at % Mn

The behaviour of this alloy is very similar to Pd-3.75 at % Mn as Fig. (V.26) shows. However, the ordering temperature Tc which is at 4.5°K is less well defined. Below Tc the incremental resistivity is linear in temperature. At temperatures up to approximately 0.5 Tc the incremental resistivity varies as $T^{1.5}$ Fig. (V.27). Above the ordering temperature this alloy is more strongly temperature dependent than the previous one.

Alloys of Higher Concentrations

The incremental resistivities of Pd containing 4.5, 5.3 and 8.4 at % Mn are plotted in Fig. (V.28) as a function of temperature. None of these alloys show a clear ordering temperature. The incremental resistivity of the alloys containing 8.4 and 4.5 at % Mn behaves as $T^{1.5}$ at temperatures well into the helium temperature range Figs. (V.29) and (V.30). Pd-5.3 at % Mn, however, varies as $T^{1.5}$ up to about 1°K Fig. (V.30).

If the range of the $T^{1.5}$ behaviour of the resistivity is a measure of the magnitude of the ordering temperature, then among the alloys investigated here Pd-5.3 at % Mn appears to have the lowest ordering temperature. This is consistent with the Tc-concentration curve shown in Fig. (V.31).

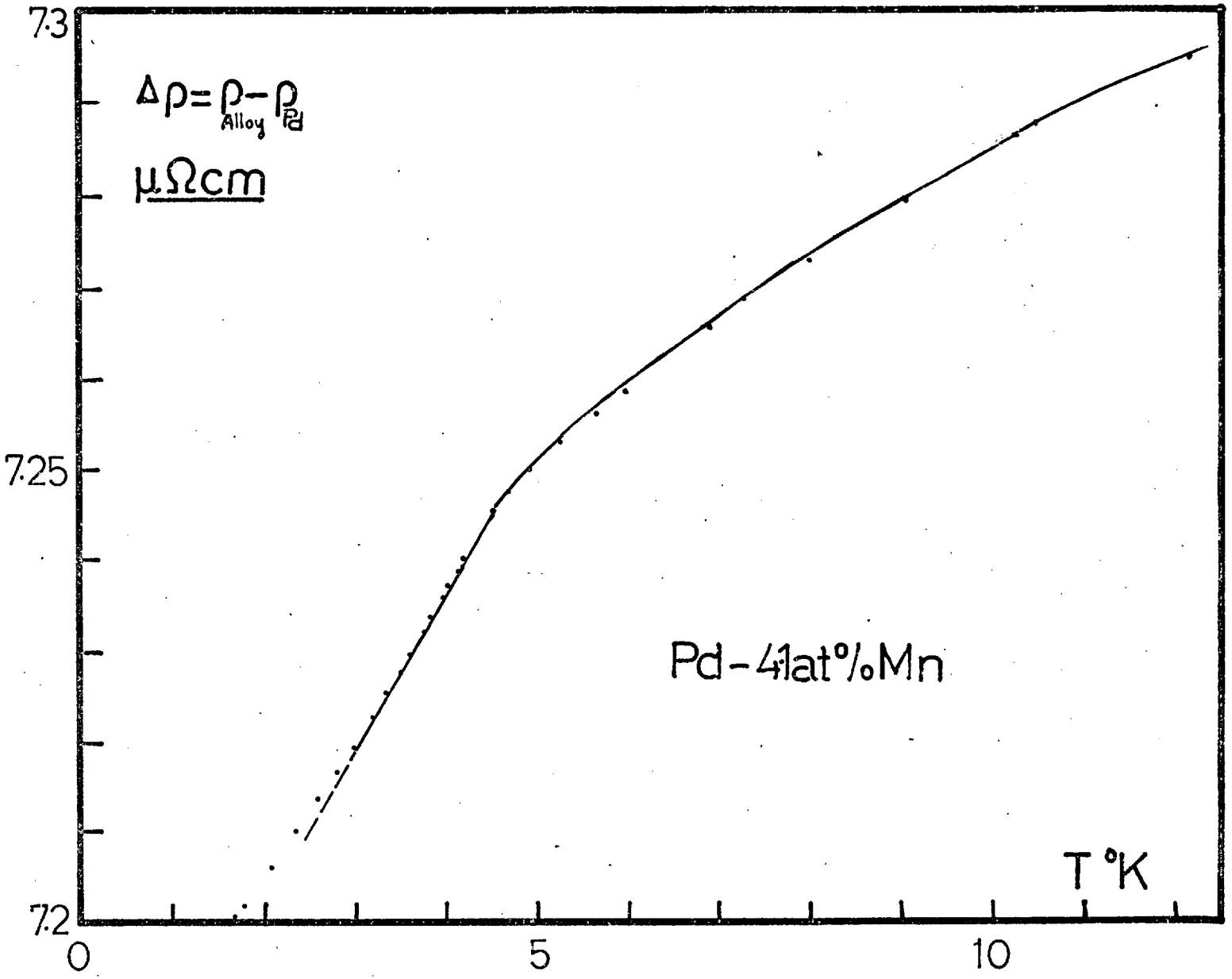

Fig. (V.26)

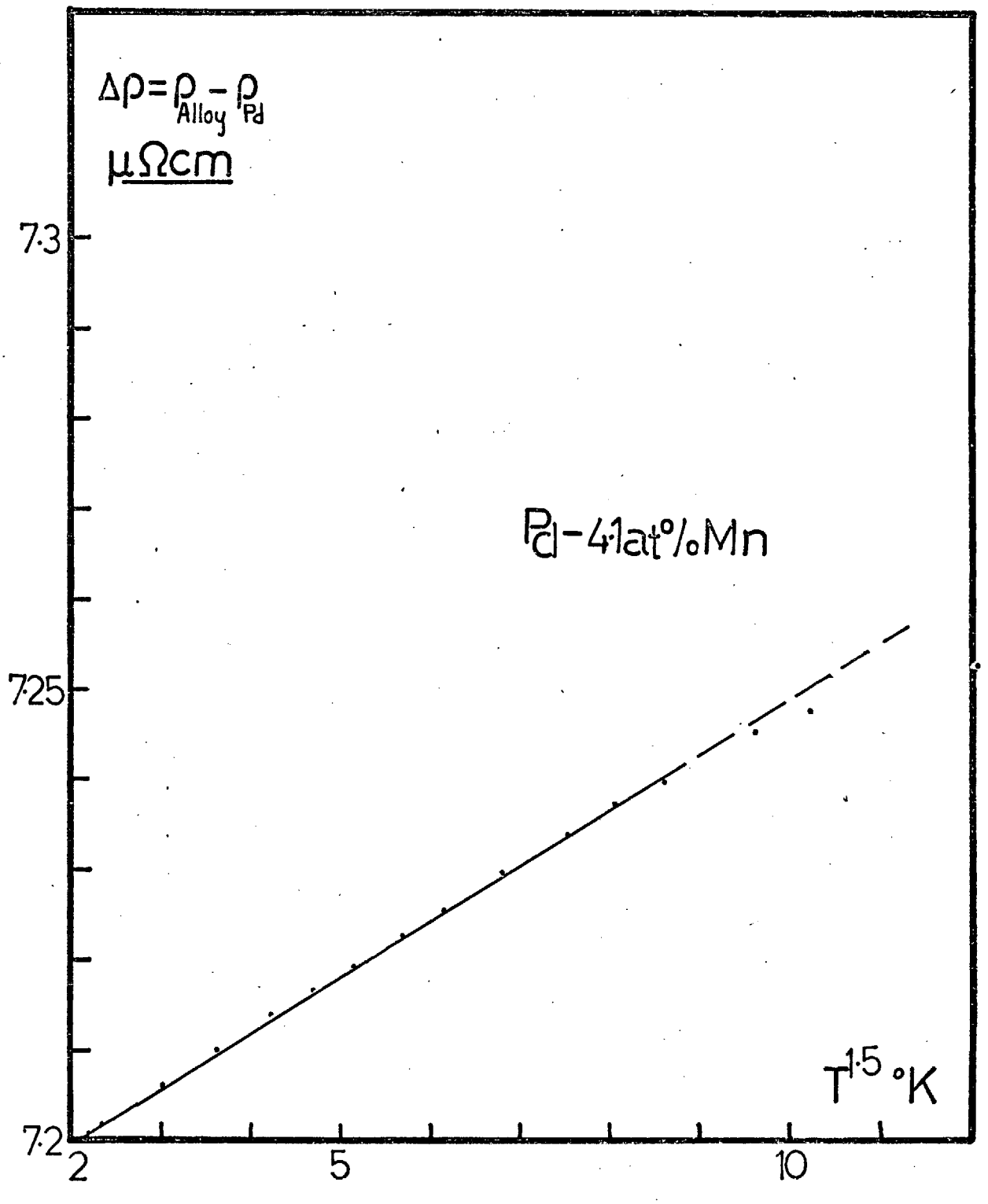

Fig. (V.27)

Fig. (V.28)

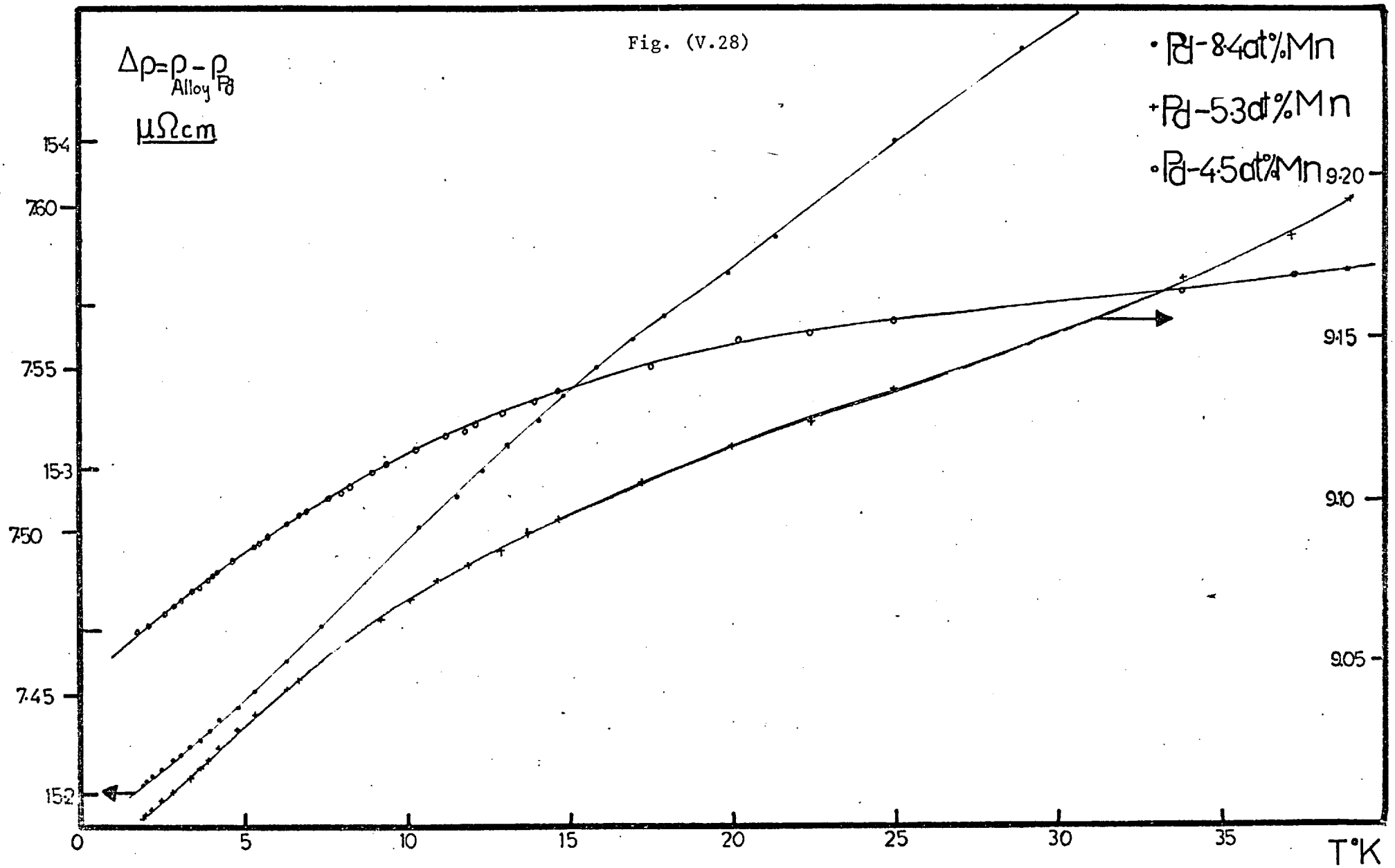
Δρ=ρ Alloy − ρ Pd
μΩcm
• Pd-8·4at%Mn
+ Pd-5·3at%Mn
◦ Pd-4·5at%Mn
15·4
7·60
7·55
15·3
7·50
7·45
15·2
9·20
9·15
9·10
9·05
0
5
10
15
20
25
30
35
T°K

Fig. (V.29)

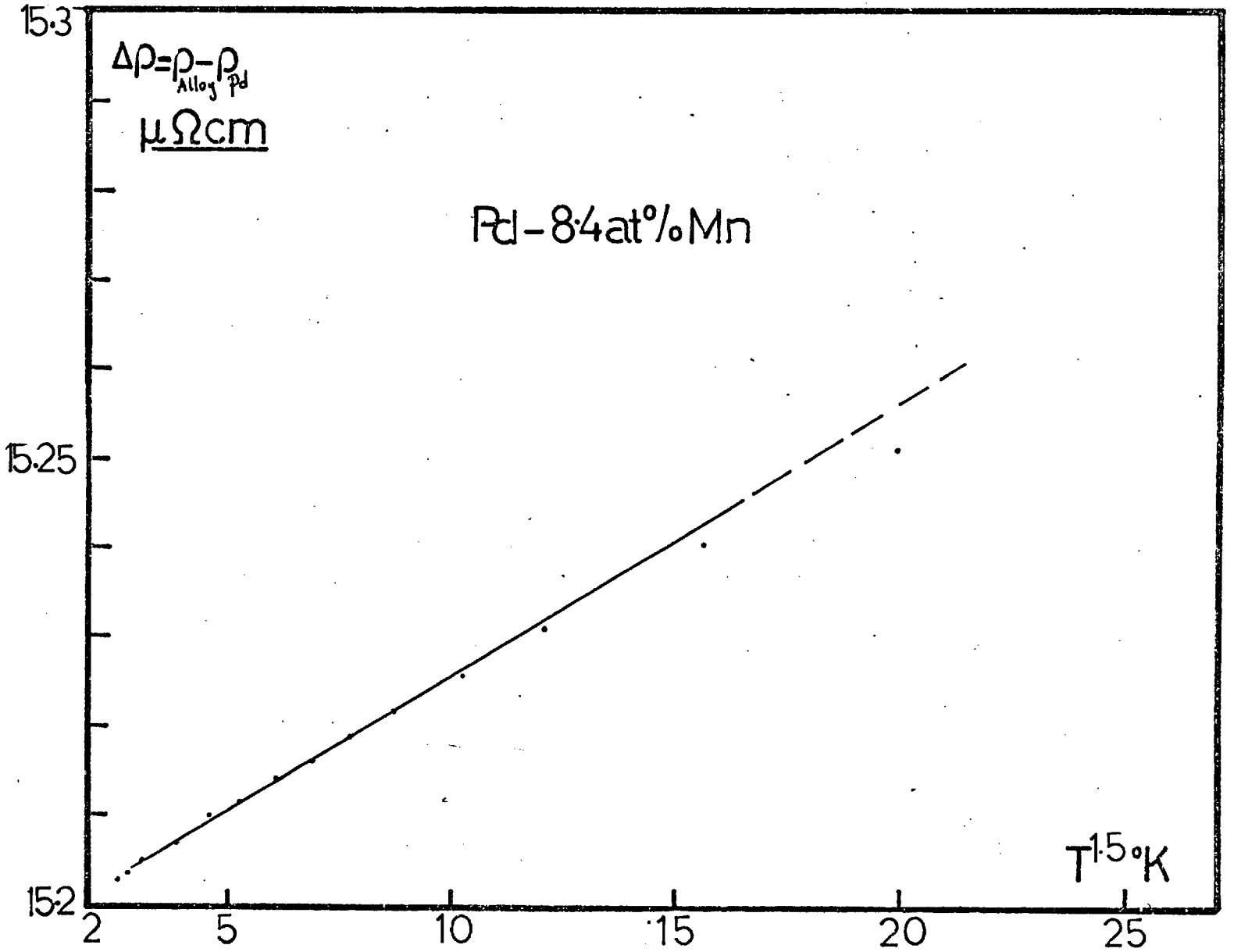
15·3
15·25
15·2
$\Delta\rho=\rho_{Alloy}-\rho_{Pd}$
μΩcm
Pd-8·4at%Mn
2
5
10
15
20
25
$T^{1.5}$°K

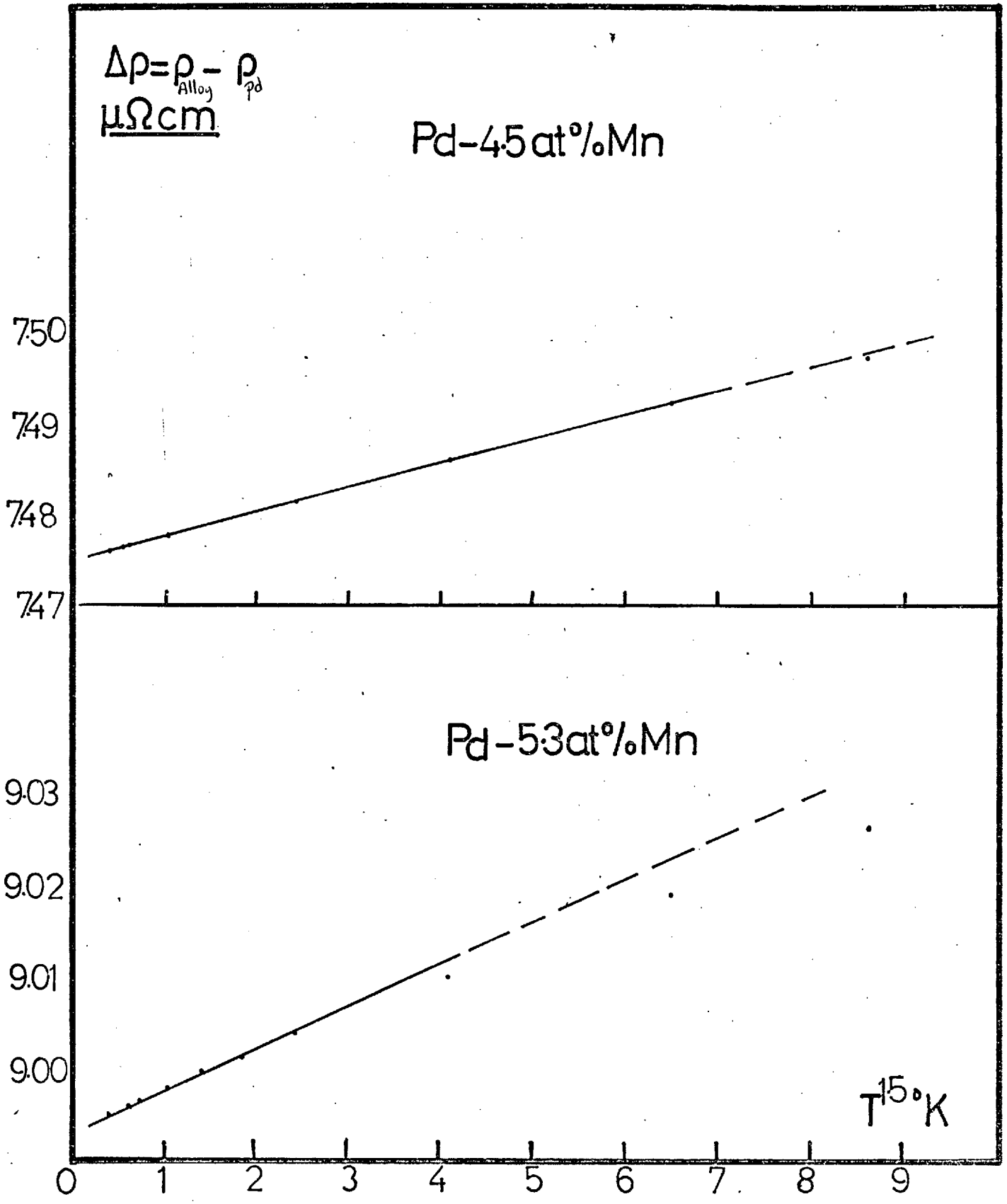
Δρ=ρ Alloy − ρ Pd
μΩcm
Pd-4.5at%Mn
7.50
7.49
7.48
7.47
Pd-5.3at%Mn
9.03
9.02
9.01
9.00
T15°K
0
1
2
3
4
5
6
7
8
9

Fig. (V.30)

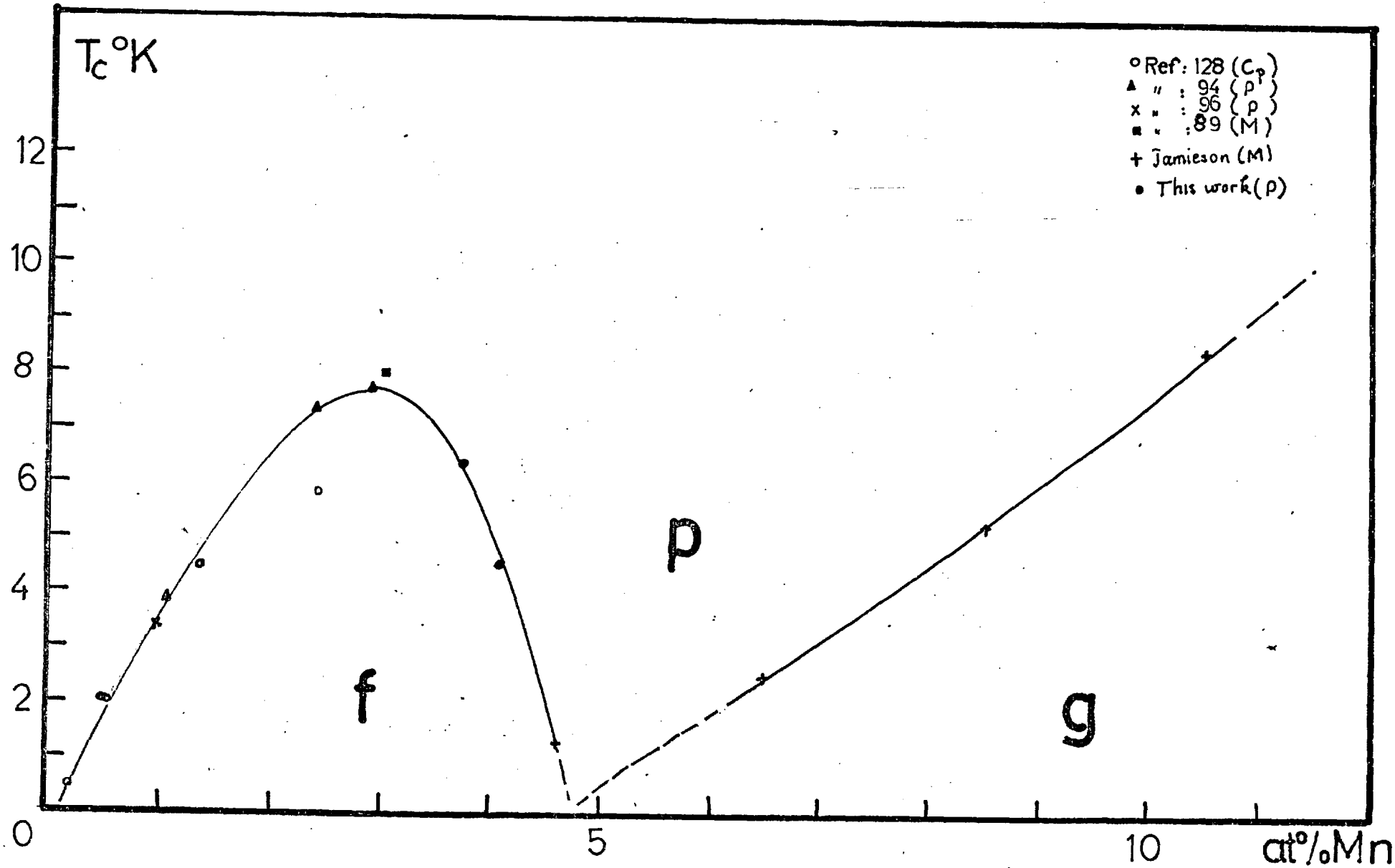
T_c °K
12
10
8
6
4
2
0
5
10
at°/₀Mn
f
p
g
° Ref: 128 (C_p)
▲ " : 94 (ρ')
x " : 96 (ρ)
■ " : 89 (M)
+ Jamieson (M)
• This work(ρ)

Fig. (V.31)

DISCUSSION

A tentative phase diagram of the Pd-Mn alloy system is shown in Fig. (V.31). At low concentrations the Curie temperature varies as Tc~3.6c (c in at %) unlike Pd-Fe and Pd-Co where Tc~40c. This implies that the strength of interaction between Mn atoms is an order of magnitude smaller than those of Fe or Co in palladium. At low concentrations the incremental resistivity-temperature graphs show a rather sharp transition from ferromagnetism to paramagnetism which indicates a more uniform range of interactions between manganese atoms. Measurements by Boerstoel (128) on dilute ($c \lesssim 2.45$ at %) alloys show fairly sharp peaks in specific heat which support the above statement.

In alloys containing up to 4.1 at % Mn, the prominent features of the incremental resistivity are the following:-

(i) Below T_c, $\Delta\rho$ decreases linearly with decreasing temperatures.

(ii) At temperatures sufficiently lower than Tc, $\Delta\rho$ varies as $T^{1.5}$.

These behaviours have been predicted by Long and Turner (Chapter II, Section 6) for the ferromagnetic alloys of Pd with Fe, Co and Mn.

The resistivity measurements of Williams and Loram (94) of Nieuwenhuys and Boerstoel (96) and this work show that the transition temperature becomes progressively less well defined and decreases with increasing manganese concentration. Above 4.3 at % Mn the resistivity becomes a smooth function of temperature, and it is no longer possible to detect the ordering temperatures. At sufficiently low temperatures again a $T^{1.5}$ behaviour is observed in the incremental resistivity. The magnetization and susceptibility measurements of Roult and Burger (109) and Jamieson show that the Curie temperature decreases further with increasing Mn concentration. Jamieson has obtained an ordering temperature of 1.25°K for Pd-4.6 at % Mn from the conventional σ^2 versus $\frac{H}{\sigma}$ (Arrott

plots). Above about 4.8 at % Mn the ordering temperature starts increasing (approximately linearly) with increasing manganese concentration. The variation of Tc with Mn concentration, Fig. (V.31), suggests a progressive transition from ferro to antiferromagnetic ordering. This can be interpreted as follows:-

At low concentrations Mn atoms interact through the polarization clouds they induce in Pd d-band. Recent works by Star at al (110) and Coles (pr.comm) show that these are giant clouds (Star et al observed a magnetic moment of $\mu = 7\text{-}8\mu_B$ per atom) similar to those found in Pd-Fe and Pd-Co. The interaction between these giant polarization clouds, which extend over a large distance due to the enhancement of the host matrix, is ferromagnetic. However, with increasing Mn concentration the direct Mn-Mn interaction which is shown by Moriya (95) and Kim (11) to be antiferromagnetic, competes with and, eventually suppresses, this ferromagnetic interaction.

The incremental resistivity of Pd-8.4 at % Mn varies, as we have seen, as $T^{3/2}$ at temperatures up to $4^{o}K$. The magnetization and susceptibility measurements by Jamieson show that the alloys containing more than about 6.5 at % Mn display the characteristic behaviours seen in spin glass systems, namely susceptibility maxima, time and temperature dependent remanence, etc. A $T^{3/2}$ behaviour is also observed by Mydosh and Ford (144) in the incremental resistivity of Au-Fe alloys with low Fe concentrations, where the alloys are well established as being spin glass systems.

3. Rh-Co Alloy System

Introduction

This alloy system is like Pd-Ni, isoelectronic and the susceptibility of the host metal is exchange enhanced. However, the enhancement in rhodium is much smaller than that in palladium and the local exchange enhancement on a cobalt atom in rhodium is very small compared to that of a nickel atom in palladium. Therefore the localized spin fluctuation effects on the electrical resistivity (103) and magnetic susceptbility (113), (112) of dilute Rh-Co alloys are small, and the appearance of localized moment behaviour is to be expected at a much higher cobalt concentration. The investigation of a Rh-11 at % Co by Murani (113) has shown that even at this concentration the cobalt atoms are well away from the magnetic state.

We report below the resistivity and magnetization measurements of rhodium containing between 11 and 44 at % Co.

(a) Resistivity

The resistivity-temperature plots of the alloys are shown in Figs. (V.32), (V.33) and (V.34) where the numbers on the curves indicate cobalt concentration in at %. The most notable features of the alloys displayed by the graphs are the following:-

(i) The alloys with cobalt concentration well away from 20 at % have only very weakly temperature dependent resistivities at low temperatures. The dependence becomes stronger on approaching this concentration from either side.

(ii) The resistivity of alloys around 20 at % Co is very strongly temperature dependent and is linear in temperature over a considerable range. Away from this concentration the power of T increases. At 11and

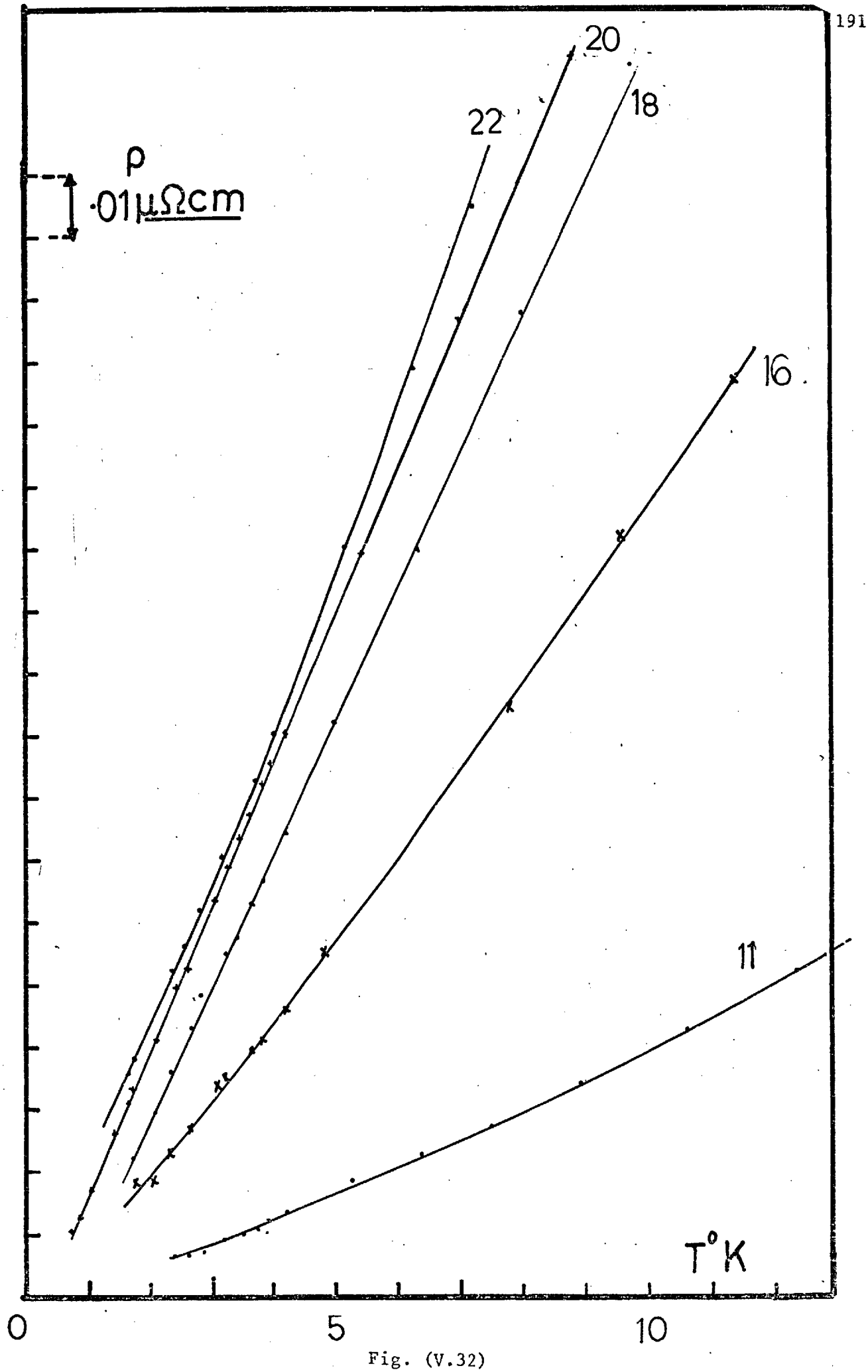

Fig. (V.32)

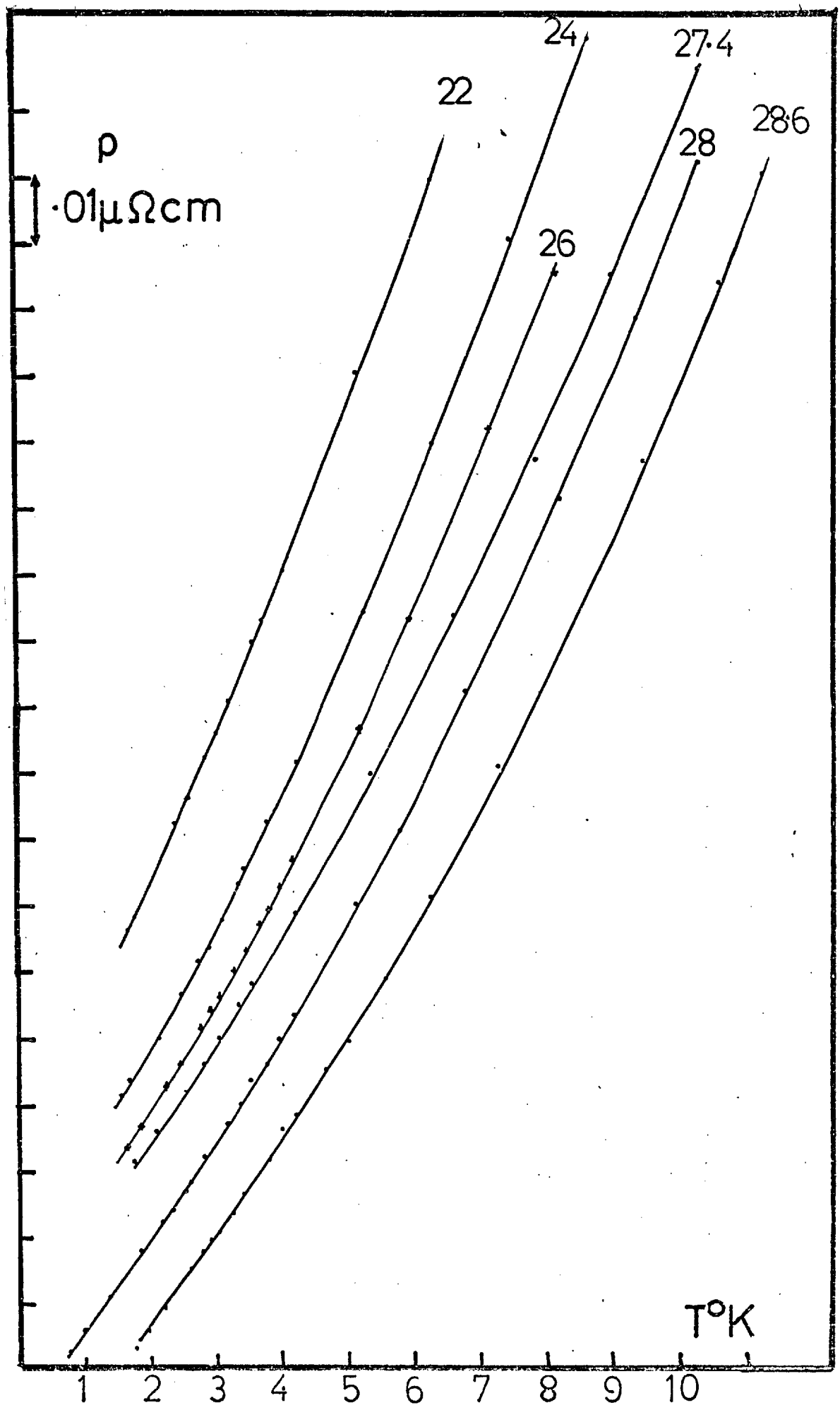

Fig. (V.33)

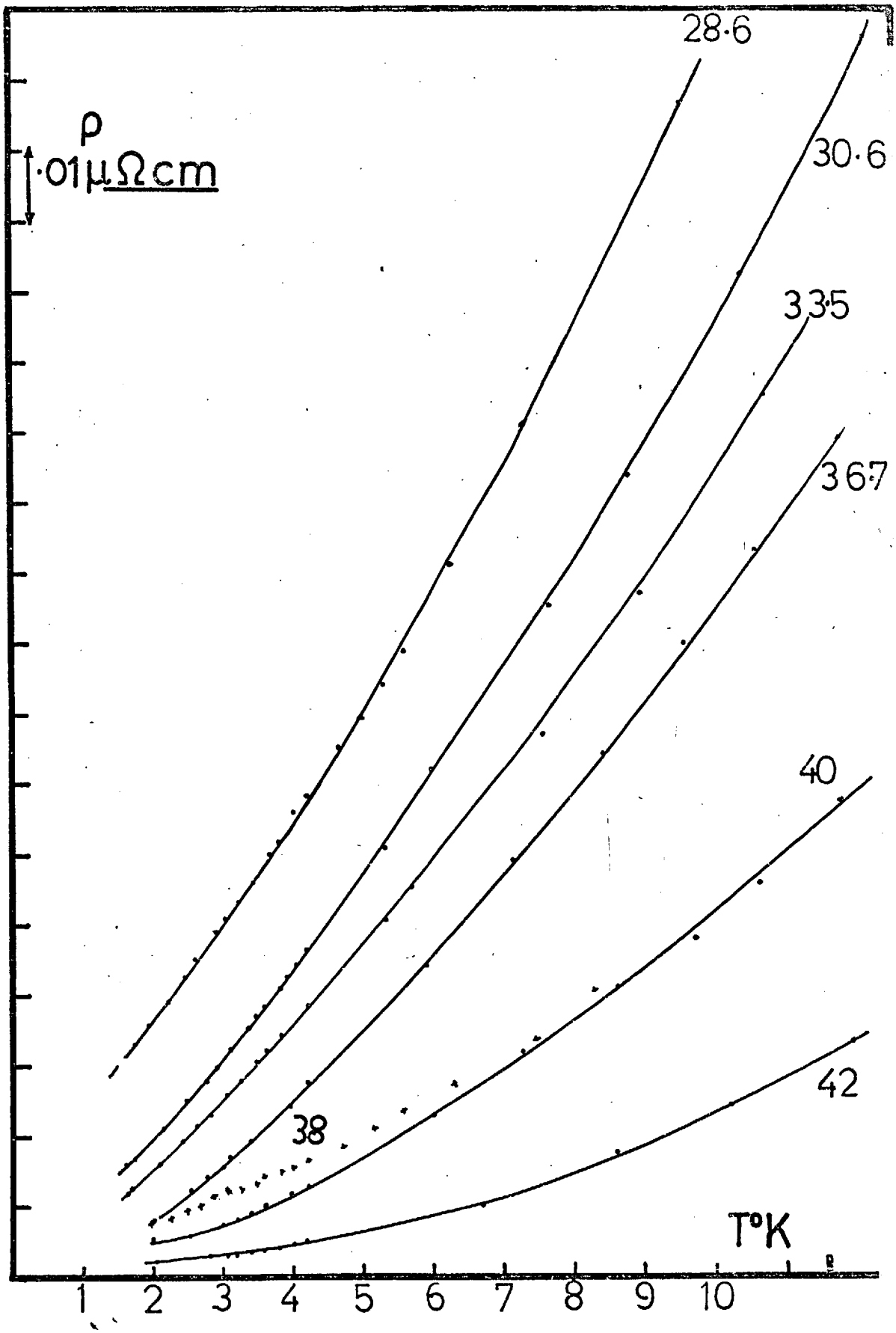

Fig. (V.34)

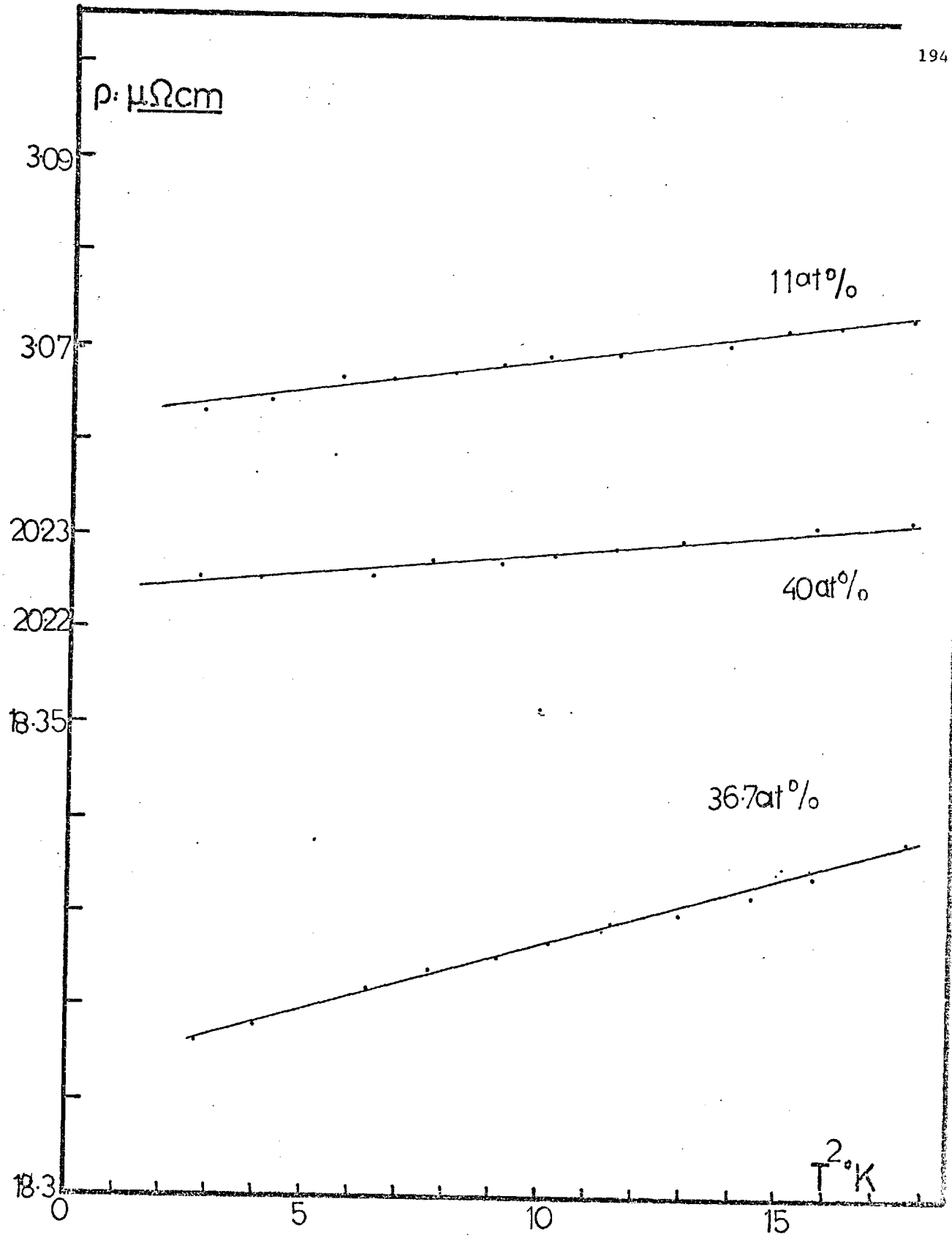

Fig. (V.35)

36.7 at % Co the power T reaches to 2 as shown in Fig. (V.35). However, the scattering mechanisms in these two alloys are different in nature as will be explained later.

A noticeable anomaly occurs in the resistivity of the alloy with 38 at % Co at about 3°K as can be seen in Fig. (V.34).

The resistivities of the alloys containing 16,20 at 28 at % Co were measured in the He^3 temperature range by Rusby at the National Physical Laboratories. Those of the first two are displayed in Fig. (V.36). The resistivity of the alloy 16 at % Co is linear in temperature down to 0.5°K, but that of 20 at % Co is linear only down to about 1.2°K. Below this temperature, deviation towards a higher power of temperature occurs.

The resistivities of alloys containing between 20 and 33.5 at % Co are plotted in Fig. (V.37) as a function of $T^{1.5}$. It is clear that there is a gradual increase in power of T. Only alloys with more than about 28 at % Co behave as $T^{1.5}$ at low temperatures. In these alloys hysteretic behaviour starts appearing in low temperature magnetization-field plots.

The resistivities of alloys containing between 33.5 and 42 at % Co are plotted in Fig. (V.38) as a function of T^2. The two concentrated alloys behave as T^2 over a larger temperature range than other alloys. The alloy containing 33.5 at % Co varies, of course, as $T^{1.5}$ as we have pointed out above.

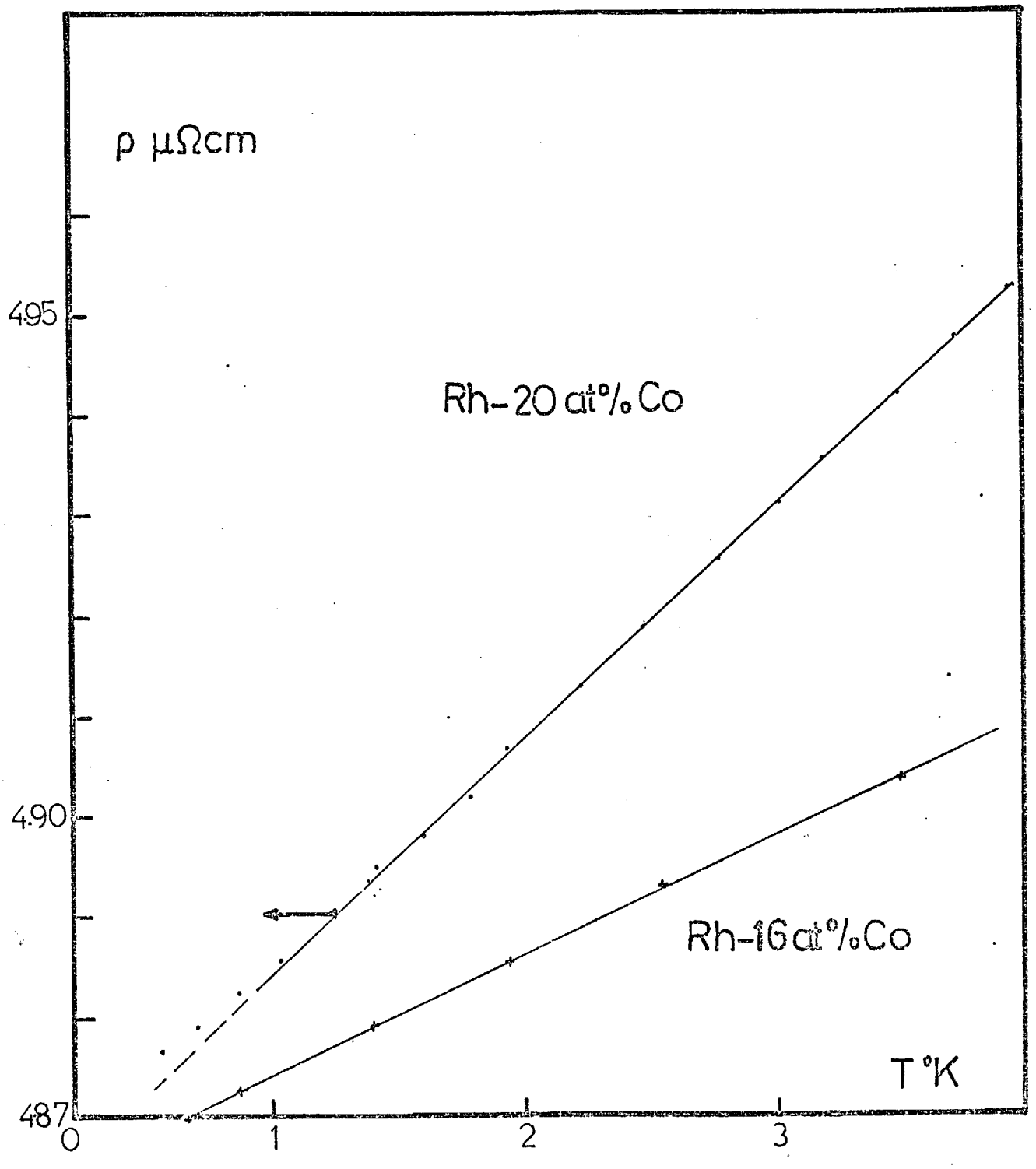

Fig. (V.36)

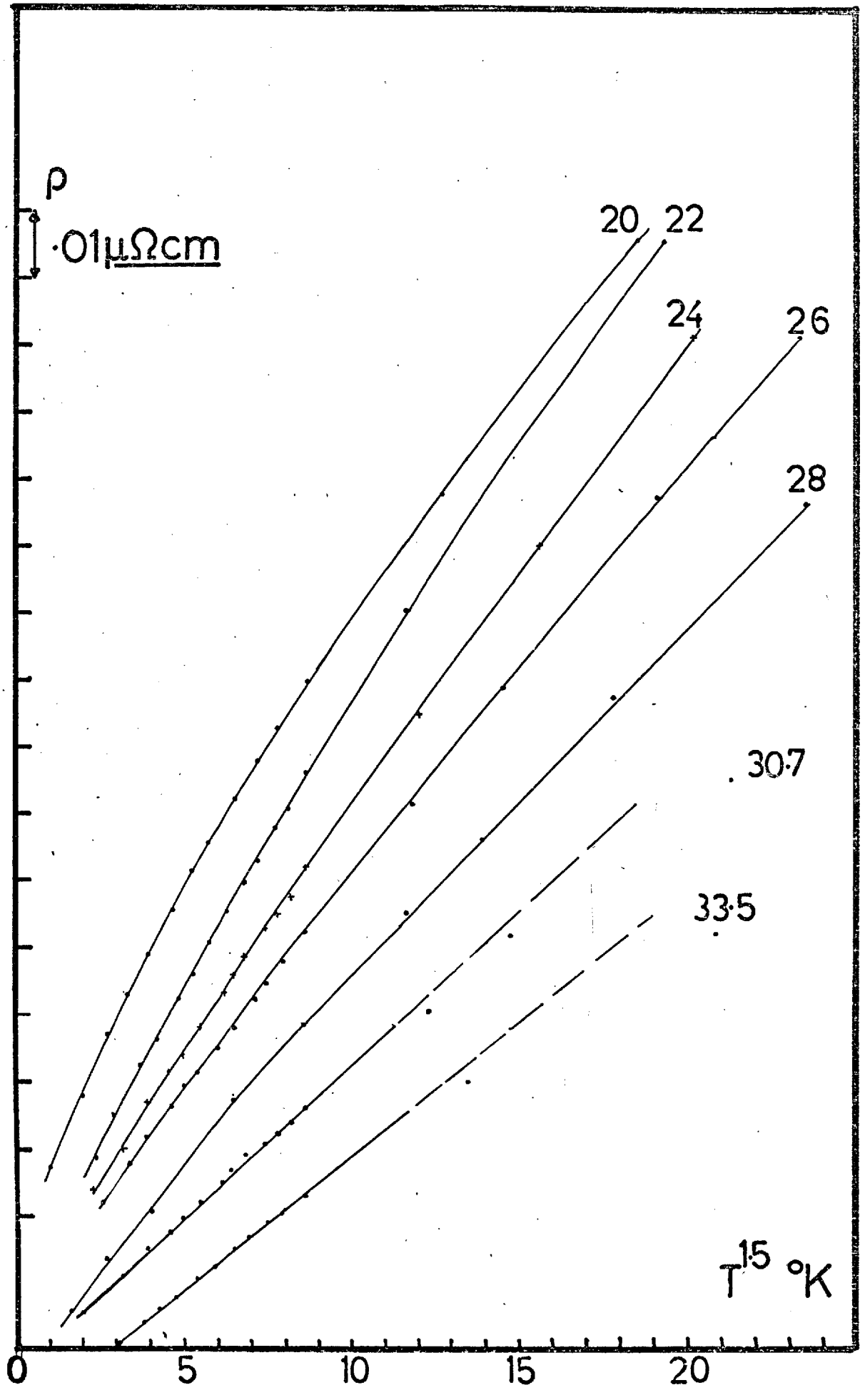

Fig. (V.37)

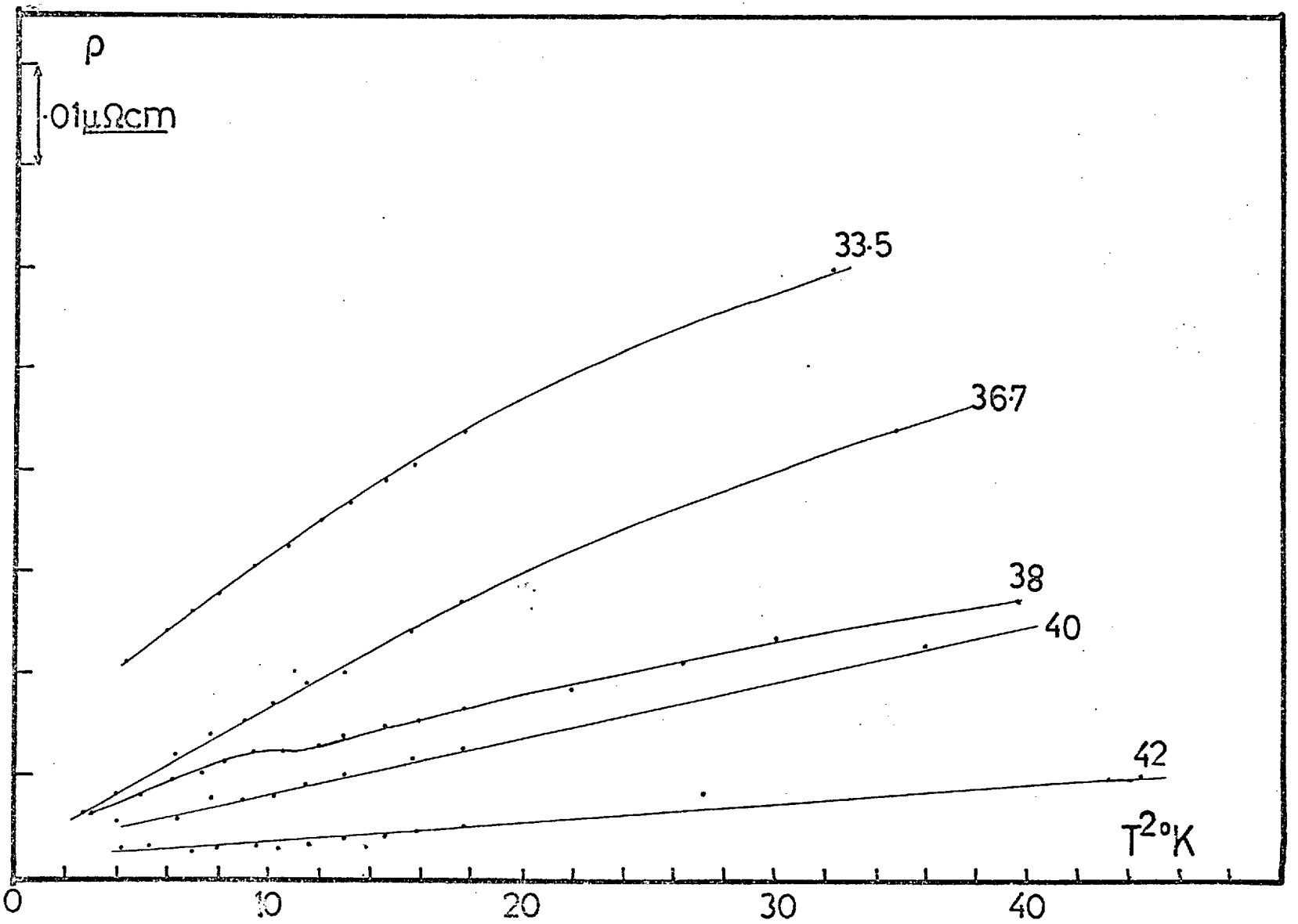

Fig. (V.38)

(b) Magnetization and Susceptibility

Magnetization and susceptibility measurements have been made, with the help of Dr. H. Jamieson, on seven different alloys containing between 28 and 42 at % Co. The susceptibility of the alloys (measured in 0.5kG) is shown in Fig. (V.39) as a function of temperature up to 295°K. All the alloys display a susceptibility maximum. The temperature Tm of this maximum moves to higher values with increasing cobalt concentration.

This type of broad maximum in the susceptibility has been found in many alloy systems such as Cu-Mn (118), Rh-Fe (121), Au-Co (122), etc. One aspect of the Rh-Co alloys susceptibility is different from that of the above alloy systems. In Rh-Co the magnitude of the susceptibility at the corresponding Tm increases, and the peak stays sharp, with increasing cobalt concentration. On the other hand, in the above alloy systems it decreases (after an initial increase), and the peaks broaden with increasing impurity concentration. Thus Rh-Co is more like Au-Fe where susceptibility maximum stays fairly sharp, and χ(Tm) increases with concentration, although this is found at very much lower solute concentration in Au-Fe.

The magnetization field plots at 1.6°K of Rh-36.7 at % Co, Rh-38 at % Co and Rh-40 at % Co are shown in Fig. (V.40) where small concentration difference between the first two alloys has produced a drastic change in the character of the hysteresis loop. We also draw attention to the similarity of hysteresis loops of the two more concentrated alloys.

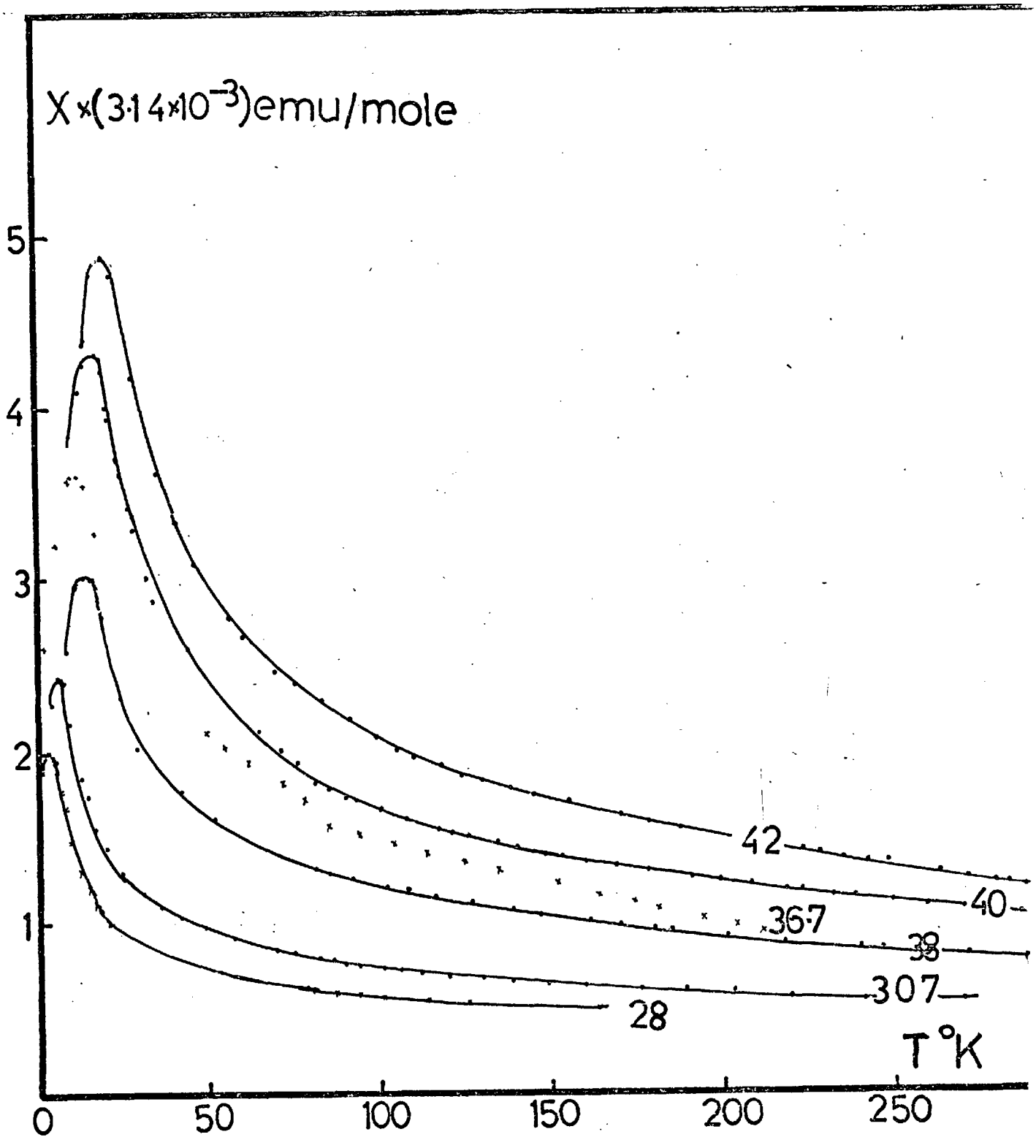

Fig. (V.39)

(For 38% alloy the factor is $3.18 \cdot 10^{-3}$)

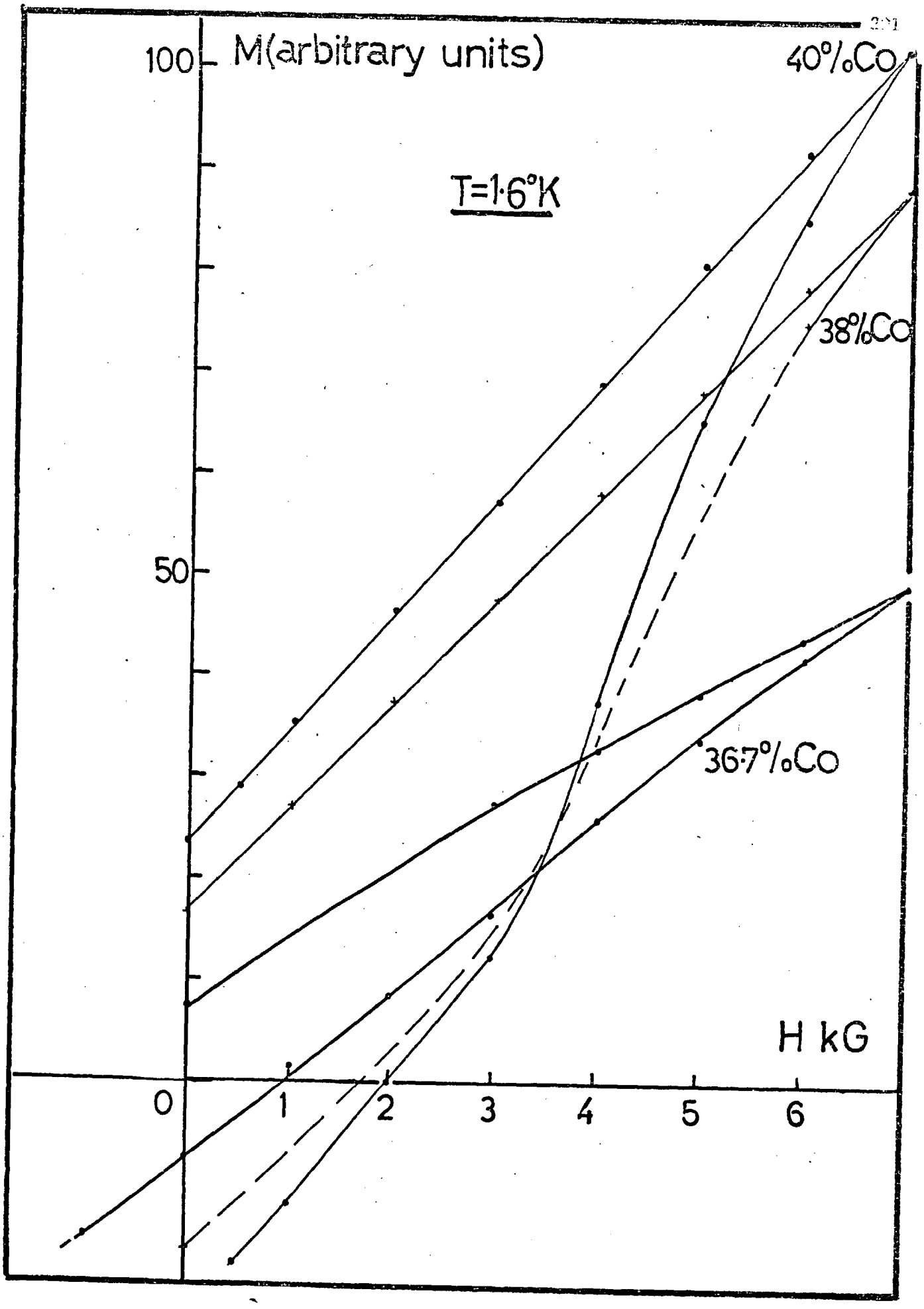

Fig. (V.40)

DISCUSSION

The resistivity change between 1.7° and 4.2°K for all the alloys studied is shown in Fig. (V.41). We believe this is a more appropriate procedure than plotting the quantity: $\Delta\rho = \rho - \rho_o$ in which case uncertainties due to the extrapolation to T = 0°K are inevitably involved.

The resistivity of the most dilute alloys is found to vary as T^2 over a considerable temperature range, and the coefficient of T^2 term is found to be small. Rusby (private communication) has reported that Rh-1 at % Co alloy varies as T^2 up to about 80°K. The coefficient of T^2 being $17.3 \times 10^{-12} \Omega cm/K^2$, which is less than even that of pure palladium. This, on the basis of the Kaiser-Doniach and Rivier-Zlatić theory implies that the cobalt atoms in the dilute limit have a very high spin fluctuation temperature, i.e. are far from being magnetic.

As the concentration is increased the range of T^2 decreases while its coefficient increases. The temperature dependent resistivity starts increasing much faster than linearly with concentration as is clear from Fig. (V.41), and becomes linear in temperature at progressively lower temperatures with increasing cobalt concentration. The figure reveals a critical concentration of about 20 at % Co. However, the non-linear low temperature behaviour shown in Fig. (V.36) suggests that at this concentration stable moments already exist which are probably few, and occur in the locality of cobalt atoms with relatively larger number of nearest neighbour cobalt atoms.

In this alloy system it seems appropriate to think of a range of spin fluctuation temperatures, the lower limit having reached zero at about 20 at % Co where the temperature dependent resistivity peaks, indicating a transition into a magnetic state, but this state is not ferromagnetic as

Fig. (V.41)

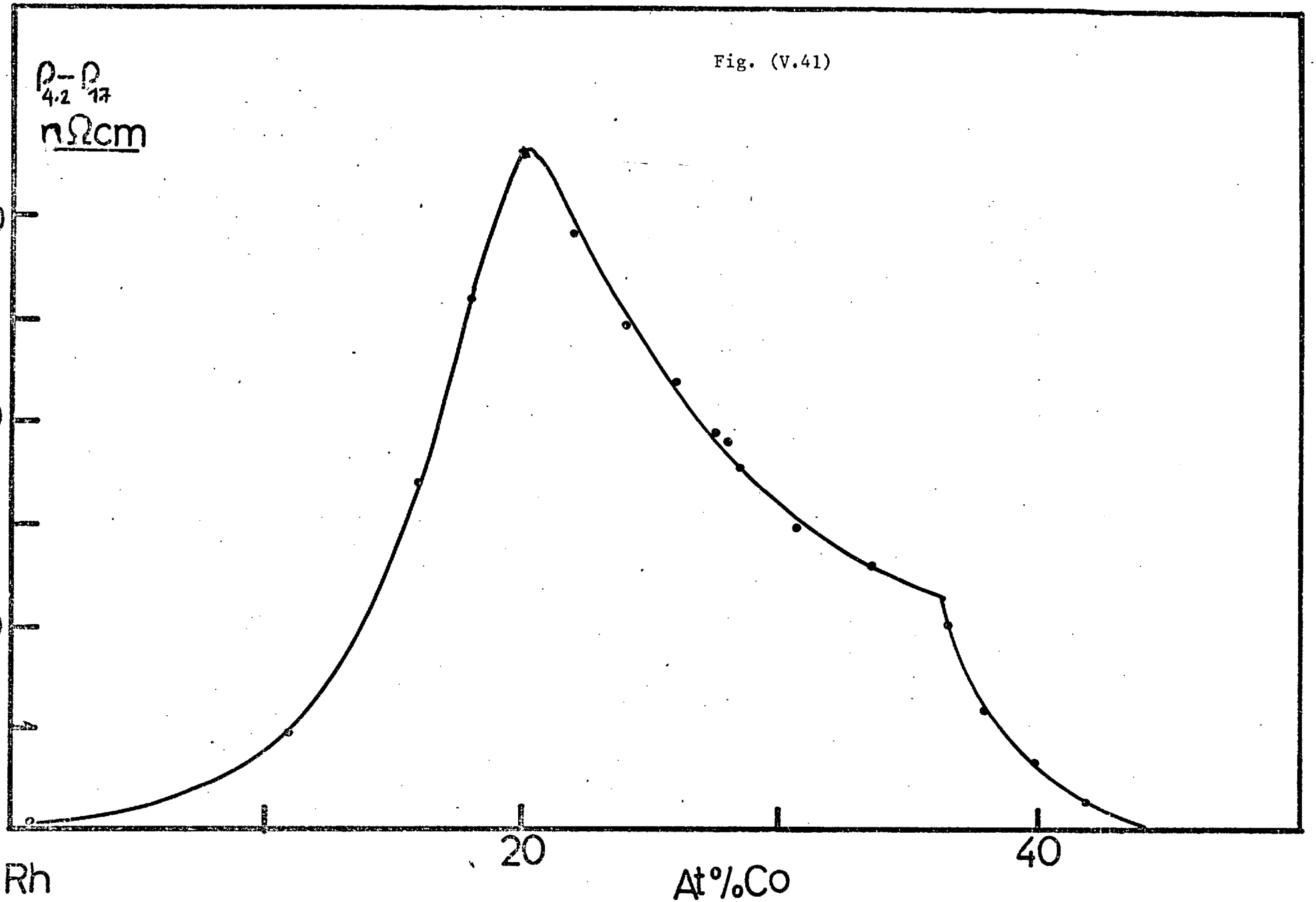

Fig. (V.42)

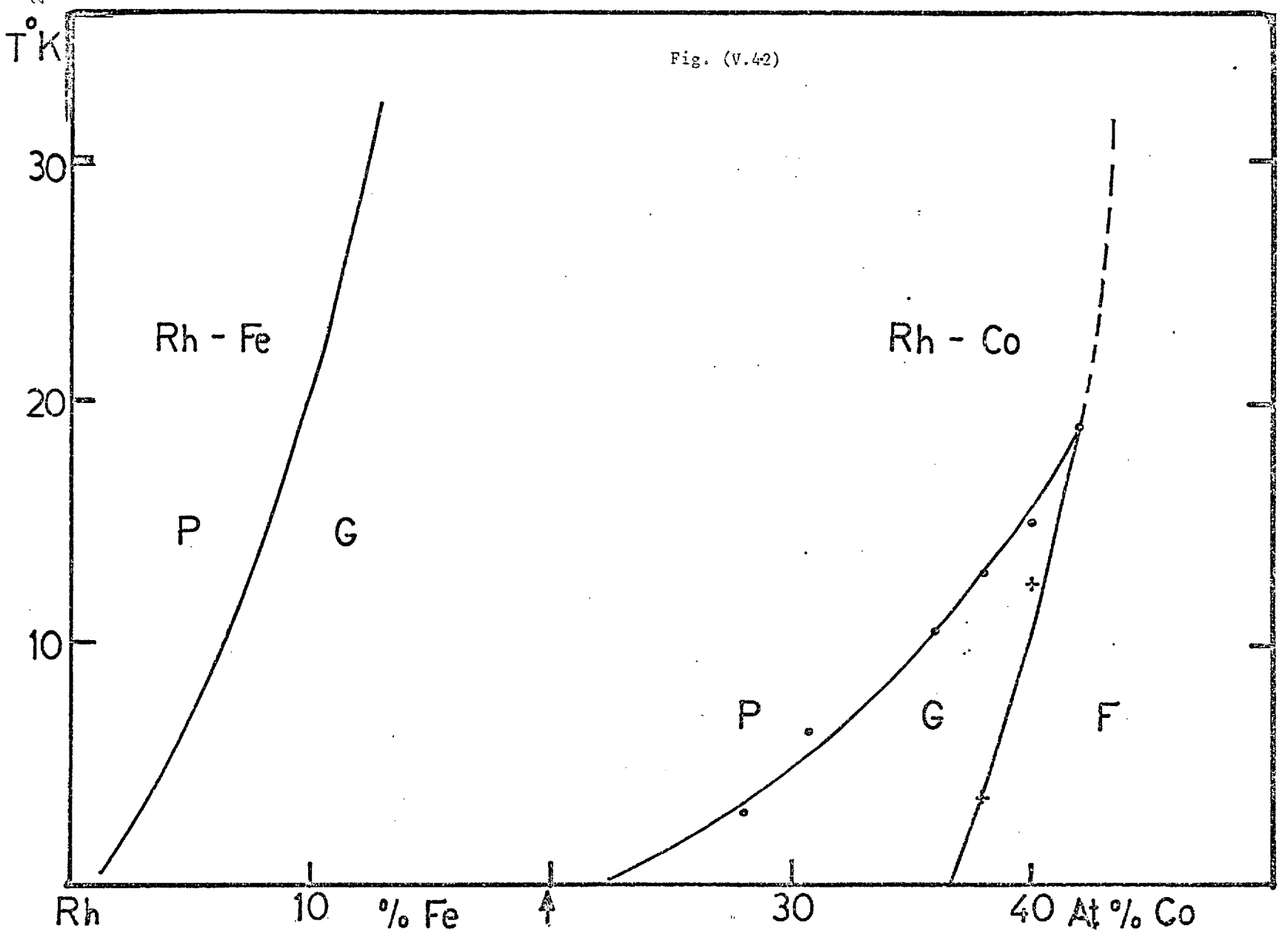

was the case with Pd-Ni alloy system. The transition at this concentration is, like Rh-Fe, into a spin glass phase as suggested by the broad susceptibility maxima.

Between 20 and 36.7 at % Co, alloys present all the characteristics seen in spin glass systems,namely susceptibility maxima, time and temperature dependent remanence and field cooling effects.

At about 37 at % Co the low temperature temperature-dependent term in resistivity drops abruptly Fig. (V.41). We associate this with a transition into a dominantly ferromagnetic phase where the ordering temperature rises rapidly with increasing cobalt concentration. The drastic change in the character of the hysteresis loop about this concentration is also striking as shown in Fig. (V.40).

The combined results of the resistivity and magnetization measurements are employed to produce a phase diagram which is shown in Fig. (V.42), where the crosses are obtained from the resistance anomaly and the dots correspond to the temperature of the susceptibility maximae. The graph suggests that by 44 at % Co the Curie temperature is well above 20^{o}K in agreement with higher temperature investigation of Vogt et al (145). Our own magnetic measurements on a 44 % alloy suggest that it may undergo transition to hcp structure.

The temperature dependent resistivities of Pd-Ni and Rh-Co alloys with critical concentrations are shown in Fig. (V.43) together with those of two alloys which have strong temperature dependence. The resistivity of Rh-Co is very strongly temperature dependent as is clear from the figure. At low temperatures the phonon terms are negligible for both Pd-Ni and Rh-Co alloys, therefore the low temperature resistivity in these alloys is of magnetic origin, ie. is due principally to spin dependent scattering.

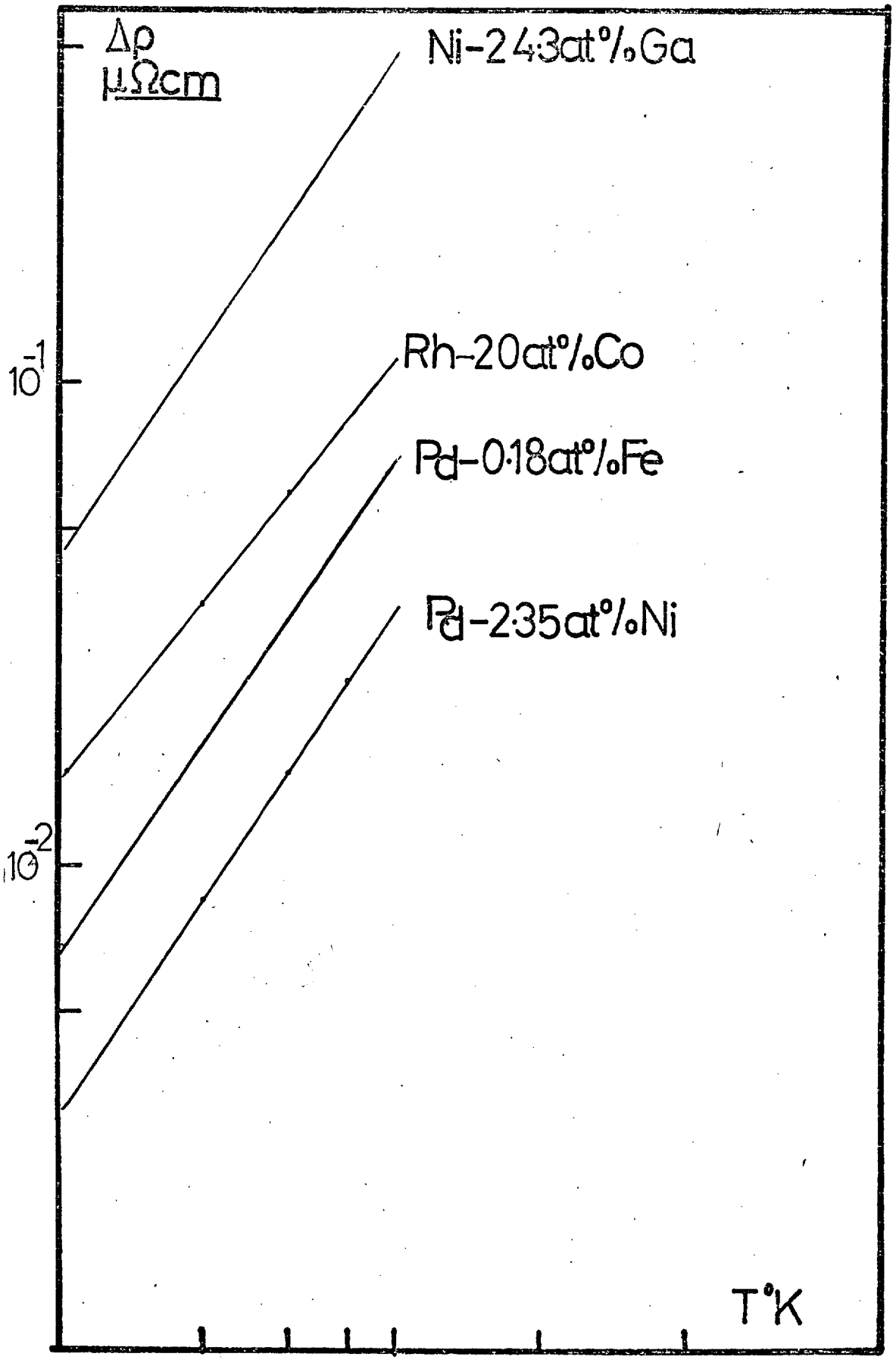

Fig. (V.43)

The resistivities of Pd-Mn and Rh-Co alloys in the spin glass region have in general a $T^{1.5}$ behaviour. Similar temperature dependence has been found in the Au-Fe alloy system by Mydosh and Ford (144). Such a $T^{1.5}$ dependence is most probably a universal feature of spin glass systems, and is possibly due to scattering by spin wave excitations localized within various clusters or regions.

To the author's knowledge, at present no theory exists which is applicable to spin glass resistivity. We hope that the data obtained here will prove useful for future attempts to clarify this problem.

From this work it is clear that the electrical resistivity measurements lead to less ambiguous conclusions especially near the critical points such as Curie temperature or critical concentration. However, the most appropriate procedure is clearly the study of the same sample by the resistance and susceptibility measurements.

REFERENCES

1. J. Friedel, Can. J. Phys. 34, 1190, 1956; Nuovo Cimento Suppl.7, 1953; Metallic Solid Solutions (J. Friedel, A.Guinier Eds) Benjamin, New York, 1963; J. Phys. Rad. 19, 573, 1958.
2. C. Kittel, Q. Theory of Solids - J. Willey and Sons, 1963.
3. E. C. Stoner, J. Phys. Rad. 12, 372, 1951.
4. B.T. Matthias, M. Peter, J.J. Williams, A.M. Clogston, E. Corenzwit and R.C. Sherwood, Phys. Rev. Letters. 5, 542, 1960.

   A.M. Clogston, B.T. Matthias, M. Peter, J.J. Williams, E. Corenzwit and R.C. Sherwood, Phys. Rev. 125, 541, 1962.
5. P.W. Anderson, Phys. Rev. 124, 41, 1961.
6. K. Yosida, A. Okiji and S. Chikazumi, Progr. Theoret. Phys. (Kyoto) 33, 559, 1965.
7. A.J. Heeger, Solid State Physics, Vol 23, 283, 1969.
8. P.W. Wolff, Phys. Rev. 124, 1030, 1961.
9. A.M. Clogston, Phys. Rev. 125, 439, 1962.
10. V. Jaccarino and L.R. Walker, Phys. Rev. Letters 15, 258, 1965.
11. D.J. Kim, Phys. Rev. B1, 3725, 1970.
12. N. River and M.J. Zuckermann, Phys. Rev. Letters 21, 904, 1968.
13. N. River, M.Sunjic and M.J. Zuckermann, Phys. Letters 28A, 492, 1969.
14. N. Rivier, Thesis, University of Cambridge, 1968.
15. T. Kasuya, Progr. Theoret. Phys. 16, No. 1, 45, 1956.
16. Y. Nagaoka, Phys. Rev. 138, A1112, 1965.
17. D.J. Scalapino, Phys. Rev. Letters 16, 937, 1966.
18. J.R. Shrieffer and P.A.Wolff, Phys. Rev. 149, 491, 1966.
19. P.W. Anderson and A.M. Clogston, Bull. Am. Phys. Soc. 6, 124, 1961.
20. C. Zener, Phys. Rev. 1, 440, 1951.
21. K. Yosida, Phys. Rev. 106, 893, 1957.
22. M.A. Rudemann and C. Kittel, Phys. Rev. 96, 99, 1954.
23. B. Caroli, J. Phys. Chem. Solids, 28, 1427, 1967.

24. A.Blandin, Thesis, University of Paris, 1961.

25. A. Blandin and J. Friedel, J. Phys. Rad. 20, 160, 1959.

26. G.G. Law and T.M. Holden, Proc. Phys. Soc. 89, 119, 1966.

27. P.A. Wolff, Phys. Rev. 120, 814, 1960.

28. B. Giovannini, M. Peter and J.R. Schrieffer, Phys. Rev. Letters 12, 736, 1964.

29. A.W. Overhauser, J. Applied Phys. 34, 1019, 1963.

30. R.E. Watson and A.J. Freeman, Phys. Rev. 152, 566, 1966; Phys. Rev. 178, 725, 1969.

31. D.J. Kim and B.B. Schwartz, Phys. Rev. 20, No. 5, 1968.

32. W. Marshall, Phys. Rev. 118, No. 6, 1519, 1960.

33. J.E. Zimmerman and F.E. Hoare, J. Phys. Chem. Solids 17, 52, 1960.

34. F.J. Due Chatenier and J. De Nobel, Physika 32, 1966.

35. M.W. Klein and R. Brout, Phys. Rev. 132, 2412, 1963.

36. S.H. Liu, Phys. Rev. 157, 1967.

37. H.E. Stanley, Intro. to Phase Trans. and Crit. Phenom. Oxford University Press, 1971.

38. C. Herring, Magnetism Vol IV. G.T. Rado and H. Suhl, Editors. Academic Press, New York, 1966.

39. E.P. Wohlfarth, Lecture Notes, Czechoslovak Summer School, 1965.

40. P.A.M. Dirac, Proc. Royal Soc. (London) A123, 714, 1929.

41. See for example, F. Reif, "Fundamentals of Statistical and Thermal Physics", McGraw Hill, 1965.

42. A. Blandin, Proc. Int. Course on Condensed Matter, Trieste, 1967.

43. E. Vogt, Phys. Stat. Sol.(b) 50, 653, 1972.

44. E.P Wohlfarth, J. Inst. Maths. Applics. 4, 359, 1968.

45. W. Treutman, Z. Angew Phys. 30, 5, 1970.

46. J.M. Ziman, "Principles of the Thoery of Solids", Cambridge University Press, 1965.

47. A.H. Wilson, "The Theory of Metals", 2nd Ed. Cambridge University Press, 1965.

48. J. Winter, "Magnetic Resonance in Metals", Oxford University Press, 1971.

49. R.M. White, "Quantum Theory of Magnetism", McGraw Hill, 1970.

50. P.W. Anderson, Many Body Physics (C. de Wit and R.Balian, Eds), 1967 Lecture Notes, Les Houches Summer School, Gordon & Breach, New York, 1968, Page 229.

51. T. Izuyama, D.J. Kim and R. Kubo, J. Phys. Soc. Japan 18, No. 7, 1025, 1963.

52. S. Doniach, Proc. Phys. Soc. 91, 86, 1967.

53. A.P. Klein and A.J. Heeger, Phys. Rev. 144, 458, 1966.

54. S. Doniach, Proc. Inter. School of Physics (Enrico Fermi) Course 37, Page 255, 1967.

55. P.G. De Gennes, J. Phys. Rad. 23, 510, 1962.

56. H. Jones, Handbuch der Physik 19, 227, 1956.

57. N.F. Mott and H. Jones, "The Theory of the Properties of Metals and Alloys", Oxford 1936, Dover 1958.

58. N.F. Mott, Advance in Phys. 13, 325, 1964.

59. J.L. Olsen, Electron Transport in Metals Interscience, New York and London, 1962.

60. G.T. Meaden, "Electrical Resistance of Metals", Plenum Press, 1965.

61. D.K.C. MacDonald, Handbuch der Physik 14, 137, 1956.

62. I. Mannari, Prog. Theor. Phys. 22, 335, 1959.

63. S.H. Liu, J. Appl. Phys. 35, 1087, 1964.

64. D.L. Mills and P. Lederer, J. Phys. Chem. Solids 27, 1805, 1966.

65. N.F. Mott, Proc. Royal Soc. (London) A153, 699, 1936.

66. T. Kasuya, Prog. Theor. Phys. Japan 16, 58, 1956.

67. P.G. De Gennes and J. Friedel, J. Phys. Chem. Solids 4, 71, 1958.

68. K. Yosida, Phys. Rev. 107, 396, 1957.

69. P.D. Long and R.E. Turner, J. Phys. C: Metal Phys. Suppl. No.2 P, S127, 1970.

70. B.R.Coles, Phil. Mag. Suppl. 7, 40, 1958.

71. S. Doniach and E.P. Wohlfarth, Proc. Royal Soc. A295, 442, 1967.

72. J. Kondo, Prog. Theo. Phys. 32, 37, 1964.

73. G. Boato, M. Bugo and C. Rizzuto, Nuovo Cimento, 45, 226, 1966.

74. A.I. Schindler and M.J. Rice, Phys. Rev. 164, 759, 1967.

75. P. Lederer and D.L. Mills, Phys. Rev. 165, 837, 1968.

76. A.B. Kaiser and S. Doniach, Int. J. Magnetism 1, 11, 1971.

77. N. Rivier and V. Zlatic, J. Phys. F.2, L.99, 1972.

78. J. Mathon, Proc. Royal Soc. A306, 355, 1968.

79. S. Doniach and S. Engelsberg, Phys. Rev. Letters 17, 1966.

80. S. Engelsberg, W.F. Brinkman and S. Doniach, Phys. Rev. Letters 20, 1040, 1968.

81. A.H. Morrish, "The Physical Principles of Magnetism". J.W. and Sons, New York, 1965.

82. J.T. Schriempf, A.I. Schindler and D.L. Mills, Phys. Rev. 187, 959, 1967.

83. M.G. Leger and W.B. Muir, (Preprint)

84. G. Chouteau, R. Fourneaoux, K. Gobrecht and R. Tourner, Phys. Rev. Letters 20, 193, 1968.

85. J.H.J. Fluitman, B.R. De Vries, R. Boom and C.J. Schinkel, Phys. Letters. 28A, 506, 1968.

86. F.R. de Boer, Thesis, University of Amsterdam, 1969.

87. J.H.J. Fluitman, R. Boom, P.F. de Schatel, C.J. Schinkel, J.L.L. Tilanus and B.R. de Vries, J. Phys. C. Solid State Physics,

88. J.W. Loram, R.J. White and A.D.G. Grassie, 1972 Physics Rev. (to be published).

89. D. Shaltiel, J.H. Wernick, H.J. Williams and M. Peter, Phys. Rev. 135, A1346, 1964.

90. R.H. Taylor and D. Griffiths, (To be published)

91. H. Jamieson, R.H. Taylor, A. Tari and B.R. Coles (to be published).

92. M.P. Sarachik and D. Shaltiel, J. Appl.Phys. 38, 1155, 1967.

93. C.W. Chen, L.R. Edwards and S. Legvold, Phys. Stat. Sol. 26, 611, 1968.

94. G. Williams and J.W. Loram, S. State Comm. 7, 1261, 1969.

95. T. Moriya, Proc. Int. School of Phys. Enrico Fermi Course 37, Academic Press, New York, 1967.

96. G.J. Nieuwenhuys and B.M. Boerstoel, Phys. Letters 33A, 281, 1970.

97. M.P. Kawatra, S. Skalski, J.A. Mydosh and J.I. Badnick, J. Appl. Phys. 40, 1202, 1969.

98. G. Williams and J.W. Loram, J. Phys. Chem. Solids, 30, 1827, 1969.

99. G. Williams, J. Phys. Chem. Solids 31, 529, 1970.

100. M.E. Colp and G.Williams, Phys. Rev. B.5, No.7, 2599, 1972.

101. S. Skalski, M.P. Kawatra, J.A. Mydosh and J.I. Badnick, Phys. Rev. B2, 3613, 1970.

102. B.R. Coles, Phys. Letters 8, 243, 1964.

103. H. Nagasawa, Phys. Letters, 32A, 271, 1970.

104. O. Laborde and P. Radhakrishna, Phys. Letters, 37A, 209, 1971.

105. R. Rusby (Private Communication).

106. R.W. Houghton, M.P. Sarachik and J.S. Kouvel, S. State Comm. 10, 369, 1972.

107. J. Crangle and W.R. Scott, J. Appl. Phys. 36, 921, 1965.

108. M.J. Besmus and A. Herr, Phys. Letters 39A, 1972.

109. J. Rault and J.P. Burger, C.R. Acad. Sc. Paris, 269, 1085, 1969.

110. W.M. Star, S. Foner, E.J. McNiff Jr., Phys. Letter 39A, 189, 1972.

111. B.M. Boerstoel, J.J. Zwart and J. Hansen, Physika 57, 397, 1972.

112. R.E. Walstedt, R.C. Sherwood and J.H. Wernick, J. Appl. Phys. 39, 555, 1968.

113. A.P. Murani, Thesis, University of London, 1969.

114. J.S. Kouvel and J.B. Comly, Phys. Rev. Letters, 24, 598, 1970.

115. F. Acker and R. Huguenin, Phys. Letters, 38A, 343, 1972.

116. E. Bucker, W.F. Brinkman, J.P. Maita and H.J. Williams, Phys. Rev. Letters 18, 1125, 1967.

117. W.C. Muellner and J.S. Kouvel, Proc. 17th Conf. Magnetism and Magnetic Materials, Chicago, Illinois, November 1971.

118. J. Owen, M. Browne, W.D. Knight and C. Kittel, Phys. Rev. 102, 1501, 1956.

J. Owen, M. Browne, V. Arp and A.F. Kipp, J. Phys. Chem. Solids 2, 85, 1957.

119. R.W. Schmitt and I.S. Jacobs, J. Phys. Chem. Solids 3, 324, 1957.

120. J.S. Kouvel, J. Phys. Chem. Solids, 21, 57, 1961; J. Phys. Chem. Solids, 24, 795, 1963.

121. A.P. Murani and B.R. Coles, J. Phys. C. No.2, S159, 1970.

122. M.H. Bancroft, Phys. Rev. B2, 2597, 1970.

123. S. Chakravorty, P. Panigrahy and P. A. Beck, J. Appl. Phys. 42, 1698, 1971.

124. P.A. Beck, Metallurgical Trans. 2, 2015, 1971.

125. A.I. Schindler and C.A. Macliet, Phys. Rev. Letters 20, 15, 1968.

126. A.I. Schindler, N.R.L. Report 7057 (Washington:NRL) 1970.

127. C.A. Macliet, A.I. Schindler and D.J. Gillespie, Phys. Rev.1.3283, 1970.

128. B.M. Boerstoel, Thesis University of Amsterdam, 1970.

129. R. Berman, J.C.F. Brock and D.J. Huntley, Cryogenics, 1964.

130. J.R. Clement and E.H. Quinell, Phys. Rev. 79, 1028, 1952.

131. G.K. White, Experimental Tech. in Low Temperature Physics", Oxford University Press, 1968.

132. M. Hansen, "Constitution of Binary Alloys", McGraw Hill, New York, 1958.

133. R.P. Elliot, "Constitution of Binary Alloys", 1st. Supp. McGraw Hill, New York, 1965.

134. A.I. Schindler and B.R. Coles, J. Appl. Physics, 39, No.2, 956, 1968.

135. R.M. Bozarth, D.D. Davis, and J.H. Warnick, J. Phys. Soc. Japan. Suppl. 17, 112, 1962.

136. J.H.J. Fluitman, Thesis University of Amsterdam, 1970.

137. E.P. Wohlfarth and P.F. de Chatel, Preprint.

138. C. Hargitai, S. Shtrickman and E.P Wohlfarth, Phys. Letters 39A, 87, 1972.

139. S. Shtrickman and E.P. Wohlfarth, Physika, 60, 427, 1972.

140. E.D. Thompson, E.P. Wohlfarth and A.C. Bryan, Proc. Royal Soc. 83, 59, 1964.

141. J.M. Ziman, "Electrons and Phonons" Oxford University Press, 1960.

142. M. McDougald and A.J. Manuel, J. Appl. Phys. 39, 961, 1968.

143. G. Williams, Phys. Rev. B5, 236, 1972.

144. J.A. Mydosh and P.J. Ford, Con. Proc. of the Symposium on Amorphous Magnetism, Wayne State University, August 1972.

145. E. Vogt, F. Bölling and W. Treutman, Ann. der Physik 25, 280, 1970.

Electrical resistivity and the transition to ferromagnetism in the palladium–nickel alloys

Abstract· The resistivity (ρ) at temperatures below 4·2 K of palladium alloys with 2 to 6 at% nickel has been measured and fitted to the expression $\rho - \rho_0 = AT^n$. The behaviour of A clearly indicates the critical concentration for the para- to ferromagnetic transition at 2·32 ± 0·03 at% nickel. Well away from this composition n is close to 2·0, but decreases on approaching it from either side.

The alloy system **Pd**Ni has been widely studied as an example of a system where strong local exchange enhancement on solute atoms leads, as their concentration increases, to long range ferromagnetic ordering; although it is, in a way, atypical in the significant enhancement effects present in the pure solvent, which lead to a long range response and rather small critical concentration.

Some of the early information on electrical resistivity (Schindler and Rice 1967, Schindler and Coles 1968) provided some information on such effects, but more recently measurements have been made of the specific heat (Schindler and Mackliet 1968, Chouteau *et al.* 1968), magnetic diffuse scattering of neutrons (Aldred *et al.* 1970) the electron transport properties (Schriempf *et al.* 1970), and magnetoresistance (Schindler and La Roy 1971). An excellent survey of theory and experiment is given by Schindler (1970).

The theory of the electrical resistivity in the dilute limit has been discussed by Lederer and Mills (1968) and by Kaiser and Doniach (1971). The physically more realistic approach of a local enhancement on the nickel atoms used by these workers leads to a T^2 behaviour of the resistivity of the paramagnetic alloys at low temperatures, but has not been extended through the critical concentration. Mathon (1968), however, has used the earlier model (Schindler and Rice 1967) of a general exchange enhancement increasing with nickel concentration, to explore the behaviour through the critical concentration. The peak in the imaginary part of the wavevector and frequency dependent susceptibility ($\chi(\boldsymbol{q}, \omega)$) moves to lower ω as the enhancement increases, causing the scattering by spin fluctuations to increase, reaching a maximum at the critical concentration. (On both sides of it the magnetic scattering can be considered as given by spin fluctuations; in the strong ferromagnetic limit at low temperatures these are straightforward spinwaves, and T^2 behaviour is again observed). Near the critical concentration we may write the spin fluctuation scattering as AT^n, but the value of n is predicted by Mathon to fall to 5/3. Fluitman (1970) has examined this scattering in near-critical Ni_3Ga and Ni_3Al finding very large A values, and n values falling to 1·5. Schindler and Gillespie (1971) have observed a sharp peak in A at the critical concentration in PtNi alloys (fitting their data to AT^2) but the curve is asymmetric and A_{max} comparatively small.

In this letter we report results which define rather closely the critical concentration in PdNi, and reveal the character of the temperature dependence.

Specimens containing 2·25, 2·35, 2·42, 2·50, 3·0, 4·0 and 5·8 at% nickel were prepared by careful arc melting of the component metals (the upper limits of the iron contents being 3 ppm), forging with nonferrous implements and homogenization at 1200° C. They (and two other alloys† containing 3·5 and 4·5 at% nickel) were then rod-rolled between protective plastic sheets, drawn to wire of about 0·8 mm diameter, etched to remove surface contamination and annealed again at 1200° C for 2 days. In view of the similarity of the components the amounts of them used to prepare the alloys are at least as good a guide to the final compositions as would be provided by most methods of quantitative analysis.

The resistances were measured by conventional potentiometric techniques and the

† These had been used in the neutron scattering experiments of Aldred *et al* (1970)

temperatures by monitoring the helium bath pressure or by a carbon resistance thermometer calibrated during the run.

As with other 'itinerant electron ferromagnets' (cf $ZrZn_2$, see Olsen 1961 and Ni_3Al, see Fluitman 1970) and unlike the 'good moments' systems (eg PdFe, see Williams and Loram 1969) the Curie point is not easy to detect in the ρ–T curve, although values of 5·8 K for the alloy with 2·50% nickel and 20·8 K for that with 3·0% are suggested by the data. The critical concentration is very easily detected, however, by examining the value of A given by fitting the data below 4·2 K (where ρ and T are known most accurately) to the expression

$$\rho = \rho_0 + AT^n$$

We consider this a more appropriate procedure than the assumption of a T^2 spin fluctuation term and a T^5 lattice scattering term for these alloys in which $\rho - \rho_0$ at 4·2 K is always greater than 100 times the lattice scattering term for pure palladium. The values of ρ_0, A and n are shown in the table 1 and those of A are plotted in figure 1 together with the

Table 1. The values of the parameters in the expression for the electrical resistivity at temperatures below 4·2 K.

Composition (at% Ni)	ρ_0† ($10^{-6}\ \Omega$ cm)	A ($10^{-12}\Omega$ cm K^{-n})	n‡
2·25	0·67[6]	2500	1·40
2·35	0·89[3]	2790	1·50
2·42	0·80[3]	1580	1·76
2·50	0·98[8]	1420	1·74
3·00	1·13[9]	607	1·9
3·50	1·28[4]	320	2·0
4·00	2·04[8]	138	2·0[4]
4·50	2·47[7]	120	2·0[6]
5·83	3·06[5]	80	2·1

† The uncertainties in these values (~±2%) arise mainly from inaccuracies in determining the dimension; they are rather larger for the 2·42% alloy.

‡ The uncertainties are ±0·05 for alloys near the critical concentration, rising to ±0·1 at 5·8% Ni.

coefficient of the T^2 term extracted for more dilute alloys by Schindler (1970). The peak in A is extremely pronounced and yields C_{crit} as 2·32 ± 0·03 at% nickel, compared with values of rather less than 2·0 suggested by Crangle and Scott (1965) and Chouteau *et al.* (1968) on the basis of magnetic measurements which, by their nature, cannot give as sharp an indication as zero field measurements. This value is in good agreement with the results given by fitting a coherent potential approximation (Harris and Zuckermann 1971) to susceptibility data for paramagnetic alloys

Rather general arguments lead one to expect n to be 2·0 for either paramagnon or magnon scattering at very low temperatures, but they cease to be valid close to critical temperatures and concentrations. Mathon (1968) derives a limiting value of 5/3 but, our experimental values clearly become less than this. Iron impurity (to the extent of 400 ppm) has been shown to produce a lowering of n from 1·65 to 1·4 for a nearly ferromagnetic Ni_3Ga alloy (Fluitman 1970) but we think it unlikely that significant amounts of any 'local moment' impurity exists in our samples.

The curve for A closely approaches the symmetry required by Mathon's theory, understandably more so than the NiGa and NiAl systems where the component elements have very different electronic structures. The very much smaller values of A for PdNi suggest however that the magnetization of the palladium matrix remains rather small in the vicinity of the critical composition.

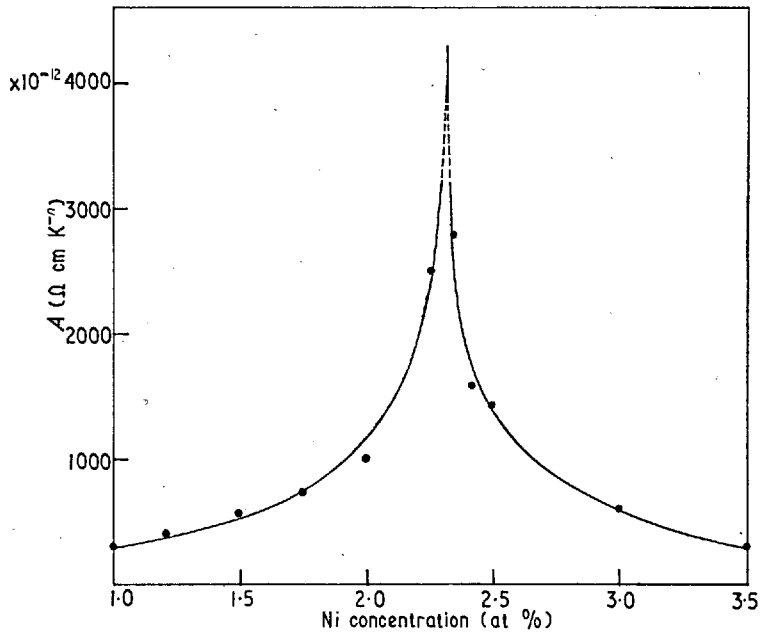

Figure 1. Plot of the coefficient A against Ni concentration. Data points for alloys with up to 2% nickel are from Schindler (1970) who took $n = 2{\cdot}0$. The value of A for the 2% alloy would rise if this restriction were lifted.

We acknowledge gratefully the metallurgical help and advice of Dr H. E. N. Stone.

Department of Physics,
Imperial College,
London SW7 2BZ

A. TARI
B. R. COLES
11th October 1971

ALDRED, A. T., RAINFORD, B. D., and STRINGFELLOW, M. W., 1970, *Phys. Rev. Lett.*, **24**, 897–9.
CHOUTEAU, G., FOURNEAUX, R., GOBRECHT, K., and TOURNIER, R., 1968, *Phys. Rev. Lett.*, **20**, 193–5.
CRANGLE, J., and SCOTT, W. R., 1965, *J. appl. Phys.*, **36**, 921–8.
FLUITMAN, J. H. J., 1970, *PhD Thesis* University of Amsterdam.
HARRIS, R., and ZUCKERMANN, M. J., 1971, *Phys. Rev.* to be published.
KAISER A. B., and DONIACH, S., 1971, *Int. J. Magnetism*, **1**, 11–22.
LEDERER, P., and MILLS, D. L., 1968, *Phys. Rev.*, **165**, 837–44.
MATHON, J., 1968 *Proc. R. Soc. A*, **306**, 355–68.
OLSEN, C. E., 1961, *J. Phys. Chem. Solids*, **19**, 228–9.
SCHINDLER, A. I., 1970, *NRL Report* 7057 (Washington: NRL).
SCHINDLER, A. I., and COLES, B. R., 1968, *J. appl. Phys.*, **39**, 956–7.
SCHINDLER, A. I., and GILLESPIE, D. J., 1971, *Proc. XIIth Int. Conf. Low Temp., Japan*, Ed. E. Kanda (Tokyo: Academic Press).
SCHINDLER, A. I., and LAROY, B. C., 1971, *Solid St. Commun.*, to be published.
SCHINDLER, A. I., and MACKLIET, C. A., 1968, *Phys. Rev. Lett.*, **20**, 15–8.
SCHINDLER, A. I., and RICE, M. J., 1967, *Phys. Rev.*, **164**, 759–64.
SCHRIEMPF, J. T., SCHINDLER, A. I., and MILLS, D. L., 1970, *Phys. Rev.*, **187**, 959–73.
WILLIAMS, G., and LORAM, J. W., 1969, *J. Phys. Chem. Solids*, **30**, 1827–33.